Title

Exploring the process of microbial methane production: a characterization of the ATP requirement for the activation of methyl coenzyme-M reductase

ISBN

9798189270284

Author

Adler, Sophia Allessio

Publication Date

2026-05-01

Peer reviewed|Thesis/dissertation

Exploring the process of microbial methane production: a characterization of the ATP requirement for the activation of methyl coenzyme-M reductase

By

Sophia Allessio Adler

A dissertation submitted in partial satisfaction of the

requirements for the degree of

Doctor of Philosophy

in

Molecular and Cell Biology

in the

Graduate Division

of the

University of California, Berkeley

Committee in charge:

Professor Dipti D. Nayak, Chair

Professor Michael A. Marletta

Professor Sabeeha S. Merchant

Professor Kathleen Collins

Spring 2026

Abstract

Exploring the process of microbial methane production:
a characterization of the ATP requirement for the activation of methyl coenzyme-M reductase

By

Sophia Allessio Adler

Doctor of Philosophy in Molecular and Cell Biology

University of California, Berkeley

Professor Dipti D. Nayak, Chair

The need for an urgent response to the climate crisis has become ever present. Both 2023 and 2024 were the hottest recorded in Earth's history [1–3] with temperatures reaching 1.5 C above pre-industrial levels. If this level of warming continues over a 20-year period, it will violate the limit set by the Paris Climate Accord[1] just a decade ago. The impacts of this warming are widely considered catastrophic to humankind, and the World Health Organization has categorized climate change as the single greatest threat to human health[4]. To appropriately respond to and mitigate global warming, a detailed understanding of its specific mechanistic causes is paramount.

Methane is considered one of the most critical greenhouse gasses, coming second only to carbon dioxide in terms of heat-trapping contributions in the atmosphere[5]. The contributions of methane to the atmosphere consist of both biotic and abiotic sources, both of which are included in the anthropogenic sources of greenhouse gasses primarily driving global warming[5]. It is estimated that about 75% of all atmospheric methane comes from biological sources which include, but are not limited to, agriculture, landfills, and natural wetlands[6]. The class of organisms responsible for the biotic methane contribution is the methanogen, a type of Archaeon found in diverse and widespread anaerobic environments across the globe[6,7]. Despite the ecological, evolutionary, and metabolic diversity of methanogens, the enzyme responsible for methane formation, methyl-coenzyme M reductase (MCR), is both ubiquitous throughout and unique to this class of organisms[8–10]. The reaction catalyzed by MCR consists of the reduction of a methyl group from methyl-coenzyme M with reducing equivalents provided by coenzyme B which produces methane and a heterodisulfide of coenzyme M and coenzyme B[11–14]. The subsequent reduction of this heterodisulfide couples this process to adenosine triphosphate (ATP) production and thus serves as the essential energy generating mechanism for these organisms[6,15].

Given that MCR is of critical importance to global carbon cycling, it's necessary to obtain a detailed understanding of the ways in which this enzyme functions *in vivo*. MCR's discovery predates the classification of Archaea as a unique domain of life, and initial descriptions of the methyl-reducing cell fraction were obtained from a "methane bacteria"[11,13,14]. Despite the discovery of this enzyme nearly

fifty years ago, the majority of research surrounding it has been restricted to in vitro biochemical characterizations mainly due to the dearth of genetic tools available to manipulate methanogens until recently [16–19]. The discoveries made surrounding MCR's structure and activity have been critical to the development of methanogenesis inhibitors, like 2-bromoethanesulfunate (BES) and 3-nitrooxypropanol (3-NOP), which have proven to be useful for experimental perturbations of methanogenesis and the reduction of enteric methane emissions from cattle[20–24]. Despite these strides made in understanding MCR biology, much remains to be uncovered about how this enzyme is assembled, regulated, and activated in vivo.

MCR is a heterohexamer composed of α_2, β_2, and γ_2 subunits and two active sites, each of which coordinate the nickel containing tetrapyrrole, cofactor F430[25]. The extreme oxygen sensitivity of MCR can be attributed to F430 because of the extraordinarily low redox potential of the Ni^{1+}/Ni^{2+} pair (between -600 mV and -700 mV)[26]. The catalytic mechanism of MCR requires that F430 is initially in the reduced Ni^{1+} oxidation state, is oxidized during catalysis, and returns to Ni^{1+} upon reaction completion and product release[27]. The installation of F430 and its reduction to Ni^{1+} are processes that require a suite of accessory proteins to accomplish[28,29]. Furthermore, since the initial purification and characterization of MCR it has been known that a sub-stoichiometric amount of ATP is required for sustained activity in addition to several protein-containing cell fractions[11,12,30]. As increased attention has been focused on MCR in light of its effects on the climate, so too has increased attention been paid to these accessory proteins which are required for the cell to have a mature and functional MCR. The work described in my thesis focuses on those proteins that are required for the ATP-based reductive activation of MCR, with particular focus on component A2, an ATP binding protein known to be associated with MCR through both genomic and biochemical evidence.

Chapter 1 of this thesis provides necessary background by reviewing literature surrounding the cellular components needed for MCR function within methanogenic archaea. This chapter provides a description and overview of the "Methanogenesis Maker Proteins" (MMPs), a classification assigned to a group of genes that co-occur with MCR in genomes[31]. Most of these MMPs have functions yet to be determined, but this chapter offers an overview of several MMPs with specifically characterized roles. It begins by describing the biosynthetic pathways for the coenzymes and cofactor used by MCR, coenzyme M, coenzyme B, and F430, and highlights which steps are performed by MMPs. Next, the current understanding of the MCR-associated proteins required for assembly and activation of the enzyme are summarized, including the installation of F430 by McrD and the McrC based activation complex. Finally, this chapter concludes by highlighting several new tools, both genomic and biochemical, that have been developed recently and could provide even more insight into MCR function. This chapter includes a table with all currently described MMPs, known functions, and associated annotations to ease comparisons between published work.

Chapter 2 dives deep into role of component A2, an ATP-binding protein introduced in Chapter 1. Component A2 has long been associated with MCR activation, but its specific biochemical role has remained elusive. In this chapter we use a suite of genetic and biochemical experiments to prove that component A2 is a bona-fide ATPase whose activity is stimulated by the presence of MCR. We uncover that the ATPase activity of this enzyme is oxygen sensitive and can be interrupted by specific

point mutations introduced into the nucleotide binding domains or into the zinc binding motif. Further analysis with these point mutants reveals that the interaction between A2 and MCR is dependent on the ability of the ATPase to bind ATP but is not dependent on hydrolysis or on zinc binding, leading to a model of interaction where A2 first binds ATP, interacts with MCR, and then hydrolyzes ATP, likely leading to conformational changes in MCR that allow the reductive activation of F430. Additionally, we perform a phylogenetic analysis to show that the zinc binding motif is unique to this class of remodeling ATPases and that component A2 has likely undergone horizontal gene transfer and clusters with a variant of MCR that performs the reverse reaction by oxidizing short chain alkanes. The work described in this chapter provides the first evidence that component A2 is an ATPase whose activity is directly modulated by interaction with MCR, a discovery that will be critical for further characterization of the full mechanism of reductive activation for MCR.

Chapter 3 builds on a discovery outlined in chapter 2 that component A2 in *M. acetivorans* is part of a polycistronic "MCR activation operon" that contains six other MMPs. In this chapter we use CRISPR *interference* (CRISPRi) as a tool to study the effects of diminished gene expression of both the MCR operon and the MCR activation operon, given the essentiality of both. We find that the MCR operon behaves as a traditional polycistronic operon with a single transcription start site when perturbed with CRISPRi. Interestingly, we find that the MCR activation operon does not behave in the same way, indicating the possibility of multiple transcription start sites being present. We also perform growth analysis of each of these knockdown strains and find that, as expected, decreased expression of MCR has a significant effect on growth rate. In contrast, we determine that decreased expression of component A2 does not have a significant effect on growth rate, indicating that the amount of this enzyme required by the cell under standard laboratory conditions is very low.

Together, the work described in this dissertation explores the role of the proteins associated with MCR function and specifically characterizes the ATP requirement for MCR activation. This work furthers our understanding of MCR function *in vivo*, allowing future studies to continue to draw a more detailed map of how this unique and complicated enzyme functions. Additionally, a clearer mechanistic understanding of MCR activation will allow for further applications towards the goal of methane emission mitigation. This work, combined with past and future experimentation, will continue to bring us closer to a full and complete picture of microbial methane production.

Table of Contents

Dedication

My dissertation work is dedicated to my great aunt, Pearl Oyle.

Without whom, I would not have moved to California, and
who would have loved to know that I became a scientist.

Acknowledgments

First and foremost, I would like to thank my advisor and mentor, Professor Dipti Nayak. Her unending passion for research (and especially for methanogens) and her scientific rigor have been a guiding force throughout my PhD. Dipti welcomed me into her lab five years ago, near the beginning of the lab's inception, and it has been truly a joy to see the lab flourish throughout my time here. I have learned so much from her about how to ask and answer an interesting scientific question, and then, just as importantly, how to communicate your science to other people. Her encouragement and excitement have helped immensely to bring me through this journey.

The members of the Nayak lab have also been a critical part of this journey. It has been a pleasure to work with each of the postdocs- Dinesh, Jonathan, Fernando, and Gray. I have learned so much science from each of you. A special thank you to Fernando- it was a pleasure to sit back-to-back with you all these years. And to Gray- thank you for always having a listening ear for my questions and being down to chat about MCR. The group of grad students that inaugurated the Nayak lab with me, Blake, Katie, and Alienor, have had a lifelong impact on me. It has been truly a privilege to undergo this journey with you. You each inspire me to laugh more, spend more time outside, be kinder, and to listen more. And to the younger students in the lab- Maddie, Annelise, Gavin, and Lindsey. I am consistently inspired by your enthusiasm and passion. Thank you for always being there to chat about either science or life. In the broader Berkeley scientific community, I would like to thank my thesis committee- Dr. Michael Marletta, Dr. Sabeeha Merchant, and Dr. Kathy Collins- for their support, feedback, and encouragement. I would also like to thank Shayan, you were the first friend I made when I moved to Berkeley in 2020 and you have continued to be a light in my life. Thank you for undergoing this journey alongside me. Additionally, I would like to thank Dr. Sarah Wengryniuk, who gave me my first ever research opportunity as a sophomore in college. Dr. Daniele Ramella also shaped my scientific journey at Temple University. His mentorship and encouragement were truly life changing. I am very grateful I took his general chemistry class nearly ten years ago.

My family has provided me with unending support and love throughout my PhD journey. To my parents- Marianne and Joe- you have always believed in me, always encouraged me, and always showed me how to have care and kindness in everything I pursue. Thank you. I love you both so much. And to Zoe, I am endlessly lucky to have a sister who is also my best friend. The joy you infuse into everyday life is infectious. Thank you for being the best sister ever. I love you dearly.

To all my friends littered across Philadelphia, Washington D.C., Minneapolis, the East Bay, Los Angeles, and San Francisco- you are too numerous to name but know that you have all touched my life and my time during my PhD very deeply. Especially to my friends in San Francisco, the community we have is full of life, laughter, dancing, and silliness, and for that I am deeply grateful. Thank you all for hang outs, arts and crafts, dinners, weekend trips, and just generally wonderful times. It has meant so much to have you all in my life. Thank you for anchoring me during these last several years. And to Arya and Patty, I remember you both always. I am eternally grateful for the time I had with each of you.

To Riley- my companion in so much of life. I cannot put into words what your love and support has meant to me throughout this journey. You continue to push me to think deeply, to laugh more, and to find joy in every corner of life. I love to explore with you, to walk up a hill, cross a river, or enter a completely unknown space. Thank you for our never-ending conversations. It has brought me immeasurable joy to do this with you by my side.

And finally, to the great natural landscapes in California. I have found comfort in your mountains and deserts. My love of science is driven by my deep desire to understand how the world around me functions, and this continues into my exploration of the outdoors. Thank you for letting me escape to your alpine forests, your dried lake beds, your hot springs, your sand dunes, and your ferocious waves crashing down on seaside cliffs. May we continue to care for the earth around us.

...

"and the universe said I love you
and the universe said you have played the game well
and the universe said everything you need is within you
and the universe said you are stronger than you know
and the universe said you are the daylight
and the universe said you are the night
and the universe said the darkness you fight is within you
and the universe said the light you seek is within you
and the universe said you are not alone
and the universe said you are not separate from every other thing
and the universe said you are the universe tasting itself, talking to itself, reading its own code"

excerpt from 'End Poem' by Julian Gough

Chapter 1

Assembly and maturation of methyl-coenzyme M reductase in methanogenic archaea

The discovery of a methyl-reducing fraction by what was then thought to be a "methanobacterium" predates the understanding of Archaea as a distinct domain of life from bacteria. Despite the early characterization of MCR as the enzyme responsible for this newly identified microbial methane production, a lack of genetic tools and capabilities to manipulate methanogens left scientists to study this enzyme mostly in isolation for several decades. The increases in prevalence of relevant tools and methods in the last 20 years has allowed for a renewed interest in characterizing how this enzyme functions within the context of the cell. As contributions to this field grow, it has become clear that MCR is truly an enzyme that 'takes a village'. This chapter was published as a review in 2025 and reflects the field's understanding at the time of what it takes for the cell to assemble and activate a fully functional MCR. The remainder of this dissertation focuses in on the protein components required to activate MCR, specifically component A2, and addresses what remains to be characterized about the other proteins implicated in MCR activation.

Sophia A. Adler[1], Grayson L. Chadwick[1]*, Dipti D. Nayak[1,2]*

[1]Department of Molecular and Cell Biology, University of California, Berkeley, CA, USA
[2]Department of Plant and Microbial Biology, University of California, Berkeley, CA, USA

*Address correspondence to: Dr. Grayson L. Chadwick (chadwick@berkeley.edu) and Dr. Dipti D. Nayak (dnayak@berkeley.edu)
This chapter was published as a review in the journal *Current Opinion in Microbiology* in 2025.
DOI: https://doi.org/10.1016/j.mib.2025.102637

Abstract

Methanogenesis is a mode of energy metabolism found in anaerobic microorganisms within the archaeal domain of life. All methanogens use the enzyme methyl-coenzyme M reductase (MCR) to produce methane. MCR is an exquisitely oxygen-sensitive enzyme that catalyzes a unique radical-based reaction, which requires many unusual cofactors and coenzymes. A persistent and increasing interest in MCR from both climate and energy perspectives has led to the development of new tools to study methanogens. These tools have, in turn, led to a flourish of new developments pertaining to MCR assembly and activation of late. In this review, we highlight the discovery of new proteins involved in MCR biogenesis in vivo, discuss the major missing pieces in our understanding, and present some of the newest technological developments enabling this ongoing work.

1.1 Introduction

Methanogenic archaea (methanogens) are a group of microorganisms that produce methane as a by-product of energy metabolism. Collectively, these microbes generate nearly one billion tons of methane each year[9]. Context-dependent control of methanogenesis is a grand challenge for biologists and engineers. This process must be stifled where it negatively impacts planetary health and stimulated where generation of methane is beneficial for energy production. Both goals can be met if we understand how methanogens generate methane. All studied methanogens use the enzyme methyl-coenzyme M reductase (MCR) to produce methane[9,32] (**Fig 1.2.1**). Besides the three structural subunits (McrA, McrB, McrG) of MCR (**Fig 1.2.1**), many accessory proteins are also required for its assembly and activation. Some of these proteins are also classified as methanogenesis marker proteins (MMPs)[10,31] (**Table 1.2.1**), as they are only found in genomes that encode MCR or other alkyl-coenzyme M reductases (ACRs). Such proteins are known to catalyze the production of coenzymes and cofactors, install posttranslational modifications (PTMs), and perform ATP-dependent activation of MCR. Uncovering the entire repertoire of these MCR-associated proteins and characterizing their role in the production of holo-MCR is crucial for a holistic understanding of this keystone enzyme. This effort will also facilitate heterologous expression of active MCR in a non-native host for industrial processes. Accordingly, this review will focus on integrating recent genomic surveys to identify MCR-associated proteins with genetic and biochemical efforts to study their functions.

1.2 MCR-associated proteins involved in the biosynthesis of cofactors and coenzymes

At least three unique cofactors are required for MCR activity: coenzyme M (CoM-SH or CoM) that serves as a methyl-carrier, coenzyme B (CoB-SH or CoB) that serves as a reductant, and an active site metallocofactor, F430, that is involved in catalysis. The genes used in the biosynthetic pathway(s) for CoM and F430 have been elucidated — and MMPs catalyze certain key reactions in both pathways — whereas these details are yet to be determined for CoB.

Even though CoM is essential for methanogenesis, it is not unique to methanogens, as bacteria also use it in alkene metabolism[33]. The biosynthetic pathway for CoM in bacteria has evolved convergently[33] and is distinct from the two pathways found in methanogens. In methanogens, the two pathways converge on sulfopyruvate, the penultimate precursor of CoM (**Fig 1.2.1A**). The final enzyme in CoM biosynthesis replaces the aldehyde group in sulfoacetaldehyde with a thiol moiety, and this unusual reaction is mediated by MMP16, which has now been designated as ComF[34,35] (**Table 1.2.1**). The exact mechanism of ComF is yet to be determined, and, interestingly, mutants lacking this enzyme can still generate CoM in the presence of exogenous sulfide. Thus, unknown pathways for CoM synthesis likely exist in methanogens and are a rich avenue for future work.

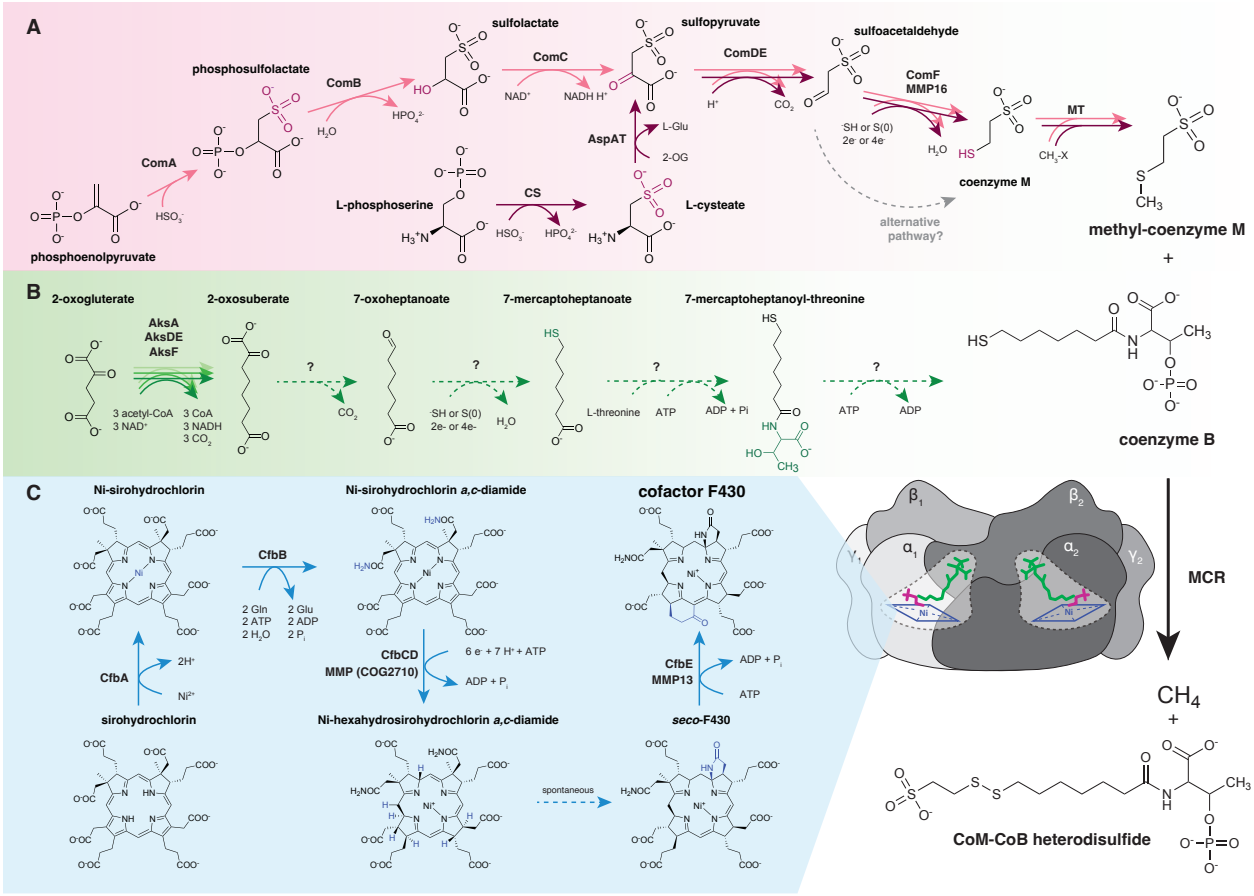

Figure 1.2.1 Biosynthetic pathways for coenzyme M, coenzyme B, and F430. The reaction catalyzed by MCR to generate methane is shown on the right. (a) The two known pathways for coenzyme M biosynthesis in methanogenic archaea are distinguished by light pink and dark pink arrows. The gray dotted arrow denotes a reaction that occurs without the given enzyme[35], so an alternative pathway is possible. The addition of new groups is highlighted in pink. Each characterized gene[36–41] is denoted above the reaction arrows. Cysteate synthase (CS) and aspartate aminotransferase (AspAT) are abbreviated as such. The methyl transfer (MT) reaction to generate methyl-coenzyme M is performed by different methyl transferase enzymes depending on the source of the methyl group. (b) The putative biosynthetic pathway for coenzyme B is shown in green arrows. The addition of new groups is highlighted in green. The first three reactions for chain elongation to generate 2-oxoglutarate are shown over a single arrow and performed by homocitrate synthase (AksA), homoaconitase (AksDE), and homocitrate dehydrogenase (AksF), respectively[42–44]. Dotted arrows with question marks denote putative steps catalyzed by unknown enzymes. (c) The biosynthetic pathway for generating F430 is shown with blue arrows. The relevant coenzyme F430 biosynthesis enzyme (CfbABCDE) is denoted above or beside the arrow[45,46]. Coenzyme M (pink), coenzyme B (green), and F430 (blue) are found in the two active sites of methyl-coenzyme M reductase (MCR; shown in gray), a heterohexamer with $\alpha_2\beta_2\gamma_2$ stoichiometry of three subunits, McrA (α), McrB (β), McrG (γ).

Unlike CoM, CoB (7-mercaptoheptanoylthreonine phosphate) is only found in archaea that encode MCR and/or other ACRs. While the biosynthetic pathway of CoB has not been fully characterized, the hydrocarbon chain of CoB is generated by α-keto acid chain elongation, that is, by

sequential addition of an acetyl group from acetyl-CoA followed by subsequent dehydration, hydroxylation, oxidation, and decarboxylation[42]. This is likely followed by thiolation, threonynylation, and phosphorylation through unidentified enzymes (**Fig 1.2.1B**).

F430, a nickel-containing tetrapyrrole, is also strictly found in MCR and other ACRs. In MCR, F430 is present in both active sites and plays a critical role in electron transfer during catalysis[25]. The biosynthesis of F430 starts with a sirohydrochlorin precursor and requires five enzymes encoded by the cfbABCDE gene cluster[45] (**Fig 1.2.1C**). The penultimate step in F430 synthesis, that is, the formation of a lactam ring, occurs spontaneously in vitro[46]. However, it is plausible that an unknown enzyme may catalyze this reaction in vivo. Interestingly, CfbC and CfbD, which together perform an ATP-dependent six-electron reduction step, are homologous to NifH and NifD, two key components of the nitrogenase complex, respectively. Since F430 is strictly associated with MCR, at least two genes involved in its biosynthesis, cfbDE, have also been designated as MMPs (**Table 1.2.1**). Variants of F430 have been identified in the active site of MCR from anaerobic methanotrophic archaea (ANME)[47,48] but are not universally conserved across them. While the impact of these variants on the reaction kinetics and reversibility has been modeled in silico[49], their significance in vivo is yet to be determined.

TIGRFAM associated annotation	arCOG[a]	COG	pfam	TIGRFAM	Gene Name	Description	Reference	MA locus tag[b]	numbering system in Borrel et. al. 2019[10]
Mmp1	arCOG02882	COG1944	pfam02624	TIGR03266	YcaO	Involved in thioglycine PTM installation on MCR	[50]	MA0165	20
Mmp2	arCOG00640	COG2144	pfam00586, pfam02769	TIGR03267		Predicted Selenophosphate synthetase-related protein		MA4193	16
Mmp3	arCOG04900	COG4070		TIGR03268		Part of McrC derived "activation complex" of MCR Predicted Peptidyl-prolyl cis-trans isomerase (rotamase), cyclophilin family	[28]	MA3997	4
Mmp4	arCOG00854	COG4002		TIGR03270		Predicted methyltransferase MtxX, phosphotransacetylase family enzyme		MA1806	15
Mmp5	arCOG04903	COG4050	pfam09885	TIGR03271		DUF2112		MA3995	6
Mmp6	arCOG04901	COG4029	pfam09875	TIGR03272		DUF2102		MA3996	5
Mmp7	arCOG03226	COG4052	pfam04609	TIGR03274		Part of McrC derived "activation complex" of MCR McrC like fold	[28]	MA3992	9
Mmp8	arCOG04893	COG4022	pfam09872	TIGR03275		DUF2099		MA0039, MA2220, MA2238	18

Mmp9	arCOG04853	COG4008		TIGR03277		Predicted metal-binding transcription factor		MA0693	25
Mmp10	arCOG00950	COG1625	pfam04055, pfam04459	TIGR03278	Mmp10	Cobalamin-requiring radical SAM methyltransferase that creates the methylarginine PTM on Mcr	[51–53]	MA4551	33
Mmp11	arCOG01116	COG1571		TIGR03280		Predicted DNA-binding protein containing a Zn-ribbon domain		MA1981	17
Mmp12	arCOG04885	COG4020		TIGR03281		Predicted ATPAse/kinase of ASKHA (acetate and sugar kinases, HSC70, actin) superfamily		MA3856	32
Mmp13	arCOG02822	COG0770	pfam08245	TIGR01085	CfbE/MurF	Coenzyme F430 biosynthesis enzyme	[45,46]	MA3630	14
Mmp14	arCOG04866	COG4065	pfam09887	TIGR03285		DUF2114		MA4519	26
Mmp15	arCOG02679	COG1924	pfam01869	TIGR03286		Predicted HSP70-class ATPase domain		MA3994	7
Mmp16	arCOG00621	COG1900	pfam01837	TIGR03287	ComF	CoM synthase	[35]	MA3299	
Mmp17	arCOG04904	COG4051	pfam09886	TIGR03291		Part of McrC derived "activation complex" of MCR	[28]	MA3993	8
	arCOG04857	COG4058	pfam02745, pfam02249	TIGR03256	McrA	MCR subunit alpha		MA4546	1
	arCOG04860	COG4054	pfam02783, pfam02241	TIGR03257	McrB	MCR subunit beta		MA4550	2
	arCOG04858	COG4057	pfam02240	TIGR03259	McrG	MCR subunit gamma		MA4547	3
	arCOG03225	COG4056	pfam04609	TIGR03264	McrC	MCR protein C- related to Mcr activation	[28,54]	MA4548	11
	arCOG04859	COG4055	pfam02505	TIGR03260	McrD	MCR protein D- related to assembly, F430 installation	[29]	MA4549	12
	arCOG03231	COG4069	pfam09890			DUF2117		MA1307, MA1397, MA1297, MA1743	19
	arCOG04847	COG4090	pfam09897			DUF2124		MA1711	21
	arCOG04846	COG4014	pfam09871			DUF2098, part of McrC derived "activation complex" of Mcr	[28]	MA4518	22
	arCOG04902	COG4048	pfam09884			DUF2111		MA4431, MA4362	24
	arCOG03221	COG4063	pfam04208	TIGR01111	MtrA	Tetrahydromethanopterin S-methyltransferase, subunit A	[44,55]	MA0272	27
	arCOG04867	COG4062	pfam05440	TIGR04166	MtrB	Tetrahydromethanopterin S-methyltransferase, subunit B	[44,55]	MA0273	28

	arCOG04868	COG4061	pfam04211	TIGR01148	MtrC	Tetrahydromethanopterin S-methyltransferase, subunit C	[44,55]	MA0274	29
	arCOG04869	COG4060	pfam04207	TIGR01112	MtrD	Tetrahydromethanopterin S-methyltransferase, subunit D	[44,55]	MA0275	30
	arCOG03380	COG4064	pfam04210		MtrG	Tetrahydromethanopterin S-methyltransferase, subunit G	[44,55]	MA0270	
	arCOG04870	COG4059	pfam04206	TIGR01113	MtrE	Tetrahydromethanopterin S-methyltransferase, subunit E	[44,55]	MA0276	31
	arCOG04844	COG4033	pfam08979			DUF1894		MA0129, MA0126	34
	arCOG04845	COG4081	pfam09001			DUF1890		MA0128	35
	arCOG03215	COG4066	pfam09888			DUF2115		N/A	36
	arCOG04894	COG4073	pfam09892			DUF2119		MA2005	37
	arCOG03213	COG4079	pfam09894			DUF2121		MA2311	38
	arCOG00185	COG1123	pfam00005	TIGR03269	atwA/ GsiA	Component A2, ABC family, related to Mcr activation	[28,54,56]	MA3998	10
	arCOG04888	COG2710	pfam00148	TIGR03282	CfbD	Coenzyme F430 biosynthesis enzyme, homolog of NifD	[45,46]	MA3628	13
	arCOG01579	COG4087	pfam00702	TIGR01511		Soluble p-type ATPase (disputed)	[57,58]	MA3999	23

Table 1.2.1 List of methanogenesis marker proteins. Highlighted in green are MMPs specifically mentioned in this chapter. [a]archaeal COG identifier. [b]relevant gene locus in *Methanosarcina acetivorans.*

1.3 MCR-associated proteins involved in the assembly, activation, and catalysis

In recent years, many proteins involved in the assembly and activation of MCR have been characterized, and these can be subdivided into three categories: a) PTM installation, b) assembly, and c) ATP-dependent reductive activation of MCR.

Across methanogens, MCR has a large suite of PTMs that are broadly conserved (1-N-methyl-histidine, thioglycine, and 5-(S)-methyl-arginine) or highly variable (S-methyl-cysteine, 2-(S)-methyl-glutamine, didehydroaspartate, and 6-hydroxy-tryptophan)[51,59]. The enzymes involved in the installation of some of these PTMs were described recently [50,52,60,61]. Two proteins designated as MMP1 and MMP10 install PTMs universally conserved within MCR in methanogens, thioglycine, and 5-(S)-methyl-arginine, respectively (**Table 1.2.1**). Curiously, despite their universal presence, neither of these PTMs was essential for the growth of methanogens under laboratory conditions. Based on these physiological assessments, it is likely that these PTMs tweak the stability of MCR or help coordinate substrates without playing a critical role during catalysis[50,52]. None of the PTMs are surface exposed; it is thus likely that they are installed co-translationally (**Fig 1.3.1A**). This hypothesis is supported by two

lines of evidence. First, assembly intermediates of MCR (apo-MCR) that lack substrates still contain the full suite of PTMs[29]. Additionally, small peptide substrate surrogates have been shown to be modified by PTM installing machinery[53].

After the installation of PTMs, F430 must be loaded into the active site of apo-MCR, and it is likely that McrD plays a role in this process (**Fig 1.3.1A**). Using cryo-electron microscopy (cryo-EM), two McrD-bound asymmetric assembly intermediates were resolved, which completely or partially lack F430. The structure of McrD alone was also independently confirmed by X-ray crystallography[62]. Although these structures indicate a central role for McrD in MCR assembly, it was also shown to be nonessential, indicating that the cell has unknown additional or compensatory ways of installing F430[29]. The dispensability of McrD, as well as the PTMs described earlier, suggests that laboratory growth captures only a sliver of the environmental conditions these microorganisms have encountered through billions of years of Earth history.

Once the active site is loaded, the nickel coordinated by F430 must be reduced to Ni(I) for the enzyme to be catalytically active[63]. All probable catalytic mechanisms for MCR rely on Ni(I) for catalysis to initiate[27] and also regenerate Ni(I) after cycling through either Ni(II) or Ni(III) intermediates. Additionally, the Ni(I) form of MCR is inactivated by unintended oxidation to Ni(II) ($E^{\circ} = -650$ mV)[26]. An elaborate process of incubating cells under 100% H2 or CO[64,65] [27,28] before enzyme purification and treatment of purified enzyme with Ti (III) citrate at high pH (9.0) allows for reactivation of MCR from Methanothermobacter marburgensis in vitro[63]. A structure of this active Ni(I) form of MCR from M. marburgensis was determined very recently[66]. Additionally, there is some evidence that exposure to light in the presence of CoM, CoB, and Ti(III) citrate might activate purified MCR, although the underlying mechanism is not clear[67]. Since Ti(III) citrate or light is not a biologically relevant reducing agent for methanogens, these processes have not elucidated specific proteins that may be relevant to activation in vivo. In 2014, Prakash et al. showed that MCR could be activated by the addition of a putative ATP-binding component A2[56] and a multiprotein fraction containing McrC, called A3a, and ATP[54]. Building on these in vitro activation studies, a cryo-EM structure of an ATP-dependent activation complex of MCR was recently identified (**Fig 1.3.1A**). This complex contains MCR bound to McrC, MMP3, MMP7, MMP17, as well as component A2 and was isolated by affinity-purification of McrC in the methanogen Methanococcus maripaludis[28]. Perhaps the most notable feature of this activation complex is the presence of three putative "L-clusters", or [8Fe-9S-C] clusters, forming a path from the external surface of the complex to F430 in the active site (**Fig 1.3.1A**). Despite the ambiguity of the interstitial carbide, this is the first time an L-cluster-like moiety has been observed in an enzyme family beyond nitrogenases, which strengthens the evolutionary relationship of these two ancient microbial metabolisms. Like the McrD-bound assembly intermediates described above, the activation complex is asymmetric[28], suggesting that both assembly and activation proceed via a two-stroke mechanism, akin to what has been proposed for catalysis[68]. Additionally, the McrA N-terminus in both the assembly and activation structures is unfolded beginning at roughly the same position (**Fig 1.3.1B**).

Despite these recent strides, much work remains to uncover the specific function of each protein found in the activation complex. Additionally, the electron donor for F430 reduction in vivo is still

unknown. While it is proposed that the hydrogenase-based electron bifurcation complex could associate with and participate in the reductive activation of MCR[54], many methanogens, like *Methanosarcina acetivorans*, do not express or encode hydrogenases[69,70]. There may be different electron donor for this process in different methanogens, which further validates the need to study MCR assembly and activation across diverse model methanogens. Additionally, the discovery of intermediates in MCR biogenesis also revives a line of inquiry regarding the localization of MCR within the cell. Earlier work using immunogold labeling led to mixed results — MCR seemed to localize to the membrane in *Methanococcus voltae*[71], but was, at different instances, observed in either the cytosol or membrane of *Methanobacterium thermoautotrophicum*[71,72]. These discrepancies may have arisen from different localization patterns for assembly intermediates, and further investigation into the localization of MCR intermediates using cryo-electron tomography (cryo-ET) tools may elucidate the spatial and temporal nature of such complexes.

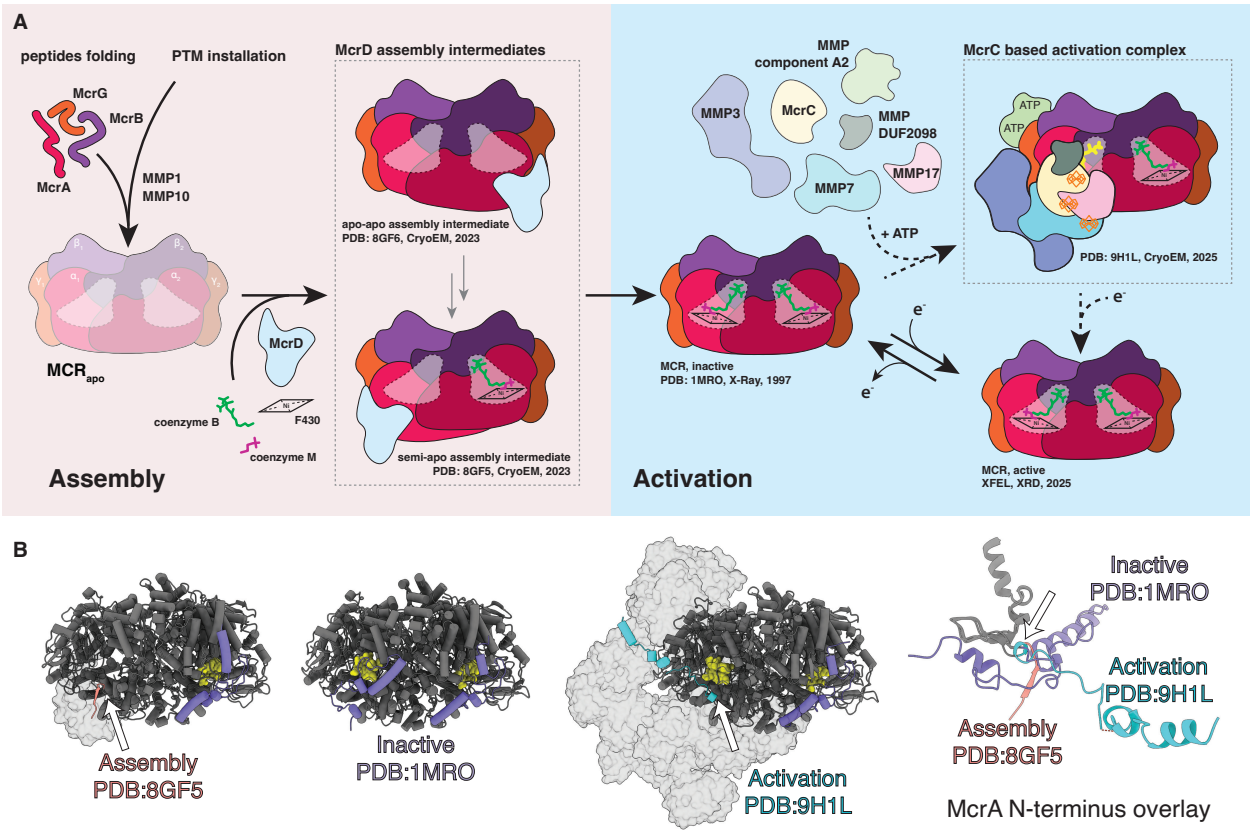

Figure 1.3.1 Assembly and activation intermediates of MCR. (a) All colored protein cartoons represent structures that have been experimentally determined with the relevant PDB (Protein Data Bank) number, method, and year of publication listed. Faded cartoons have not been experimentally determined. Within the active site, coenzyme M (CoM) is in pink, coenzyme B (CoB) is in green, the heterodisulfide of CoM and CoB (CoM-S-SCoB) is in yellow, and F430 is in black. From left to right: MCR folding with co-translational installation of some PTMs with relevant MMPs listed. McrD-based assembly intermediates are shown as the apo-apo form (top) and semi-apo (bottom), where F430, CoM,

and CoB are installed into only one active site at a time to generate the inactive Ni(II) structure of MCR. The transition to the active Ni(I) form has been achieved using chemical reducing agents like Ti(III) citrate, indicated by the introduction of electrons (e-) (lower arrows). An activation complex containing McrC is likely to lead to the same outcome, but this process remains poorly understood. Within the McrC-based activation complex, the three L-cluster-like moieties are depicted in orange. (b) Experimentally determined structures highlighting the unfolding of the McrA subunit N-terminus during assembly and activation. From left to right: McrD-bound assembly complex, inactive MCR, MCR bound to activation complex, overlay of N-terminal regions of McrA. All MCR subunits are depicted in dark gray except for the N-terminal regions of McrA that vary dramatically from one another. The fully resolved N-terminal region found symmetrically in the 1MRO crystal structure is broadly similar to those found in the right side of 8GF5 and 9H1L and is depicted in purple (up to residue L69 in 1MRO). On the left side of the assembly and activation structures where the accessory proteins are bound (transparent surfaces), all of the residues up to that point are colored in pink and teal, respectively. The F430 cofactor is shown in yellow. The point at which the N-terminus unfolds relative to the crystal structure is highlighted with the white arrows and is shown in detail on the right. Note: not all residues corresponding to 1–69 in the crystal structure are resolved in either the assembly or activation structures.

1.4 New tools continue to reveal new facets of MCR biochemistry

Recent advances in our understanding of MCR have been facilitated by the development of new tools to study methanogens. The application of CRISPR-Cas9 gene editing[16] broadened the landscape of genetic manipulations that was accessible in methanogens by allowing for the manipulation of essential genes like MCR[73]. The expansion of the CRISPR-Cas toolbox, with the development of Cas12a-based editing[19,74] and CRISPR interference (CRISPRi)[18,75] further broadens the modes of genetic manipulation. These tools have already proven important by finding back-up pathways for synthesizing key cofactors[35] or determining that highly conserved PTMs of MCR only show phenotypic effects under certain growth conditions[61]. Unbiased genome-wide forward genetic tools, like random bar code transposon-site sequencing (RB- TnSeq)[76,77], could facilitate high-throughput screening of mutants relevant to MCR biochemistry. This screening approach can be deployed to identify backup pathways for genes that are seemingly dispensable or for the discovery of conditionally essential genes needed for MCR function beyond standard laboratory growth, such as in the presence of oxidative stress or nutrient limitation.

Tools to advance imaging of methanogens in recent years may also prove promising to resolve the spatial and temporal dynamics of MCR in vivo. Historically, the use of fluorescent protein tags in methanogens has been challenging given the high autofluorescence of methanogens and that the most common chromophores require oxygen for maturation. FAST (Fluorescence-Activating and absorption-Shifting Tag) is oxygen independent and fluoresces upon binding to a membrane-permeable fluorogenic ligand[78]. The use of FAST-tagged proteins[79] for live cell imaging[78] and flow cytometry[80] opens the door for more precise characterization of in vivo protein–protein interactions and dynamics of protein expression across various genetic backgrounds and growth conditions, which could be applied to the questions posed above regarding interactions between MCR and protein components of

the assembly and activation machinery. The use of a fluorescent reporter could also address questions regarding MCR localization and compartmentalization.

1.5 Conclusions

The work presented in this review highlights the great strides that have been made in our understanding of methane production by MCR. Broadening the scope of proteins essential for MCR biogenesis provides a wider range of targets for the development of specific inhibitors of methanogenesis. Although antimethanogenic feed additives, like Bovear (3-nitroxypropanol or 3-NOP), are being used in commercial agriculture, they have limited efficacy. A cocktail of inhibitors that target different steps in MCR biogenesis may prove to be more efficacious. Additionally, identifying the minimal gene set required to engineer methanogenesis in a heterologous host will be tremendously useful to produce biomethane as a fuel and energy source. Taken together, the current pace of tool development for methanogens with an increasing interest in the fascinating biochemistry of MCR provides a hopeful outlook for the future of the field.

1.5.1 Acknowledgments

We would like to thank members of the Nayak Lab for helpful discussions and for providing comments on this manuscript.

Chapter 2

Component A2 is a redox-sensitive archaeal ATPase activated by methyl-coenzyme M reductase

This chapter zooms in on one piece of the MCR activation complex, component A2. We use both genetic and biochemical techniques to provide the first thorough characterization of this enzyme. We find that component A2 is a bona-fide ATPase that is both oxygen sensitive and modulated by interaction with MCR. We also perform a phylogenetic analysis to determine that component A2 has likely co-evolved with its MCR counterpart, specifically with ACR, and undergone horizontal gene transfer to do so. These findings situate component A2 as a unique archaeal remodeling ATPase involved in the reductive activation of MCR.

Sophia A. Adler[1], Dipti D. Nayak[1,2]*

[1]Department of Molecular and Cell Biology, University of California, Berkeley, CA, USA
[2]Department of Plant and Microbial Biology, University of California, Berkeley, CA, USA

*Address correspondence to: Dr. Dipti D. Nayak (dnayak@berkeley.edu)
This chapter has been submitted as a manuscript and can be found as a pre-print at bioRxiv at the following DOI: https://doi.org/10.64898/2026.03.18.712670

Abstract

Methyl-coenzyme M reductase (MCR) is the primary source of biogenic methane on Earth. In the active site of MCR, a nickel (Ni)-containing porphyrin (F430) must be in the Ni1+ oxidation state to initiate catalysis. The reductive activation of MCR, i.e., reduction of F430 to its Ni1+ state, is an ATP-dependent process, but the underlying ATPase and its precise role remain unknown. Component A2 is an ATP-binding protein that associates with MCR but was reported to lack ATPase activity. Hence, it was proposed to function solely as an ATP-carrier protein. However, recent structural insights into the MCR activation complex suggest that component A2 may hydrolyze ATP to drive conformational changes required for enzyme activation. Here, we provide direct biochemical evidence that component A2 is a bona fide ATPase that hydrolyzes ATP under strictly anaerobic conditions and only upon interaction with MCR. Mutational analyses reveal that component A2 must be bound to ATP prior to association with MCR and that residues involved in ATP hydrolysis do not impact protein-protein interaction. The two nucleotide-binding domains of A2 act cooperatively but display asymmetric contributions to ATP hydrolysis and MCR engagement. In addition, a distinctive N-terminal zinc-binding motif (ZBM) is required for maximal ATPase activity but is dispensable for MCR binding.

Phylogenetic analyses reveal that this ZBM distinguishes component A2 from related ABC-type ATPases. Together, these findings identify component A2 as a distinct class of remodeling ATPases that powers conformational changes underlying the reductive activation of MCR.

2.1 Introduction

Methyl-coenzyme M reductase (MCR)-encoding archaea plays a prominent role in the global methane cycle by catalyzing a reversible reaction shown below[9]:

$$CH_3 - S - CoM + CoB - SH \leftrightarrow CH_4 + CoM - S - S - CoB$$

In methanogenic archaea, MCR mediates the final step of methanogenesis to generate methane. In anaerobic methanotrophic archaea (ANME), MCR activates methane to methyl-coenzyme M, which is the first step in its eventual oxidation to carbon dioxide[59,81]. Despite substantial sequence-level divergence, the overall structure and active site architecture of MCR is extremely well-conserved across archaea[32]. The ~300 kDa MCR heterohexamer is comprised of three subunits arranged in an $\alpha_2\beta_2\gamma_2$ conformation and contains two active sites that are 50 Å apart and proposed to be functionally coupled (Fig. 1)[25,32,82]. Each active site has a non-covalently bound prosthetic group, factor 430 (F430), that is only found in MCR and other members of the alkyl-coenzyme M reductase (ACR) enzyme family[32,59,83,84]. F430 is a Ni-containing tetrapyrrole that must be reduced to its Ni^{1+} oxidation state, through a process known as reductive activation, for MCR to be catalytically active[85–87]. As the mid-point potential of the Ni^{2+}/Ni^{1+} couple is extremely low (between -600 mV and -700 mV relative to a standard hydrogen electrode)[26], the reductive activation of MCR requires many accessory proteins (**Fig 2.1.1**)[28,88]. In the absence of these proteins, the Ni atom in F430 gets rapidly oxidized to Ni^{2+} and MCR becomes catalytically inactive, even when purified under anaerobic conditions[89].

For nearly fifty years it has been known that the reductive activation of MCR is an ATP-dependent process, but the underlying reason is not clearly understood. In 1979, Gunsalus and colleagues showed that *Methanothermobacter thermoautotrophicus* cell extracts required trace amounts of ATP for methane production from methyl-coenzyme M and estimated that ~1 mol of ATP was required for ~15 mols of methane produced[90]. Subsequently, Rouvier et al. isolated an ATP-binding protein, designated as component A2 or AtwA, that was required for optimal methane production by cell extracts of *M. theroautotrophicus*[91]. Initial reports indicated that component A2 is a soluble, colorless, air-tolerant protein of the ABC-type ATPase family that lacks any detectable ATP hydrolysis activity[91,92]. Component A2 could not perform electron transfer either to or from common electron carriers like FAD, NAD, NADP, or F_{420}[91]. Based on these analyses, component A2 was designated as an ATP-carrier protein[90–92] that delivers ATP to another enzyme, often speculated to be a homolog of the dinitrogenase reductase (NifH)[54], which can hydrolyze ATP and transfer electrons to F430 for the reductive activation of MCR. However, NifH homologs have not, to our knowledge, been shown to copurify with MCR even though they are universally conserved in MCR-encoding archaea[45,46].

Recently, a cryo-EM structure of the MCR activation complex shed new light on the putative function of component A2[28]. The MCR activation complex contains component A2 bound asymmetrically to one γ subunit (McrG). In addition, the MCR activation complex also contains McrC and other methanogenesis marker proteins (MMPs) – Mmp3, Mmp7, and Mmp17 – that coordinate three complex Fe-S clusters, which closely resemble the [8Fe-9S-C] L clusters involved in the maturation of nitrogenases (**Fig 2.1.1**). Even though component A2 does not interact directly with McrC and the MMPs in the activation complex, it is postulated to stabilize the N-terminal "latch" of the α subunit (McrA) to make the active site more accessible for electron transfer to F430 through the putative L clusters. To this end, Ramirez-Amador and colleagues showed that addition of ATP stabilizes the MCR activation complex and postulated that this occurs through structural rearrangements that occur when component A2 hydrolyzes ATP. This hypothesis directly contradicts previous biochemical evidence that component A2 is merely an ATP-carrier protein. Furthermore, since component A2 is bound to ATP —not ADP — in the activation complex, it is still plausible that it delivers ATP to another ATPase domain protein, like MMP15, that could transiently associate with the activation complex, making it difficult to capture structurally[93].

Here, we resolve a longstanding conundrum regarding the role of component A2 in the reductive activation of MCR by complementary in vivo and in vitro analysis of the protein from *Methanosarcina acetivorans*. Our results show that component A2 is a bona fide ATPase that hydrolyzes ATP only upon interaction with MCR under anaerobic conditions, and that interaction with MCR is predicated on A2 first binding ATP. In addition, our evolutionary analyses indicate that component A2 belongs to a unique class of redox-active remodeling ATPases that have co-evolved with members of the ACR family within archaea.

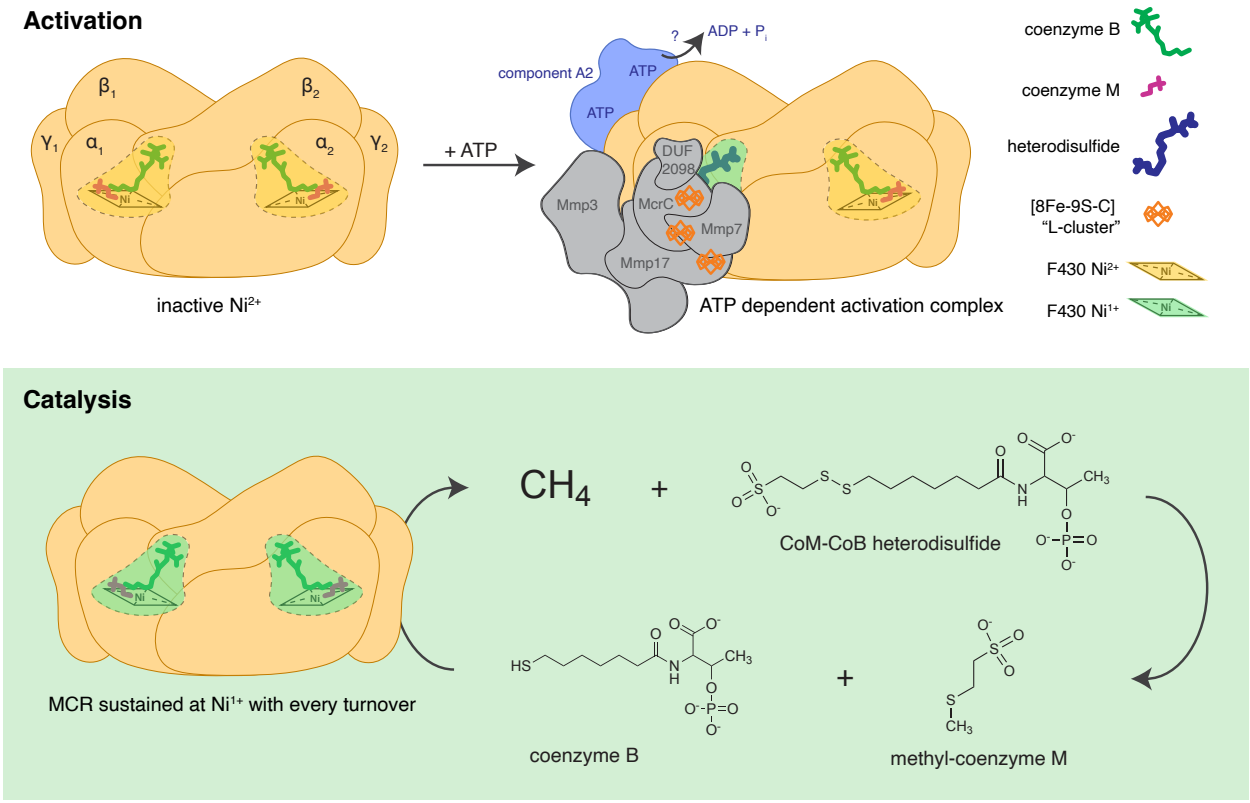

Figure 2.1.1 Cartoon depicting the reductive activation and catalytic activity of MCR. (Top) Reductive activation of MCR is an ATP-dependent process. Component A2 (light blue) and other methanogenesis marker proteins or MMPs (gray) are required to generate the Ni^{1+} form of F430 (green) for activation of MCR from its Ni^{2+} oxidation state (yellow) to its Ni^{+1} oxidation state (green). (Bottom) The reaction catalyzed by MCR requires an external input of electrons for the reduction of the methyl-group in methyl-coenzyme M to methane, which is provided by coenzyme B. The Ni^{1+} form of F430 is regenerated at the end of each reaction cycle so ATP-dependent activation is not required for each molecule of methane generated.

2.2 Results

2.2.1 Component A2 is essential and constitutively expressed in Methanosarcina acetivorans

In *M. acetivorans*, component A2 is encoded by MA_3998 (MA_RS20860) and is found in the vicinity of six genes encoding methanogenesis marker proteins (MMPs) (**Fig 2.2.1.1A**), some of which have also been implicated in the activation of MCR (**Fig 2.2.1.1B**) and all of which are highly conserved across genomes containing MCR/ACR[28,94]. Component A2 and these six others neighboring MMPs are often referred to as the MCR activation operon, but it is unclear if these genes are co-transcribed and the degree to which they are expressed. First, to test if component A2 is in an operon with the other six MMPs (shown in **Fig 2.2.1.1A**), we extracted RNA from *M. acetivorans* and performed RT-PCR with primers that span intergenic regions across the putative operon as shown in **Fig S2.1A**. We were able to

observe PCR products for all the intergenic regions tested, which experimentally validates that these seven genes are, indeed, organized as an MCR activation operon (**Fig S2.1A**). Next, we mapped RNA-sequencing reads from previous transcriptomics experiments with *M. acetivorans*[73,95,96] to the MCR activation operon. The average expression of the MCR activation operon does not vary significantly across growth substrates and remains unchanged in response to MCR-limitation (**Fig S2.1B and C**). The read depth and coverage of the MCR activation operon is ~40-fold lower than the MCR operon (*mcrBDCGA*) (**Fig 2.2.1.1C**, **Fig S2.2**). Taken together, these data suggest that component A2 is part of the MCR activation operon, which is constitutively expressed at much lower levels than MCR operon in *M. acetivorans.*

Based on their proposed function, component A2 and other genes in the MCR activation operon are likely to be essential in methanogens, but this hypothesis, to the best of our knowledge, has not been explicitly tested. To test the essentiality of the MCR activation operon, we designed CRISPR-editing plasmids to generate in-frame chromosomal deletions of each gene individually[16]. For component A2, transformation of the CRISPR-editing plasmids did not produce any viable colonies (**Fig S2.3**). For the rest of the genes- Mmp5, Mmp6, Mmp17, Mmp7, Mmp3, and Mmp15- in the MCR activation operon, a few antibiotic-resistant transformants were detected (**Fig S2.3**). However, PCR with primers flanking the gene of interest revealed either a mixed population of the wildtype (WT) and the mutant allele or only the WT allele, suggesting that genome editing was either incomplete or unsuccessful, respectively (**Fig S2.3**). A similar observation was also made in recent attempts to delete *nifB*[97], another essential gene in *M. acetivorans*. Altogether, we were unable to successfully delete component A2 or any of the neighboring MMPs in *M. acetivorans,* which corroborates their proposed role in the activation of MCR, an enzyme essential for growth and viability.

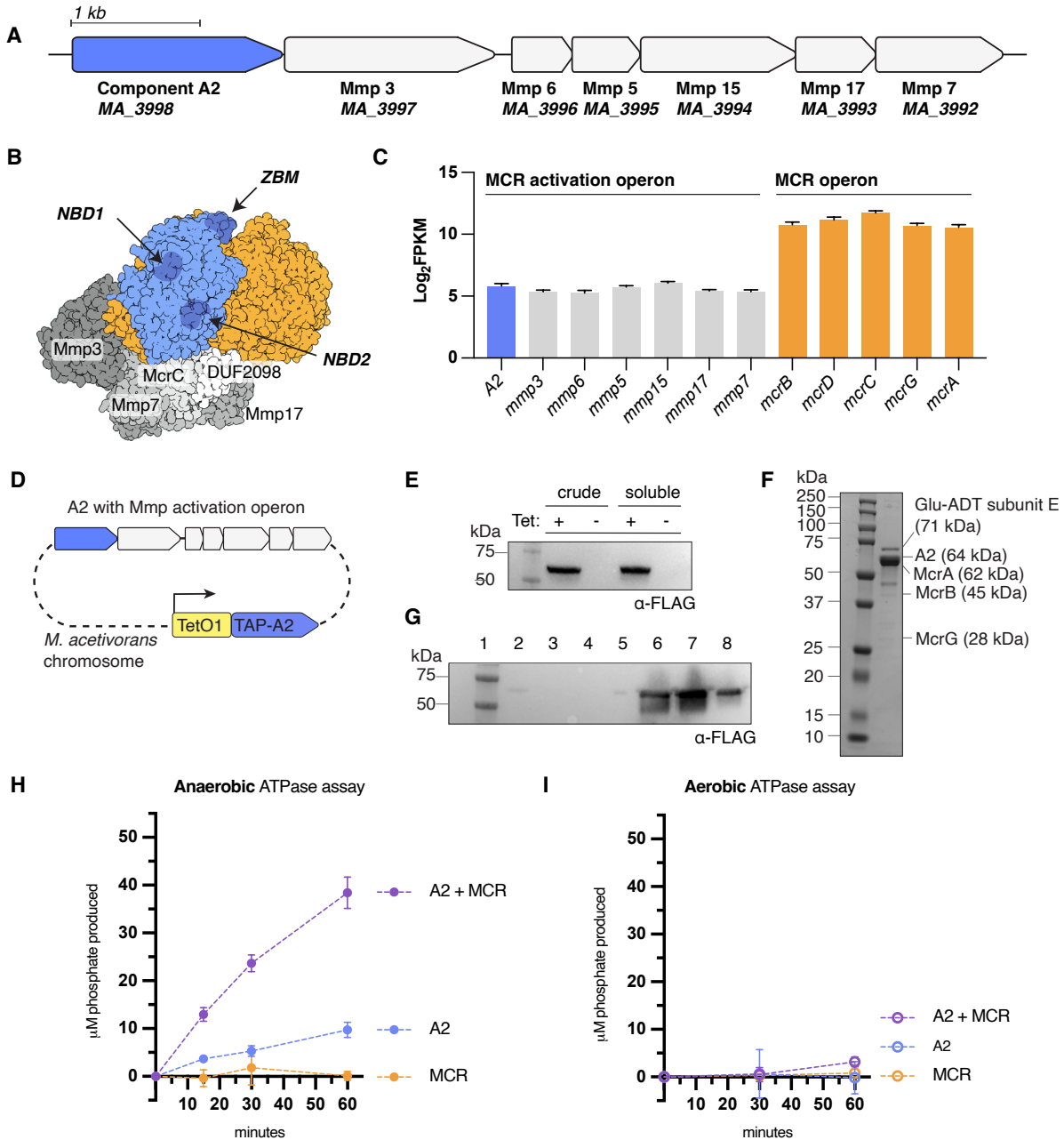

Figure 2.2.1.1 Component A2 is an oxygen-sensitive ATPase that hydrolyzes ATP upon interaction with MCR. (a) Genomic arrangement of the MCR activation operon in *M. acetivorans* with scale bar depicting 1 kilobase pair. (b) Structure of the putative MCR activation complex (PDB: 9H1L) with MCR in orange, component A2 (with relevant domains highlighted) in blue, and the other methanogenesis marker proteins in gray. NBD refers to Nucleotide Binding Domain and ZBM refers to Zinc Binding Motif. (c) Log_2 transformed FPKM (Fragments Per Kilobase of transcript per Million mapped reads) of the MCR activation operon and the MCR operon in *M. acetivorans* grown in high-salt (HS) minimal medium supplemented with trimethylamine (TMA) at 37 °C. (d) Genotype of an *M. acetivorans* strain expressing a second copy of component A2 in trans under the control of a tetracycline inducible promotor. (e) Anti-FLAG immunoblot showing the inducible production of component A2

upon the addition of 100 μg/mL tetracycline (tet) to the growth medium in crude and soluble cell lysates with 13.9 μg total protein loaded into each lane. (f) Anti-FLAG immunoblot of aerobic affinity-purification of A2 with a Streptactin resin. The lanes represent the following: (1) ladder, (2) cell lysate, (3) flow-through, (4) first wash, (5) second wash, (6) first elution, (7) second elution, and (8) third elution. (g) SDS-PAGE gel showing anaerobic purification of full-length TAP-tagged component A2 (64 kDa with tag). (h) Anaerobic ATPase assay of component A2 alone (blue), MCR alone (purple), and component A2 combined with MCR (orange). Each reaction contained 500 μg/mL of each protein indicated with 200 μM ATP, 10 mM MgCl2, 20 mM HEPES, 300 mM NaCl, and 1% glycerol. Reactions were incubated at 37 °C. Inorganic phosphate production was measured at 0, 15, 30, and 60 minutes using the malachite green reagent. (I) Aerobic ATPase assay of component A2 alone (blue), MCR alone (purple), and component A2 combined with MCR (orange). Proteins were purified anaerobically then removed from the anaerobic chamber and reactions were set up on the bench top. The same assay conditions as (c) were used, but time points were taken at 0, 30, and 60 minutes. Error bars represent the standard deviation of three technical replicates for each reaction.

2.2.2 *Component A2 hydrolyzes ATP after interacting with MCR under anaerobic conditions*

Since the native component A2 locus is essential and constitutively expressed at low levels in *M. acetivorans* (**Fig 2.2.1.1C**), we generated a strain to overexpress it in trans for facile purification and biochemical characterization of its proposed function (**Fig 2.2.1.1D**). Expressing component A2 in trans also allowed us to study catalytically inactive mutants as the chromosomal locus retained its original function, which, as noted above, appears to be essential for cell viability. To this end, we fused a **t**andem-**a**ffinity **p**urification (TAP) tag, comprised of a Twin-Strep-1X-FLAG sequence, at the N-terminus of component A2 and expressed it under the control of the P*mcrB*(tetO1) tetracycline inducible promoter in the pJK027A vector backbone[17]. We chose to add a TAP tag the N-terminus of component A2 as it is far from the interaction interface with MCR and is also known to not disrupt ATP-binding[28,54]. The resulting plasmid (pSAA004) was integrated in the chromosome of *M. acetivorans* (WWM73) at the φC31 attachment site as described previously[17]. Whole genome sequencing was performed to verify the genotype of the strain used for protein purification (**Table S2.1**) and the production of TAP-tagged component A2 was detected by immunoblotting against the FLAG-tag when expression was induced with 100 μg/mL tetracycline (**Fig 2.2.1.1E**). Overexpression of component A2 did not lead to an observable growth defect, which indicated that elevated levels of this protein are not toxic or lethal to *M. acetivorans* (**Fig S2.4**). Anaerobic affinity purification of TAP-tagged component A2 yielded colorless, soluble, full-length protein of ~ 64 kDa (**Fig 2.2.1.1F and G**). In addition to component A2, we observed nine additional bands that either correspond to McrB, McrG or degradation products of component A2 itself (**Fig 2.2.1.1F** and Table S2). A band corresponding to Glutamyl-tRNA(Gln) amidotransferase subunit E (**Table S2.2**) was observed in all protein preparations of component A2 (even the mutant forms; see below) hence was not considered to impact any of the data presented here. Since McrA is the same size as component A2, we used an anti-McrA antibody to confirm that it also copurifies with this protein (**Fig S2.5E**). A reverse pulldown with TAP-tagged MCR (**Fig S2.5C**) confirmed the interaction between component A2 and MCR (**Table S2.3**).

While it is well established that component A2 binds ATP[28,91,98], it is unclear if its role in the

context of MCR activation is to serve as an ATP carrier for an alternate ATPase or to perform ATP hydrolysis by itself[54]. To disentangle these two hypotheses, we explored if component A2 can hydrolyze ATP in isolation or in conjunction with MCR using the Malachite green assay to quantify free inorganic phosphate (P_i) produced during the process (see more details in the Materials and Methods section). When component A2 was purified under anaerobic conditions, we detected robust ATPase activity, ~ 38 nmol Pi released/mg protein after 60 minutes of incubation for three independent preparations (**Fig 2.2.1.1H**, **2.2.3.1J**). In contrast, when we purified component A2 under aerobic conditions, no free Pi was detected under the same conditions (**Fig S2.5F**). To rule out the possibility that the ATP hydrolysis in anaerobic preparations of component A2 was due to co-purifying contaminant(s), we assayed the ATPase activity of anaerobically prepared A2 after air exposure. Treatment with air and oxic buffers abolished ATPase activity (**Fig 2.2.1.1I**), which suggests that component A2 is an oxygen-sensitive protein and can only hydrolyze ATP under reducing conditions.

Next, we tested if the addition of MCR impacts ATP hydrolysis by component A2 in vitro. Anaerobic preparations of MCR from stationary-phase cultures of M. acetivorans had no detectable ATPase activity whereas ATP hydrolysis was observed in MCR preparations from exponential-phase cultures, likely because component A2 copurifies with it (**Fig S2.5H**). Hence, we only used MCR derived from stationary-phase cultures to test its impact on ATPase activity of component A2 (**Fig 2.2.1.1H**). The addition of an equal amount of MCR by weight to component A2 increased its ATPase activity under anaerobic conditions by 2.2-fold (**Fig 2.2.1.1H**, **2.2.3.1J**, and **Fig S2.5G**). In contrast, no detectable ATPase activity was observed when MCR was added to component A2 under aerobic conditions (**Fig 2.2.1.1I**). These data are consistent with the hypothesis that the ATPase activity of component A2 alone is due to the small amount of MCR that copurifies with it, which is further enhanced by the addition of MCR. Taken together, our in vitro analyses suggest that component A2 is a redox-sensitive ATPase that hydrolyzes ATP only after it interacts with MCR.

2.2.3 At least one nucleotide-binding domain and the zinc-binding motif are important for ATP hydrolysis by component A2

Component A2 from *M. acetivorans* contains two nucleotide binding domains (NBDs) as well as a $CXXCX_{12}CXXC$ Zn^{2+}-binding motif (ZBM) (**Fig 2.2.3.1A-C**). The two NBDs are highly conserved in component A2 sequences across archaea and each of them contains a Walker A motif (GxxGxGK[T/S]) and Walker B motif (hhhhDE) (**Fig 2.2.3.1A and B**). The lysine residue (K) of the Walker A motif is known to be critical for ATP-binding[99], and the glutamate residue (E) of the Walker B motif deprotonates water in the first step of ATP hydrolysis and is essential for catalysis[100]. To eliminate ATP-binding, we mutated the lysine residues in the two Walker A motifs to alanine by generating a K43A/K329A double point mutant of component A2. To specifically abolish ATPase activity, without impacting ATP-binding, we generated a E200A/E459A double point mutant of component A2. Additionally, we generated single point mutants, K43A, K329A, E200A, and E459A, to determine if catalytic activity is dependent on both NBDs and if the two NBDs act asymmetrically. All point mutants were expressed and purified from *M. acetivorans* using the strategy described for the WT allele in **Fig 2.2.2.1** (*F*igs. S6-S8).

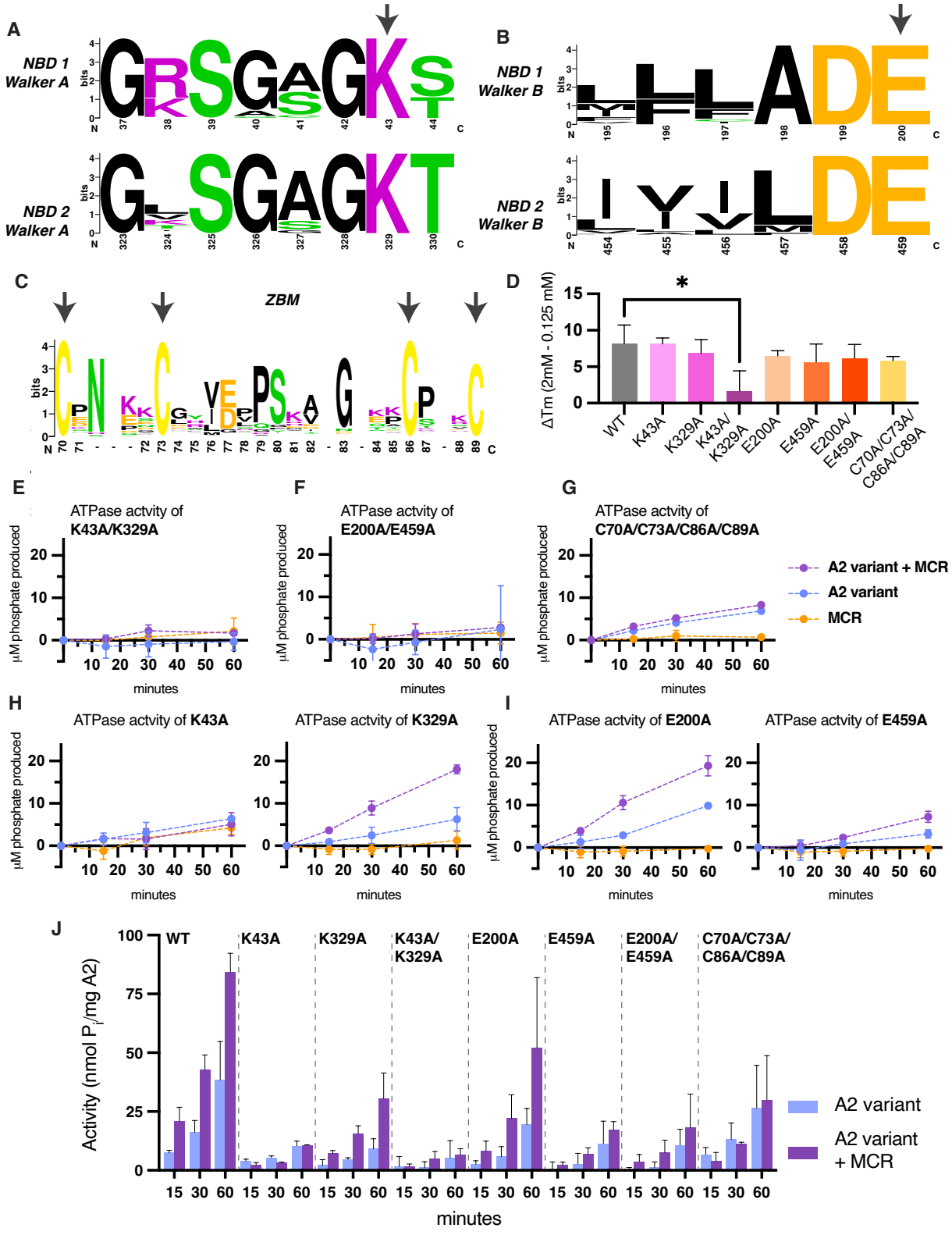

Figure 2.2.3.1 Nucleotide binding domains (NBDs) and zinc binding motif (ZBM) of component A2 are highly conserved and disrupt ATPase activity. (a-c) Sequence alignment of 888

component A2 sequences assigned to HMM (Hidden Markov Model) TIGR03269. The x-axis indicates position number in *Methanosarcina acetivorans*. Arrows indicate the (a) mutated residues K43 and K329, (b) D200 and D459, and (c) C70, C73, C86, and C89. (d) Change in melting temperature (ΔTm) of component A2 variants in buffer with 2 mM ATP versus 125 μM ATP. Error bars represent standard deviation of the mean ΔTm of three independent preparations of the protein (except for E200A and E459A, which represent the data for two and four protein preparations, respectively) and Welch's unpaired t-test was performed to assess statistical significance; * indicates P-value < 0.05. (e-i) Anaerobic ATPase assay of each indicated component A2 variant (blue), MCR alone (orange), and the component A2 variant combined with MCR (purple). Each reaction contained 500 μg/mL of each protein with 200 μM ATP, 10 mM $MgCl_2$, 20 mM HEPES, 300 mM NaCl, and 1% glycerol. Reactions were incubated at 37 °C. Inorganic phosphate production was measured at 0, 15, 30, and 60 minutes using malachite green reagent. Error bars represent the standard deviation of three technical replicates. (j) ATPase activity for each component A2 variant alone and upon addition of MCR. Error bars represent the standard deviation of three independent preparations of each variant of A2, except C70A/C73A/C86A/C89A for which only two independent preparations were performed.

To validate the proposed role of each of these NBD residues, we performed differential scanning fluorimetry (DSF) (or thermal shift assays) in the presence of low (0.125 mM) or high (2 m) concentrations of ATP in the buffer[101]. All DSF assays were performed aerobically with anaerobically purified enzyme, and the first differential of the melt curve had a single, major peak, which we infer corresponds to the melting temperature ('Tm') of component A2 (**Fig 2.2.3.1D** and **Fig S2.9**). Switching from low to high ATP concentrations in the buffer increased the Tm (referred to as the ΔTm) of all mutants of components A2 by > 5.0 °C, apart from the K43A/K329A double mutant (**Fig 2.2.3.1D** and **Fig S2.9**). These data suggest that ATP-binding stabilizes component A2 and that the K43A/K329A double mutant, as expected, does not experience this shift in Tm because it cannot bind ATP. Like the NBDs, the $CXXCX_{12}CXXC$ ZBM is highly conserved across all component A2 sequences too (**Fig 2.2.3.1C**), which suggests that it is functionally relevant. To test the role of the ZBM, we generated a C70A/C73A/C86A/C89A mutant. The ZBM mutant was stabilized by the presence of ATP in the buffer (**Fig 2.2.3.1D**), which indicates that it can still bind ATP.

Next, we measured the anaerobic ATPase activity of all the point mutants either by themselves or in the presence of an equal amount of MCR by weight. The K43A/K329A double mutant produced <6 nmol Pi/mg protein after 60 minutes of incubation, which did not increase upon the addition of MCR (**Fig 2.2.3.1E, J,** and **Fig S2.10A**). ATP hydrolysis was similarly attenuated in the E200A/E459A mutant (**Fig 2.2.3.1F, J** and **Fig S2.10B**). The C70A/C73A/C86A/C89A mutant had ~50% activity of the WT by itself, which did not increase upon the addition of MCR (**Fig 2.2.3.1G, J,** and **Fig S2.10C**). These data suggest that the NBDs are essential whereas the ZBM is critical for optimal ATPase activity.

To test if the two NBDs work synergistically or independently, we assayed the ATPase activity of the single point mutants. While neither single mutant behaved like WT, the K329A mutant had ~ 2.9 times higher activity than the K43A mutant in the presence of MCR (**Fig 2.2.3.1H, J,** and **Fig S2.11A-B**). Similarly, the E200A mutant had ~ 3 times higher activity than the E459A mutant (**Fig 2.2.3.1I, J,**

and **Fig S2.11C-D**). These data suggest that the NBDs have an asymmetric but synergistic contribution to ATP hydrolysis.

2.2.4 Only ATP-bound component A2 can interact with MCR

There are two models for ATP hydrolysis by the component A2-MCR complex that are equally consistent with the activity data noted above. One is that component A2 binds ATP first, ATP-bound component A2 interacts with MCR, and then ATP hydrolysis occurs (**Fig 2.2.4.1A**). Alternately, component A2 binds MCR first, ATP binds to the component A2-MCR complex, which is followed by hydrolysis (**Fig 2.2.4.1A**). To distinguish between these two possibilities, we leveraged DSF to observe complex formation between component A2 and MCR either in the presence or absence of different adenine nucleotides. All DSF assays were performed aerobically with anaerobically purified enzyme, so that the interaction between component A2 and MCR could be decoupled from ATP hydrolysis. In the presence of ATP, the first differential of the melt curve for component A2 and MCR individually showed a single peak at 45.5 ± 1.3 °C and 67.2 ± 0.8 °C respectively, which corresponds to the Tm of these two proteins (**Fig 2.2.4.1B, C,** and **Fig S2.12A-B**). When component A2 and MCR are combined in the presence of ATP, a third peak at 60.8 ± 0.6 °C appears in the melt curve (**Fig 2.2.4.1D** and **Fig S2.12C**). We interpret that this third peak corresponds to the Tm of the complex of component A2 and MCR. This third peak is absent when MCR and component A2 are combined in the absence of ATP or in the presence of ADP (**Fig 2.2.4.1D, E,** and **Fig S2.12D-F**). All tested concentrations of ATP showed some presence of this component A2-MCR peak (**Fig 2.2.4.1E** and **Fig S2.12G**). In contrast, a peak corresponding to the component A2-MCR complex was not detected regardless of the [ADP] (**Fig 2.2.4.1E** and **Fig S2.12H**).

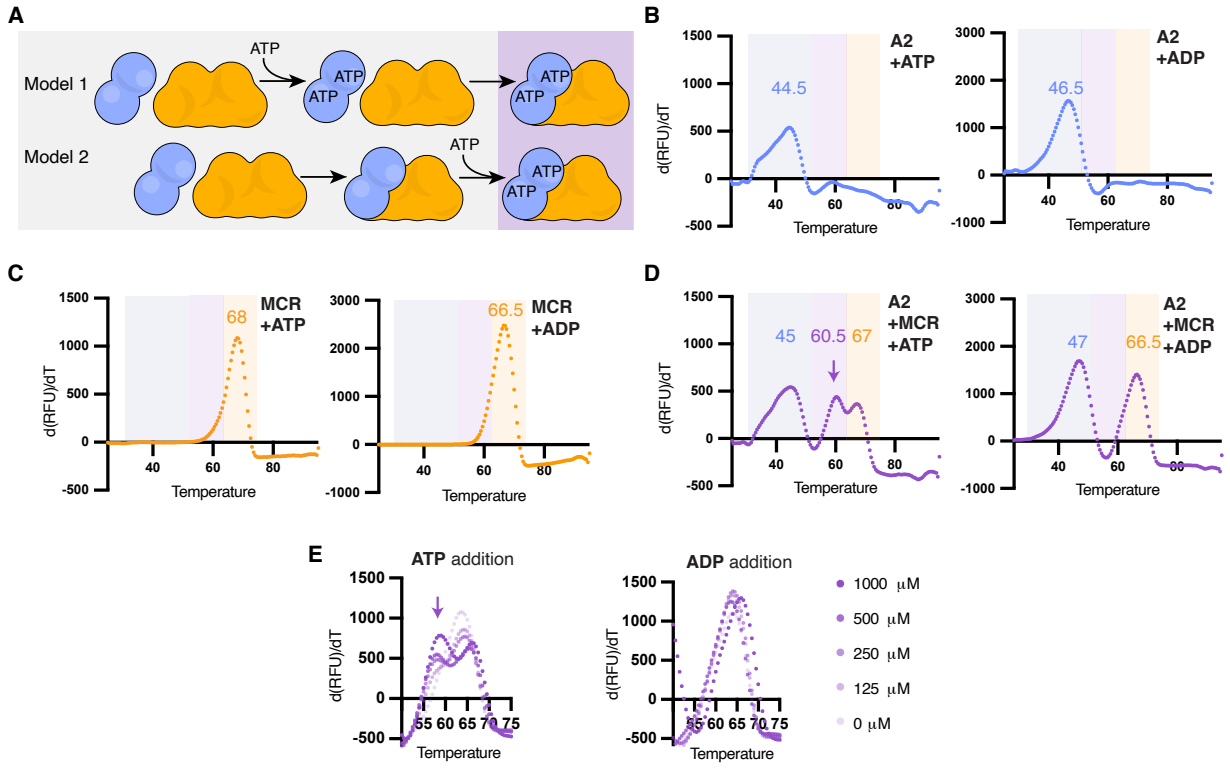

Figure 2.2.4.1 Only ATP-bound component A2 can interact with MCR. (a) Cartoons showing two models of ATP-based interaction between component A2 and MCR. In Model 1, component A2 (blue) binds MCR (in orange) and the component A2-MCR complex interact with ATP. In Model 2, component A2 is bound to ATP (in blue) prior to engagement with MCR (in range). (b-d) Differential scanning fluorimetry (DSF) of (b) component A2, (c) MCR, and (d) component A2 combined with MCR. Samples contained 2 mM ATP (left panel) or ADP (right panel), 10 mM $MgCl_2$, 20 mM HEPES, 300 mM NaCl, and 1% glycerol. (e) DSF of component A2 combined with MCR with increasing concentrations as indicated of ATP (left) or ADP (right) and the same assay conditions as (b-d). The peak corresponding to the component A2-MCR complex (purple arrow) only appears in the presence of ATP. All samples in panels b-e contain 0.5 mg/mL of each protein indicated.

AlphaFold[102] predicted structures of apo-component A2 compared to the ATP- and ADP-bound versions reveal significant conformational changes (**Fig S2.13**). Additionally, the AlphaFold predicted structure of ATP-bound component A2 is in high agreement with the MCR-bound component A2 from the activation complex[28] (**Fig S2.13E**). These structural predictions further support our model that only ATP-bound component A2 can interact with MCR (see **Fig 2.2.4.1A**).

2.2.5 A catalytically dead component A2 can still interact with MCR

Based on our model so far, mutations in the Walker A motif of the NBDs that disrupt ATP-binding in component A2 would abolish interaction with MCR. However, whether the Walker B motif of the NBD or the ZBM contributes to the interaction between component A2 and MCR is not as intuitive. To test the role of each of these motifs in MCR interaction, we assessed the amount of MCR

that copurifies with each component A2 mutant by immunoblotting against a previously described anti-McrA antibody[73]. As expected, the K43A/K329A double mutant, which cannot bind ATP, copurifies with practically no MCR compared to WT (**Fig 2.2.5.1A** and **Fig S2.14**). However, each of the single mutants (K43A and K329A) could still interact with MCR but to slightly lesser degree than WT. The E459A, E200A/E459A and C70A/C73A/C86A/C89A mutants co-purified with similar amounts of MCR as WT (**Fig 2.2.5.1A** and **Fig S2.14**). However, the E200A mutant had diminished interaction with MCR, like the K43A and K329A mutants. To further corroborate these findings, we performed DSF assays of each of these mutants alone and with MCR in the presence of ATP. No evidence of the component A2-MCR complex could be detected when the K43A/K329A mutant was combined with MCR in the presence of ATP (**Fig 2.2.5.1B** and **Fig S2.15A**). In contrast, a peak corresponding to the Tm of the component A2-MCR complex was observed for all the other mutants (**Fig 2.2.5.1C-H** and **Figs S15 and S16**). These data indicate that the interaction between MCR and component A2 is dependent on ATP-binding but not linked to ATP hydrolysis.

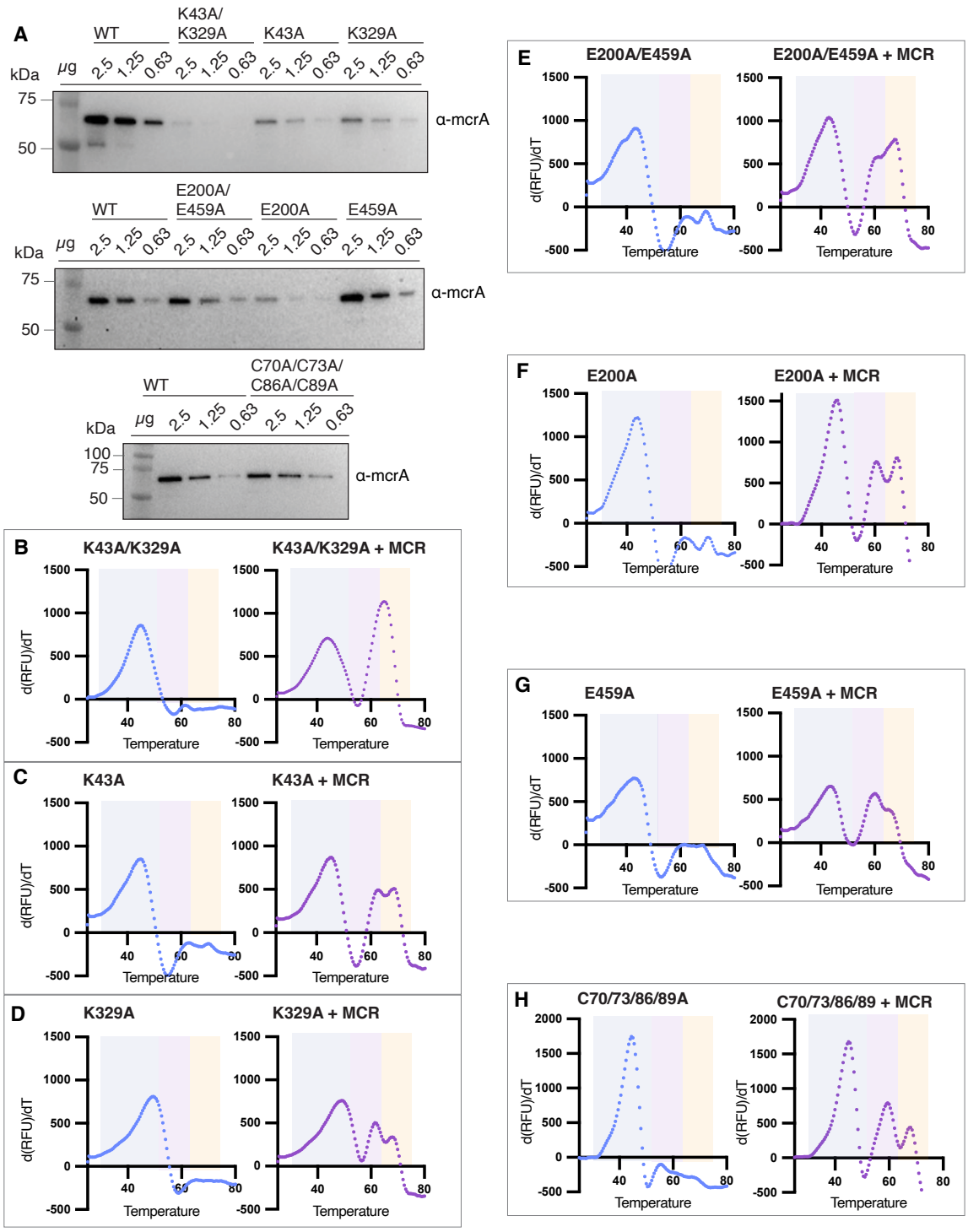

Figure 2.2.5.1 Interaction of MCR and component A2 is not coupled to ATP hydrolysis. a) Immunoblots with anti-McrA specific antibodies to evaluate the amount of MCR that copurifies with variants of component A2: K43A/K329A, K43A, and K329A (top), E200A/E459A, E200A, and E459A (middle) and C70A/C73A/C86A/C89A (bottom). Each blot shows a 2X dilution series for each

indicated protein starting at 2.5 μg. (b-h) Differential scanning fluorimetry (DSF) of component A2 variants alone (left) or combined with MCR (right). Peaks with a blue background correspond to component A2, with an orange background correspond to MCR, and with a purple background correspond to component A2-MCR complex. Samples contained 2 mM ATP, 10 mM $MgCl_2$, 20 mM HEPES, 300 mM NaCl, 0.5 mg/mL of each indicated protein, and 1% glycerol.

2.2.6 Component A2 has co-evolved with members of the alkyl-coenzyme M reductase (ACR) superfamily

To study the evolutionary history of component A2, we built a phylogenetic tree using 80 sequences that capture the sequence diversity of the protein as well as the taxonomic breadth of archaea that encode them (**Fig 2.2.6.1**, Dataset 1). Many archaea, including *M. acetivorans,* also encode a component A2 homolog that contains both NBDs but lacks the ZBM, and we designated these proteins as the outgroup to root the component A2 tree. The phylogeny of component A2 is not consistent with vertical inheritance and indicates that it has undergone rampant HGT within archaea. For example, component A2 sequences from archaea within the Halobacteriota can be found in at least 8 distinct clades that have a bootstrap support of 100 (**Fig 2.2.6.1**). *Methanoliparia* encode both MCR and ACR[103] and two distantly related component A2 sequences. Each component A2 sequence from *Methanoliparia* either clusters with sequences derived from archaea that encode MCR or ACR. Methanogens that encode multiple MCR isozymes[104] (members of the Methanobacteriota) only encode one component A2 (Dataset 1) and there are no obvious distinctions between the component A2 sequences derived from ANME and methanogens either. Altogether, these observations suggest that the MCR-specific component A2 is likely to be compatible with all MCRs but not with ACRs and vice versa. Finally, even though component A2 sequences from ACR-encoding archaea are more closely related to each other than to their counterparts from MCR-encoding archaea (**Fig 2.2.6.1**), they do not form a highly divergent monophyletic clade like ACRs do relative to MCR[83]. This is likely because all component A2 sequences perform the same core function of ATP hydrolysis regardless of which ACR they associate with, in contrast with the significant sequence divergence ACR has undergone to accommodate divergent substrates.

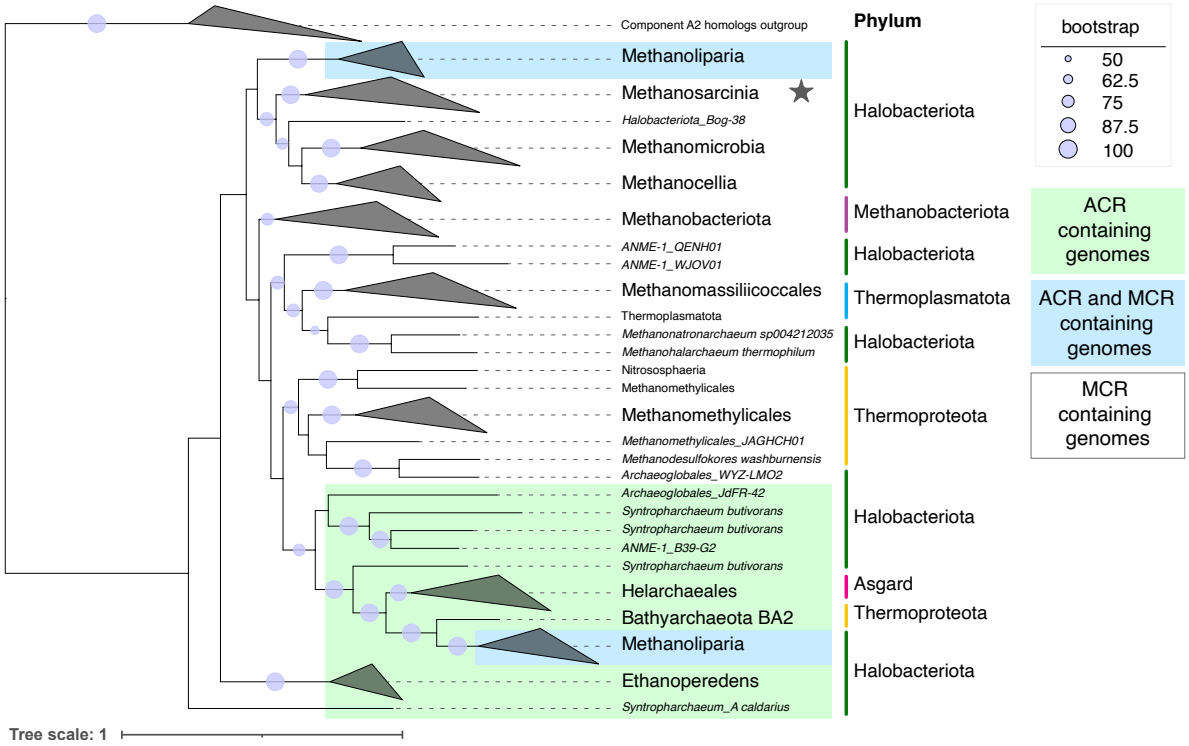

Figure 2.2.6.1 Phylogenetic analysis of component A2 across alkyl-coenzyme M reductase (ACR)-encoding archaea. Phylogenetic tree of component A2 amino acid sequences derived from genomes encoding alkyl coenzyme-M reductase (ACR) in green, methyl-coenzyme M reductase (MCR) in white, and both in blue. All 888 protein sequences with the TIGRFAM Hidden Markov Model (HMM) TIGR0326 assigned to component A2 were obtained from the Genome Taxonomy Database (GTDB) R214. These sequences were clustered at 70% sequence similarity and any truncated sequences or sequences with large insertions (as described in the Methods) were removed, which resulted in a final set of 80 component A2 sequences. The outgroup comprises of 20 sequences of a component A2 homolog lacking a zinc-binding motif (ZBM) that was identified using the sequence from *M. acetivorans* (MA_3967 or MA_RS20695) as a search query. The clade containing the component A2 sequence from *M. acetivorans* is indicated by a star.

2.3 Discussion

In this study, we established an over-expression system in *M. acetivorans* to experimentally evaluate the role of component A2 in the reductive activation of MCR. Many hypotheses regarding the role of component A2 have been made with protein purified from *E. coli* or from indirect measurements using methane production rates as a proxy for ATPase activity. We suspect that the use of heterologously produced protein and an insensitive assay technique have led to confounding results for decades. By directly measuring Pi production by component A2 derived from *M. acetivorans*, we show that this enzyme is a bona fide ATPase, whose activity is dependent on redox conditions (**Fig 2.2.2.1H and I**)

and is modulated by its association with MCR (**Fig 2.2.2.1H**). Even though both NBDs of component A2 are required for interaction with MCR and for optimal ATP hydrolysis they are not functionally equivalent (**Fig 2.2.3.1E-J**). Mutations in the Walker B motif of NBD2 impede ATP hydrolysis far more than mutations in the Walker B motif of NBD1 (**Fig 2.2.3.1I**). In contrast, mutations in the Walker B motif of NBD1 substantially lower component A2-MCR interactions whereas mutations in the Walker B motif of NBD2 do not affect protein-protein interaction at all (**Fig 2.2.5.1A**). We hypothesize that the universally conserved ZBM renders component A2 redox-sensitive (**Fig 2.2.3.1C**). It is quite likely that the ZBM acts as a "redox-switch" where reduced cysteine residues bind Zn^{2+} and oxidation of these residues reduces rates of ATP hydrolysis (**Fig 2.2.3.1G**)[105]. This redox switch in component A2 might ensure that the reductive activation of MCR only occurs under environmental conditions that are conducive for catalysis, i.e., in the absence of oxygen or other oxidants.

The evolutionary ties between the maturation machinery for nitrogenases and MCR have been discussed previously[28] but are worth revisiting considering our findings. While nitrogenases requires ATP hydrolysis for electron transfer during catalytic turnover[106], MCR requires ATP input only for cofactor reduction during enzyme maturation. Thus, the net demand for ATP hydrolysis is much lower for MCR than nitrogenases. Furthermore, in nitrogenases, ATP hydrolysis is directly coupled to a redox gating mechanism that triggers electron flow from a [4Fe-4S] cluster in NifH to the P-cluster in NifDK, which is the terminal electron donor for N_2 reduction[107]. Our data suggest that component A2, by itself, is unlikely to be involved in a redox gating mechanism for MCR activation but might facilitate this process through a series of cascading events that are somehow linked to ATP hydrolysis. Our DSF assays reveal a distinct peak for the component A2-MCR complex, which indicates that the two proteins interact even in the absence of McrC and the other MMPs that are putatively involved in transferring electrons to F430 in the active site of MCR (**Fig 2.2.4.1D and E**). That said, even when an equal amount of MCR is added to component A2, the rate of ATP hydrolysis only increases by 2.2-fold and the reaction does not proceed to completion (**Fig 2.2.2.1H and 2.2.3.1J**). These results suggest that ATP hydrolysis is only triggered when component A2 interacts with a certain sub-population of MCR, likely MCR bound to the electron transfer components of the activation complex. By decoupling MCR interaction from ATP hydrolysis, component A2 might be able to rapidly associate with MCR but only hydrolyze ATP when MCR is primed for reductive activation. Our proposal is also consistent with the mode of action for type I/II ABC transporters where conformational changes in the membrane-bound transporter that are triggered by the interaction of the substrate with the substrate-binding protein ultimately led to hydrolysis by the ATPase component[108]. The conformational cues in MCR induced by other components of the activation complex that ultimately trigger ATP hydrolysis by component A2 are currently unknown but an exciting area of investigation for future studies.

In summary, this work provides clear experimental evidence that component A2 is an unusual, yet bona fide ATPase involved in the activation of MCR. We also establish a pipeline for holistic and mechanistic analyses of essential components involved in the biogenesis of MCR in vivo. A detailed understanding of how each component of the activation complex interacts with MCR will be necessary

for a complete understanding of the intricate pathway involved in the maturation of MCR within the cell.

2.4 Materials and Methods

2.4.1 Media and culture conditions

All *M. acetivorans* strains were grown at 37 °C without shaking in hermetically sealed Balch tubes or 1-liter anaerobic bottles in bicarbonate-buffered high-salt (HS) medium containing either 50 mM (for standard passaging) or 100 mM (for protein purification) Trimethylamine.HCl (TMA) as the growth substrate. All *E. coli* strains were grown shaking at 37 °C in lysogeny broth (LB) with 20 μg/mL chloramphenicol.

2.4.2 Plasmid construction

The vector to overexpress component A2 (MA_3998 or MA_RS20860) in *M. acetivorans* was constructed using the pJK027A vector backbone. Briefly, MA_3998 was amplified from the *M. acetivorans* genome and the 2X Strep- 1X FLAG TAP tag was added to the N-terminus of the protein via primer overhangs. The amplified PCR product was assembled into pJK027A linearized with *NdeI* and *HindIII* via Gibson Assembly as previously described[109]. Site directed mutagenesis of component A2 to generate the K43A, K329A, K43A/K329A, E200A, E459A, and E200A/E459A variants was conducted with primers containing the desired point mutations. The C70A/C73A/C86A/C89A allele of A2 was generated as a synthetic construct (Twist Biosciences, South San Francisco, CA, USA). All plasmids were transformed into *E. coli* strain WWM4489[110], a derivative of DH10B, by electroporation (MicroPulser Electroporator, Bio-Rad, Hercules, CA, USA) and the resulting transformants were grown in LB supplemented with 20 μg/mL chloramphenicol and10 mM rhamnose to induce high copy number of the plasmid[110]. All plasmids were extracted using the Zyppy Miniprep Kit (Zymo Research, Tustin, CA) and verified by Sanger sequencing at the UC Berkeley DNA Sequencing Facility. All primers used were obtained from Integrated DNA Technologies, Coralville, IA, USA. All primers and plasmids used in this study can be found in Supplemental Tables 2.4 and 2.5.

2.4.3 Transformation of Methanosarcina acetivorans

M. acetivorans strain WWM73[17] was transformed with the component A2 overexpression plasmids by liposome-mediated transformation as previously described[111]. Each transformation reaction was performed with 2 μg plasmid DNA and 20 mL of *M. acetivorans* cells grown to late-exponential phase high-salt (HS) minimal medium with 50 mM trimethylamine.hydrochloride (TMA) as the sole carbon and energy source containing HS-media. Transformants were then plated on agar-solidified HS-medium with 50 mM TMA and 2 μg/mL puromycin. Plates were incubated at 37 ºC for 2-3 weeks in an intrachamber anaerobic incubator with an H_2S /CO_2/N_2 (1,000 ppm/20%/balance) headspace. Colonies were picked into 10 mL of HS-medium with 50 mM TMA and 2 μg/mL puromycin and incubated at 37 ºC without shaking. Once grown, integration of the plasmid onto the chromosome was

confirmed by PCR using diagnostic primers listed Supplemental table S2.4. PCR product sequences were verified by Sanger sequencing at the UC Berkeley DNA Sequencing Facility. Strains generated for this study are listed in Supplemental table S2.6.

2.4.4 Genomic DNA extraction and whole-genome sequencing

Genomic DNA was extracted from 2 mL of culture grown to saturation using the QIAGEN DNeasy Blood & Tissue kit (QIAGEN, Hilden, Germany) according to manufacturer's protocol. Library preparation and Illumina sequencing was conducted by SeqCenter (Pittsburgh, PA, USA). The resulting sequencing reads were analyzed *breseq* v0.35.5[112] using default settings.

2.4.5 Growth curves of Methanosarcina acetivorans

Growth curves were performed by preculturing strains in HS-TMA media without shaking at 37 ºC (HeraTherm General Protocol Microbiological Incubator, Thermo Fisher Scientific, Waltham, MA) in sealed Balch tubes. From early stationary phase cells, 0.5 mL culture was transferred into three replicate tubes with 100 μg/mL tetracycline and three replicate tubes without tetracycline. All tubes contained 2 μg/mL puromycin to maintain the integrated plasmid. Growth was measured by monitoring the optical density at 600 nm (Genesys 50, Thermo Fisher Scientific, Waltham, MA). All tubes containing tetracycline were wrapped in aluminum foil to prevent light-based degradation of the chemical. The growth rate was calculated from the slope of the linear fit of the $\log_{10}$-transformed optical density versus time with a minimum five points in the exponential phase with the highest R^2 value (minimum cut-off ≥ 0.99).

2.4.6 Anaerobic purification of proteins

500 mL cultures of *M. acetivorans* were grown in HS-media supplemented with 100 mM TMA in 1-liter anaerobic bottles sealed with butyl rubber stoppers (Chemglass Life Sciences, Vineland, NJ, USA) at 37 ºC. Cultures were supplemented with 2 μg/mL puromycin and 100 μg/mL tetracycline to induce protein expression and grown to late-exponential phase (for component A2) or stationary phase (for methyl-coenzyme M reductase; MCR). All the steps of protein purification were conducted under anaerobic conditions in a Coy chamber (Coy Lab Products, Grass Lake, MI, USA) with a N_2/H_2 (96-97%/ 3-4%) headspace. All buffers were made anaerobic by sparging with 100% N_2 for 30 minutes and were filter sterilized following sparging. Cells were harvested by spinning (Sorvall Legend XTR, Thermo Fisher Scientific, Waltham, MA, USA) at 6000 RPM at 4 °C for 10 minutes in a gas-tight sealed polypropylene Nalgene centrifuge bottles. After harvesting, cells were anaerobically lysed via osmotic pressure in 20 mM HEPES, 1% glycerol buffer, pH 8 (Buffer A) with the addition of 0.25X Roche cOmplete EDTA-free Protease Inhibitor Cocktail (MilliporeSigma, Burlington, MA, USA) and DNase I (Thermo Fisher Scientific, Waltham, MA, USA). After lysis, 5 M NaCl was added to crude cell lysate for a final concentration of 300 mM NaCl. Crude cell lysate was cleared by spinning at 10,000 RPM at 4 °C for 30 minutes. To purify protein, cleared cell lysate was applied twice to 0.25-0.5 mL Strep-Tactin Superflow plus resin (Qiagen, Hilden, Germany) equilibrated with 10 mL anaerobic Buffer A + 300

mM NaCl. After washing the resin with 12 mL of Buffer A + 300 mM NaCl, the protein of interest was eluted with Buffer A + 300 mM NaCl + 2.5 mM desthiobiotin (Sigma-Aldrich, St. Louis, MO, USA). Purified protein was stored at room temperature in the anaerobic chamber, unless otherwise stated[113]. Protein concentration was determined by Pierce Bradford Plus Protein Assay Reagent (Thermo Fisher Scientific, Waltham, MA, USA) using Bovine Serum Albumin (BSA) for calibration curve generation.

2.4.7 ATPase assays

All ATPase assays were performed under anaerobic conditions in the Coy anaerobic chamber unless otherwise stated. Assays were performed with component A2 within 48 hours of purification. Component A2 was stored anaerobically at room temperature (RT) prior to use. ATPase reactions were performed in anaerobically in 110 μL reaction volume incubated at 37 °C containing 20 mM HEPES, 1% glycerol, 300 mM NaCl, 10 mM $MgCl_2$, 200 μM ATP, and 500 μg/mL of either component A2, MCR, or both. Reactions were started with addition of protein. Reactions were set up in technical triplicate and 25 μL aliquots were taken at 0, 15, 30, and 60-minute time points. To quench reaction time points, aliquots were immediately added to an equivalent volume of ice cold 20 mM EDTA, pH 8, and removed from the anaerobic chamber. Aliquots were stored on ice until the final time point was taken. ATPase activity was evaluated immediately following the final time point by measuring the production of inorganic phosphate using malachite green solution (Echelon Biosciences, Salt Lake City, UT, USA). Each 50 μL aliquot was plated in duplicate in a 96-well plate and 80 μL of malachite green solution was added to each well and mixed by pipetting. After allowing color development for 25 minutes at RT, the absorbance was measured at 620 nm on an Epoch 2 microplate reader (BioTek, Winooski, VT, USA). Absorbance was converted to phosphate concentration using a 0-100 μM phosphate calibration curve and plotted against time to determine ATPase activity over the course of the reaction. Reactions were internally normalized to the 0-minute time point to only measure change in phosphate production over the course of the 60-minute incubation.

2.4.8 Differential Scanning Fluorimetry

Anaerobically purified component A2 or MCR was removed from the anaerobic chamber to set up reactions for differential scanning fluorimetry at RT on the bench top. Each sample contained 500 μg/mL indicated protein, 20 mM $MgCl_2$, ATP at concentration indicated in figure legend (ranging from 0 – 2 mM), 20 mM HEPES, 300 mM NaCl, and 1% glycerol at pH 8. SYPRO Orange Protein Gel Stain (Invitrogen, Thermo Fisher Scientific, Waltham, MA, USA) was added to a final concentration of 5X and each sample was gently pipetted to mix and dispensed into 96-well PCR plates (Applied Biosystems, Thermo Fisher Scientific, Waltham, MA, USA) and sealed with adhesive optical film. Using a CFX96 Touch Real-Time PCR Detection System (Bio-Rad, Hercules, CA, USA) fluorescence was measured in the FRET channel (450-730 nm range of excitation/emission wavelengths) along a temperature gradient from 25°C to 95°C in increments of 0.5°C every 30 seconds. The first derivative of the fluorescence emission as a function of temperature (dRFU/dT) was plotted and the melting temperature (T_m) was defined as the peak(s) of the first derivative. Melt curves were repeated with biological triplicate (independent protein purifications) as indicated.

2.4.9 SDS-PAGE and Immunoblotting of FLAG-tagged proteins and of MCR

Samples containing protein as indicated in figure captions were combined with Laemmli sample buffer (Bio-Rad, Hercules, CA, USA) and 2.5% β-mercaptoethanol and then heated at 95°C for 8 minutes. Samples were then loaded into 12% precast Tris-Glycine denaturing SDS-PAGE gels (Mini-PROTEAN TGX, Bio-Rad, Hercules, CA, USA). Bio-Rad Precision Plus Prestained Protein Standard was used as a molecular weight standard. Gels were run at 100-150 V until the dye front reached the bottom of the cassette. Gels were stained with Coomassie GelCode Blue (Thermo Fisher Scientific, Waltham, MA, USA). For immunoblotting, protein was transferred from the gel to the PVDF (polyvinylidene fluoride) membrane with the Trans-Blot Turbo Transfer System and Midi-PVDF Transfer Pack (Bio-Rad, Hercules, CA, USA) following manufacturer's instructions. Following transfer, membranes were rinsed for 5 minutes with water, 5 minutes with PBS (137 mM NaCl, 2.7 mM KCl, 10 mM Na_2HPO_4, 1.8 mM KH_2PO_4), and blocked for 1 hour at RT with 5% nonfat milk dissolved in PBS. For visualization of FLAG-tagged proteins, membranes were then rinsed in PBS 4X for 5 minutes prior to incubation with mouse monoclonal anti-FLAG M2 HRP-conjugated antibody (Sigma-Aldrich, St Louis, MO) diluted 1:66666 in PBS-T (PBS with 0.05% Tween-20) for 1 hour at RT. Following incubation with antibody, membranes were rinsed 3X in PBS-T and then 3X in PBS for 5 minutes each. Alternatively, for visualizing McrA, membranes were rinsed in PBS 4X for 5 minutes following blocking and then incubated overnight at 4°C with polyclonal rabbit antibodies raised against McrA (1:10000 dilution) (GenScript, Piscataway, NJ, USA) in PBS-T. The following day membranes were rinsed in PBS-T 4X for 5 minutes each and then incubated with anti-rabbit horseradish peroxidase (HRP) conjugate antibodies (1:100000 dilution) (Promega, Madison, WI, USA) for 2 hours at room temperature and finally rinsed 3X in PBS-T and then 3X in PBS for 5 minutes each. For both FLAG and McrA visualization, the signal was developed by addition of the Immobilon Western Chemiluminescent HRP Substrate (MilliporeSigma, Burlington, MA, USA) in the dark. Both SDS-PAGE gels and immunoblots were visualized on a ChemiDoc MP Imaging System (Bio-Rad, Hercules, CA, USA).

2.4.10 Mass spectrometry Sample Identification

Mass spectrometry-based identification of proteins extracted from SDS-PAGE gels were performed by either Applied Biomics, Inc (Hayward, CA, USA) or QB3/Chemistry Mass Spectrometry Facility at UC Berkeley. Applied Biomics performed sample preparation in house. For samples analyzed at the UC Berkeley QB3/Chemistry Mass Spectrometry Facility sample preparation was performed as follows. Bands from Coomassie stained SDS-PAGE gel were excised with a razor blade and diced, and gel pieces were washed for 20 minutes in 500 µL of 100 mM NH_4HCO_3 and the supernatant was discarded. Gel pieces were then incubated in 150 µL of 100 mM NH_4HCO_3 and 10 µL of 45 mM DTT for 15 minutes at 50 °C. Next 10 µL of 100 mM iodoacetamide was added and the mixture was incubated for 15 minutes in the dark at RT. The supernatant was discarded gel pieces were washed with 500 µL of a 50:50 mix of acetonitrile and 100mM NH_4HCO_3 with shaking for 20 minutes. After the supernatant was discarded, gel pieces were incubated with 50 µL of acetonitrile for 15 minutes. Solvent was removed and gel fragments were dried in a speed vac. Gel pieces were then reswelled with 10 µL of

25 mM NH_4HCO_3 containing 0.1 μg sequencing-grade modified trypsin (Promega, Madison, WI, USA). After 15 minutes, 20 μL of additional NH_4HCO_3 was added and the reaction was incubated overnight at 37 °C. Remaining peptides from the gel pieces were extracted twice with 50 μl of 60% acetonitrile/0.1% formic acid for 20 minutes, then once with 25 μl acetonitrile, and samples were dried in a speed-vac.

2.4.11 RNA extraction and cDNA synthesis

M. acetivorans strain WWM60 was grown to mid-exponential phase and 1 mL of culture was added to an equivalent volume of Trizol (Life Technologies, Carslbad, CA) prewarmed to 37 °C. Following incubation for 5 minutes at RT, 2 mL of 100% cold ethanol was added, and RNA was extracted according to the manufacturer's instructions using the Qiagen RNeasy Mini Kit (Qiagen, Hilden, Germany). Concentration of the RNA was determined using a Nanodrop One UV Spectrophotometer (Thermo Fisher Scientific, Waltham, MA) and stored at −80 °C. To eliminate any minor amounts of contaminating genomic DNA, RNA was treated with DNase according to the manufacturer's instructions using TURBO-DNA free kit (Thermo Fisher Scientific, Waltham, MA, USA). Next, to synthesize cDNA, reactions were set up with 2.5 ng/μL random hexamers, 10 ng/μL DNase-treated RNA, 0.5 mM dNTPs, 5 mM DTT, First-strand buffer, and 10 U/μL Superscript III. Prior to the addition of DTT, First-strand buffer, and Superscript III, the reaction was incubated at 65 °C for 5 minutes and then placed on ice for 1 minute. Following the addition of the rest of the reagents, the reaction was incubated at 25 °C for 5 minutes, then 50 °C for 60 minutes, and finally 70 °C for 15 minutes. The resulting cDNA was stored at -20°C. All reagents used for cDNA synthesis were obtained from Thermo Fisher Scientific, Waltham, MA, USA.

2.4.12 Protein structural prediction and visualization

AlphaFold 3[102] was used for structural models of *M. acetivorans* component A2 (MA_3998) alone and with ATP or ADP. Protein domains were identified using InterPro v108[114]. Protein structures were visualized using ChimeraX v1.7.1[115].

2.4.13 Protein sequence alignment

Protein sequences with the assigned TIGRFAM Hidden Markov Model (HMM)[116] TIGR03269 were downloaded from the Genome Taxonomy Database (GTDB) R214, which included 888 sequences. A multiple sequence alignment (MSA) MUSCLE v5.1 alignment[117] was performed using Geneious software v 2024.0.2. The MSA of individual motifs of interest (NBD1 walker-A, NBD2 walker-A, NBD1 walker-B, NBD2 walker-B, and zinc binding motif) were extracted from the full sequence alignment. Each individual motif contained the following number of sequences from the MSA: 867 in NBD1 walker-A, 888 in NBD2 walker-A, 883 in NBD1 walker-B, 880 in NBD2 walker-B, and 870 in the zinc binding motif. Individual sequence motifs were visualized with WebLogo v3[118].

2.4.14 Phylogenetic analysis

All 888 sequences were clustered based on 70% sequence similarity using Cluster Database at High Identity with Tolerance (CD-HIT)[119] with default parameters. Clustering provided a list of 86 sequences that were further trimmed based on sequence length to omit truncated sequences or sequences with large insertions. Sequences were retained if they fell within ±10% of the mean sequence length, and the component A2 sequence from *M. acetivorans* was manually added in, due to its relevance to this work. This resulted in a final set of 80 sequences. The tree was built using these 80 sequences along with 20 sequences for the outgroup. The outgroup was determined by using Basic Local Alignment Search Tool (BLAST) to find 20 sequences that are most like the component A2 homolog from *M. acetivorans* MA_3967 (MA_RS20695). A multiple sequence alignment (MSA) was performed using the MUSCLE v5.1 plug-in[117] in Geneious software v2024.0.2. A tree was then built using the Randomized Axelerated Maximum Likelihood (RAxML) algorithm v8.2.11[120] with protein model GAMMABLOSUM62 and 100 bootstrap replicates. The tree was visualized using iTOL v7 (Interactive Tree of Life)[121].

Chapter 3

Dissection of the expression of the MCR activation operon using CRISPR *interference*

In the final chapter of my dissertation, I present experiments following up on the discoveries made in chapter 2 that the MCR activation operon is transcribed as a single full-length transcript and does not change significantly in response to growth substrate or MCR-limitation. In this set of experiments, I use CRISPR *interference* (CRISPRi) to knockdown the expression of either MCR or component A2 and used qPCR to measure both the expression of the targeted gene as well as the genes downstream in the operon. In addition, I also performed growth analyses to determine if lowering expression of these essential genes has a measurable impact on growth under standard laboratory conditions.

Sophia A. Adler[1], Dipti D. Nayak[1,2]

[1]Department of Molecular and Cell Biology, University of California, Berkeley, CA, USA
[2]Department of Plant and Microbial Biology, University of California, Berkeley, CA, USA

Abstract

Given the importance of MCR to global carbon cycling, a detailed map of its function, regulation, and interacting partners is critical to effectively implement applied techniques like specific inhibitors to methanogenesis and, perhaps, vaccines against methanogens. Additionally, the utility of methane as a clean burning fuel means that fully re-engineering methanogenesis in a scalable host microbe could offer a renewable replacement for traditional fossil fuels. For either scenario, an understanding of both the expression and regulation of MCR, the key enzyme responsible for methane production, is paramount. To this end we sought to more fully understand the expression of the MCR activation operon and how changes in expression affect growth of *M. acetivorans*. In the previous chapter, we established that the MCR activation operon has transcription across all gene boundaries, proving that there is a full-length transcript produced across the entire operon. Here, we utilize CRISPRi to show that despite the presence of a full-length transcript of this operon, the knockdown of component A2- the first gene of the operon- unexpectedly fails to alter the transcription of most of the downstream genes. This contrasts with the knockdown in expression of McrB, the first gene in the MCR operon, which showed the expected polar effect and lowered transcription of McrA, the final gene in the operon. Additionally, growth analyses show that despite much lower expression of component A2, growth of this strain was not significantly different from wildtype growth. These results highlight the areas of research that deserve further investigation so that a full understanding of the regulation and expression of the MCR activation operon may be obtained.

3.1 Introduction

The importance of understanding MCR biology for global carbon cycling cannot be understated. MCR is used by both the methane generating methanogens as well as the methane consuming ANME (anaerobic methanotrophic archaea). Globally, methanogens are found in both extreme environments, like deep-sea hydrothermal vents[122–124] and hypersaline lakes[125,126], as well as more mesophilic locations like rice fields[127], peat bogs[128], landfills[129], and the digestive systems of humans[130], animals[131], and event insects[132]. Given that MCR is the enzyme responsible in each of these environments for methane contributions, as well as the methane sinks provided by ANME in anoxic marine and freshwater environments, a detailed understanding of the expression and regulation of this enzyme is required.

MCR is encoded on a polycistronic operon containing a total of five genes, three of which form the subunits which make up the holoenzyme[13,32]. The other two genes, *mcrD* and *mcrC*, are involved in insertion and then reductive activation of F430, respectively[28,29] (**Fig 3.1.1A**). Another polycistronic operon located elsewhere in the genome has been implicated in the reductive activation of MCR: this operon contains seven genes, *component A2, mmp3, mmp6, mmp5, mmp15, mmp17,* and *mmp7,* four of which were identified as being part of the McrC containing activation complex of MCR[28] (**Fig 3.1.1A**). The other three genes have also been predicted to interact with MCR via this activation complex[93], but more direct evidence is needed to understand the nature of this interaction. This operon, deemed the "MCR activation operon," is extremely highly conserved in genomes that contain MCR, even more so than other genes that consistently co-occur genomically with MCR[10]. Since MCR is known to be essential[73] and the MCR activation operon is very likely essential (see chapter 2), we sought a method to study the effect on growth of decreased transcription of both operons. CRISPR *interference* (CRISPRi) is a highly effective and reversible technique used to knock down the expression of a gene of interest by exploiting a deactivated version of *S. pyogenes* Cas9 (dCas9)[18,75,133–135]. The dCas9 contains a mutated endonuclease domain such that double stranded DNA cutting is disabled, but sequence specific DNA binding is retained[134]. When dCas9 is targeted to a gene of interest via the sgRNA, it melts the dsDNA and sits on the chromosome preventing RNA polymerase from proceeding down the open reading frame[135]. Thus, transcription is halted and expression of the target gene is decreased. When either the sgRNA or dCas9 is expressed from an inducible promoter, the system becomes tunable and the targeting of essential genes can be modulated accordingly (**Fig 3.1.1B**). When CRISPRi is used to target a gene in a polycistronic operon, a polar effect is observed. This results in the genes downstream of the target also decreasing in expression[135] (**Fig 3.1.1C**). When pooled CRISPRi screens are performed, the polar effect must be taken into consideration when interpreting phenotypic data, but, given that genes expressed on the same transcript are typically functionally related, it can also be useful to study the effect of the knock down of the entire transcript when the first gene is targeted.

In this chapter we utilize CRISPRi in our model methanogen *M. acetivroans* to knock down the gene expression of both the MCR operon and the MCR activation operon. Interestingly we only observe significant changes to growth when the genes in the MCR operon are targeted directly.

Additionally, we find that the MCR activation operon does not exhibit the expected polar effect when the first gene is knocked down, indicating that the structure of this operon may be more complex than initially understood.

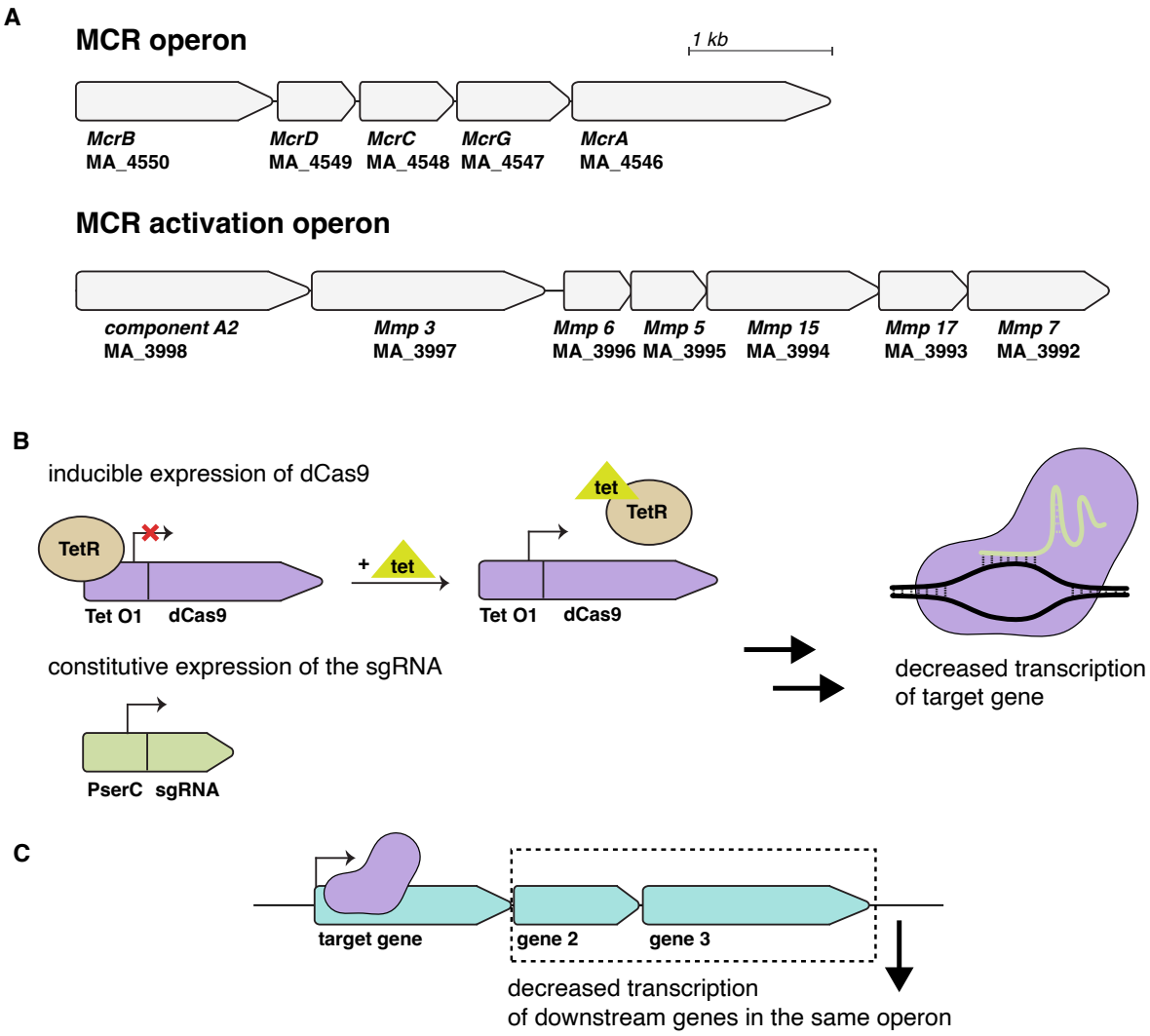

Figure 3.1.1 Structure of MCR and MCR activation operons and CRISPRi expression system (a) Cartoons depicting the MCR (top) and MCR activation (bottom) operons drawn to scale with a scale bar depicting 1 kilobase. (b) Cartoon of the CRISPRi expression system utilized in this study. When tetracycline (tet) is added, it binds TetR and causes de-repression of the PmcrB-TetO1 promoter. The sgRNA is constitutively expressed from the PserC promoter. (c) Cartoon depicting the polar effect which occurs when the first gene of an operon is targeted by dCas9 (purple).

3.2 Results

3.2.1 CRISPRi can be effectively used to lower expression of MCR in M. acetivorans

To begin our investigation into the expression and subsequent knock down of the genes within the MCR activation operon, we first sought to establish the ability of this system to knockdown a highly expressed, well characterized operon. To this end we built *M. acetivorans* strains expressing a plasmid containing both a constitutively expressed sgRNA targeting a gene of interest and a tetracycline inducible, catalytically deactivated Cas9 (dCas9) (**Fig 3.1.1B**). When tetracycline is added to the culture, it binds the repressor, TetR, which causes it to release the operator sequence (TetO1) and permits transcription of dCas9 (**Fig 3.1.1B**). This expression system allows the growth and maintenance of strains targeting the knockdown of essential genes. Alternative approaches, like lowering the expression of essential genes directly by swapping the native promotor, can select for escape mutants given that the growth of such strains is typically highly reduced compared with wild type. Inducible expression of dCas9, however, allows for expression of the target gene when tetracycline is absent.

To lower the expression of MCR, we generated knock-down (KD) strains targeting either the first gene, *mcrB*, or the last gene, *mcrA*, in the operon. To measure the expression of these genes compared to WT, RT-qPCR was performed with RNA extracted immediately prior to tetracycline addition, 5 hours post, and 10 hours post addition. The initial RNA extraction was performed when the cells were in mid-exponential growth. Given that the doubling time of *M. acetivorans* is ~12 hours when grown on trimethylamine, each of the following time points were also within exponential growth. When the relative expression of mcrB was measured in both the KD and WT strains, both the 5-hour and 10-hour time point showed a significant reduction in gene expression (**Fig 3.2.1.1A**). McrB expression was lowered to ~37% and ~28% of WT levels at the 5- and 10-hour time points, respectively (**Fig 3.2.1.1A**). Similarly, when *mcrA* was targeted the expression of *mcrA* was decreased to ~29% and ~18% of WT levels at 5- and 10- hours post induction of dCas9, respectively (**Fig 3.2.1.1B**). This result showed proof of concept that CRISPRi could be effectively use in our model methanogen, *M. acetivorans*, to lower the expression of an essential gene of interest.

It has been previously established that MCR is transcribed at high levels in the cell[73], and that it is not growth rate limiting in substrate rich environments when transcription is this high. Previous work established that when MCR expression was limited by directly promotor swapping the native MCR promotor for an inducible promotor, growth was not inhibited until *mcrA* transcripts were reduced to 1/3 of WT levels[73]. Given that our CRISPRi constructs were also able to reduce MCR expression to below this threshold we wanted to confirm that the KD strains would also confer a growth defect. As expected, both the *mcrA* KD and *mcrB* KD showed a significant growth defect compared with WT (**Fig 3.2.1.1C and D**). Interestingly, the *mcrA* KD also grew significantly worse than the mcrB knockdown. This is possibly because the KD of *mcrA* appeared to be slightly stronger than *mcrB* (**Fig 3.2.1.1A and B**). It is also plausible that lowering the expression of only the last gene in the operon alters the stoichiometry of the protein complex in such a way that is more detrimental than having the expression of each gene in the operon lowered concurrently.

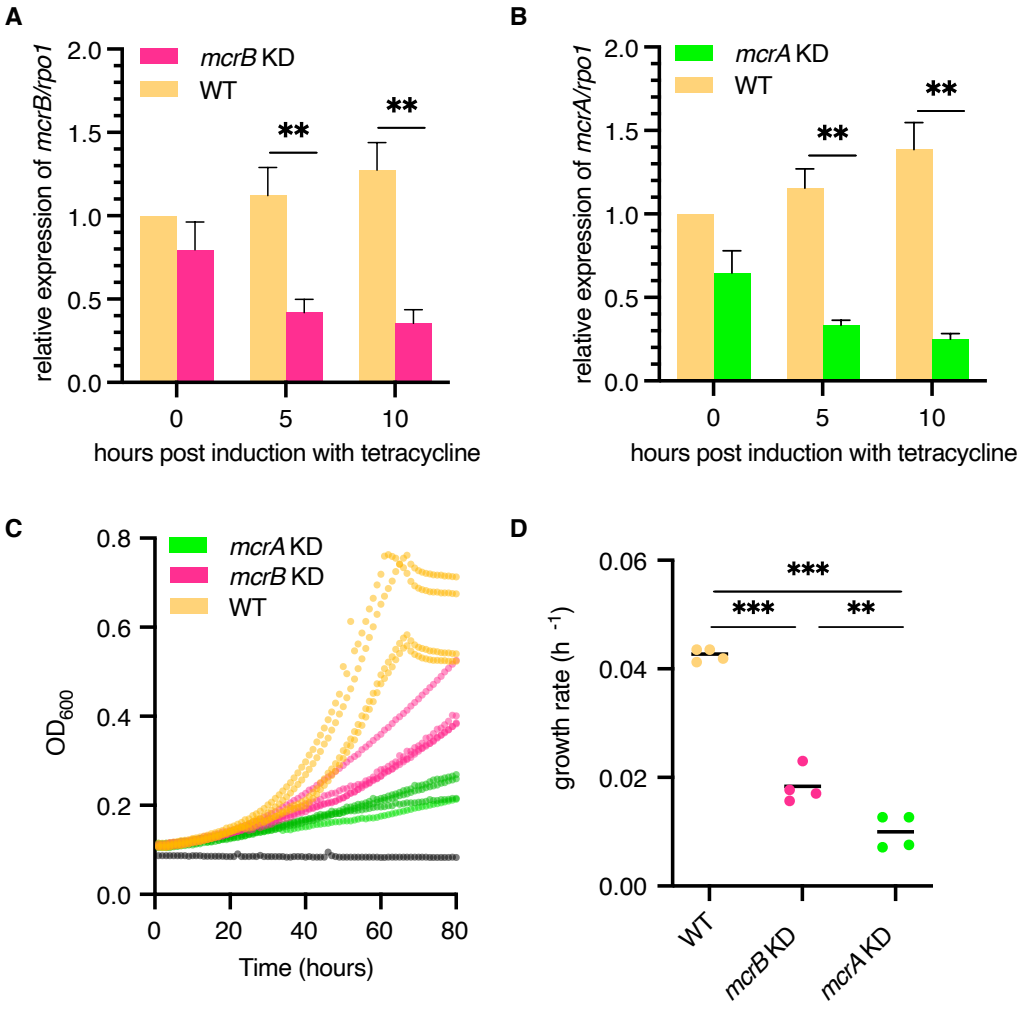

Figure 3.2.1.1 Inducible knock down of expression of *mcrB* and *mcrA* causes a growth defect. (a) Relative expression of *mcrB* in WT (orange) and the *mcrB* KD strain (pink). Time points were taken immediately prior to 100 μg/mL tetracycline addition, 5 hours, and 10 hours after. Expression of *mcrB* measured with RT-qPCR was internally normalized to the housekeeping gene *rpo1* within each strain, and then each time point is displayed as the relative expression compared to the 0 time point for WT, set to 1. (b) Relative expression of *mcrA* in WT (orange) and the *mcrA* KD strain (green), with the same parameters as (a). (c) Growth curves of WT, *mcrA* KD, and *mcrB* KD when grown with 100 μg/mL tetracycline. A blank well is shown in black. Four replicates growth curves were conducted for each strain. (d) Growth rates corresponding to the curves plotted in (c). Error bars represent the standard deviation of 3 biological replicates. Statistical significance was tested by unpaired Welch's t test. ** indicates p-value <0.01 and *** indicates a p-value <0.001.

3.2.2 The MCR and MCR activation operons exhibit differing polar effects

Given our ultimate goal of examining the change in expression of the MCR activation operon when knocking down the first gene, we first sought to characterize the behavior of the MCR operon under equivalent conditions. There is only one known promotor and transcription start site (TSS)[136] upstream of the MCR operon, so we expected that when the expression of the first gene of the operon, *mcrB*, was knocked down, the subsequent expression of the downstream genes would follow, as is well established in CRISPRi based screens[137,138]. When targeting *mcrB* we found, as expected, that the expression of *mcrG* and *mcrA* were decreased to ~21% and ~35% of WT levels after 10 hours induction of dCas9, respectively (**Fig 3.2.2.1**).

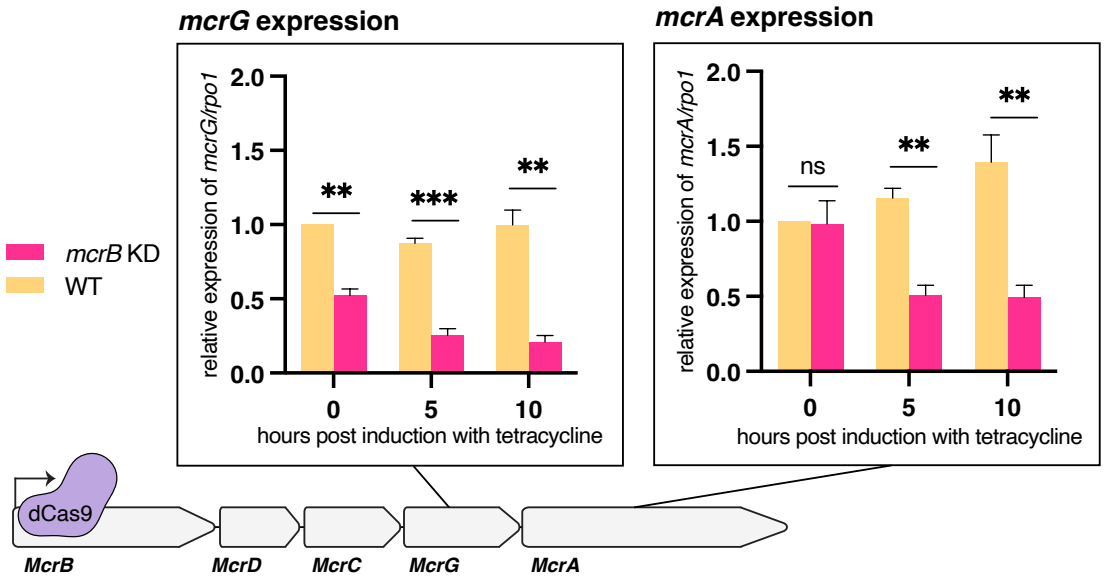

Figure 3.2.2.1 Polar effect of *mcrB* knockdown in expression. Relative expression of *mcrG* and *mcrA* in WT (orange) and the *mcrB* KD strain (pink). Time points were taken immediately prior to 100 μg/mL tetracycline addition, 5 hours, and 10 hours after. Expression of *mcrG* and *mcrA* measured with RT-qPCR was internally normalized to the housekeeping gene *rpo1* within each strain, and then each time point is displayed as the relative expression compared to the 0 time point for WT, set to 1. Error bars represent the standard deviation of 3 biological replicates. Statistical significance was tested by unpaired Welch's t test. ** indicates p-value <0.01 and *** indicates a p-value <0.001. 'ns' indicates p-value > 0.05.

To examine the MCR activation operon, we built a knock down strain targeting *component A2*. When we looked at the expression of *component A2* itself, we found that, as expected, the expression was significantly decreased compared to WT- about 19% of WT levels 10 hours after induction of Cas9 (**Fig 3.2.2.2A**). Interestingly, the expression of A2 was already decreased to ~32% prior to tetracycline addition (**Fig 3.2.2.2A**). This could indicate that the sgRNA targeting *component A2* had very high affinity such that any small amount of "leaky" expression of dCas9 from the tetracycline inducible

promotor would already cause a decrease in expression. Regardless of inducibility, the knock down in expression was effective, and we expected the downstream genes in the operon to behave similarly, as observed for the MCR operon. However, we observed that only *mmp3* showed a minimal, but still significant, decrease in expression in this strain (**Fig 3.2.2.2B**). The rest of the downstream genes that we quantified, *mmp6, mmp15,* and *mmp7*, lacked significant changes in expression compared with WT at each time point measured (**Fig 3.2.2.2C, D, and E**).

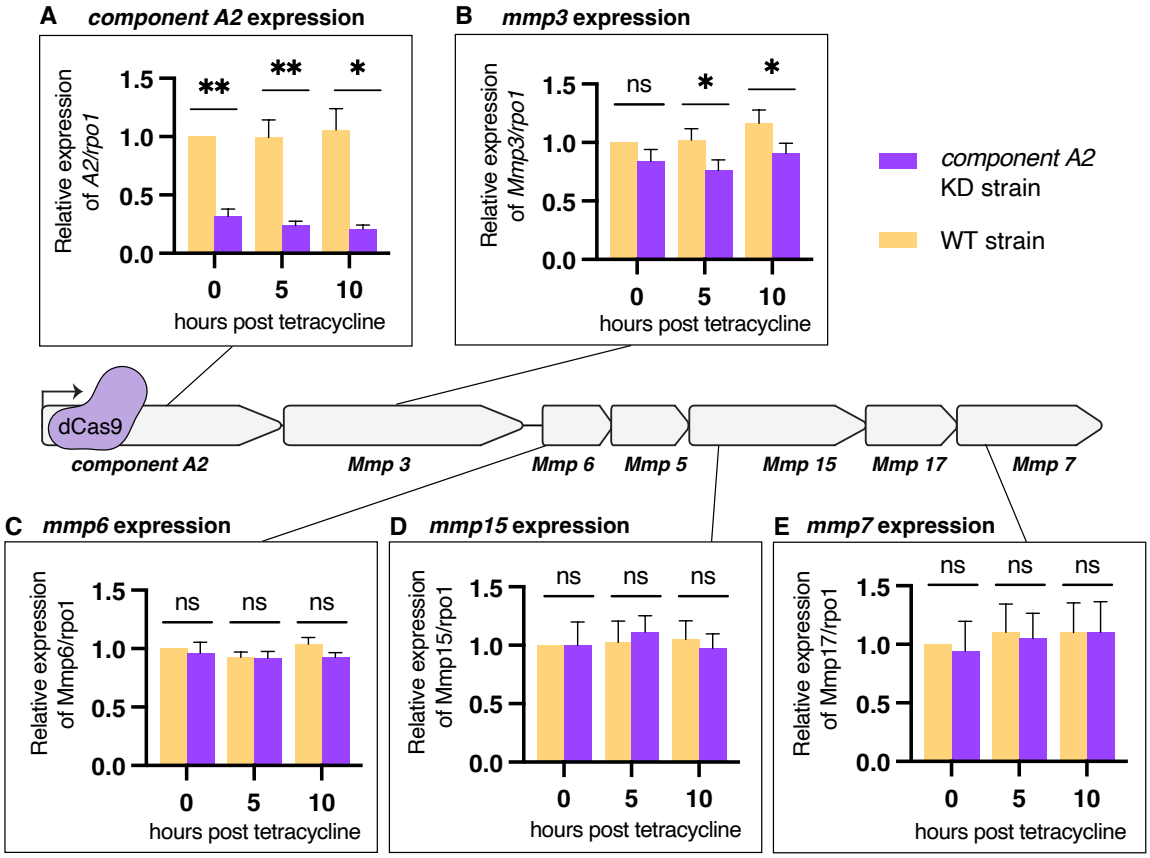

Figure 3.2.2.2 Knockdown of *component A2* fails to have polar effect on all downstream genes in the operon. (a) Relative expression of *component A2* in WT (orange) and the *component A2* KD strain (purple). Time points were taken immediately prior to 100 µg/mL tetracycline addition, 5 hours, and 10 hours after. Expression of *component A2 was* measured with RT-qPCR was internally normalized to the housekeeping gene *rpo1* within each strain, and then each time point is displayed as the relative expression compared to the 0 time point for WT, set to 1. (b-e) Relative expression of *mmp3* (b), *mmp6* (c), *mmp15* (d), and *mmp7* (e) in WT (orange) and the *component A2* KD strain (purple). Error bars represent the standard deviation of 3 biological replicates. Statistical significance was tested by unpaired Welch's t test. * Indicates p-value <0.05 and ** indicates p-value <0.01. 'ns' indicates p-value > 0.05.

3.2.3 Decreased expression of component A2 does not affect growth rate

As explored in chapter 2, *component A2* plays a critical role as the ATPase in the MCR activation complex and was unable to be deleted from *M. acetivorans*. It also is extremely highly conserved among MCR encoding genomes, indicating its role has been essential throughout methanogen evolution. However, it is expressed at much lower levels than MCR itself (**Fig 2.2.1.1**), so whether the knockdown to ~19% of WT levels would have a significant effect on growth was yet to be determined. Additionally, as stated previously, it is known that MCR is expressed above rate-limiting levels under standard laboratory growth of *M. acetivorans*. To determine if knock down in expression of *component A2* would affect growth, we performed growth curves and calculated the growth rate of WT and the *component A2* KD strain with the addition of 100 μg/mL tetracycline to the growth medium. We found that there was no significant change in growth rate in the *component A2* KD strain compared to WT (**Fig 3.2.3.1**), unlike the KD strains of both *mcrB* and *mcrA*. Interestingly, two of the four replicates for the *component A2* KD strain exhibited a temporary stall in growth midway through exponential growth (**Fig 3.2.3.1A**). It is unclear whether this phenotype is an artifact of the method of measurement or a result of lower expression of *component A2*. Regardless, the lack of change to growth rate (**Fig 3.2.3.1A**) indicates that very little of *component A2* is necessary for the cell under standard laboratory conditions.

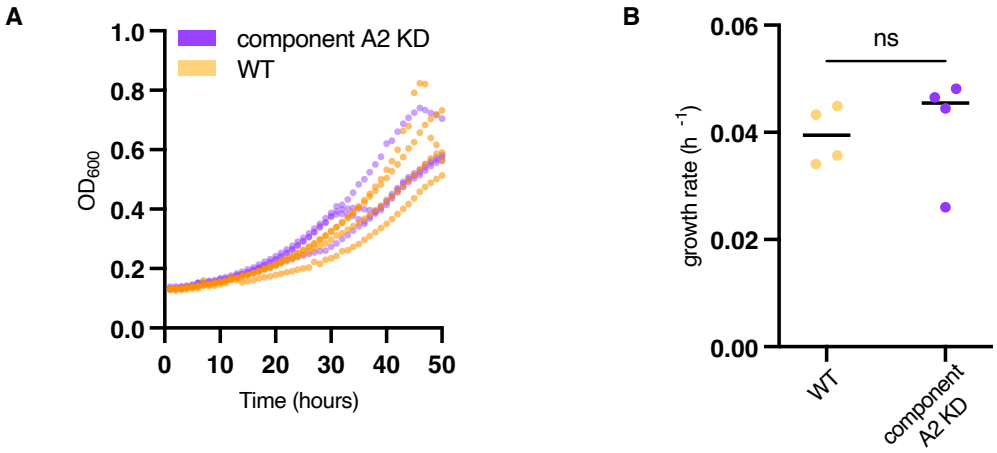

Figure 3.2.3.1 Knockdown of *component A2* does not show growth rate defect. (a) Growth curves of WT (orange) and *component A2* KD (purple) when grown with 100 μg/mL tetracycline. Four replicates growth curves were conducted for each strain. (b) Growth rates corresponding to the curves plotted in (a). Statistical significance was tested by unpaired Welch's t test. 'ns' indicates p-value >0.05.

3.3 Discussion

This chapter contributes to the growing field of knowledge surrounding the MCR activation operon and its putative role for MCR maturation and continued function in the cell. Although we initially set out to characterize the growth phenotype when the expression of the MCR activation

operon was artificially lowered using CRIPSRi, we observed an interesting phenomenon that indicated disparate polar effects of CRISPRi knock down between the MCR operon and the MCR activation operon.

When measuring the expression in the *mcrB* KD strain of downstream genes (*mcrG* and *mcrA*) we observed the polar effect expected of an operon that contains only one promotor and TSS (**Fig 3.2.2.1**). However, when we measured the expression in the *component A2* KD strain of downstream genes (*mmp3*, *mmp6*, *mmp15*, and *mmp7*), only the gene directly adjacent to *component A2* (*mmp3*) displayed a very moderate decrease in expression. The most likely explanation for this result is that there is a second internal promoter and TSS within one of the first two genes of this operon, which allows for two isoforms of the transcript to be generated- a short form containing the genes downstream and to the exclusion of *component A2* and long form containing the entirety of the operon. The "long form" of this transcript was described and characterized in chapter 2. The "short form" is putative and would require more thorough analysis to be sure of its existence. It is, however, well characterized that many operons in prokaryotic systems do not exhibit the expected polar effect when CRISPRi screens are applied. A 2018 study from Wang et. al.[139] found in a pooled CRISPRi screen in *E. coli* that 35% of polycistronic targets with known-to-be-essential downstream genes exhibited no phenotype when compared to the essential gene itself being targeted. This lack of polar effect indicated to the authors that these operons may contain undefined promotors and thus multiple lengths of transcript could be produced. Another study[140] performed in *E. coli*, which used RNA sequencing to map promoters, terminators, and operonic structure genome wide, found that nearly half of polycistronic operons contained multiple promoters (some of which also contained multiple terminators). Although work characterizing operons containing internal promoters has been more limited in Archaea, examples like the *arcBCD* operon used for arginine fermentation, which has been shown to produce three transcript lengths, have been well described[141,142] alongside more global approaches to identify TSSs[143–145].

Although the genes downstream of *component A2* remained at WT or near-WT levels in the KD strain, we still sought to determine if the decreased expression of A2 alone would confer a growth phenotype. Interestingly, there was no difference in growth rate between the *component A2* KD and WT under standard laboratory conditions. It is possible that standard growth of *M. acetivorans*, which is performed under a highly reducing environment, does not provide enough oxidative stress to observe a phenotype under decreased levels of component A2. Given that this ATPase- as described in chapter 2- is oxygen sensitive and involved in the reductive activation of cofactor F430 within MCR, it is plausible that increasing the oxidative stress to the cells by decreasing the amount of reductant in the media would cause a more severe phenotype in the *component A2* KD strain than in WT.

Through bioinformatic and experimental data it is now well established that the genes encoded on the MCR activation operon play a critical role in MCR function in the cell. However, regulatory elements controlling the expression of MCR and MCR-related genes still represent a significant gap in knowledge. In fact, only one known trans-acting regulatory factor has been described[146] for the MCR operon. This putative transcriptional regulator was characterized in *Methanothermobactor thermautotrophicus,* a methanogen which encodes two copies of the MCR operon. Thus, it is unclear if

this regulatory element is relevant to the majority of methanogens which, like *M. acetivorans,* only encode one copy of the MCR operon. Alternative TSSs could represent another way to regulate MCR associated genes. The results presented in this chapter highlight the importance of continuing to investigate the expression and regulation of MCR related genes, given the possibility that multiple isoforms of the MCR activation operon exist and are perhaps expressed under differing conditions in the cell. Additionally, this chapter highlights the utility of CRISPRi in studying operonic structure in Archaea, a topic which still remains vastly understudied.

3.4 Materials and Methods

3.4.1 Plasmid construction and strain generation

The vectors to generate knockdowns in *mcrB*, *mcrA,* and *component A2* in *M. acetivorans* were constructed using the pJK027A vector backbone. Briefly, dCas9 from *S. pyogenes* was amplified from pBFC0103. The amplified PCR product was assembled into pJK027A linearized with *NdeI* and *HindIII* via Gibson Assembly as previously described[109] to generate the base plasmid pGLC014, which was used to construct all CRISPRi plasmids. For each plasmid, a synthetic construct (Twist Biosciences, South San Francisco, CA, USA) was generated containing the sgRNA targeting the gene of interest driven off the PserC promoter. For independent replication in *M. acetivorans*, cointegrates of all plasmids were generated using Gateway BP clonase II Enzyme Mix (ThermoFisher, Waltham, MA, USA) and verified by restriction digest. All plasmids were transformed into *E. coli* strain WWM4489[110], a derivative of DH10B, by electroporation (MicroPulser Electroporator, Bio-Rad, Hercules, CA, USA) and the resulting transformants were grown in LB supplemented with 20 μg/mL chloramphenicol, 50 μg/mL kanamycin, and10 mM rhamnose to induce high copy number of the plasmid[110]. All plasmids were extracted using the Zyppy Miniprep Kit (Zymo Research, Tustin, CA) and verified by Sanger sequencing at the UC Berkeley DNA Sequencing Facility. All primers used were obtained from Integrated DNA Technologies, Coralville, IA, USA. All primers and plasmids used in this chapter can be found in Supplemental Tables S3.1 and S3.2. See section *2.4.3* for details on *M. acetivorans* strain generation. All strains generated for this chapter in Supplemental Table S3.3.

3.4.2 Media and culture conditions

All *M. acetivorans* strains were grown at 37 °C without shaking in hermetically sealed Balch tubes or 1-liter anaerobic bottles in bicarbonate-buffered high-salt (HS) medium containing 50 mM Trimethylamine-HCl (TMA) as the growth substrate for standard passaging. For plate reader growth assays, modified HS-TMA media was used that omitted bicarbonate and was instead buffered by 50 mM 1,4-piperazinediethanesulfonic acid (PIPES) adjusted to a final pH of 6.8. All *E. coli* strains were grown shaking at 37 °C in lysogeny broth (LB) with 20 μg/mL chloramphenicol and/or 50 μg/mL kanamycin.

3.4.3 RNA extraction for measuring knockdown in expression

To obtain measurements of gene expression of genes of interest in both the WT (WWM60) and KD strains (DDN223, DDN224, and DDN249), cultures were growth with 2 μg/mL puromycin in triplicate at 37 °C without shaking until reaching an OD between 0.3-0.4. Cultures were removed from the incubator, and 1 mL aliquots were taken and immediately added to an equivalent volume of Trizol (Life Technologies, Carslbad, CA) prewarmed to 37 °C. Immediately following this step, tetracycline was added to each culture to a final concentration of 100 μg/mL and cultures were returned to the incubator. For aliquots removed: following incubation for 5 minutes at RT, 2 mL of 100% cold ethanol was added, and RNA was extracted according to the manufacturer's instructions using the Qiagen RNeasy Mini Kit (Qiagen, Hilden, Germany). After extraction, concentration was determined using a Nanodrop One UV Spectrophotometer (Thermo Fisher Scientific, Waltham, MA) and RNA was stored at −80 °C until further use. After 5 hours and 10 hours of incubation with tetracycline, equivalent RNA extractions were performed as described for the 0 hour time point with the omission of additional tetracycline.

3.4.4 RT-qPCR

To perform RT-qPCR, RNA was first treated with DNase according to the manufacturer's instructions using TURBO-DNA free kit (Thermo Fisher Scientific, Waltham, MA, USA) to eliminate any minor amounts of contaminating DNA. Next, to synthesize cDNA, reactions were set up with 2.5 ng/μL random hexamers, 10 ng/μL DNase-treated RNA, 0.5 mM dNTPs, 5 mM DTT, First-strand buffer, and 10 U/μL Superscript III. Prior to the addition of DTT, First-strand buffer, and Superscript III, the reaction was incubated at 65 °C for 5 minutes and then placed on ice for 1 minute. Following the addition of the rest of the reagents, the reaction was incubated at 25 °C for 5 minutes, then 50 °C for 60 minutes, and finally 70 °C for 15 minutes. The resulting cDNA was stored at -20°C. All reagents used for cDNA synthesis were obtained from Thermo Fisher Scientific, Waltham, MA, USA. For qPCR, all primers were tested for both efficiency and specificity. Efficiency was measured by performing a serial dilution of WT cDNA to generate a standard curve. The efficiency was calculated by plotting the mean Ct of each dilution vs. the $-\log_2(\text{dilution})$ and transforming the slope of this graph with $2^{1/\text{slope}}$ and multiplying by 100 to define the efficiency as a percentage. Primers were only used that had an efficiency between 95-105% and were within 5% of the efficiency of the housekeeping gene, *rpo1*. Specificity was determined by performing a melt curve after cycling with a ramp of 0.5 °C per second up to 95 °C. Primer pairs were used if they generate only one product which produces a single peak in the melt curve. Each qPCR reaction was set up with a 1:20 dilution of the cDNA, 10 μM forward and reverse primers, and Power SYBR Green PCR Master Mix (Thermo Fisher Scientific, Waltham, MA, USA). The thermocycler was run with an initial 10-minute melt at 95 °C, followed by 40X cycles of 15 seconds at 95 °C and 1 minute at 60°C. qPCR reactions were plated in triplicate in 96-well PCR plates (Applied Biosystems, Thermo Fisher Scientific, Waltham, MA, USA) and sealed with adhesive optical film. A CFX96 Touch Real-Time PCR Detection System (Bio-Rad, Hercules, CA, USA) was used for running the reaction. Results were analyzed using the ΔΔCt Livak method[147], with *rpo1* as an internal housekeeping gene.

3.4.5 Growth assays

Growth assays were performed as previously described[148]. Briefly, 1.8 mL cultures were plated into 24-well flat-bottomed tissue culture plate (Corning Life Sciences, Durham, NC, USA) inside the anaerobic chamber (Coy Laboratory Products, Grass Lake, MI, USA) and sealed with optical film. All growth assays were performed in PIPES-buffered media as described above containing 2 μg/mL puromycin (for KD strains) and 100 μg/mL tetracycline (all strains). Plates were incubated in a microplate reader (Agilent BioTek Epoch 2, Agilent, Santa Clara, CA, USA) at 37°C, with brief shaking only before each reading every 1 hour. The growth rate was calculated from the slope of the linear fit of the $\log_{10}$-transformed optical density versus time with a minimum 20 points in the exponential phase with the highest R^2 value (minimum cut-off ≥ 0.97).

Conclusions

The continued warming of the earth is driven predominately by anthropogenic sources of greenhouse gasses[149]. The largest contribution to this warming is made by carbon dioxide and methane, with methane contributing an outsized effect due to its much larger warming potential compared with carbon dioxide[5]. The majority of methane in earth's atmosphere is produced by a single class of organism, methanogenic archaea, and each of these organisms use the same enzyme to produce methane, MCR[9]. In addition, the closely related ANME (anaerobic methanotrophic archaea) and ANKA (anaerobic alkane oxidizing archaea) use MCR and the closely related ACR for methane and short chain alkane oxidation, respectively[59]. Together, this places MCR in a critical role for global carbon cycling, especially when determining sources and sinks of methane and developing tools to mitigate methane emissions.

For several decades the work surrounding MCR focused either on *in vitro* biochemical characterization of its activity or on bulk measurements made by growing methanogens under varying laboratory conditions. In the past decade, a renewed interest in understanding MCR function in vivo has occurred, due largely to the advances made in tool development to genetically manipulate these organisms (see chapter 1.4). This has allowed for advances in our understanding of MCR assembly, cellular abundance, and activation. The work presented in this thesis joins this suite of recent discoveries to try and detangle the complicated biology of this enzyme. We were able to define and characterize the ATPase activity of component A2, a protein first described in association with MCR in 1985[91], but until now little focus has been paid towards it. Based on the work presented here, we provide a model to describe the interaction between component A2 and MCR, where ATP binding by component A2 is required first to enable interaction with MCR, and subsequent hydrolysis of ATP is modulated by this interaction. Although the work in this thesis has advanced our understanding of MCR activation and the specific role of component A2, many future studies to further characterize the exact mechanism of MCR assembly and reductive activation are required. Despite clear evidence, as described in chapter 1, that McrD assists in the installation of F430, the deletion of gene yields viable cells[29]. It is currently unknown how F430 installation occurs in the absence of McrD, and this remains ripe for future studies. Additionally, despite the huge advances made in characterizing aspects of the MCR activation complex[28], the source of electrons for reductive activation remains unknown. Uncovering the role of each component of this activation complex will help to answer this question as well as provide evolutionary context for MCR. Additionally, the regulation of each of the components involved in MCR assembly and activation is an area of work that is still, largely, unchartered.

As pieces of this puzzle continue to be put together, a more solid foundation will be established for generating specific inhibitors of methanogenesis. Although feed additives like 3-NOP are FDA approved, having an arsenal of antibiotics that may be used in this context will be paramount. The combination of biotechnological innovation with greater societal changes will be the greatest toolset available in the fight against global warming. Overall, the work I have described here characterized one of the essential parts of the MCR activation complex, component A2, and provided a framework for using *M. acetivorans* as a host for both genomic and biochemical studies of the MCR activation complex.

References

1. Bevacqua, E., Schleussner, C.-F. & Zscheischler, J. A year above 1.5 °C signals that Earth is most probably within the 20-year period that will reach the Paris Agreement limit. *Nat. Clim. Chang.* **15**, 262–265 (2025).
2. Foster, G. & Rahmstorf, S. Global Warming Has Accelerated Significantly. *Geophysical Research Letters* **53**, e2025GL118804 (2026).
3. NOAA National Centers for Environmental Information. *Monthly Global Climate Report for Annual 2024*. (2025) doi:https://www.ncei.noaa.gov/access/metadata/landing-page/bin/iso?id=gov.noaa.ncdc:C00672.
4. Parums, D. V. A Review of the Increasing Global Impact of Climate Change on Human Health and Approaches to Medical Preparedness. *Med Sci Monit* **30**, e945763-1-e945763-8 (2024).
5. Shan, Y. *et al.* Global methane footprints growth and drivers 1990-2023. *Nat Commun* **16**, 8184 (2025).
6. Mand, T. D. & Metcalf, W. W. Energy Conservation and Hydrogenase Function in Methanogenic Archaea, in Particular the Genus *Methanosarcina*. *Microbiol Mol Biol Rev* **83**, e00020-19 (2019).
7. Liu, Y. & Whitman, W. B. Metabolic, Phylogenetic, and Ecological Diversity of the Methanogenic Archaea. *Annals of the New York Academy of Sciences* **1125**, 171–189 (2008).
8. Vázquez-Salazar, A., Hernández-Morales, R., Mixcoha, E., Muñiz-Trejo, R. & Muñoz-Velasco, I. Methyl-coenzyme M reductase in archaeal methanogenesis: evolution, mechanism, and biotechnological perspectives. *Front. Catal.* **6**, (2026).
9. Thauer, R. K., Kaster, A.-K., Seedorf, H., Buckel, W. & Hedderich, R. Methanogenic archaea: ecologically relevant differences in energy conservation. *Nat Rev Microbiol* **6**, 579–591 (2008).
10. Borrel, G. *et al.* Wide diversity of methane and short-chain alkane metabolisms in uncultured archaea. *Nat Microbiol* **4**, 603–613 (2019).
11. Ellefson, W. L. & Wolfe, R. S. Role of component C in the methylreductase system of Methanobacterium. *Journal of Biological Chemistry* **255**, 8388–8389 (1980).
12. Ellefson, W. L. & Wolfe, R. S. Component C of the methylreductase system of Methanobacterium. *Journal of Biological Chemistry* **256**, 4259–4262 (1981).
13. Gunsalus, R. P. & Wolfe, R. S. Methyl coenzyme M reductase from Methanobacterium thermoautotrophicum. Resolution and properties of the components. *Journal of Biological Chemistry* **255**, 1891–1895 (1980).
14. Wolfe, R. S. & McBride, B. C. New coenzyme of methyl transfer, coenzyme M. *Biochemistry* **10**, 2317–2324 (1971).
15. Downing, B. E. & Nayak, D. D. Innovations in the electron transport chain fuel archaeal methane metabolism. *Trends in Biochemical Sciences* **50**, 425–437 (2025).
16. Nayak, D. D. & Metcalf, W. W. Cas9-mediated genome editing in the methanogenic archaeon Methanosarcina acetivorans. *Proceedings of the National Academy of Sciences of the United States of America* **114**, 2976–2981 (2017).

17. Guss, A. M., Rother, M., Zhang, J. K., Kulkkarni, G. & Metcalf, W. W. New methods for tightly regulated gene expression and highly efficient chromosomal integration of cloned genes for *Methanosarcina* species. *Archaea* **2**, 193–203 (2008).
18. Du, Q. *et al.* An improved CRISPR and CRISPR interference (CRISPRi) toolkit for engineering the model methanogenic archaeon Methanococcus maripaludis. *Microbial Cell Factories* **23**, 239 (2024).
19. Zhu, P., Somvanshi, T., Bao, J. & Scheller, S. CRISPR/Cas12a toolbox for genome editing in Methanosarcina acetivorans. *Frontiers in Microbiology* **14**, 1235616 (2023).
20. Boyd, J. M., Ellsworth, A. & Ensign, S. A. Characterization of 2-Bromoethanesulfonate as a Selective Inhibitor of the Coenzyme M-Dependent Pathway and Enzymes of Bacterial Aliphatic Epoxide Metabolism. *J Bacteriol* **188**, 8062–8069 (2006).
21. Liu, H., Wang, J., Wang, A. & Chen, J. Chemical inhibitors of methanogenesis and putative applications. *Appl Microbiol Biotechnol* **89**, 1333–1340 (2011).
22. Ni, G. *et al.* Methanogenesis inhibition remodels microbial fermentation and stimulates acetogenesis in ruminants. *Proceedings of the National Academy of Sciences* **122**, e2514823122 (2025).
23. Duin, E. C. *et al.* Mode of action uncovered for the specific reduction of methane emissions from ruminants by the small molecule 3-nitrooxypropanol. *Proc Natl Acad Sci U S A* **113**, 6172–6177 (2016).
24. Xie, X. *et al.* Mitigating enteric methane emissions: An overview of methanogenesis, inhibitors and future prospects. *Anim Nutr* **21**, 84–96 (2025).
25. Ermler, U., Grabarse, W., Shima, S., Goubeaud, M. & Thauer, R. K. Crystal Structure of Methyl-Coenzyme M Reductase: The Key Enzyme of Biological Methane Formation. *Science* **278**, 1457–1462 (1997).
26. Holliger, C., Pierik, A. J., Reijerse, E. J. & Hagen, W. R. A spectroelectrochemical study of factor F430 nickel(II/I) from methanogenic bacteria in aqueous solution. *J. Am. Chem. Soc.* **115**, 5651–5656 (1993).
27. Wongnate, T. *et al.* The radical mechanism of biological methane synthesis by methyl-coenzyme M reductase. *Science* **352**, 953–958 (2016).
28. Ramírez-Amador, F. *et al.* Structure of the ATP-driven methyl-coenzyme M reductase activation complex. *Nature* https://doi.org/10.1038/s41586-025-08890-7 (2025) doi:10.1038/s41586-025-08890-7.
29. Chadwick, G. L., Joiner, A. M. N., Ramesh, S., Mitchell, D. A. & Nayak, D. D. McrD binds asymmetrically to methyl-coenzyme M reductase improving active-site accessibility during assembly. *Proc. Natl. Acad. Sci. U.S.A.* **120**, e2302815120 (2023).
30. Rouvière, P. E., Bobik, T. A. & Wolfe, R. S. Reductive activation of the methyl coenzyme M methylreductase system of Methanobacterium thermoautotrophicum delta H. *J Bacteriol* **170**, 3946–3952 (1988).
31. Gao, B. & Gupta, R. S. Phylogenomic analysis of proteins that are distinctive of Archaea and its main subgroups and the origin of methanogenesis. *BMC Genomics* **8**, 86 (2007).

32. Ginovska, B., Raugei, S., Ragsdale, S. W., Ohmer, C. & Sarangi, R. Structural and Mechanistic Advances in the Chemistry of Methyl-Coenzyme M Reductase (MCR). *Acc. Chem. Res.* **58**, 824–833 (2025).
33. Wu, H.-H. *et al.* The pathway for coenzyme M biosynthesis in bacteria. *Proceedings of the National Academy of Sciences of the United States of America* **119**, e2207190119 (2022).
34. White, R. H. Identification of an Enzyme Catalyzing the Conversion of Sulfoacetaldehyde to 2-Mercaptoethanesulfonic Acid in Methanogens. *Biochemistry* **58**, 1958–1962 (2019).
35. Chadwick, G. L., Williams, M. C., Shalvarjian, K. E. & Nayak, D. D. Methanogenesis marker 16 metalloprotein is the primary coenzyme M synthase in Methanosarcina acetivorans. *PLOS Genetics* **21**, e1011695 (2025).
36. Graham, D. E., Xu, H. & White, R. H. Identification of coenzyme M biosynthetic phosphosulfolactate synthase: a new family of sulfonate-biosynthesizing enzymes. *The Journal of Biological Chemistry* **277**, 13421–13429 (2002).
37. Graham, D. E., Graupner, M., Xu, H. & White, R. H. Identification of coenzyme M biosynthetic 2-phosphosulfolactate phosphatase. A member of a new class of Mg(2+)-dependent acid phosphatases. *European Journal of Biochemistry / FEBS* **268**, 5176–5188 (2001).
38. Graupner, M., Xu, H. & White, R. H. Identification of an archaeal 2-hydroxy acid dehydrogenase catalyzing reactions involved in coenzyme biosynthesis in methanoarchaea. *Journal of Bacteriology* **182**, 3688–3692 (2000).
39. Graham, D. E., Taylor, S. M., Wolf, R. Z. & Namboori, S. C. Convergent evolution of coenzyme M biosynthesis in the Methanosarcinales: cysteate synthase evolved from an ancestral threonine synthase. *The Biochemical Journal* **424**, 467–478 (2009).
40. Helgadóttir, S., Rosas-Sandoval, G., Söll, D. & Graham, D. E. Biosynthesis of phosphoserine in the Methanococcales. *Journal of Bacteriology* **189**, 575–582 (2007).
41. Graupner, M., Xu, H. & White, R. H. Identification of the gene encoding sulfopyruvate decarboxylase, an enzyme involved in biosynthesis of coenzyme M. *Journal of Bacteriology* **182**, 4862–4867 (2000).
42. Howell, D. M., Graupner, M., Xu, H. & White, R. H. Identification of enzymes homologous to isocitrate dehydrogenase that are involved in coenzyme B and leucine biosynthesis in methanoarchaea. *Journal of Bacteriology* **182**, 5013–5016 (2000).
43. Howell, D. M., Harich, K., Xu, H. & White, R. H. Alpha-keto acid chain elongation reactions involved in the biosynthesis of coenzyme B (7-mercaptoheptanoyl threonine phosphate) in methanogenic Archaea. *Biochemistry* **37**, 10108–10117 (1998).
44. Drevland, R. M., Jia, Y., Palmer, D. R. J. & Graham, D. E. Methanogen homoaconitase catalyzes both hydrolyase reactions in coenzyme B biosynthesis. *The Journal of Biological Chemistry* **283**, 28888–28896 (2008).
45. Zheng, K., Ngo, P. D., Owens, V. L., Yang, X.-P. & Mansoorabadi, S. O. The biosynthetic pathway of coenzyme F430 in methanogenic and methanotrophic archaea. *Science* **354**, 339–342 (2016).
46. Moore, S. J. *et al.* Elucidation of the biosynthesis of the methane catalyst coenzyme F430. *Nature* **543**, 78–82 (2017).

47. Mayr, S. *et al.* Structure of an F430 variant from archaea associated with anaerobic oxidation of methane. *Journal of the American Chemical Society* **130**, 10758–10767 (2008).
48. Allen, K. D., Wegener, G. & White, R. H. Discovery of multiple modified F(430) coenzymes in methanogens and anaerobic methanotrophic archaea suggests possible new roles for F(430) in nature. *Applied and Environmental Microbiology* **80**, 6403–6412 (2014).
49. Polêto, M. D., Allen, K. D. & Lemkul, J. A. Structural Dynamics of the Methyl-Coenzyme M Reductase Active Site Are Influenced by Coenzyme F430 Modifications. *Biochemistry* **63**, 1783–1794 (2024).
50. Nayak, D. D., Mahanta, N., Mitchell, D. A. & Metcalf, W. W. Post-translational thioamidation of methyl-coenzyme M reductase, a key enzyme in methanogenic and methanotrophic Archaea. *eLife* **6**, e29218 (2017).
51. Lyu, Z. *et al.* Posttranslational Methylation of Arginine in Methyl Coenzyme M Reductase Has a Profound Impact on both Methanogenesis and Growth of Methanococcus maripaludis. *Journal of Bacteriology* **202**, 10.1128/jb.00654-19 (2020).
52. Deobald, D., Adrian, L., Schöne, C., Rother, M. & Layer, G. Identification of a unique Radical SAM methyltransferase required for the sp3-C-methylation of an arginine residue of methyl-coenzyme M reductase. *Scientific Reports* **8**, 7404 (2018).
53. Radle, M. I., Miller, D. V., Laremore, T. N. & Booker, S. J. Methanogenesis marker protein 10 (Mmp10) from Methanosarcina acetivorans is a radical S-adenosylmethionine methylase that unexpectedly requires cobalamin. *The Journal of Biological Chemistry* **294**, 11712–11725 (2019).
54. Prakash, D., Wu, Y., Suh, S.-J. & Duin, E. C. Elucidating the Process of Activation of Methyl-Coenzyme M Reductase. *J Bacteriol* **196**, 2491–2498 (2014).
55. Welander, P. V. & Metcalf, W. W. Loss of the mtr operon in Methanosarcina blocks growth on methanol, but not methanogenesis, and reveals an unknown methanogenic pathway. *Proceedings of the National Academy of Sciences* **102**, 10664–10669 (2005).
56. Kuhner, C. H., Lindenbach, B. D. & Wolfe, R. S. Component A2 of methylcoenzyme M reductase system from Methanobacterium thermoautotrophicum delta H: nucleotide sequence and functional expression by Escherichia coli. *J Bacteriol* **175**, 3195–3203 (1993).
57. Aziz, I. *et al.* Structural and mechanistic basis of the central energy-converting methyltransferase complex of methanogenesis. *Proceedings of the National Academy of Sciences of the United States of America* **121**, e2315568121 (2024).
58. Bramkamp, M., Gaßel, M., Herkenhoff-Hesselmann, B., Bertrand, J. & Altendorf, K. The Methanocaldococcus jannaschii protein Mj0968 is not a P-type ATPase. *FEBS Letters* **543**, 31–36 (2003).
59. Gendron, A. & Allen, K. D. Overview of Diverse Methyl/Alkyl-Coenzyme M Reductases and Considerations for Their Potential Heterologous Expression. *Frontiers in Microbiology* **13**, 867342 (2022).
60. Nayak, D. D. *et al.* Functional interactions between posttranslationally modified amino acids of methyl-coenzyme M reductase in Methanosarcina acetivorans. *PLOS Biology* **18**, e3000507 (2020).

61. Rodriguez Carrero, R. J. *et al.* Genetic and biochemical characterization of a radical SAM enzyme required for post-translational glutamine methylation of methyl-coenzyme M reductase. *mBio* **16**, e0354624 (2025).
62. Sutherland-Smith, A. J. *et al.* The crystal structure of methanogen McrD, a methyl-coenzyme M reductase-associated protein. *FEBS open bio* **14**, 1222–1229 (2024).
63. Goubeaud, M., Schreiner, G. & Thauer, R. K. Purified methyl-coenzyme-M reductase is activated when the enzyme-bound coenzyme F430 is reduced to the nickel(I) oxidation state by titanium(III) citrate. *European Journal of Biochemistry / FEBS* **243**, 110–114 (1997).
64. Rospert, S., Böcher, R., Albracht, S. P. & Thauer, R. K. Methyl-coenzyme M reductase preparations with high specific activity from H2-preincubated cells of Methanobacterium thermoautotrophicum. *FEBS Letters* **291**, 371–375 (1991).
65. Zhou, Y., Dorchak, A. E. & Ragsdale, S. W. In vivo activation of methyl-coenzyme M reductase by carbon monoxide. *Frontiers in Microbiology* **4**, 69 (2013).
66. Ohmer, C. J. *et al.* Structure of active methyl-CoM reductase, Earth's main methane producer. 2025.04.26.650772 Preprint at https://doi.org/10.1101/2025.04.26.650772 (2025).
67. Olson, K. D., McMahon, C. W. & Wolfe, R. S. Photoactivation of the 2-(methylthio)ethanesulfonic acid reductase from Methanobacterium. *Proceedings of the National Academy of Sciences of the United States of America* **88**, 4099–4103 (1991).
68. Goenrich, M., Duin, E. C., Mahlert, F. & Thauer, R. K. Temperature dependence of methyl-coenzyme M reductase activity and of the formation of the methyl-coenzyme M reductase red2 state induced by coenzyme B. *Journal of Biological Inorganic Chemistry* **10**, 333–342 (2005).
69. Guss, A. M., Kulkarni, G. & Metcalf, W. W. Differences in hydrogenase gene expression between Methanosarcina acetivorans and Methanosarcina barkeri. *Journal of Bacteriology* **191**, 2826–2833 (2009).
70. Welte, C. & Deppenmeier, U. Membrane-bound electron transport in Methanosaeta thermophila. *Journal of Bacteriology* **193**, 2868–2870 (2011).
71. Ossmer, R. *et al.* Immunocytochemical localization of component C of the methylreductase system in Methanococcus voltae and Methanobacterium thermoautotrophicum. *Proceedings of the National Academy of Sciences of the United States of America* **83**, 5789–5792 (1986).
72. Aldrich, H. C., Beimborn, D. B., Bokranz, M. & Schönheit, P. Immunocytochemical localization of methyl-coenzyme M reductase in Methanobacterium thermoautotrophicum. *Arch. Microbiol.* **147**, 190–194 (1987).
73. Chadwick, G. L., Dury, G. A. & Nayak, D. D. Physiological and transcriptomic response to methyl-coenzyme M reductase limitation in Methanosarcina acetivorans. *Applied and Environmental Microbiology* **90**, e0222023 (2024).
74. Bao, J., de Dios Mateos, E. & Scheller, S. Efficient CRISPR/Cas12a-Based Genome-Editing Toolbox for Metabolic Engineering in Methanococcus maripaludis. *ACS synthetic biology [electronic resource]* **11**, 2496–2503 (2022).
75. Dhamad, A. E. & Lessner, D. J. A CRISPRi-dCas9 System for Archaea and Its Use To Examine Gene Function during Nitrogen Fixation by Methanosarcina acetivorans. *Applied and Environmental Microbiology* **86**, (2020).

76. Wetmore, K. M. *et al.* Rapid quantification of mutant fitness in diverse bacteria by sequencing randomly bar-coded transposons. *mBio* **6**, e00306-15 (2015).
77. Day, L. A. *et al.* High-throughput genetics enables identification of nutrient utilization and accessory energy metabolism genes in a model methanogen. *mBio* **15**, e0078124 (2024).
78. Hernandez, E. & Costa, K. C. The Fluorescence-Activating and Absorption-Shifting Tag (FAST) Enables Live-Cell Fluorescence Imaging of Methanococcus maripaludis. *Journal of Bacteriology* **204**, e0012022 (2022).
79. Plamont, M.-A. *et al.* Small fluorescence-activating and absorption-shifting tag for tunable protein imaging in vivo. *Proceedings of the National Academy of Sciences of the United States of America* **113**, 497–502 (2016).
80. Adlung, N. & Scheller, S. Application of the Fluorescence-Activating and Absorption-Shifting Tag (FAST) for Flow Cytometry in Methanogenic Archaea. *Applied and Environmental Microbiology* **89**, e0178622 (2023).
81. Hallam, S. J. *et al.* Reverse Methanogenesis: Testing the Hypothesis with Environmental Genomics. *Science* **305**, 1457–1462 (2004).
82. Shima, S. *et al.* Structure of a methyl-coenzyme M reductase from Black Sea mats that oxidize methane anaerobically. *Nature* **481**, 98–101 (2011).
83. Lemaire, O. N. & Wagner, T. A Structural View of Alkyl-Coenzyme M Reductases, the First Step of Alkane Anaerobic Oxidation Catalyzed by Archaea. *Biochemistry* **61**, 805–821 (2022).
84. Laso-Pérez, R. *et al.* Anaerobic Degradation of Non-Methane Alkanes by " *Candidatus* Methanoliparia" in Hydrocarbon Seeps of the Gulf of Mexico. *mBio* **10**, e01814-19 (2019).
85. Rospert, S., Böcher, R., Albracht, S. P. J. & Thauer, R. K. Methyl-coenzyme M reductase preparations with high specific activity from H_2-preincubated cells of *Methanobacterium thermoautotrophicum*. *FEBS Letters* **291**, 371–375 (1991).
86. Rouvière, P. E., Bobik, T. A. & Wolfe, R. S. Reductive activation of the methyl coenzyme M methylreductase system of Methanobacterium thermoautotrophicum delta H. *J Bacteriol* **170**, 3946–3952 (1988).
87. Ellefson, W. L., Whitman, W. B. & Wolfe, R. S. Nickel-containing factor F430: chromophore of the methylreductase of Methanobacterium. *Proc. Natl. Acad. Sci. U.S.A.* **79**, 3707–3710 (1982).
88. Adler, S. A., Chadwick, G. L. & Nayak, D. D. Assembly and maturation of methyl-coenzyme M reductase in methanogenic archaea. *Current Opinion in Microbiology* **87**, 102637 (2025).
89. Thauer, R. K. Methyl (Alkyl)-Coenzyme M Reductases: Nickel F-430-Containing Enzymes Involved in Anaerobic Methane Formation and in Anaerobic Oxidation of Methane or of Short Chain Alkanes. *Biochemistry* **58**, 5198–5220 (2019).
90. Gunsalus, R. P. & Wolfe, R. S. Methyl coenzyme M reductase from Methanobacterium thermoautotrophicum. Resolution and properties of the components. *Journal of Biological Chemistry* **255**, 1891–1895 (1980).
91. Rouvière, P. E., Escalante-Semerena, J. C. & Wolfe, R. S. Component A2 of the methylcoenzyme M methylreductase system from Methanobacterium thermoautotrophicum. *J Bacteriol* **162**, 61–66 (1985).

92. Nagle, D. P. & Wolfe, R. S. Component A of the methyl coenzyme M methylreductase system of Methanobacterium: resolution into four components. *Proc. Natl. Acad. Sci. U.S.A.* **80**, 2151–2155 (1983).
93. Shelton, E. B. *et al.* An Expanded Molecular Model for the Activation of Methyl-Coenzyme M Reductase. *Biochemistry* **64**, 4424–4436 (2025).
94. Borrel, G. *et al.* Wide diversity of methane and short-chain alkane metabolisms in uncultured archaea. *Nat Microbiol* **4**, 603–613 (2019).
95. Shalvarjian, K. E. *et al.* Methanogenic archaea encoding Pyrrolysine maintain ambiguous amber codon usage. *Proceedings of the National Academy of Sciences* **122**, e2517473122 (2025).
96. Downing, B. E., Gupta, D., Shalvarjian, K. E. & Nayak, D. D. Genus-specific remodeling of carbon and energy metabolism facilitates acetoclastic methanogenesis in Methanosarcina spp. and Methanothrix spp. *Journal of Bacteriology* **208**, e00448-25 (2026).
97. Saini, J., Dhamad, A., Muniyasamy, A., Alverson, A. J. & Lessner, D. J. The nitrogenase cofactor biogenesis enzyme NifB is essential for the viability of methanogens. Preprint at https://doi.org/10.1101/2023.10.20.563283 (2023).
98. Kuhner, C. H., Lindenbach, B. D. & Wolfe, R. S. Component A2 of methylcoenzyme M reductase system from Methanobacterium thermoautotrophicum delta H: nucleotide sequence and functional expression by Escherichia coli. *J Bacteriol* **175**, 3195–3203 (1993).
99. Hanson, P. I. & Whiteheart, S. W. AAA+ proteins: have engine, will work. *Nat Rev Mol Cell Biol* **6**, 519–529 (2005).
100. Orelle, C., Dalmas, O., Gros, P., Di Pietro, A. & Jault, J.-M. The Conserved Glutamate Residue Adjacent to the Walker-B Motif Is the Catalytic Base for ATP Hydrolysis in the ATP-binding Cassette Transporter BmrA. *Journal of Biological Chemistry* **278**, 47002–47008 (2003).
101. Khan, M. F. *et al.* Determination of Protein–Ligand Binding Affinities by Thermal Shift Assay. *ACS Pharmacol. Transl. Sci.* **7**, 3096–3107 (2024).
102. Abramson, J. *et al.* Accurate structure prediction of biomolecular interactions with AlphaFold 3. *Nature* **630**, 493–500 (2024).
103. Zhou, Z. *et al.* Non-syntrophic methanogenic hydrocarbon degradation by an archaeal species. *Nature* **601**, 257–262 (2022).
104. Bonacker, L. G., Baudner, S., Mörschel, E., Böcher, R. & Thauer, R. K. Properties of the two isoenzymes of methyl-coenzyme M reductase in Methanobacterium thermoautotrophicum. *Eur J Biochem* **217**, 587–595 (1993).
105. Pace, N. J. & Weerapana, E. Zinc-Binding Cysteines: Diverse Functions and Structural Motifs. *Biomolecules* **4**, 419 (2014).
106. Howard, J. B. & Rees, D. C. Structural Basis of Biological Nitrogen Fixation. *Chem. Rev.* **96**, 2965–2982 (1996).
107. Rutledge, H. L. & Tezcan, F. A. Electron Transfer in Nitrogenase. *Chem Rev* **120**, 5158–5193 (2020).
108. Rice, A. J., Park, A. & Pinkett, H. W. Diversity in ABC transporters: Type I, II and III importers. *Crit Rev Biochem Mol Biol* **49**, 426–437 (2014).

109. Gibson, D. G. *et al.* Enzymatic assembly of DNA molecules up to several hundred kilobases. *Nat Methods* **6**, 343–345 (2009).
110. Kim, S. Y. *et al.* Different biosynthetic pathways to fosfomycin in Pseudomonas syringae and Streptomyces species. *Antimicrob Agents Chemother* **56**, 4175–4183 (2012).
111. Metcalf, W. W., Zhang, J. K., Apolinario, E., Sowers, K. R. & Wolfe, R. S. A genetic system for Archaea of the genus Methanosarcina: liposome-mediated transformation and construction of shuttle vectors. *Proc Natl Acad Sci U S A* **94**, 2626–2631 (1997).
112. Deatherage, D. E. & Barrick, J. E. Identification of mutations in laboratory evolved microbes from next-generation sequencing data using breseq. *Methods Mol Biol* **1151**, 165–188 (2014).
113. Duin, E. C., Prakash, D. & Brungess, C. Methyl-Coenzyme M Reductase from Methanothermobacter marburgensis. in *Methods in Enzymology* vol. 494 159–187 (Elsevier, 2011).
114. Blum, M. *et al.* InterPro: the protein sequence classification resource in 2025. *Nucleic Acids Research* **53**, D444–D456 (2025).
115. Meng, E. C. *et al.* UCSF ChimeraX: Tools for structure building and analysis. *Protein Science* **32**, e4792 (2023).
116. Haft, D. H. TIGRFAMs: a protein family resource for the functional identification of proteins. *Nucleic Acids Research* **29**, 41–43 (2001).
117. Edgar, R. C. Muscle5: High-accuracy alignment ensembles enable unbiased assessments of sequence homology and phylogeny. *Nat Commun* **13**, 6968 (2022).
118. Crooks, G. E., Hon, G., Chandonia, J.-M. & Brenner, S. E. WebLogo: A Sequence Logo Generator: Figure 1. *Genome Res.* **14**, 1188–1190 (2004).
119. Li, W. & Godzik, A. Cd-hit: a fast program for clustering and comparing large sets of protein or nucleotide sequences. *Bioinformatics* **22**, 1658–1659 (2006).
120. Stamatakis, A. RAxML version 8: a tool for phylogenetic analysis and post-analysis of large phylogenies. *Bioinformatics* **30**, 1312–1313 (2014).
121. Letunic, I. & Bork, P. Interactive Tree Of Life (iTOL) v5: an online tool for phylogenetic tree display and annotation. *Nucleic Acids Res* **49**, W293–W296 (2021).
122. Stetter, K. O. History of discovery of the first hyperthermophiles. *Extremophiles* **10**, 357–362 (2006).
123. Holden, J. F. & Sistu, H. Formate and hydrogen in hydrothermal vents and their use by extremely thermophilic methanogens and heterotrophs. *Front Microbiol* **14**, 1093018 (2023).
124. Zeng, X., Alain, K. & Shao, Z. Microorganisms from deep-sea hydrothermal vents. *Mar Life Sci Technol* **3**, 204–230 (2021).
125. Mathrani, I. M., Boone, D. R., Mah, R. A., Fox, G. E. & Lau, P. P. Methanohalophilus zhilinae sp. nov., an Alkaliphilic, Halophilic, Methylotrophic Methanogen. *International Journal of Systematic and Evolutionary Microbiology* **38**, 139–142 (1988).
126. Sorokin, D. Y. *et al.* Discovery of extremely halophilic, methyl-reducing euryarchaea provides insights into the evolutionary origin of methanogenesis. *Nat Microbiol* **2**, 17081 (2017).
127. Rajendran, S. *et al.* Methane Emission from Rice Fields: Necessity for Molecular Approach for Mitigation. *Rice Science* **31**, 159–178 (2024).

128. L Bräuer, S., Basiliko, N., M P Siljanen, H. & H Zinder, S. Methanogenic archaea in peatlands. *FEMS Microbiol Lett* **367**, fnaa172 (2020).
129. Grégoire, D. S., George, N. A. & Hug, L. A. Microbial methane cycling in a landfill on a decadal time scale. *Nat Commun* **14**, 7402 (2023).
130. Hoegenauer, C., Hammer, H. F., Mahnert, A. & Moissl-Eichinger, C. Methanogenic archaea in the human gastrointestinal tract. *Nat Rev Gastroenterol Hepatol* **19**, 805–813 (2022).
131. Volmer, J. G., McRae, H. & Morrison, M. The evolving role of methanogenic archaea in mammalian microbiomes. *Front. Microbiol.* **14**, (2023).
132. Brune, A. Symbiotic digestion of lignocellulose in termite guts. *Nat Rev Microbiol* **12**, 168–180 (2014).
133. Jinek, M. *et al.* A Programmable Dual-RNA–Guided DNA Endonuclease in Adaptive Bacterial Immunity. *Science* **337**, 816–821 (2012).
134. Qi, L. S. *et al.* Repurposing CRISPR as an RNA-Guided Platform for Sequence-Specific Control of Gene Expression. *Cell* **152**, 1173–1183 (2013).
135. Zhang, R., Xu, W., Shao, S. & Wang, Q. Gene Silencing Through CRISPR Interference in Bacteria: Current Advances and Future Prospects. *Front. Microbiol.* **12**, (2021).
136. Thomm, M., Sherf, B. A. & Reeve, J. N. RNA polymerase-binding and transcription initiation sites upstream of the methyl reductase operon of Methanococcus vannielii. *Journal of Bacteriology* **170**, 1958–1961 (1988).
137. Peters, J. M. *et al.* A Comprehensive, CRISPR-based Functional Analysis of Essential Genes in Bacteria. *Cell* **165**, 1493–1506 (2016).
138. Peters, J. M. *et al.* Bacterial CRISPR: accomplishments and prospects. *Current Opinion in Microbiology* **27**, 121–126 (2015).
139. Wang, T. *et al.* Pooled CRISPR interference screening enables genome-scale functional genomics study in bacteria with superior performance. *Nat Commun* **9**, 2475 (2018).
140. Conway, T. *et al.* Unprecedented High-Resolution View of Bacterial Operon Architecture Revealed by RNA Sequencing. *mBio* **5**, 10.1128/mbio.01442-14 (2014).
141. Ruepp, A. & Soppa, J. Fermentative arginine degradation in Halobacterium salinarium (formerly Halobacterium halobium): genes, gene products, and transcripts of the arcRACB gene cluster. *Journal of Bacteriology* **178**, 4942–4947 (1996).
142. Koide, T. *et al.* Prevalence of transcription promoters within archaeal operons and coding sequences. *Mol Syst Biol* **5**, MSB200942 (2009).
143. Jäger, D., Förstner, K. U., Sharma, C. M., Santangelo, T. J. & Reeve, J. N. Primary transcriptome map of the hyperthermophilic archaeon Thermococcus kodakarensis. *BMC Genomics* **15**, 684 (2014).
144. Li, J. *et al.* Global mapping transcriptional start sites revealed both transcriptional and post-transcriptional regulation of cold adaptation in the methanogenic archaeon Methanolobus psychrophilus. *Sci Rep* **5**, 9209 (2015).
145. Li, J. *et al.* The archaeal RNA chaperone TRAM0076 shapes the transcriptome and optimizes the growth of Methanococcus maripaludis. *PLOS Genetics* **15**, e1008328 (2019).

146. Shinzato, N. *et al.* Specific DNA Binding of a Potential Transcriptional Regulator, Inosine 5′-Monophosphate Dehydrogenase-Related Protein VII, to the Promoter Region of a Methyl Coenzyme M Reductase I-Encoding Operon Retrieved from Methanothermobacter thermautotrophicus Strain ΔH. *Applied and Environmental Microbiology* **74**, 6239–6247 (2008).
147. Livak, K. J. & Schmittgen, T. D. Analysis of relative gene expression data using real-time quantitative PCR and the 2(-Delta Delta C(T)) Method. *Methods* **25**, 402–408 (2001).
148. Baskevitch, A. S. & Nayak, D. D. Histones and nucleoid-associated proteins in Methanosarcina acetivorans mediate recovery from stress and stasis. 2025.11.24.690127 Preprint at https://doi.org/10.1101/2025.11.24.690127 (2025).
149. Calvin, K. *et al. IPCC, 2023: Climate Change 2023: Synthesis Report. Contribution of Working Groups I, II and III to the Sixth Assessment Report of the Intergovernmental Panel on Climate Change [Core Writing Team, H. Lee and J. Romero (Eds.)]. IPCC, Geneva, Switzerland.* https://www.ipcc.ch/report/ar6/syr/ (2023) doi:10.59327/IPCC/AR6-9789291691647.
150. Adler, B. A. *et al.* CRISPRi-ART enables functional genomics of diverse bacteriophages using RNA-binding dCas13d. *Nat Microbiol* **10**, 694–709 (2025).

Appendix A. Supplementary information to Chapter 2

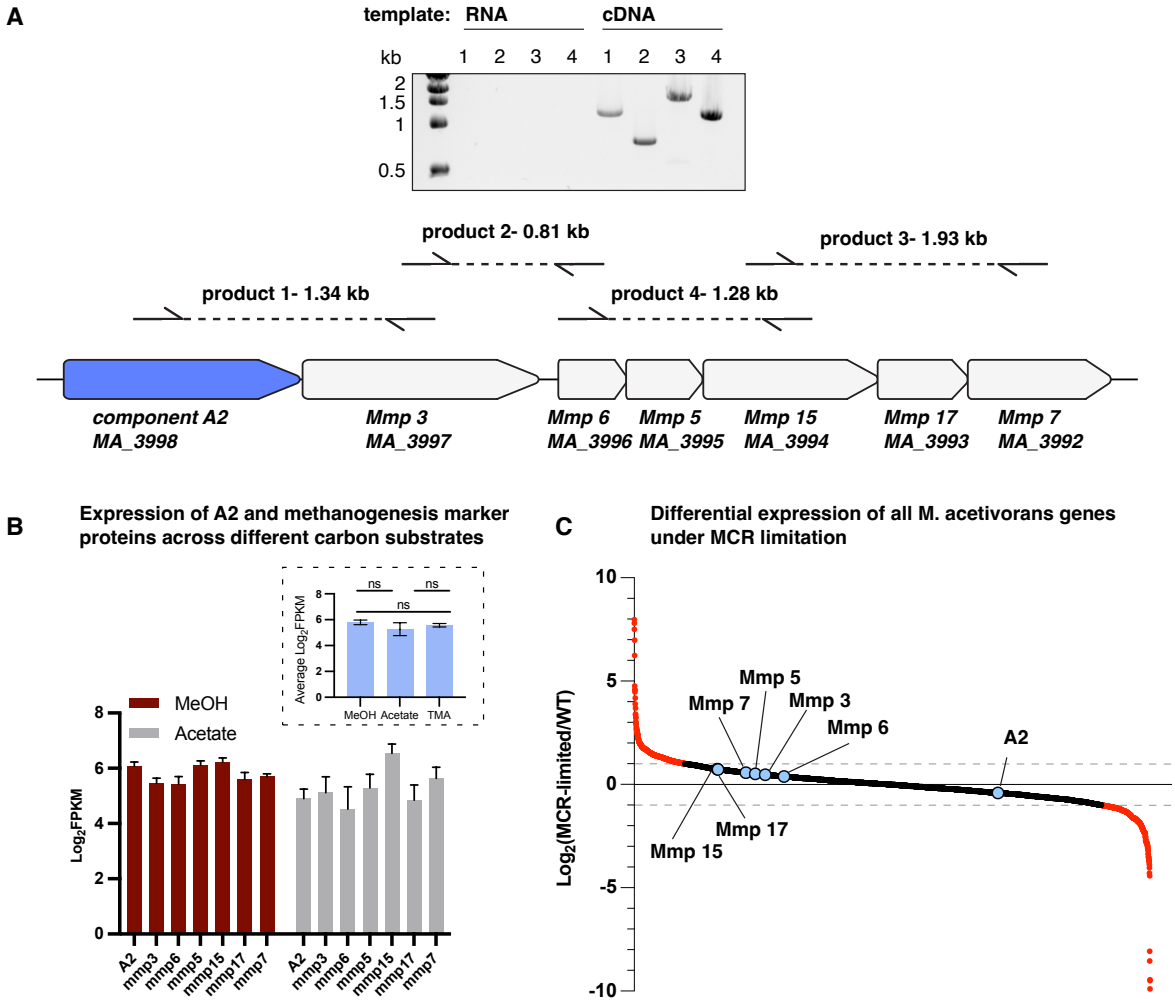

Fig S2.1. Expression analysis of the methyl-coenzyme M reductase (MCR) activation operon in *Methanosarcina acetivorans*. (a) Agarose gel electrophoresis showing the PCR products generated from the primer pairs across all gene boundaries for the MCR activation operon with either RNA or cDNA synthesized from the RNA as the template used for the PCR reactions. Lanes 1-4 correspond to the products for the primers pairs labelled 1-4 on the chromosome map shown below. Component A2 is highlighted in blue. (b) expression of genes in the MCR activation operon on during growth on high-salt (HS) minimal-medium supplemented with 125 mM methanol (MeOH; maroon) or 40 mM acetate (gray) as the sole carbon and energy substrate at 37 °C. Error bars represent the standard deviation for three replicates. Inset shows average expression of the MCR activation operon on MeOH, TMA, and acetate. Error bars represent the standard deviation of three replicates. Statistical significance tested by unpaired Welch's t test. ns indicates a p-value > 0.05 (c) Differential expression of all genes in *M. acetivorans* between strains WWM60 (parent) and DDN032 (P*mcrB*(tetO1)-*mcrBDCGA*) grown

without tetracycline to curtail growth by limiting the level of MCR in the cell. Genes are ordered along the x-axis from highest to lowest differential expression. Genes with a log2-fold change > 1 or <1 are show in red and genes with a log2-fold change in expression between -1 and 1 are shown in black. Genes in the MCR activation operon are highlighted.

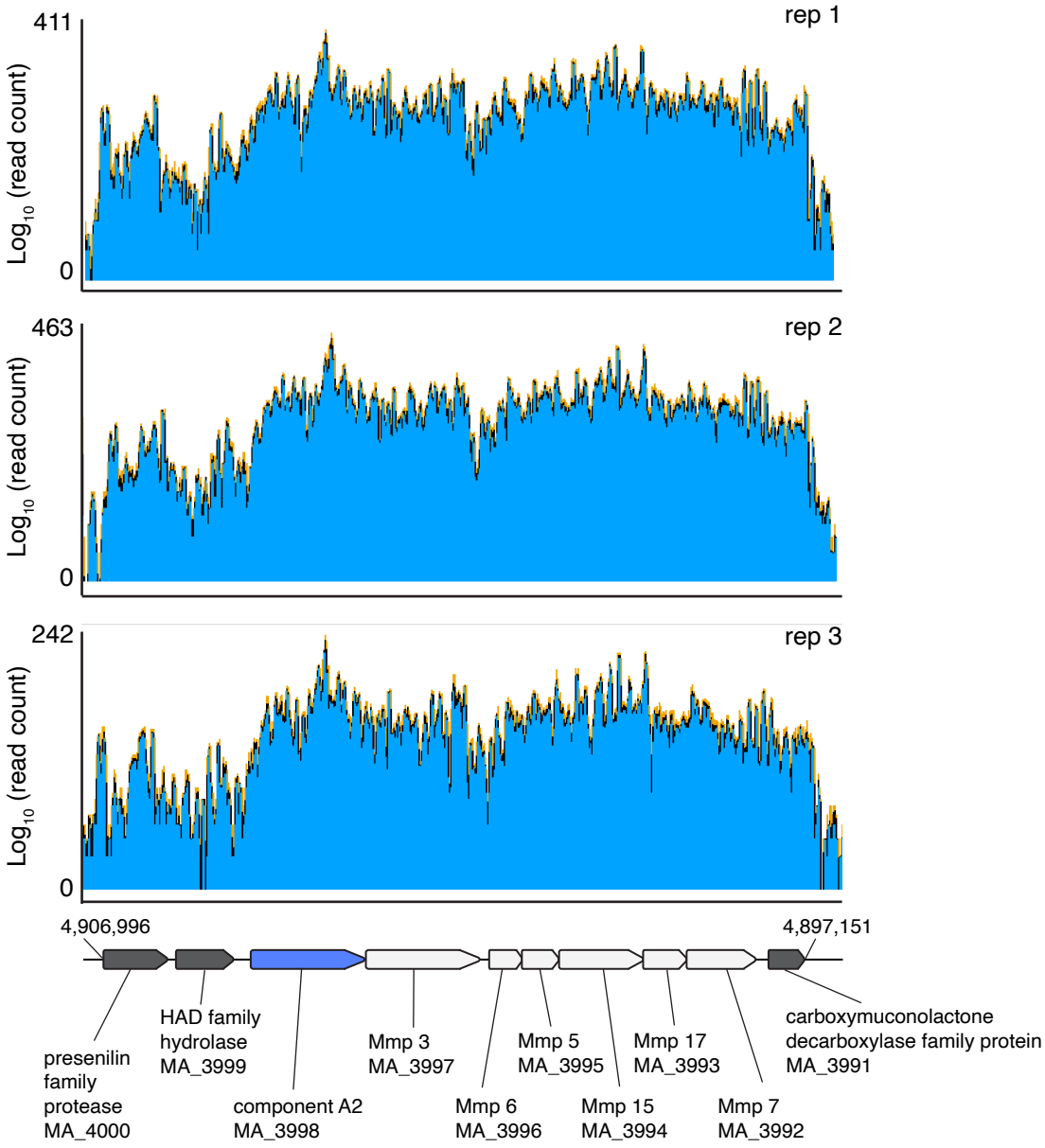

Fig S2.2 RNAseq reads [95] mapped across the genomic region of *M. acetivorans* containing the MCR activation operon. Paired-end RNA read coverage of the MCR activation operon during growth on TMA and ~2 kilobase up stream and ~1s kilobase down stream genes included. Three technical replicates (denoted as rep1, rep2, and rep3) are shown. Reads are aligned to the chromosomal locus as indicated below.

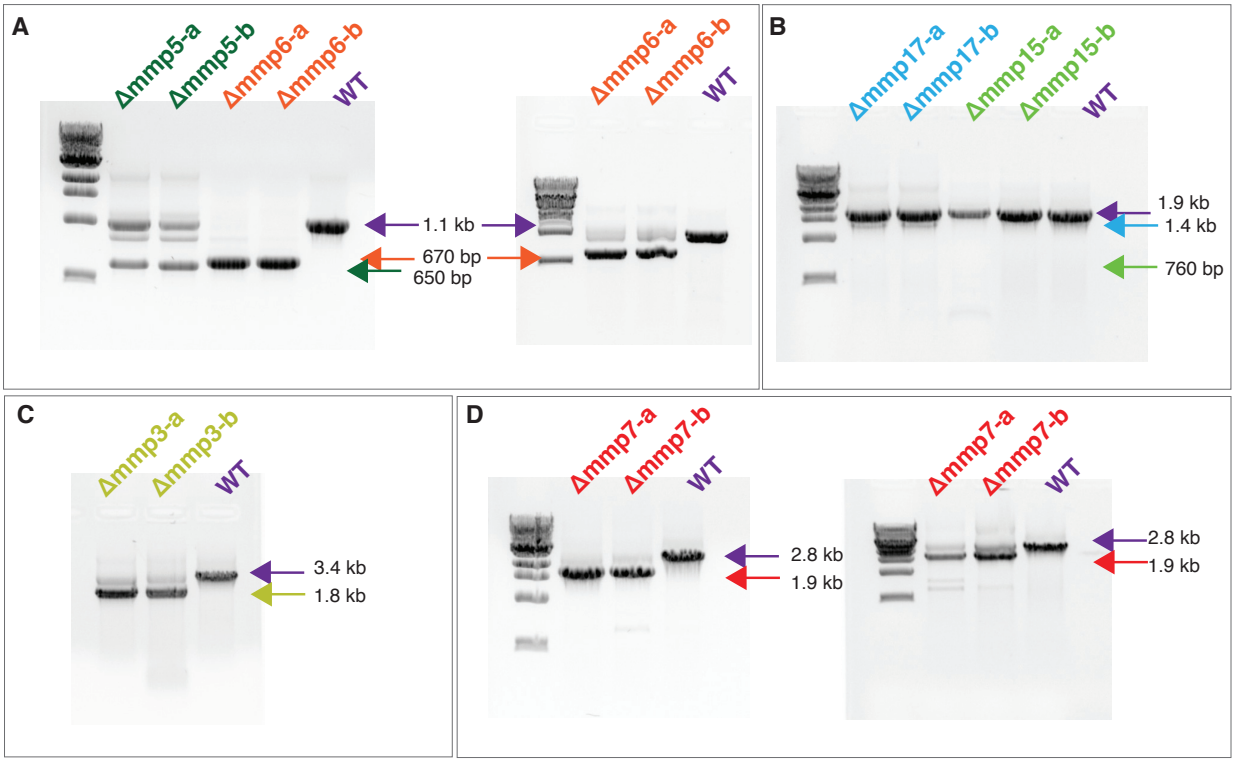

Fig S2.3 Attempts to delete genes in the MCR activation operon fail to yield clean deletion mutants. Example gels showing the PCR product generated with primers flanking the gene of interest from puromycin resistant colonies post transformation of the CRISPR-editing plasmid. (a) Diagnostic PCR for puromycin-resistant colonies (labeled a-b) when WWM60 was transformed with CRISPR-editing plasmids to delete Mmp5 and Mmp6, respectively. The PCR product corresponding to the wildtype (WT) allele is shown in purple, the PCR product corresponding to the deletion of Mmp5 is shown in dark green, and the PCR product corresponding to the deletion of Mmp6 is shown in orange (left). The gel on the right shows the appearance of a PCR product corresponding to the WT allele several passages of the Δmmp6 cultures. (b) Diagnostic PCR for puromycin-resistant colonies (labeled a-b) when WWM60 was transformed with CRISPR-editing plasmids to delete Mmp17 and Mmp15, respectively. The PCR product corresponding to the wildtype (WT) allele is shown in purple, the PCR product corresponding to the deletion of Mmp17 is shown in light blue, and the PCR product corresponding to the deletion of Mmp15 is shown in light green. (c) Diagnostic PCR for puromycin-resistant colonies (labeled a-b) when WWM60 was transformed with CRISPR-editing plasmids to delete Mmp3. The PCR product corresponding to the wildtype (WT) allele is shown in purple and the PCR product corresponding to the deletion of Mmp3 is shown in chartreuse. (d) Diagnostic PCR for puromycin-resistant colonies (labeled a-b) when WWM60 was transformed with CRISPR-editing plasmids to delete Mmp7. The PCR product corresponding to the wildtype (WT) allele is shown in purple and the PCR product corresponding to the deletion of Mmp3 is shown in red (left). The gel on the right shows the increased appearance of the PCR product corresponding to the WT allele after several round of passages of the Δmmp7 cultures.

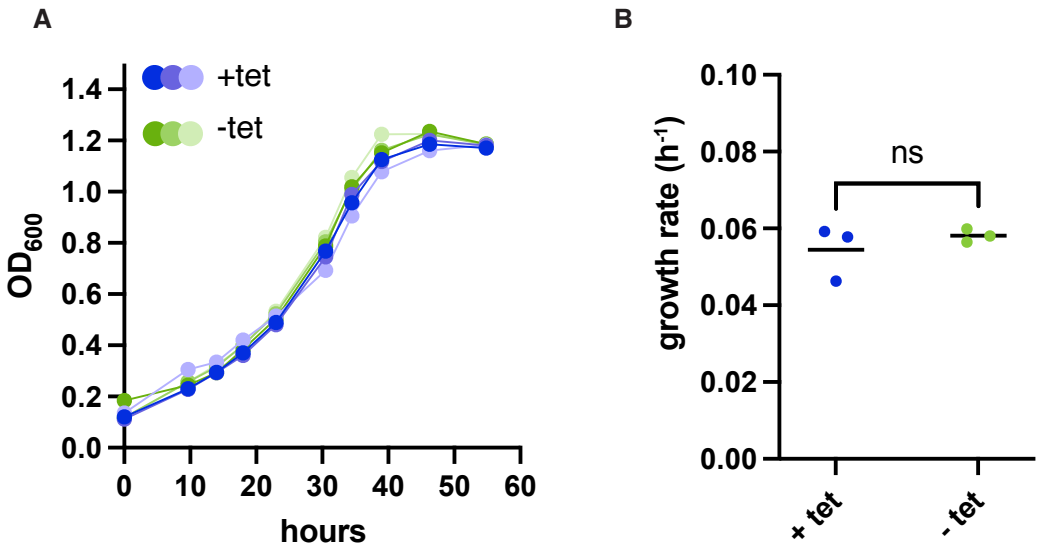

Fig S2.4 Analysis of growth when component A2 is overexpressed in *M. acetivorans*. (a) Growth curves of DDN122 expressing component A2 from the P*mcrB*(tetO1) tetracycline inducible promoter when expression of component A2 is induced by addition of 100 μg/mL tetracycline (+ tet, blue dots) or uninduced in the absence of tetraclycine (- tet, green dots). Cells were grown in 50 mM TMA-HS media supplemented with 2 μg/mL puromycin and 100 μg/mL tetracycline, if protein expression was induced (blue dots). Three replicates growth curves were conducted for each condition. (b) Growth rates corresponding to the curves plotted in (a). Statistical significance was tested by unpaired Welch's t test. ns indicates a p-value > 0.05.

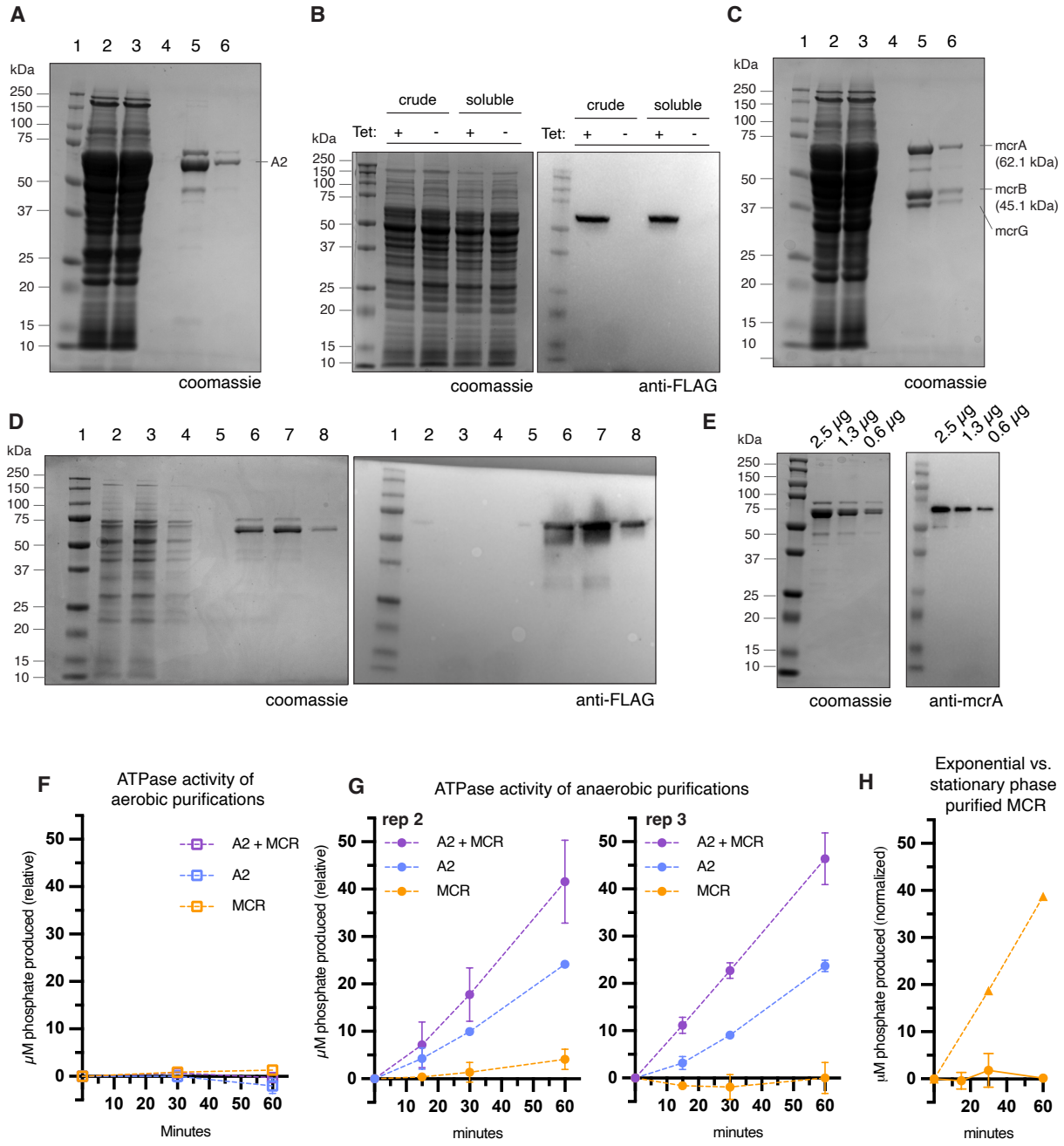

Fig S2.5 Purification of component A2 and MCR to determine ATPase activity. (a) SDS-PAGE gel representing various steps in the anaerobic affinity purification of component A2 using a Streptactin resin. Lanes as indicated are (1) ladder, (2) cleared lysate, (3) flow through, (4) second wash, (5) first elution, (6) second elution. (b) anti-FLAG western blot (right) showing the inducible production of component A2 in crude and soluble cell lysates of DDN122 and the corresponding SDS-PAGE gel (right) as a protein loading control. (c) SDS-PAGE Coomassie-stained gel showing the purification of MCR with the same lanes as (a). (d) anti-FLAG western blot (right) and SDS-PAGE Coomassie stained gel (left) as a protein loading control of component A2 purification with lanes as follows: (1) ladder,

(2) cell lysate, (3) flow through, (4) first wash, (5) second wash, (6) first elution, (7) second elution, and (8) third elution. (e) anti-mcrA western blot (right) and SDS-PAGE Coomassie-stained gel (left), as a protein loading control, of purified component A2 diluted 2X from 2.5 μg to 0.6 μg per lane as indicated. (f) Aerobic ATPase assay of component A2 alone (blue), MCR alone (purple), and component A2 combined with MCR (orange). Each protein was purified under aerobic conditions. Each reaction contained 500 μg/mL of each protein in buffer with 200 μM ATP, 10 mM $MgCl_2$, 20 mM HEPES, 300 mM NaCl, and 1% glycerol. Reactions were incubated at 37 °C. Inorganic phosphate production was measured at 0, 30, and 60 minutes using malachite green reagent. (g) Additional biological replicates of anaerobic ATPase activity with two additional independent purification of component A2. Each reaction contained 500 μg/mL of each protein indicated with 200 μM ATP, 10 mM $MgCl_2$, 20 mM HEPES, 300 mM NaCl, and 1% glycerol. Reactions were incubated at 37 °C inside the anaerobic chamber. Inorganic phosphate production was measured at 0, 15, 30 and 60 minutes using malachite green reagent. (h) ATPase activity of MCR purified from exponential phase cells (triangles) with the same reaction conditions as (f), except time points were taken at 0, 30 and 60 minutes. The data from figure 1h for stationary phase purified MCR is included (circles) is included for comparison.

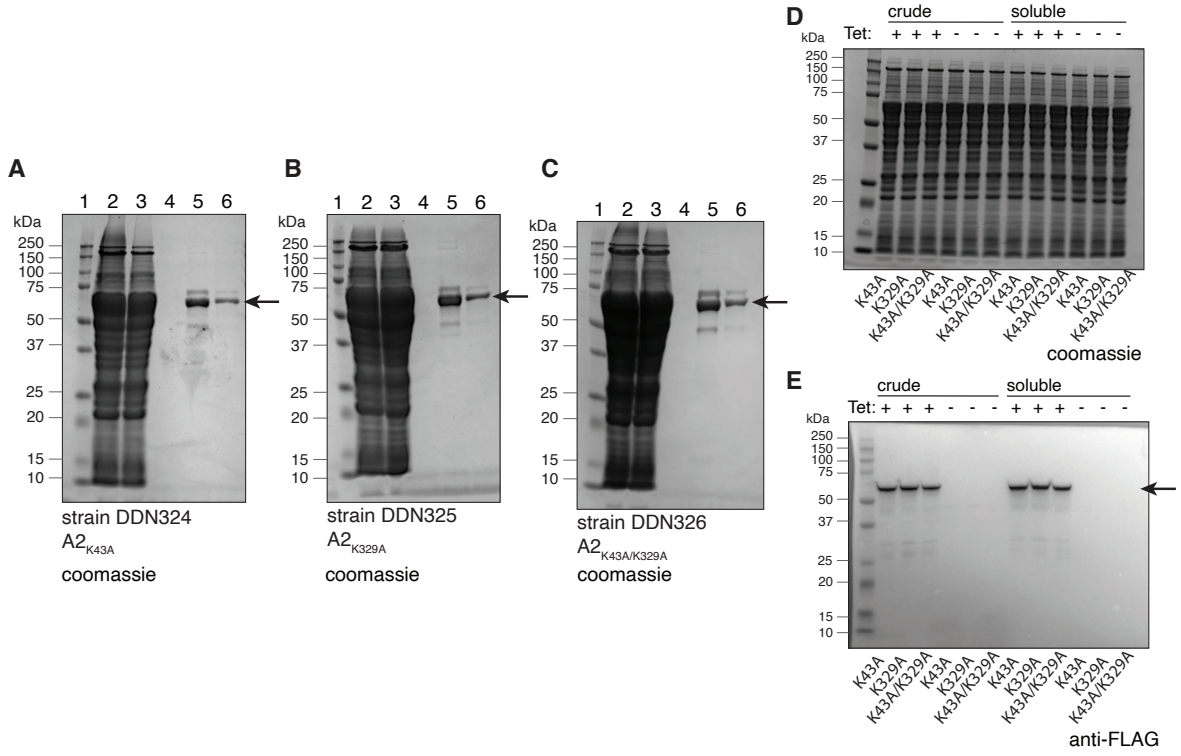

Fig S2.6 Purification of lysine point mutants of component A2. (a-c) SDS-PAGE Coomassie-stained gel showing the purification of (a) K43A, (b) K329A, and (c) K43A/K329A variants of component A2. Lanes as indicated are (1) ladder, (2) clear lysate, (3) flow through, (4) second wash, (5) first elution, (6) second elution. (d-e) anti-FLAG Western blot (e) showing the inducible production of each lysine point

mutant in crude and soluble cell lysate and (d) the corresponding SDS-PAGE Coomassie-stained gel as a protein loading control.

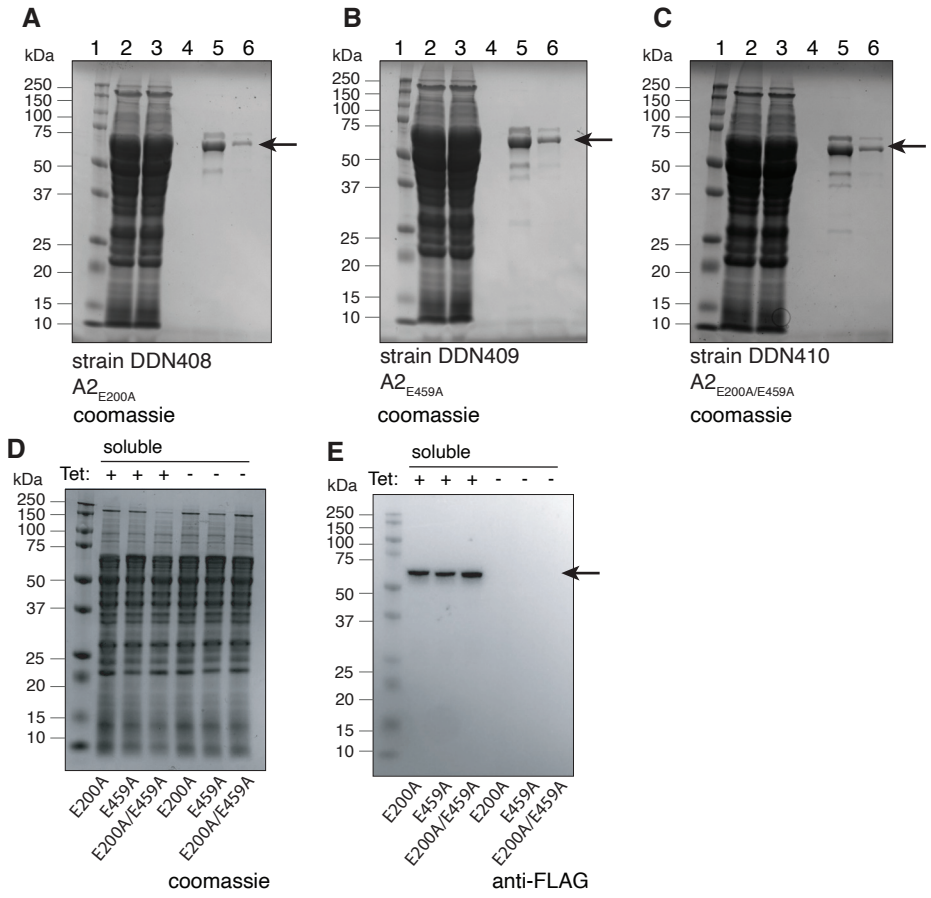

Fig S2.7 Purification of glutamate point mutants of component A2. (a-c) SDS-PAGE Coomassie-stained gel showing the purification of (a) E200A, (b) E459A, and (c) E200A/E459A. Lanes as indicated are (1) ladder, (2) clear lysate, (3) flow through, (4) second wash, (5) first elution, (6) second elution. (d-e) anti-FLAG Western blot (e) showing the inducible production of each glutamate point mutant in soluble cell lysates and the corresponding (d) SDS-PAGE Coomassie-stained gel as a protein loading control.

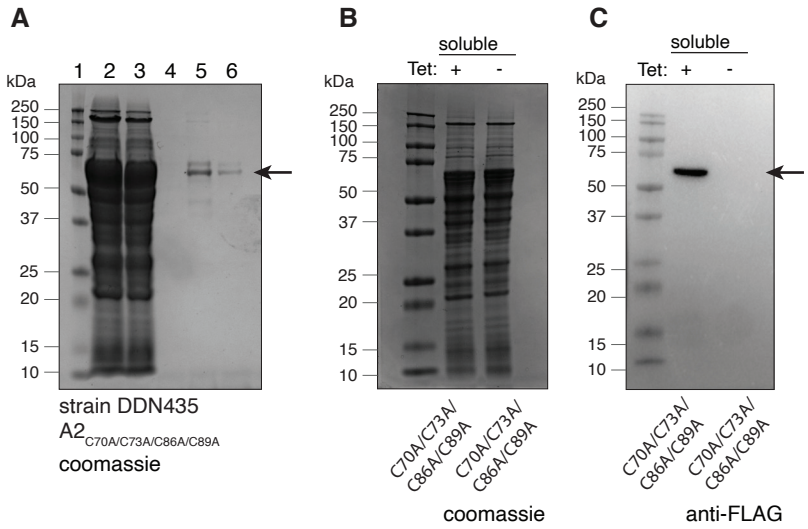

Fig S2.8 Purification of cysteine point mutants of component A2. (a) SDS-PAGE Coomassie-stained gel showing the purification of C70A/C73A/C86A/C89A point mutant of component A2. Lanes as indicated are (1) ladder, (2) clear lysate, (3) flow through, (4) second wash, (5) first elution, (6) second elution. (b-c) anti-FLAG Western blot (c) showing the inducible production of the cysteine point mutant in soluble cell lysates and the corresponding (b) SDS-PAGE Coomassie-stained gel as a protein loading control.

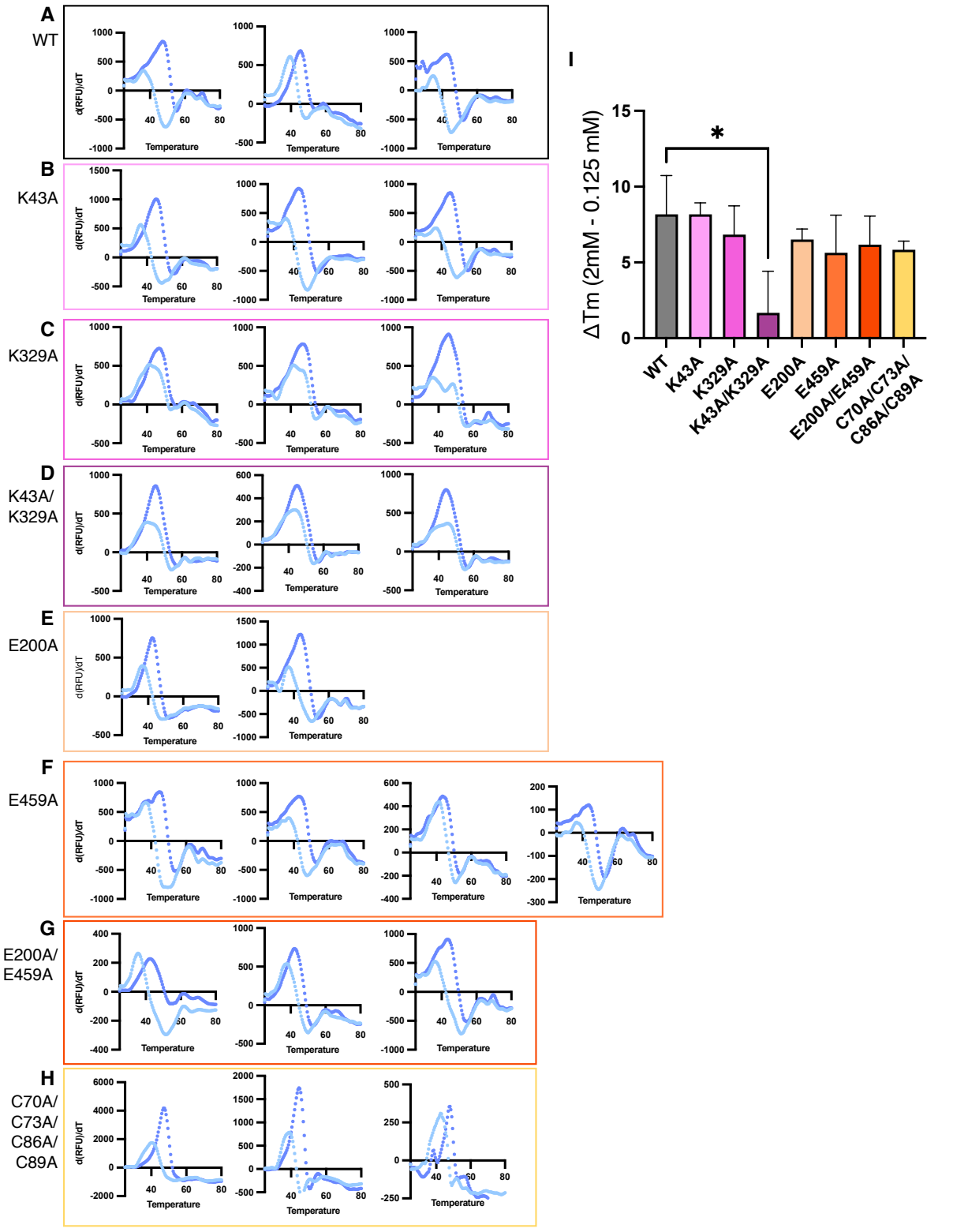

Fig S2.9 Change in melting temperature (Tm) with low (0.125 mM) and high (2 mM) concentrations of ATP across all variants of component A2. (a-h) Differential scanning fluorimetry of independent

biological replicates of each point mutant and the wildtype (WT) allele (as indicated) with 0.125 mM (light blue) and 2 mM (dark blue) ATP. (i) summary of the changes in Tm found across panels (a-h) colored according to each point mutant in panels a-h. Error bars represent standard deviation of three replicates (except for E200A and E459A, which represent the data for two and four protein preparations, respectively) and Welch's unpaired t-test was performed to assess significance; * indicates P-value < 0.05.

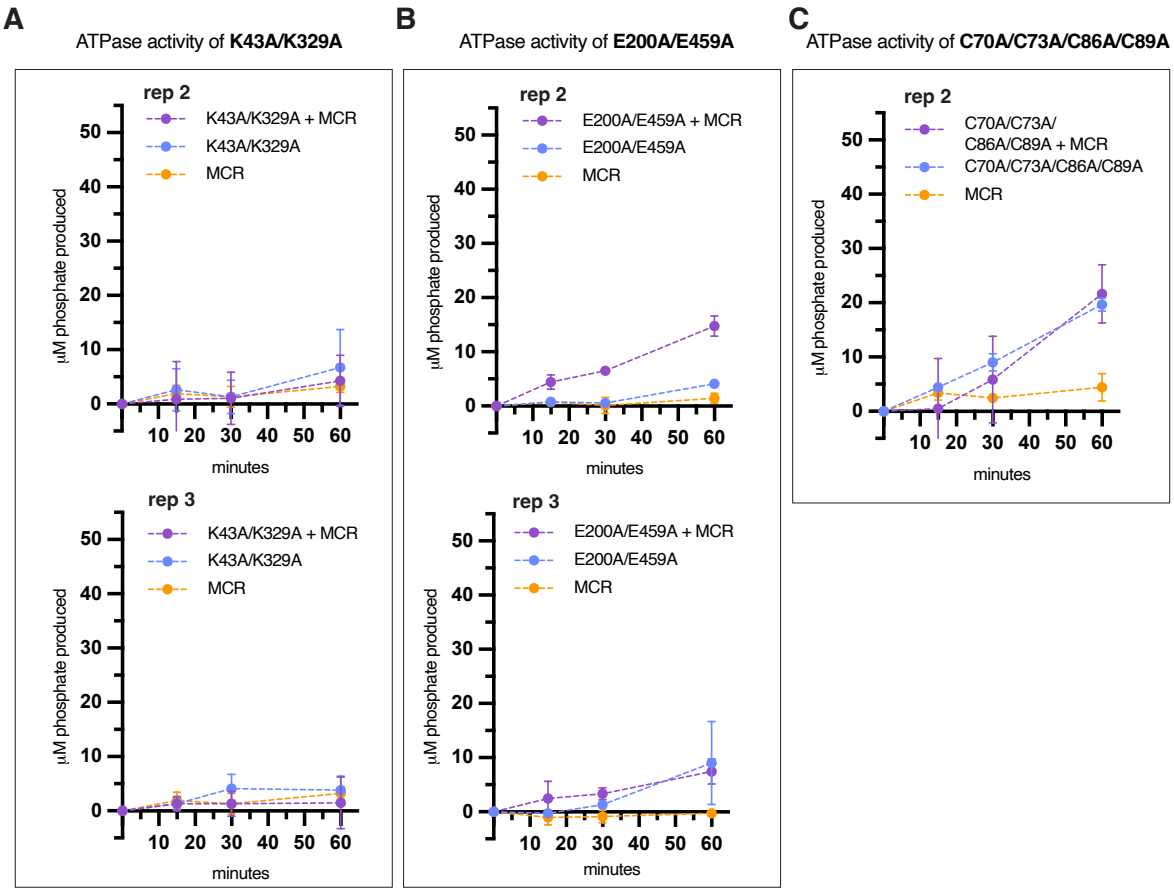

Fig S2.10 Independent replicates of the ATPase assay for K43A/K329A, E200A/K459A, and C70A/C73A/C86A/C89A mutants of Component A2. (a-c) Replicate anaerobic ATPase assays performed using independent purifications of each component A2 mutant. Each reaction contained 500 µg/mL of each protein indicated with 200 µM ATP, 10 mM $MgCl_2$, 20 mM HEPES, 300 mM NaCl, and 1% glycerol. Reactions were incubated at 37 °C. Inorganic phosphate production was measured at 0, 15, 30, and 60 minutes using malachite green reagent. Note: Replicate 1 for each mutant is shown in main text Figure 3.

A ATPase activity of K43A

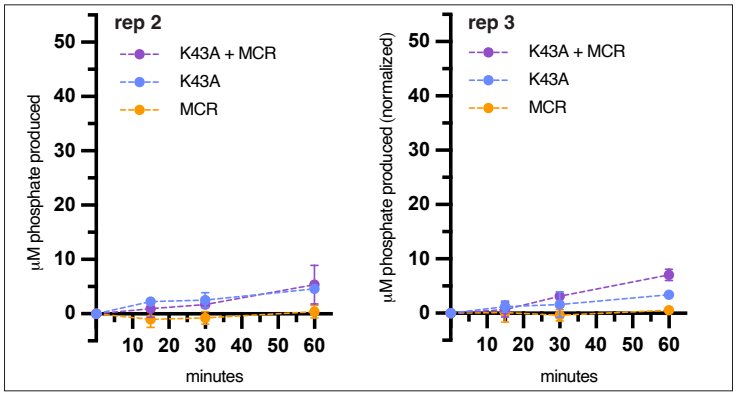

B ATPase activity of K329A

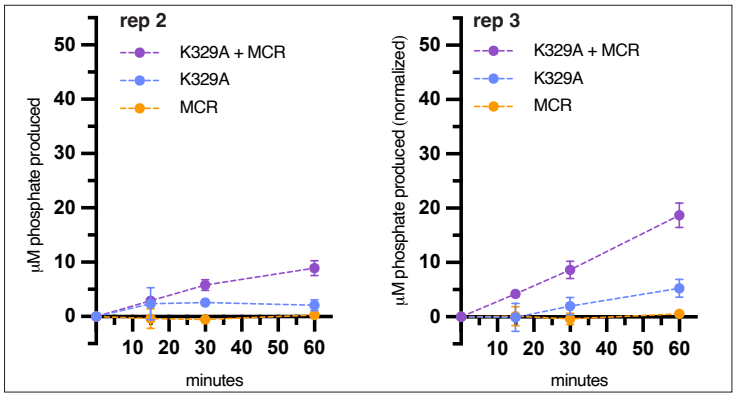

C ATPase activity of E200A

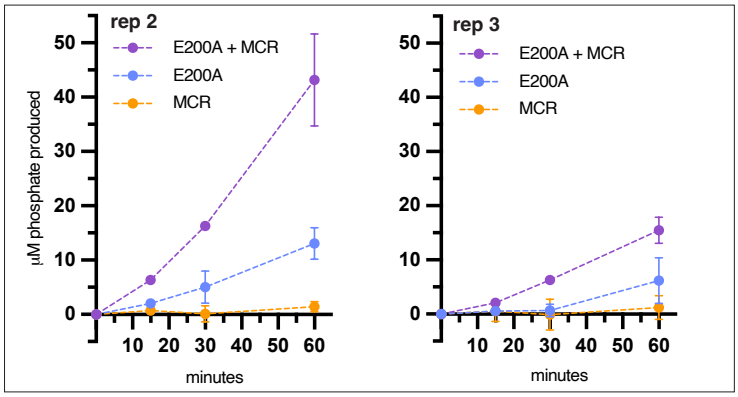

D ATPase activity of E459A

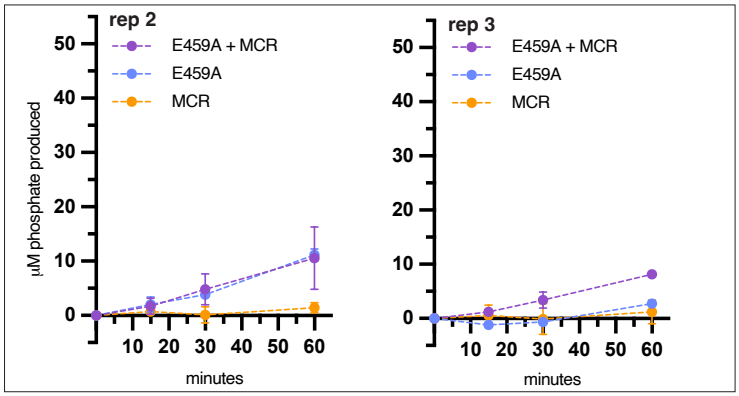

Fig S2.11 Independent replicates of the ATPase assay for K43A, K329A, E200A, and E459A mutants of component A2. (a-d) Replicate anaerobic ATPase assays performed using independent purifications of each component A2 mutant. Each reaction contained 500 μg/mL of each protein indicated with 200 μM ATP, 10 mM $MgCl_2$, 20 mM HEPES, 300 mM NaCl, and 1% glycerol. Reactions were incubated at 37 °C. Inorganic phosphate production was measured at 0, 15, 30, and 60 minutes using malachite green reagent. The same MCR fraction was used between K43A rep 3 and K329A rep 3, E200A rep 2 and E459A rep 2, and E200A rep 3 and E459A rep 3, so the MCR alone data is plotted across both plots in these panels for comparison. Note: Replicate 1 for each mutant is shown in main text Figure 3.

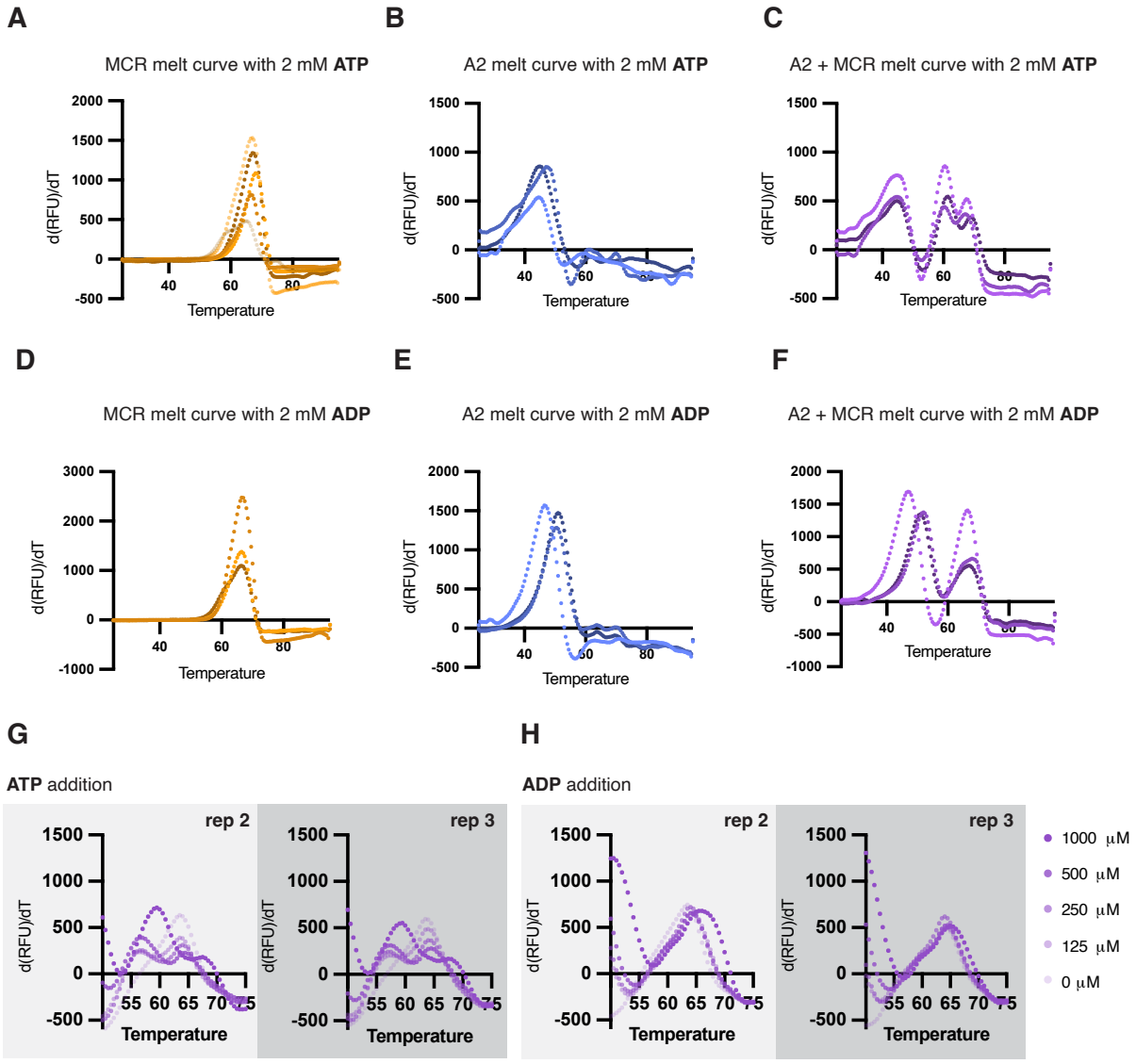

Fig S2.12 Differential Scanning Fluorimetry (DSF) of component A2 and MCR with ATP or ADP. (a-c) Multiple independent purifications of MCR (a), component A2 (b), or MCR + component A2 (c). Samples contained 0.5 mg/mL each protein, 2 mM ATP, 10 mM $MgCl_2$, 20 mM HEPES, 300 mM NaCl, and 1% glycerol. (d-f) Three independent purifications of MCR (d), component A2 (e), or MCR

+ component A2 (f). Samples contained 2 mM ADP, 10 mM $MgCl_2$, 20 mM HEPES, 300 mM NaCl, and 1% glycerol. (g-h) Two additional replicates of DSF melt curves with increasing concentrations of ATP (g) or ADP (h) and the same conditions as (a-f). Note: Replicate 1 is shown in main text Figure 4.

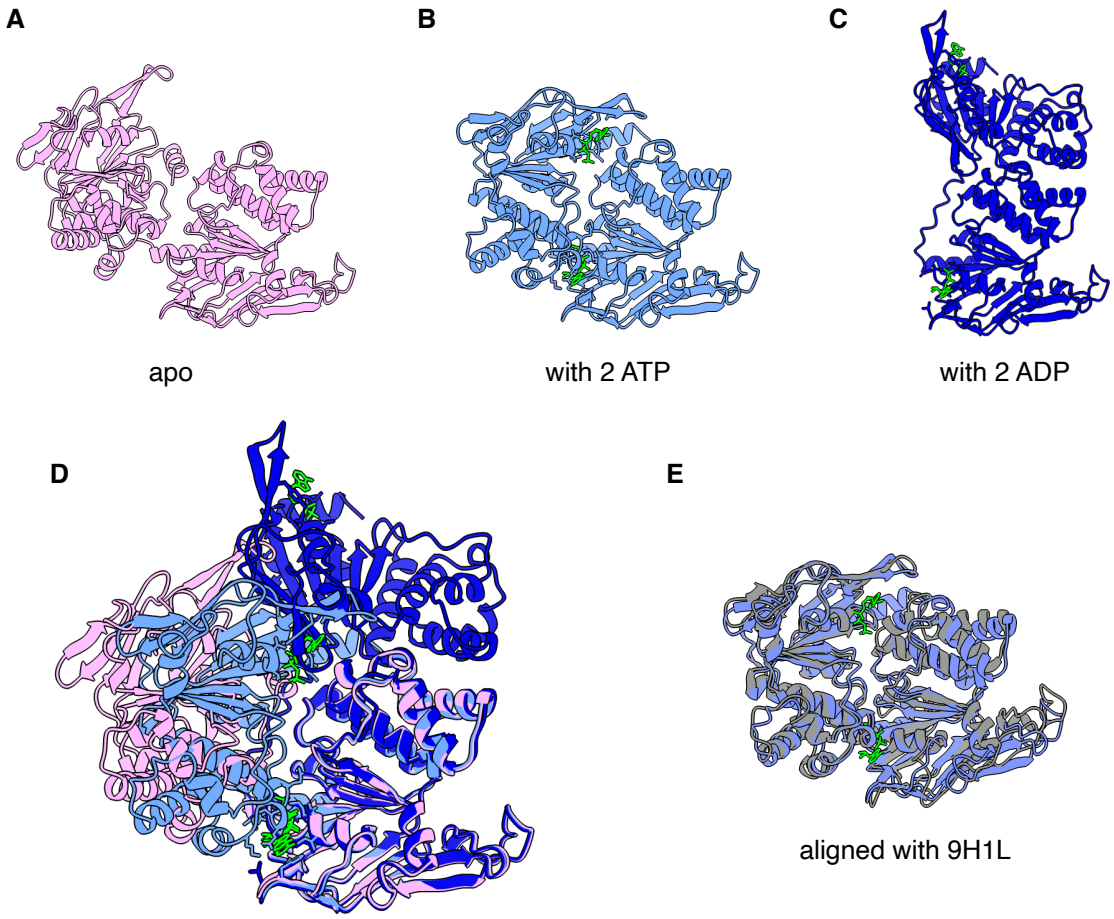

Fig S2.13 AlphaFold predicted structures of component A2 with and without nucleotides bound. (a) AlphaFold predicted structure of *M. acetivorans* component A2 without any nucleotide (pink). (b) AlphaFold predicted structure of *M. acetivorans* component A2 with 2 molecules of ATP (light blue). (c) AlphaFold predicted structure of *M. acetivorans* component A2 with 2 molecules of ADP (dark blue). (d) alignment of the predicted structures in a-c maintaining the same orientation with apo-protein (pink), ATP-bound (light blue), and ADP-bound (dark blue) forms. RMSD of apo component A2 aligned with ATP-bound component A2 is 10.262 Å, RMSD of apo component A2 aligned with ADP-bound component A2 is 30.107 Å. (e) AlphaFold predicted structure of *M. acetivorans* component A2 with 2 molecules of ATP (light blue) aligned with the resolved A2 structure from PDB: 9H1L (grey). RMSD is 2.667 Å. Each panel shows the relevant nucleotide in green.

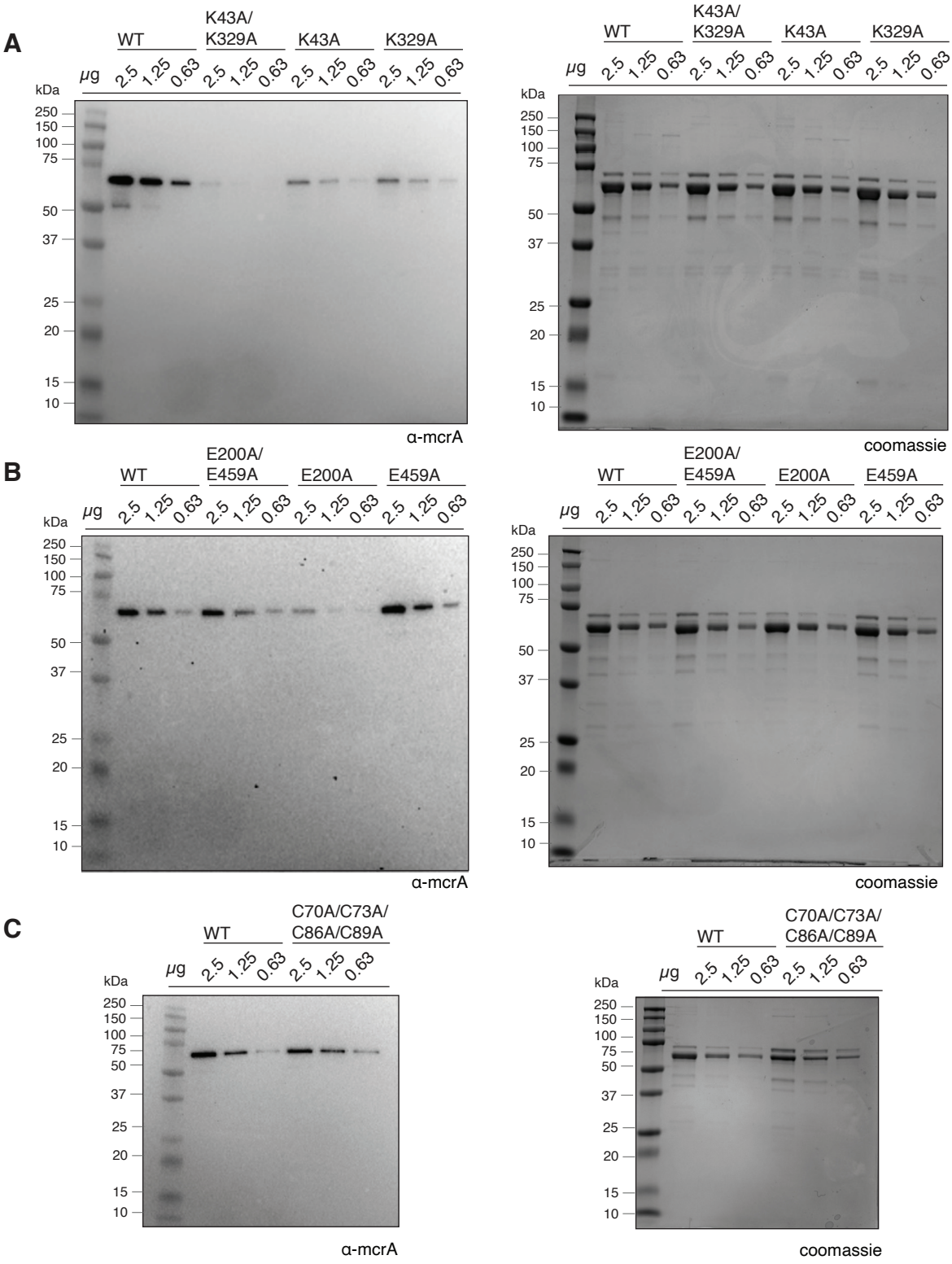
A
WT
K43A/ K329A
K43A
K329A
μg
2.5 1.25 0.63 2.5 1.25 0.63 2.5 1.25 0.63 2.5 1.25 0.63
kDa
250
150
100
75
50
37
25
20
15
10
α-mcrA
coomassie
B
WT
E200A/ E459A
E200A
E459A
μg
2.5 1.25 0.63 2.5 1.25 0.63 2.5 1.25 0.63 2.5 1.25 0.63
kDa
250
150
100
75
50
37
25
20
15
10
α-mcrA
coomassie
C
WT
C70A/C73A/ C86A/C89A
μg
2.5 1.25 0.63 2.5 1.25 0.63
kDa
250
150
100
75
50
37
25
20
15
10
α-mcrA
coomassie

Fig S2.14 Full images of western blots shown in Figure 5a. (a-b) Uncropped western blots (left) with anti-McrA specific antibodies and Coomassie stained SDS-PAGE gels (right) as a protein loading control for (a) K/A mutants, (b) E/A mutants, and (c) C/A mutant as indicated.

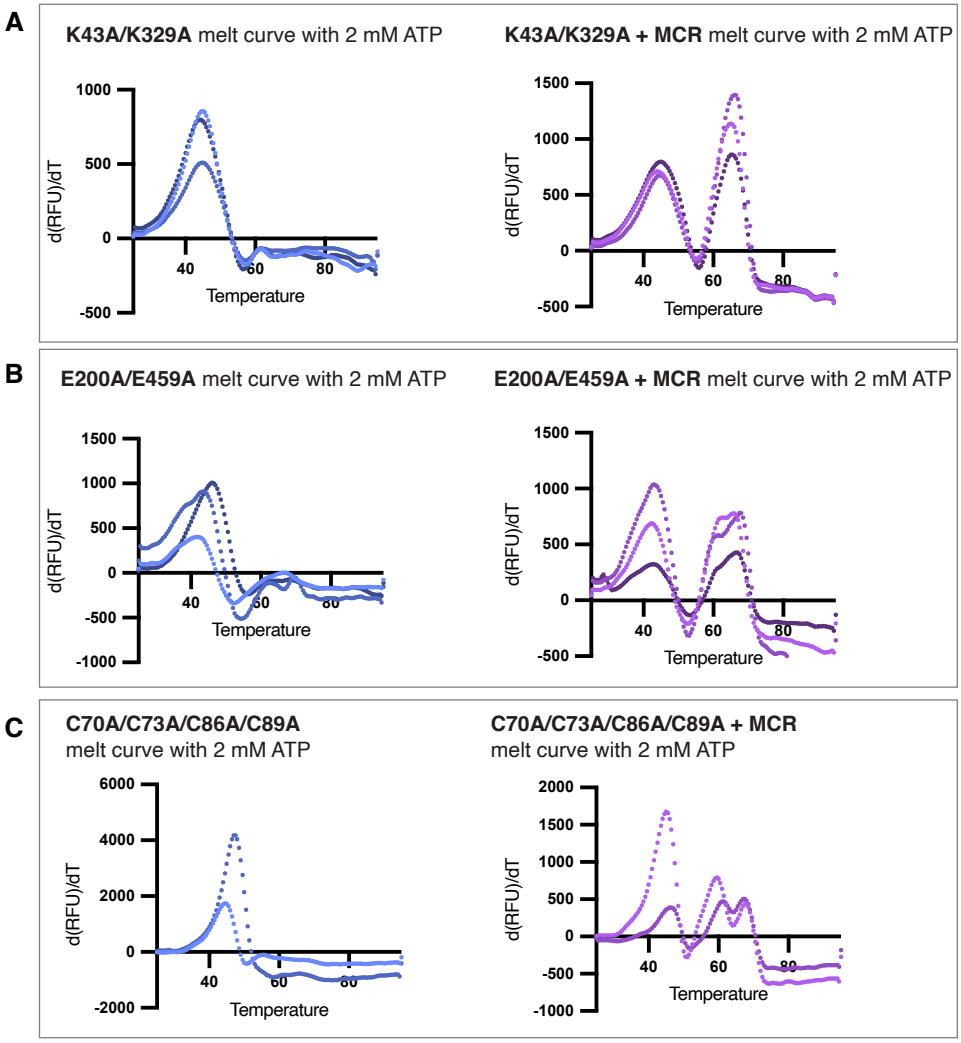

Fig S2.15 Differential scanning fluorimetry of K43A/K329A, E200A/E459A, and C70A/C73A/C86A/C89A mutants of component A2 + MCR in the presence of ATP. (a-b) Three independent purifications of (a) K43A/K329A component A2, or (b) MCR + K43A/K329A component A2. Samples contained 2 mM ATP, 10 mM $MgCl_2$, 20 mM HEPES, 300 mM NaCl, and 1% glycerol. (c-d) Three independent purifications of (c) E200A/E459A component A2, or (d) MCR + E200A/E459A component A2, with the same sample conditions as (a). (e-f) Two independent purifications of (e) C70A/C73A/C86A/C89A component A2, or (f) MCR + C70A/C73A/C86A/C89A component A2 (f), with the same sample conditions as (a). All proteins are at a concentration of 0.5 mg/mL.

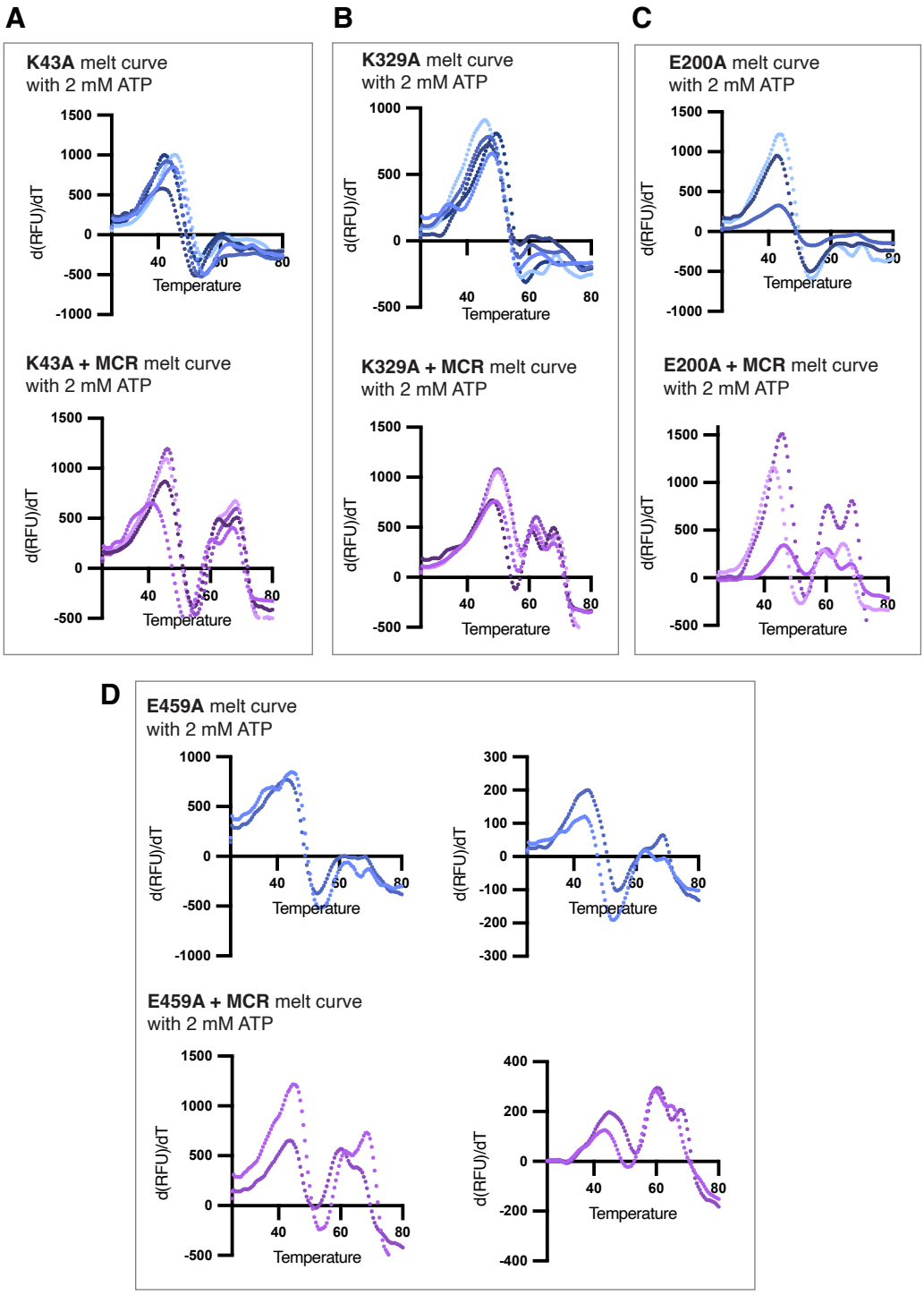

Fig S2.16 Differential Scanning Fluorimetry of K43A, K329A, E200A, and E459A mutants of component A2 + MCR with ATP. (a) Independent purifications of K43A (top), or MCR + K43A (bottom). Samples contained 2 mM ATP, 10 mM $MgCl_2$, 20 mM HEPES, 300 mM NaCl, and 1% glycerol. (b) Independent purifications of K329A (top), or MCR + K329A (bottom)., with the same sample conditions as (a). (c) Independent purifications of E200A (top), or MCR + E200A (bottom), with the same sample conditions as (a). (d) Independent purifications of E459A (top), or MCR +

E459A (bottom), with the same sample conditions as (a). All proteins are at a concentration of 0.5 mg/mL.

Table S2.1 Mutations in DDN122 (a strain generated in this study that has a second copy of component A2 under the control of the P*mcrB*(tetO1) promoter) relative to the parent strain (WWM73). Mutations were predicted using Breseq version v0.35.5 using default parameters.

position	mutation	annotation	gene	present in parent strain
487,691	+C	intergenic (+91/-1171)	*MA_0404* → / → *isf-3*	yes
954,776	$(A)_{5\rightarrow6}$	coding (27/765 nt)	*MA_0806* ←	yes
1,327,728	Δ1 bp	intergenic (+539/+2434)	*MA_1110* → / ← *MA_1114*	yes
2,100,489	2 bp→CT	intergenic (-200/+180)	*MA_1738* ← / ← *MA_1739*	yes
2,100,494	G→T	intergenic (-205/+176)	*MA_1738* ← / ← *MA_1739*	yes
2,548,151	+C	coding (6598/6654 nt)	*MA_2045* ←	yes
2,850,254	A→G	F64L (TTC→CTC)	*serC* ←	yes
2,880,667	T→G	H313Q (CAT→CAG)	*MA_2328* →	yes
3,446,809	Δ1 bp	coding (771/774 nt)	*MA_2751* →	yes
4,309,060	Δ1 bp	coding (108/12681 nt)	*MA_3471* ←	yes
4,888,175	Δ1 bp	intergenic (-67/-228)	*MA_3972* ← / → *MA_3973*	yes
4,958,953	+C	intergenic (+2396/-395)	*MA_4028* → / → *MA_4030*	yes

Table S2.2 Identification of individual SDS-PAGE bands of in-gel digests from component A2 preparation showing tryptic peptides and resulting proteins identified.

~70 kDa band

Glutamyl-tRNA(Gln) amidotransferase subunit E, MA_2862, MW: 70.8

Protein score CI% 100%

Calc. Mass	Observ. Mass	Sequence	Ion score	C. I. %
841.4638	841.4547	EVQPGRR		
852.4396	852.4212	EKLFCR		
924.4421	924.4196	LGTEFSDR		
998.5992	998.5614	LAIEAVINR		
998.5992	998.5614	LAIEAVINR	52	99.977
1013.6716	1013.6249	GSILAALLKK		
1015.553	1015.5273	QDVNISIAR		
1016.6251	1016.5781	QLNLLFIR	49	99.95
1016.6251	1016.5781	QLNLLFIR		
1080.5432	1080.5029	RLGTEFSDR		
1096.6725	1096.627	TLVGIVPEIR	62	99.998
1096.6725	1096.627	TLVGIVPEIR		
1108.5746	1108.54	RFASESGLNK		
1124.5582	1124.525	GDSIVYSLDR		
1173.6222	1173.5884	DANVNSTLIAR		
1279.6715	1279.6223	EVAEYIGMVLR	94	100
1279.6715	1279.6223	EVAEYIGMVLR		
1295.6664	1295.6144	EVAEYIGMVLR		
1347.5852	1347.5331	DIGDSDFEFFR		
1347.5852	1347.5331	DIGDSDFEFFR	103	100
1361.7423	1361.6803	GLFAAISNQEIAK		
1371.7114	1371.6622	EAIEGIPEETRK		
1379.6914	1379.6462	IVVDGSNTSGFQR		
1440.8057	1440.7471	GVQALDLIEDIVR	81	100
1440.8057	1440.7471	GVQALDLIEDIVR		
1475.7086	1475.6986	MEKYDYSELGLK		
1507.7863	1507.736	KIVVDGSNTSGFQR		
1577.9261	1577.863	LGIPLVEIATAPDIR	61	99.997
1577.9261	1577.863	LGIPLVEIATAPDIR		
1596.9067	1596.8505	GVQALDLIEDIVRR		
1623.8224	1623.776	IEEKGDSIVYSLDR		
1716.8075	1716.7592	TAFLASDGYIETSEGR	78	100
1716.8075	1716.7592	TAFLASDGYIETSEGR		
1745.8649	1745.8066	LFNMKPVDQMHVMR		
1745.8649	1745.8066	LFNMKPVDQMHVMR	78	100
1761.8597	1761.803	LFNMKPVDQMHVMR		
1807.9113	1807.8192	LGLSAFDPEEVENFIK		

1870.9592	1870.9004	ALPDGNTAYMRPLPGAAR	48	99.945
1870.9592	1870.9004	ALPDGNTAYMRPLPGAAR		
1886.9541	1886.8969	ALPDGNTAYMRPLPGAAR		
1922.8436	1922.7898	AYDTTCLIENDEEPPR		
2288.0862	2288.0342	DAIGAGPEDAFVMVADEPEKAR		
2407.1082	2407.0491	AYDTTCLIENDEEPPREL		

~60 kDa band

ABC transporter, ATP-binding protein, MA_3998, MW: 59.6

Protein score CI% 100%

Calc. Mass	Observ. Mass	Sequence	Ion score	C. I. %
844.5073	844.4847	IAIMLQR		
860.5022	860.4769	IAIMLQR		
908.4948	908.4698	RYISVDR		
968.6502	968.611	IALAQVLIK		
976.5461	976.5302	LSLYDPIR		
982.5866	982.5566	TILMHVLR	57	99.994
982.5866	982.5566	TILMHVLR		
998.5815	998.5537	TILMHVLR		
1000.6084	1000.5824	RIAIMLQR		
1003.5166	1003.5363	ELSGGEKQR		
1016.6033	1016.5746	RIAIMLQR		
1071.5105	1071.4856	TFALYGDER	66	100
1071.5105	1071.4856	TFALYGDER		
1104.6411	1104.6071	LSLYDPIRK		
1109.6677	1109.6251	NVLVGEPIIR		
1109.6677	1109.6251	NVLVGEPIIR	31	97.283
1121.5837	1121.5616	NLTVDFDGLK		
1179.535	1179.5647	VGDEWVDMTK		
1184.4558	1184.4395	MTDEMSEGER		
1206.7205	1206.6803	LVHEAIINAVK		
1350.8467	1350.814	IALAQVLIKEPR		
1350.8467	1350.814	IALAQVLIKEPR	66	100
1493.6107	1493.7108	MTDEMSEGERHR		
1508.8066	1508.765	AVELLEEVNLSHR	88	100
1508.8066	1508.765	AVELLEEVNLSHR		
1636.9016	1636.8674	KAVELLEEVNLSHR	77	100
1636.9016	1636.8674	KAVELLEEVNLSHR		
1710.9458	1710.9009	ILMGILPPTSGEVEVR		
1710.9458	1710.9009	ILMGILPPTSGEVEVR	95	100
1726.9408	1726.902	ILMGILPPTSGEVEVR		
2021.9927	2021.9484	GTESFENISGEVIYHLAR	160	100
2021.9927	2021.9484	GTESFENISGEVIYHLAR		
2110.1101	2110.1047	NPLLLLADEPTGTLDPMTAK		
2110.1501	2110.1047	IVEIGRPGTVLAQLTEEER	77	100

~50 kDa band

ABC transporter, ATP-binding protein, MA_3998, MW: 59.6

Protein score CI% 100%

Calc. Mass	Observ. Mass	Sequence	Ion score	C. I. %
844.5073	844.5098	IAIMLQR		
908.4948	908.4931	RYISVDR		
976.5461	976.5475	LSLYDPIR		
982.5866	982.5903	TILMHVLR		
982.5866	982.5903	TILMHVLR	42	99.755
998.5815	998.5963	TILMHVLR		
1000.6084	1000.6046	RIAIMLQR		
1003.5166	1003.5557	ELSGGEKQR		
1016.6033	1016.622	RIAIMLQR		
1071.5105	1071.5198	TFALYGDER	38	99.423
1071.5105	1071.5198	TFALYGDER		
1104.6411	1104.6388	LSLYDPIRK		
1109.6677	1109.6621	NVLVGEPIIR		
1109.6677	1109.6621	NVLVGEPIIR	43	99.825
1179.535	1179.6029	VGDEWVDMTK		
1206.7205	1206.7023	LVHEAIINAVK		
1493.6107	1493.7355	MTDEMSEGERHR		
1508.8066	1508.7999	AVELLEEVNLSHR		
1508.8066	1508.7999	AVELLEEVNLSHR	73	100
1636.9016	1636.897	KAVELLEEVNLSHR		
1710.9458	1710.9396	ILMGILPPTSGEVEVR		
1710.9458	1710.9396	ILMGILPPTSGEVEVR	44	99.836
2021.9927	2021.9875	GTESFENISGEVIYHLAR		
2110.1501	2110.1387	IVEIGRPGTVLAQLTEEER		

~45 kDa band

Methyl coenzyme-M reductase subunit beta, MA_4550, MW: 45

Protein score CI% 100%

Calc. Mass	Observ. Mass	Sequence	Ion Score	C. I. %
858.5407	858.5487	IILDTKR		
1071.6157	1071.6185	SLLIQAPSSR		
1071.6157	1071.6185	SLLIQAPSSR	34	98.555
1131.5891	1131.5687	AVEDGVISVDK		
1383.6387	1383.6803	SDTVDIYDDRGK		
1411.7474	1411.7524	NIMANHIAAITSR		
1411.7474	1411.7524	NIMANHIAAITSR	75	100
1416.7693	1416.7738	DGTIGTVIESIVGR		
1427.7423	1427.7592	NIMANHIAAITSR		
1658.8782	1658.879	LLESNVDIMSLAPTR	68	100

1658.8782	1658.879	LLESNVDIMSLAPTR

~27 kDa band

Methyl coenzyme-M reductase subunit gamma, MA_4547, MW: 27.6

Protein score CI% 100%

Calc. Mass	Observ. Mass	Sequence	Ion Score	C. I. %
1020.5333	1020.5558	GATVHGHSVR		
1088.5524	1088.5701	SYFAAINFR		
1088.5524	1088.5701	SYFAAINFR	62	99.997
1090.5813	1090.5734	LEGGVIIMDK		
1109.4714	1109.6082	ERDMEQCAK		
1368.6543	1368.6763	DDAEVIEWVHR		
1554.7759	1554.7944	EISDEDLTAVLGHR		
1568.7084	1568.7329	LQEDGVMFDMLDR		
1724.8094	1724.8285	LQEDGVMFDMLDRR		
1779.8075	1779.83	VQMETEMTDPALAGMR		
1817.8452	1817.8657	AYEAQYYPGATSVGANR		
1817.8452	1817.8657	AYEAQYYPGATSVGANR	64	99.999
1823.9609	1823.9769	LREISDEDLTAVLGHR		
2140.9797	2141.0093	YVQFADSMYNAPATPYF	81	100
		R		
2140.9797	2141.0093	YVQFADSMYNAPATPYF		
		R		
2170.0676	2170.0933	VDNVAFRDDAEVIEWVH		
		R		
2540.1545	2540.1855	APGSDYPSTHPPLAEMG		
		EPACSIR		

~30 kDa band

ABC transporter, ATP-binding protein, MA_3998, MW: 59.6

Sequence coverage: 43%

Positions in Master Proteins	Theo. MH+ [Da]	DeltaM [ppm]: Mascot	Deltam/z [Da]: Mascot	Sequence	Confidence
19918090 [415-424]	1064.5371	-1.32	-0.0007	AAGFEENKAK	High
19918090 [430-441]	1477.61584	-3.32	-0.00163	MTDEMSEGERHR	High
19918090 [430-441]	1493.61075	-0.29	-0.00014	MTDEMSEGERHR	High
19918090 [9-18]	1121.58372	-0.37	-0.00021	NLTVDFDGLK	High
19918090 [9-21]	1433.79986	-1.02	-0.00073	NLTVDFDGLKALK	High
19918090 [278-287]	1109.66772	-0.06	-0.00003	NVLVGEPIIR	High
19918090 [275-287]	1494.86385	-1.09	-0.00081	QEKNVLVGEPIIR	High
19918090 [430-439]	1216.44564	1.37	0.00083	MTDEMSEGER	High
19918090 [44-51]	998.58155	-1.24	-0.00062	TILMHVLR	High
19918090 [470-478]	944.57751	-0.46	-0.00022	VAVTNSILK	High

19918090 [351-360]	1179.53505	0.75	0.00044	VGDEWVDMTK	High
19918090 [351-360]	1195.52997	1.22	0.00073	VGDEWVDMTK	High
19918090 [124-132]	1071.51055	-0.23	-0.00012	TFALYGDER	High
19918090 [430-439]	1184.45581	0.86	0.00051	MTDEMSEGER	High
19918090 [454-469]	1792.87071	-2.49	-0.00223	IVIMDEPTGTMDPITK	High
19918090 [305-314]	1121.6201	-0.92	-0.00052	AVDKISFDVK	High
19918090 [155-167]	1508.80673	1.59	0.0012	AVELLEEVNLSHR	High
19918090 [73-81]	1109.5408	1.11	0.00062	CGYIERPSK	High
19918090 [315-329]	1433.76347	-2.04	-0.00146	EGEIFGLVGISGAGK	High
19918090 [174-182]	1003.5167	-1.27	-0.00063	ELSGGEKQR	High
19918090 [408-414]	786.54475	0.43	0.00017	KAIITLK	High
19918090 [154-167]	1636.9017	0.12	0.00006	KAVELLEEVNLSHR	High
19918090 [442-453]	1350.84675	0.17	0.00011	IALAQVLIKEPR	High
19918090 [361-368]	858.47919	-0.73	-0.00031	LGVDNKGR	High
19918090 [335-350]	1710.94587	-0.51	-0.00044	ILMGILPPTSGEVEVR	High
19918090 [335-350]	1726.94078	-0.04	-0.00003	ILMGILPPTSGEVEVR	High
19918090 [27-38]	1227.69433	-0.05	-0.00003	INEGEVVGILGK	High
19918090 [212-222]	1206.72048	-0.59	-0.00035	LVHEAIINAVK	High
19918090 [454-469]	1760.88088	-1.51	-0.00133	IVIMDEPTGTMDPITK	High
19918090 [454-469]	1776.8758	-0.7	-0.00062	IVIMDEPTGTMDPITK	High
19918090 [442-450]	968.65028	-0.59	-0.00029	IALAQVLIK	High
19918090 [295-304]	1163.65313	-0.85	-0.00049	YISVDRGVVR	High

Methanogenesis Marker Protein 7, MA_3992, MW: 34.3

Sequence coverage: 37%

Positions in Master Proteins	Theo. MH+ [Da]	DeltaM [ppm]: Mascot	Deltam/z [Da]: Mascot	Sequence	Confidence
499333395 [295-300]	763.47125	-0.18	-0.00007	NYILIK	High
499333395 [218-230]	1406.81142	-0.88	-0.00041	QQAKDPLAVLPAR	High
499333395 [117-126]	1271.60486	0.61	0.00039	RVSLSMDYER	High
499333395 [172-187]	1675.82859	0.55	0.00046	TEDVPGADLYVGNIGR	High
499333395 [195-210]	1774.9069	-1.38	-0.00082	TEEIEALDKLNEGVSK	High
499333395 [245-259]	1592.93702	0.79	0.00063	VLSPAPLTLQLDGLR	High
499333395 [231-244]	1712.89998	1.83	0.00104	VMKEIENQVPEIQR	High
499333395 [231-244]	1728.8949	2.08	0.00179	VMKEIENQVPEIQR	High
499333395 [118-126]	1099.50884	-2.22	-0.00122	VSLSMDYER	High
499333395 [118-126]	1115.50375	-2.33	-0.0013	VSLSMDYER	High
499333395 [118-127]	1227.6038	-2.88	-0.00177	VSLSMDYERK	High
499333395 [234-244]	1354.69612	-0.56	-0.00038	EIENQVPEIQR	High
499333395 [100-112]	1351.68993	-1.22	-0.00082	HPGANTNMIGLAR	High

499333395 [100-112]	1367.68484	-0.34	-0.00023	HPGANTNMIGLAR	High
499333395 [293-300]	1022.6067	-0.38	-0.00019	MKNYILIK	High
499333395 [262-270]	1177.55242	-1.66	-0.00098	LPYDEFHEK	High

~28 kDa band

ABC transporter, ATP-binding protein, MA_3998, MW: 59.6

Sequence coverage: 46%

Positions in Master Proteins	Theo. MH+ [Da]	DeltaM [ppm]: Mascot	Deltam/z [Da]: Mascot	Sequence	Confidence
19918090 [415-424]	1064.5371	-1.67	-0.00089	AAGFEENKAK	High
19918090 [470-478]	944.57751	-0.78	-0.00037	VAVTNSILK	High
19918090 [44-51]	998.58155	0.17	0.00008	TILMHVLR	High
19918090 [124-132]	1071.51055	1.02	0.00055	TFALYGDER	High
19918090 [39-51]	1414.78349	0.92	0.00043	SGSGKTILMHVLR	High
19918090 [192-211]	2126.10495	0.96	0.00102	NPLLLLADEPTGTLDPMTAK	High
19918090 [9-18]	1121.58372	-1.24	-0.0007	NLTVDFDGLK	High
19918090 [430-441]	1509.60567	1.1	0.00056	MTDEMSEGERHR	High
19918090 [454-469]	1760.88088	1.05	0.00093	IVIMDEPTGTMDPITK	High
19918090 [212-222]	1206.72048	3.36	0.00203	LVHEAIINAVK	High
19918090 [103-111]	1104.64117	1.32	0.00073	LSLYDPIRK	High
19918090 [27-38]	1227.69433	-1.15	-0.0007	INEGEVVGILGK	High
19918090 [361-368]	858.47919	0.19	0.00008	LGVDNKGR	High
19918090 [117-123]	860.50223	0.08	0.00004	IAIMLQR	High
19918090 [442-453]	1350.84675	-3	-0.00202	IALAQVLIKEPR	High
19918090 [154-167]	1636.9017	-1.44	-0.00118	KAVELLEEVNLSHR	High
19918090 [52-69]	2021.99269	-1.92	-0.0013	GTESFENISGEVIYHLAR	High
19918090 [174-182]	1003.5167	-0.35	-0.00018	ELSGGEKQR	High
19918090 [315-329]	1433.76347	-1.44	-0.00104	EGEIFGLVGISGAGK	High
19918090 [73-81]	1109.5408	0.89	0.0005	CGYIERPSK	High
19918090 [155-167]	1508.80673	-1.89	-0.00143	AVELLEEVNLSHR	High
19918090 [335-350]	1726.94078	-1.8	-0.00156	ILMGILPPTSGEVEVR	High
19918090 [295-304]	1163.65313	0.1	0.00006	YISVDRGVVR	High

~25 kDa band

ABC transporter, ATP-binding protein, MA_3998, MW: 59.6

Sequence coverage: 16%

Positions in Master Proteins	Theo. MH+ [Da]	DeltaM [ppm]: Mascot	Deltam/z [Da]: Mascot	Sequence	Confidence
19918090 [415-424]	1064.5371	0.05	0.00003	AAGFEENKAK	High
19918090 [27-38]	1227.69433	0.64	0.00039	INEGEVVGILGK	High
19918090 [361-368]	858.47919	-0.16	-0.00007	LGVDNKGR	High
19918090 [442-453]	1350.84675	-1.82	-0.00123	IALAQVLIKEPR	High
19918090 [174-182]	1003.5167	0.26	0.00013	ELSGGEKQR	High
19918090 [73-81]	1109.5408	-2.3	-0.00127	CGYIERPSK	High
19918090 [19-26]	927.57343	0.77	0.00036	ALKNVNLR	High
19918090 [454-469]	1760.88088	0.98	0.00087	IVIMDEPTGTMDPITK	High

Methanogenesis Marker Protein 17, MA_3993, MW: 22.7

Sequence coverage: 19%

Positions in Master Proteins	Theo. MH+ [Da]	DeltaM [ppm]: Mascot	Deltam/z [Da]: Mascot	Sequence	Confidence
499333396 [23-32]	1115.63067	-0.99	-0.00055	IIEDNLASLK	High
499333396 [141-151]	1340.73211	1	0.00067	LHENLVEFAIR	High
499333396 [33-39]	697.43554	0	0	LAPAIGR	High
499333396 [22-32]	1243.72563	0	0	KIIEDNLASLK	High
499333396 [152-160]	1032.5585	-1.52	-0.00079	ATPEGFRVR	High

~16 kDa band

conserved hypothetical protein, MA_4200, MW: 17.9

Sequence coverage: 64%

Positions in Master Proteins	Theo. MH+ [Da]	DeltaM [ppm]: Mascot	Deltam/z [Da]: Mascot	Sequence	Confidence
19918309 [44-51]	946.53564	-0.4	-0.00019	AFKELNPK	High
19918309 [1-17]	1884.00076	3.77	0.00355	MIGIISDSHDNLTAIRK	High
19918309 [1-16]	1771.90071	-0.08	-0.00007	MIGIISDSHDNLTAIR	High
19918309 [1-16]	1755.90579	1.82	0.00159	MIGIISDSHDNLTAIR	High
19918309 [126-145]	2046.98345	-3.22	-0.0033	MIDGTPVINPGECSGVLSGK	High
19918309 [126-145]	2030.98854	-1.18	-0.0012	MIDGTPVINPGECSGVLSGK	High
19918309 [52-68]	1930.9909	-1.15	-0.00074	LYFVFGNNDGDKVTLTK	High
19918309 [1-17]	1899.99567	0.02	0.00001	MIGIISDSHDNLTAIRK	High
19918309 [52-63]	1388.64811	-1.05	-0.00073	LYFVFGNNDGDK	High
19918309 [117-125]	975.4755	0.09	0.00003	GHTHDPGVR	High
19918309 [29-43]	1595.8904	-1.74	-0.00139	AVLHAGDIISPFTVR	High
19918309 [18-25]	982.53564	0.48	0.00024	AVEFFNKK	High

19918309 [18-24]	854.44068	0.62	0.00026	AVEFFNK	High
19918309 [104-116]	1377.70087	-1.34	-0.00092	ALAESGDFDVVVR	High

Table S2.3 Identification of individual SDS-PAGE bands of in-gel digests from MCR preparation showing tryptic peptides and resulting proteins identified.

~60 kDa band

ABC transporter, ATP-binding protein, MA_3998, MW: 59.6

seq coverage: 65.9%

Conf%	Observ.mass	Calc. mass	Ion%	#	Sequence
100.00%	963.71686	962.53796	76.90%	2	-.MPVFIEVK.N
18.20%	979.93097	978.53284	75.00%	1	-.M(15.9949)PVFIEVK.N
100.00%	1121.976	1121.5837	100.00%	7	K.NLTVDFDGLK.A
100.00%	1228.6326	1227.6943	100.00%	5	R.INEGEVVGILGK.S
99.80%	983.73737	982.5866	92.30%	14	K.TILMHVLR.G
57.80%	999.5153	998.5815	84.60%	2	K.TILM(15.9949)HVLR.G
100.00%	2023.1487	2021.9927	57.10%	3	R.GTESFENISGEVIYHLAR.C
100.00%	2023.6553	2021.9927	57.40%	16	R.GTESFENISGEVIYHLAR.C
100.00%	1931.0596	1929.8608	57.70%	2	K.CPVCGETLEEFEADFIK.L
59.20%	1929.4131	1929.8608	45.50%	1	K.CPVCGETLEEFEADFIK.L
99.70%	977.57355	976.5462	100.00%	2	K.LSLYDPIR.K
98.40%	1105.427	1104.6411	46.20%	17	K.LSLYDPIRK.D
11.90%	1106.187	1104.6411	50.00%	1	K.LSLYDPIRK.D
99.70%	845.13745	844.5073	100.00%	8	R.IAIMLQR.T
76.60%	861.46533	860.5022	100.00%	4	R.IAIM(15.9949)LQR.T
100.00%	1071.9497	1071.5105	100.00%	5	R.TFALYGDER.V
100.00%	1675.6926	1674.9425	87.50%	9	R.VLVNVINSLNEIGYK.G
100.00%	1676.0977	1674.9425	72.50%	2	R.VLVNVINSLNEIGYK.G
99.60%	2266.596	2268.1653	36.50%	3	K.GEDAMKKAVELLEEVNLSHR.M
28.40%	1637.2201	1636.9016	45.90%	1	K.KAVELLEEVNLSHR.M
100.00%	1509.824	1508.8068	95.00%	31	K.AVELLEEVNLSHR.M
25.90%	1508.7313	1508.8068	48.50%	1	K.AVELLEEVNLSHR.M
29.10%	2264.4473	2266.143	35.40%	2	K.AVELLEEVNLSHRM(15.9949)M(15.9949)HVAR.E
100.00%	2110.84	2110.11	72.70%	2	R.NPLLLLADEPTGTLDPMTAK.L
100.00%	2112.1482	2110.11	61.10%	2	R.NPLLLLADEPTGTLDPMTAK.L
100.00%	2127.9412	2126.105	81.80%	4	R.NPLLLLADEPTGTLDPM(15.9949)TAK.L
100.00%	2127.4265	2126.105	56.40%	2	R.NPLLLLADEPTGTLDPM(15.9949)TAK.L
100.00%	1207.6759	1206.7205	94.10%	36	K.LVHEAIINAVK.N
20.60%	2179.9954	2178.036	28.30%	1	K.NYNMSMVLTSHWPEVIEK.L
100.00%	3262.604	3260.654	33.80%	2	K.AILLENGEVVQEGDPLEVSAIFMQSVSMVR.Q

97.00%	3278.1309	3276.649	28.40%	1	K.AILLENGEVVQEGDPLEVSAIFM(15.9949)QSVSMVR.Q
100.00%	3277.5852	3276.649	41.60%	2	K.AILLENGEVVQEGDPLEVSAIFMQSVSM(15.9949)VR.Q
100.00%	3294.1882	3292.6438	30.70%	2	K.AILLENGEVVQEGDPLEVSAIFM(15.9949)QSVSM(15.9949)VR.Q
100.00%	1110.2744	1109.6677	100.00%	9	K.NVLVGEPIIR.V
92.20%	2177.3682	2176.2197	34.60%	1	R.DLSKRYISVDRGVVRAVDK.I
40.40%	909.31757	908.4948	75.00%	1	K.RYISVDR.G
100.00%	1434.0156	1433.7634	100.00%	3	K.EGEIFGLVGISGAGK.T
100.00%	1435.8513	1433.7634	56.10%	2	K.EGEIFGLVGISGAGK.T
11.20%	1954.9984	1952.0334	29.60%	1	K.EGEIFGLVGISGAGKTTTSK.I
100.00%	1711.7412	1710.9458	100.00%	6	K.ILMGILPPTSGEVEVR.V
30.70%	1713.7292	1710.9458	31.80%	1	K.ILMGILPPTSGEVEVR.V
100.00%	1727.6694	1726.9408	84.60%	7	K.ILM(15.9949)GILPPTSGEVEVR.V
100.00%	1180.3419	1179.535	86.70%	2	R.VGDEWVDMTK.L
90.70%	657.8392	658.44977	88.90%	2	K.AIITLK.A
43.30%	1264.2993	1261.8103	50.00%	1	R.HRIALAQVLIK.E
87.00%	970.3972	968.65027	100.00%	4	R.IALAQVLIK.E
100.00%	1761.7612	1760.8809	92.00%	4	R.IVIMDEPTGTMDPITK.V
100.00%	1777.364	1776.8757	96.00%	4	R.IVIMDEPTGTM(15.9949)DPITK.V
100.00%	1777.4922	1776.8757	72.00%	4	R.IVIM(15.9949)DEPTGTMDPITK.V
99.70%	947.56476	944.5775	93.30%	4	K.VAVTNSILK.A
41.00%	688.7841	686.41956	80.00%	1	K.IVEIGR.P
100.00%	2111.9724	2110.1501	58.50%	7	K.IVEIGRPGTVLAQLTEEER.I
100.00%	1443.5706	1442.7485	95.00%	2	R.PGTVLAQLTEEER.I

Table S2.4 Table of all primers and gblocks used in this study

Name	Sequence
SA025	TCATGGTCACATCCTCAGTTTGAAAAAGGTGGAGGACCAGTATTTATTGAAGTTAAAAA
SA026	TGAAAAAGGTGGCGGGTCAGGCGGGGGTTCAGGGGGTGGCTCATGGTCACATCCTCAG
SA027	ACGACAAGGGTTCCGCTGCATCCTGGTCACATCCTCAGTTTGAAAAAGGTGGCGGG
SA028	AATAAATTAAGGAGGAAATTCAATGGACTACAAAGACGATGACGACAAGGGTTCCGC
SA029	CATTATACGAAGTTATCAAGATTATATTTCTTCTGCAGCTTTGATCCT
SA030	AATAAATTAAGGAGGAAATTCAATGCCAGTATTTATTGAAGTT
SA031	GCGGAACCCTTGTCGTCATCGTCTTTGTAGTCTCCTCCACCTATTTCTTCTGCAGCTTTG
SA032	CTGACCCGCCACCTTTTTCAAACTGAGGATGTGACCAGGATGCAGCGGAACCCTTGTCGT
SA033	TCAAACTGAGGATGTGACCATGAGCCACCCCCTGAACCCCCGCCTGACCCGCCACCTTT
SA034	CATTATACGAAGTTATCAAGATTATTTTTCAAACTGAGGATGTGACCA
SA119	CTTGACCCCATGACTGCAAA
SA120	AATTTTCTCCAGATCCGAGACTTT
SA124	AGACCGGGATTCCATTTCCT
SA126	TATTTGCAAGCTCGGAAAGGA
SA131	TCTCGGTAGAAGACGGAATTCC
SA134	CTGGAAACCCCGGCTTCTT
SA137	TGCAGGGGAAATCGGGATTA
SA138	CAGGACTTGCCCAGTGGATA
SA148	GCATCAGGATTGTGGCCCCTGATCCGCTTTT
SA149	GCGGATCAGGGGCCACAATCCTGATGCAC
SA150	AATAAATTAAGGAGGAAATTCA
SA151	AGGTTGTGGTGGCGCCTGCTCCGCTTAT
SA152	AAGCGGAGCAGGCGCCACCACAACCTCTAAAAT
SA173	CTTCTGTTAGCTGACGCGCCTACGGGTACA
SA174	TGTACCCGTAGGCGCGTCAGCTAACAGAAG
SA175	GTTATTATGGACGCACCTACAGGGACCATGGAC
SA176	GTCCATGGTCCCTGTAGGTGCGTCCATAATAAC
gSAA001	AATAAATTAAGGAGGAAATTCAATGGACTACAAAGACGATGACGACAAGGGTTCCGCTGCATCCTGGTCA CATCCTCAGTTTGAAAAAGGTGGCGGGTCAGGCGGGGGTTCAGGGGGTGGCTCATGGTCACATCCTCA GTTTGAAAAAGGTGGAGGACCAGTATTTATTGAAGTTAAAAACCTAACTGTAGACTTTGACGGTCTCAAA GCCCTGAAAAATGTAAATTTAAGGATCAACGAAGGGGAAGTCGTTGGAATTCTGGGAAAAAGCGGATCA GGGAAAACAATCCTGATGCACGTGTTGCGCGGGACCGAATCTTTTGAGAATATCTCAGGCGAAGTAATC TATCATCTGGCCCGCGCAGAGAAAGCTGGATATATAGAGCGTCCAAGCAAAATAGGCCAGAAAGCCCCGG TCGCAGGGGAGACGCTTGAGGAGTTCGAAGCTG

Table S2.5 Table of all plasmids used in this study.

Plasmid	Description	Reference
pJK027A	Vector with PmcrB(tetO1) promoter fusion to uidA that contains φC31-attB and λattP	[17]
pAMG40	Vector for fosmid retrofitting containing pC2A and λattB	[17]
pDN201	pJK027A-derived plasmid with PmcrB(tetO1) promoter fusion to Spy cas9	[16]
pSAA004	derivative of pJK027A with MA3998_N_1XFLAG_2XStrep under control of PmcrB(tetO1)	this study
pSAA049	derivative of pJK027A with MA3998_C_1XFLAG_2XStrep under control of PmcrB(tetO1)	this study
pSAA050	derivative of pJK027A with MA3998_N_1XFLAG_ 2XStrep_K43A under control of PmcrB(tetO1)	this study
pSAA051	derivative of pJK027A with MA3998_N_1XFLAG_ 2XStrep_K329A under control of PmcrB(tetO1)	this study
pSAA052	derivative of pJK027A with MA3998_N_1XFLAG_ 2XStrep_K43/329A under control of PmcrB(tetO1)	this study
pSAA055	derivative of pJK027A with MA3998_N_1XFLAG_ 2XStrep_E200A under control of PmcrB(tetO1)	this study
pSAA056	derivative of pJK027A with MA3998_N_1XFLAG_ 2XStrep_E459A under control of PmcrB(tetO1)	this study
pSAA057	derivative of pJK027A with MA3998_N_1XFLAG_2XStrep_E200/459A under control of PmcrB(tetO1)	this study
pSAA058	derivative of pJK027A with MA3998_N_1XFLAG_2XStrep_C70/73/86/89A under control of PmcrB(tetO1)	this study
pDN353	pDN201 derived plasmid containing the sgRNA and repair template to generate an in-frame deletion of MA_3992	this study
pDN355	pDN201 derived plasmid containing the sgRNA and repair template to generate an in-frame deletion of MA_3993	this study
pDN356	pDN201 derived plasmid containing the sgRNA and repair template to generate an in-frame deletion of MA_3994	this study
pDN357	pDN201 derived plasmid containing the sgRNA and repair template to generate an in-frame deletion of MA_3995	this study
pDN358	pDN201 derived plasmid containing the sgRNA and repair template to generate an in-frame deletion of MA_3996	this study
pDN359	pDN201 derived plasmid containing the sgRNA and repair template to generate an in-frame deletion of MA_3997	this study
pDN360	pDN201 derived plasmid containing the sgRNA and repair template to generate an in-frame deletion of MA_3998	this study
pDN367	Cointegrate of pDN353 and pAMG40 obtained using Gateway cloning (BP Clonase II)	this study
pDN369	Cointegrate of pDN355 and pAMG40 obtained using Gateway cloning (BP Clonase II)	this study
pDN371	Cointegrate of pDN357 and pAMG40 obtained using Gateway cloning (BP Clonase II)	this study
pDN373	Cointegrate of pDN359 and pAMG40 obtained using Gateway cloning (BP Clonase II)	this study
pDN375	Cointegrate of pDN361 and pAMG40 obtained using Gateway cloning (BP Clonase II)	this study
pDN377	Cointegrate of pDN363 and pAMG40 obtained using Gateway cloning (BP Clonase II)	this study
pDN379	Cointegrate of pDN365 and pAMG40 obtained using Gateway cloning (BP Clonase II)	this study

Table S2.6 Table of all strains used in this study.

Strain	Description	Reference
WWM60	M. acetivorans delta hpt:: PmcrB-tetR	[17]
WWM1086	M. acetivorans delta hpt:: PmcrB-tetR TAP (3X-FLAG EK site 2X Strep EK site) tag at N-terminus of mcrG (WWM60/pDN329)	[50]
WWM73	M. acetivorans delta hpt:: PmcrB-tetR-phiC31int-attP	17
DDN122	M. acetivorans delta hpt:: PmcrB-tetR-phiC31int-attP att::BmcrB(tetO1) MA3998-NstrepFLAG (WWM73/att:pSAA004)	this study
DDN291	M. acetivorans delta hpt:: PmcrB-tetR-phiC31int-attP att::BmcrB(tetO1) MA3998-CstrepFLAG (WWM73/ att:pSAA049)	this study
DDN324	M. acetivorans delta hpt:: PmcrB-tetR-phiC31int-attP att::BmcrB(tetO1) MA3998-NstrepFLAG-K43A (WWM73/ att:pSAA050)	this study
DDN325	M. acetivorans delta hpt:: PmcrB-tetR-phiC31int-attP att::BmcrB(tetO1) MA3998-NstrepFLAG-K329A (WWM73/ att:pSAA051)	this study
DDN326	M. acetivorans delta hpt:: PmcrB-tetR-phiC31int-attP att::BmcrB(tetO1) MA3998-NstrepFLAG-K43A-K329A (WWM73/ att:pSAA052)	this study
DDN408	M. acetivorans delta hpt:: PmcrB-tetR-phiC31int-attP att::BmcrB(tetO1) MA3998-NstrepFLAG-E200A (WWM73/ att:pSAA055)	this study
DDN409	M. acetivorans delta hpt:: PmcrB-tetR-phiC31int-attP att::BmcrB(tetO1) MA3998-NstrepFLAG-E459A (WWM73/ att:pSAA056)	this study
DDN410	M. acetivorans delta hpt:: PmcrB-tetR-phiC31int-attP att::BmcrB(tetO1) MA3998-NstrepFLAG-E200/459A (WWM73/ att:pSAA057)	this study
DDN435	M. acetivorans delta hpt:: PmcrB-tetR-phiC31int-attP att::BmcrB(tetO1) MA3998-NstrepFLAG-C70/73/86/89 (WWM73/ att:pSAA058)	this study

Table S2.7 Table of all genomes for the sequences used to build alignment in Figure 2.2.3.1. Protein sequences with the assigned TIGRFAM Hidden Markov Model (HMM)[116] **TIGR03269** were downloaded from the Genome Taxonomy Database (GTDB) R214, which included 888 sequences. This table shows the genome accession number from which the sequence originates, the description of the genome, and the number of sequences with **TIGR03269** assigned. See section *2.4.13* for further detail.

Name	Description	# sequences
GB_GCA_001766825.1	d__Archaea;p__Halobacteriota;c__Syntropharchaeia;o__Syntropharchaeales;f__Syntropharchaeaceae;g__Syntropharchaeum;s__Syntropharchaeum butanivorans	4
GB_GCA_004212075.1	d__Archaea;p__Halobacteriota;c__Methanoliparia;o__Methanoliparales;f__Methanoliparaceae;g__Methanoliparum;s__Methanoliparum thermophilum	3
GB_GCA_004212085.1	d__Archaea;p__Halobacteriota;c__Methanoliparia;o__Methanoliparales;f__Methanoliparaceae;g__Methanolliviera;s__Methanolliviera hydrocarbonicum	3
GB_GCA_013375455.1	d__Archaea;p__Asgardarchaeota;c__Lokiarchaeia;o__Helarchaeales;f__HEL-GB-A;g__JABXJT01;s__JABXJT01 sp013375455	3
GB_GCA_016840125.1	d__Archaea;p__Asgardarchaeota;c__Lokiarchaeia;o__Helarchaeales;f__HEL-GB-A;g__JABXJT01;s__JABXJT01 sp016840125	3
GB_GCA_021409285.1	d__Archaea;p__Halobacteriota;c__Methanosarcinia;o__Methanosarcinales;f__Methanoperedenaceae;g__Methanoperedens;s__Methanoperedens sp021409285	3
GB_GCA_022710385.1	d__Archaea;p__Halobacteriota;c__Methanomicrobia;o__Methanomicrobiales;f__Methanoregulaceae;g__UBA9949;s__UBA9949 sp022710385	3
GB_GCA_023434825.1	d__Archaea;p__Methanobacteriota;c__Methanobacteria;o__Methanobacteriales;f__Methanobacteriaceae;g__Methanobacterium_D;s__Methanobacterium_D sp023434825	3
GB_GCA_902158735.1	d__Archaea;p__Halobacteriota;c__Methanoliparia;o__Methanoliparales;f__Methanoliparaceae;g__Methanolliviera;s__Methanolliviera sp902158735	3
GB_GCA_902158745.1	d__Archaea;p__Halobacteriota;c__Methanoliparia;o__Methanoliparales;f__Methanoliparaceae;g__Methanolliviera;s__Methanolliviera sp902158745	3
GB_GCA_902386135.1	d__Archaea;p__Halobacteriota;c__Methanosarcinia;o__Methanosarcinales;f__Methanoperedenaceae;g__Methanoperedens;s__Methanoperedens sp902386135	3
GB_GCA_903832665.1	d__Archaea;p__Halobacteriota;c__Methanomicrobia;o__Methanomicrobiales;f__Methanoregulaceae;g__Methanoregula;s__Methanoregula sp903832665	3
GB_GCA_905339155.1	d__Archaea;p__Halobacteriota;c__Methanosarcinia;o__Methanosarcinales;f__Methanoperedenaceae;g__Methanoperedens;s__Methanoperedens sp905339155	3
GB_GCA_000309865.1	d__Archaea;p__Methanobacteriota;c__Methanobacteria;o__Methanobacteriales;f__Methanobacteriaceae;g__Methanobacterium;s__Methanobacterium sp000309865	2
GB_GCA_000499765.1	d__Archaea;p__Methanobacteriota;c__Methanobacteria;o__Methanobacteriales;f__Methanobacteriaceae;g__Methanobacterium;s__Methanobacterium sp000499765	2
GB_GCA_001412335.1	d__Archaea;p__Halobacteriota;c__Methanomicrobia;o__Methanomicrobiales;f__Methanoregulaceae;g__SD8;s__SD8 sp001412335	2
GB_GCA_001766815.1	d__Archaea;p__Halobacteriota;c__Syntropharchaeia;o__Syntropharchaeales;f__Syntropharchaeaceae;g__Syntropharchaeum_A;s__Syntropharchaeum_A caldarius	2
GB_GCA_001940805.1	d__Archaea;p__Halobacteriota;c__Methanomicrobia;o__Methanomicrobiales;f__Methanocorpusculaceae;g__Methanocorpusculum;s__Methanocorpusculum sp001940805	2
GB_GCA_002010305.1	d__Archaea;p__Halobacteriota;c__Archaeoglobi;o__Archaeoglobales;f__JdFR-42;g__JdFR-42;s__JdFR-42 sp002010305	2
GB_GCA_002067035.1	d__Archaea;p__Halobacteriota;c__Methanomicrobia;o__Methanomicrobiales;f__Methanoregulaceae;g__Methanoregula;s__Methanoregula sp002067035	2
GB_GCA_002067065.1	d__Archaea;p__Methanobacteriota;c__Methanobacteria;o__Methanobacteriales;f__Methanobacteriaceae;g__Methanobacterium;s__Methanobacterium sp002067065	2
GB_GCA_002067095.1	d__Archaea;p__Halobacteriota;c__Methanomicrobia;o__Methanomicrobiales;f__Methanoregulaceae;g__Methanolinea_A;s__Methanolinea_A sp002067095	2
GB_GCA_002067315.1	d__Archaea;p__Halobacteriota;c__Methanocellia;o__Methanocellales;f__Methanocellaceae;g__Methanocella_A;s__Methanocella_A sp002067315	2
GB_GCA_002067635.1	d__Archaea;p__Thermoplasmatota;c__Thermoplasmata;o__Methanomassiliicoccales;f__Methanomassiliicoccaceae;g__UBA6;s__UBA6 sp002067635	2

GB_GCA_002067895.1	d__Archaea;p__Halobacteriota;c__Methanomicrobia;o__Methanomicrobiales;f__Methanoregulaceae;g__MVRE01;s__MVRE01 sp002067895	2
GB_GCA_002068435.1	d__Archaea;p__Halobacteriota;c__Methanomicrobia;o__Methanomicrobiales;f__Methanoregulaceae;g__UBA9949;s__UBA9949 sp002068435	2
GB_GCA_002287215.1	d__Archaea;p__Halobacteriota;c__Methanomicrobia;o__Methanomicrobiales;f__Methanocorpusculaceae;g__Methanocorpusculum;s__Methanocorpusculum parvum	2
GB_GCA_002494885.1	d__Archaea;p__Methanobacteriota;c__Methanobacteria;o__Methanobacteriales;f__Methanobacteriaceae;g__Methanobacterium_D;s__Methanobacterium_D sp002494885	2
GB_GCA_002495055.1	d__Archaea;p__Halobacteriota;c__Methanomicrobia;o__Methanomicrobiales;f__Methanoregulaceae;g__Methanoregula;s__Methanoregula sp002495055	2
GB_GCA_002495065.1	d__Archaea;p__Halobacteriota;c__Methanomicrobia;o__Methanomicrobiales;f__Methanoregulaceae;g__Methanoregula;s__Methanoregula sp002495065	2
GB_GCA_002495625.1	d__Archaea;p__Methanobacteriota;c__Methanobacteria;o__Methanobacteriales;f__Methanobacteriaceae;g__Methanobacterium_A;s__Methanobacterium_A sp002495625	2
GB_GCA_002496805.1	d__Archaea;p__Methanobacteriota;c__Methanobacteria;o__Methanobacteriales;f__Methanobacteriaceae;g__Methanobacterium;s__Methanobacterium sp002496805	2
GB_GCA_002498375.1	d__Archaea;p__Halobacteriota;c__Methanomicrobia;o__Methanomicrobiales;f__Methanocorpusculaceae;g__Methanocorpusculum;s__Methanocorpusculum sp002498375	2
GB_GCA_002499905.1	d__Archaea;p__Halobacteriota;c__Methanomicrobia;o__Methanomicrobiales;f__Methanoregulaceae;g__UBA9949;s__UBA9949 sp002499905	2
GB_GCA_002502245.1	d__Archaea;p__Halobacteriota;c__Methanomicrobia;o__Methanomicrobiales;f__Methanoregulaceae;g__Methanoregula;s__Methanoregula sp002502245	2
GB_GCA_002502735.1	d__Archaea;p__Halobacteriota;c__Methanomicrobia;o__Methanomicrobiales;f__Methanoregulaceae;g__Methanoregula;s__Methanoregula sp002502735	2
GB_GCA_002503825.1	d__Archaea;p__Halobacteriota;c__Methanomicrobia;o__Methanomicrobiales;f__Methanoregulaceae;g__UBA467;s__UBA467 sp002503825	2
GB_GCA_002504725.1	d__Archaea;p__Methanobacteriota;c__Methanobacteria;o__Methanobacteriales;f__Methanobacteriaceae;g__UBA587;s__UBA587 sp002504725	2
GB_GCA_002505765.1	d__Archaea;p__Methanobacteriota;c__Methanobacteria;o__Methanobacteriales;f__Methanobacteriaceae;g__Methanobacterium_D;s__Methanobacterium_D sp002505765	2
GB_GCA_002506085.1	d__Archaea;p__Halobacteriota;c__Methanomicrobia;o__Methanomicrobiales;f__Methanocorpusculaceae;g__Methanocorpusculum;s__Methanocorpusculum sp002506085	2
GB_GCA_002506105.1	d__Archaea;p__Halobacteriota;c__Methanomicrobia;o__Methanomicrobiales;f__Methanoregulaceae;g__Methanolinea_A;s__Methanolinea_A sp002506105	2
GB_GCA_002508495.1	d__Archaea;p__Halobacteriota;c__Methanomicrobia;o__Methanomicrobiales;f__Methanoregulaceae;g__Methanoregula;s__Methanoregula sp002508495	2
GB_GCA_002509485.1	d__Archaea;p__Halobacteriota;c__Methanomicrobia;o__Methanomicrobiales;f__Methanoregulaceae;g__SD8;s__SD8 sp002509485	2
GB_GCA_002509495.1	d__Archaea;p__Halobacteriota;c__Methanomicrobia;o__Methanomicrobiales;f__Methanoregulaceae;g__Methanolinea_A;s__Methanolinea_A sp002509495	2
GB_GCA_002509665.1	d__Archaea;p__Methanobacteriota;c__Methanobacteria;o__Methanobacteriales;f__Methanobacteriaceae;g__Methanobacterium_D;s__Methanobacterium_D sp002509665	2
GB_GCA_002835825.1	d__Archaea;p__Halobacteriota;c__Methanomicrobia;o__Methanomicrobiales;f__Methanoregulaceae;g__Methanoregula;s__Methanoregula sp002835825	2
GB_GCA_002839605.1	d__Archaea;p__Halobacteriota;c__Methanomicrobia;o__Methanomicrobiales;f__Methanoregulaceae;g__Methanoregula;s__Methanoregula sp002839605	2
GB_GCA_002839675.1	d__Archaea;p__Halobacteriota;c__Methanomicrobia;o__Methanomicrobiales;f__Methanoregulaceae;g__Methanoregula;s__Methanoregula sp002839675	2
GB_GCA_002839705.1	d__Archaea;p__Methanobacteriota;c__Methanobacteria;o__Methanobacteriales;f__Methanobacteriaceae;g__UBA349;s__UBA349 sp002839705	2
GB_GCA_003136075.1	d__Archaea;p__Halobacteriota;c__Methanomicrobia;o__Methanomicrobiales;f__Methanoregulaceae;g__Methanoregula;s__Methanoregula sp003136075	2
GB_GCA_003141335.1	d__Archaea;p__Halobacteriota;c__Methanomicrobia;o__Methanomicrobiales;f__Methanoregulaceae;g__Methanoregula;s__Methanoregula sp003141335	2
GB_GCA_003151535.1	d__Archaea;p__Methanobacteriota;c__Methanobacteria;o__Methanobacteriales;f__Methanobacteriaceae;g__Methanobacterium_B;s__Methanobacterium_B sp003151535	2
GB_GCA_003157235.1	d__Archaea;p__Halobacteriota;c__Methanosarcinia;o__Methanosarcinales;f__Methanosarcinaceae;g__Methanosarcina;s__Methanosarcina sp003157235	2
GB_GCA_003158115.1	d__Archaea;p__Methanobacteriota;c__Methanobacteria;o__Methanobacteriales;f__Methanobacteriaceae;g__Methanobacterium_B;s__Methanobacterium_B sp003158115	2

GB_GCA_003160755.1	d__Archaea;p__Halobacteriota;c__Syntropharchaeia;o__ANME-1;f__ANME-1;g__QEXZ01;s__QEXZ01 sp003160755	2
GB_GCA_003162115.1	d__Archaea;p__Methanobacteriota;c__Methanobacteria;o__Methanobacteriales;f__Methanobacteriaceae;g__Methanobacterium_B;s__Methanobacterium_B sp003162115	2
GB_GCA_003164415.1	d__Archaea;p__Methanobacteriota;c__Methanobacteria;o__Methanobacteriales;f__Methanobacteriaceae;g__Methanobacterium_B;s__Methanobacterium_B sp003164415	2
GB_GCA_003164755.1	d__Archaea;p__Halobacteriota;c__Methanosarcinia;o__Methanosarcinales;f__Methanosarcinaceae;g__Methanosarcina;s__Methanosarcina sp003164755	2
GB_GCA_003166335.1	d__Archaea;p__Methanobacteriota;c__Methanobacteria;o__Methanobacteriales;f__Methanobacteriaceae;g__Methanobacterium_A;s__Methanobacterium_A sp003166335	2
GB_GCA_003170075.1	d__Archaea;p__Halobacteriota;c__Methanomicrobia;o__Methanomicrobiales;f__Methanoregulaceae;g__Methanoregula;s__Methanoregula sp003170075	2
GB_GCA_003194425.1	d__Archaea;p__Halobacteriota;c__Syntropharchaeia;o__ANME-1;f__ANME-1;g__ANME1a;s__ANME1a sp003194425	2
GB_GCA_003194435.1	d__Archaea;p__Halobacteriota;c__Syntropharchaeia;o__ANME-1;f__ANME-1;g__G60ANME1;s__G60ANME1 sp003194435	2
GB_GCA_003315675.1	d__Archaea;p__Halobacteriota;c__Methanomicrobia;o__Methanomicrobiales;f__Methanocorpusculaceae;g__Methanocorpusculum;s__Methanocorpusculum sp003315675	2
GB_GCA_003336485.1	d__Archaea;p__Halobacteriota;c__Syntropharchaeia;o__ANME-1;f__ANME-1;g__QENH01;s__QENH01 sp003336485	2
GB_GCA_003491305.1	d__Archaea;p__Methanobacteriota;c__Methanobacteria;o__Methanobacteriales;f__Methanobacteriaceae;g__Methanobacterium;s__Methanobacterium sp003491305	2
GB_GCA_003557905.1	d__Archaea;p__Thermoplasmatota;c__Thermoplasmata;o__Methanomassiliicoccales;f__Methanomethylophilaceae;g__PWHV01;s__PWHV01 sp003557905	2
GB_GCA_003601795.1	d__Archaea;p__Halobacteriota;c__Syntropharchaeia;o__ANME-1;f__ANME-1;g__QEXZ01;s__QEXZ01 sp003601795	2
GB_GCA_003661125.1	d__Archaea;p__Halobacteriota;c__Syntropharchaeia;o__ANME-1;f__ANME-1;g__QMVO01;s__QMVO01 sp003661125	2
GB_GCA_003661185.1	d__Archaea;p__Halobacteriota;c__Syntropharchaeia;o__ANME-1;f__B39-G2;g__B39-G2;s__B39-G2 sp003661185	2
GB_GCA_005191415.1	d__Archaea;p__Asgardarchaeota;c__Lokiarchaeia;o__Helarchaeales;f__HEL-GB-A;g__HEL-GB-A;s__HEL-GB-A sp005191415	2
GB_GCA_009712615.1	d__Archaea;p__Methanobacteriota;c__Methanobacteria;o__Methanobacteriales;f__Methanobacteriaceae;g__Methanobacterium_B;s__Methanobacterium_B sp009712615	2
GB_GCA_011049045.1	d__Archaea;p__Halobacteriota;c__Syntropharchaeia;o__ANME-1;f__ANME-1;g__JACGMN01;s__JACGMN01 sp011049045	2
GB_GCA_012026835.1	d__Archaea;p__Halobacteriota;c__Methanosarcinia;o__Methanosarcinales;f__Methanoperedenaceae;g__Methanoperedens;s__Methanoperedens sp012026835	2
GB_GCA_012516785.1	d__Archaea;p__Halobacteriota;c__Methanomicrobia;o__Methanomicrobiales;f__Methanoregulaceae;g__UBA9949;s__UBA9949 sp012516785	2
GB_GCA_012838205.1	d__Archaea;p__Methanobacteriota;c__Methanobacteria;o__Methanobacteriales;f__Methanobacteriaceae;g__Methanobacterium;s__Methanobacterium sp012838205	2
GB_GCA_013139985.1	d__Archaea;p__Halobacteriota;c__Syntropharchaeia;o__ANME-1;f__ANME-1;g__QENH01;s__QENH01 sp013139985	2
GB_GCA_013180565.1	d__Archaea;p__Halobacteriota;c__Syntropharchaeia;o__ANME-1;f__ANME-1;g__QENH01;s__QENH01 sp013180565	2
GB_GCA_013180585.1	d__Archaea;p__Halobacteriota;c__Syntropharchaeia;o__ANME-1;f__ANME-1;g__QENJ01;s__QENJ01 sp013180585	2
GB_GCA_013180605.1	d__Archaea;p__Halobacteriota;c__Syntropharchaeia;o__ANME-1;f__ANME-1;g__QEXZ01;s__QEXZ01 sp013180605	2
GB_GCA_013331015.1	d__Archaea;p__Halobacteriota;c__Methanomicrobia;o__Methanomicrobiales;f__Methanoregulaceae;g__Methanoregula;s__Methanoregula sp11803u	2
GB_GCA_013374505.1	d__Archaea;p__Halobacteriota;c__Syntropharchaeia;o__ANME-1;f__ANME-1;g__QENJ01;s__QENJ01 sp013374505	2
GB_GCA_013375355.1	d__Archaea;p__Asgardarchaeota;c__Lokiarchaeia;o__Helarchaeales;f__JABXJV01;g__JABXJV01;s__JABXJV01 sp013375355	2
GB_GCA_013375405.1	d__Archaea;p__Asgardarchaeota;c__Lokiarchaeia;o__Helarchaeales;f__HEL-GB-A;g__JABXJT01;s__JABXJT01 sp013375405	2
GB_GCA_013403005.1	d__Archaea;p__Methanobacteriota;c__Methanobacteria;o__Methanobacteriales;f__Methanobacteriaceae;g__Methanobacterium;s__Methanobacterium sp013403005	2

GB_GCA_013415565.1	d__Archaea;p__Halobacteriota;c__Methanomicrobia;o__Methanomicrobiales;f__Methanoregulaceae;g__UBA9949;s__UBA9949 sp013415565	2
GB_GCA_015660965.1	d__Archaea;p__Halobacteriota;c__Methanomicrobia;o__Methanomicrobiales;f__Methanoregulaceae;g__MVRE01;s__MVRE01 sp015660965	2
GB_GCA_016217785.1	d__Archaea;p__Methanobacteriota;c__Methanobacteria;o__Methanobacteriales;f__Methanobacteriaceae;g__Methanobacterium;s__Methanobacterium sp016217785	2
GB_GCA_016296195.1	d__Archaea;p__Thermoplasmatota;c__Thermoplasmata;o__Methanomassiliicoccales;f__Methanomethylophilaceae;g__UBA71;s__UBA71 sp016296195	2
GB_GCA_016874685.1	d__Archaea;p__Methanobacteriota;c__Methanobacteria;o__Methanobacteriales;f__Methanobacteriaceae;g__VGTM01;s__VGTM01 sp016874685	2
GB_GCA_016928455.1	d__Archaea;p__Halobacteriota;c__Syntropharchaeia;o__ANME-1;f__ANME-1;g__JACGMN01;s__JACGMN01 sp016928455	2
GB_GCA_017399555.1	d__Archaea;p__Halobacteriota;c__Methanomicrobia;o__Methanomicrobiales;f__Methanocorpusculaceae;g__Methanocorpusculum;s__Methanocorpusculum sp017399555	2
GB_GCA_017883485.1	d__Archaea;p__Halobacteriota;c__Methanosarcinia;o__Methanosarcinales;f__Methanosarcinaceae;g__Methanosarcina;s__Methanosarcina sp017883485	2
GB_GCA_018262855.1	d__Archaea;p__Halobacteriota;c__Methanomicrobia;o__Methanomicrobiales;f__Methanoregulaceae;g__Methanolinea_A;s__Methanolinea_A sp018262855	2
GB_GCA_018263335.1	d__Archaea;p__Halobacteriota;c__Methanomicrobia;o__Methanomicrobiales;f__Methanoregulaceae;g__Methanolinea_A;s__Methanolinea_A sp002067155	2
GB_GCA_018432765.1	d__Archaea;p__Halobacteriota;c__Methanomicrobia;o__Methanomicrobiales;f__Methanoregulaceae;g__SD8;s__SD8 sp018432765	2
GB_GCA_018883755.1	d__Archaea;p__Halobacteriota;c__Methanomicrobia;o__Methanomicrobiales;f__Methanocorpusculaceae;g__Methanocorpusculum;s__Methanocorpusculum faecipullorum	2
GB_GCA_018899795.1	d__Archaea;p__Halobacteriota;c__Methanosarcinia;o__Methanosarcinales;f__Methanoperedenaceae;g__Methanoperedens;s__Methanoperedens sp018899795	2
GB_GCA_019058315.1	d__Archaea;p__Asgardarchaeota;c__Lokiarchaeia;o__Helarchaeales;f__JABXJV01;g__JABXJV01;s__JABXJV01 sp019058315	2
GB_GCA_019084405.1	d__Archaea;p__Methanobacteriota;c__Methanobacteria;o__Methanobacteriales;f__Methanobacteriaceae;g__UBA588;s__UBA588 sp019084405	2
GB_GCA_020724545.1	d__Archaea;p__Halobacteriota;c__Methanosarcinia;o__Methanosarcinales;f__Methanoperedenaceae;g__Methanoperedens;s__Methanoperedens nitroreducens_B	2
GB_GCA_020854975.1	d__Archaea;p__Methanobacteriota;c__Methanobacteria;o__Methanobacteriales;f__Methanobacteriaceae;g__Methanobacterium;s__Methanobacterium sp020854975	2
GB_GCA_020855015.1	d__Archaea;p__Methanobacteriota;c__Methanobacteria;o__Methanobacteriales;f__Methanobacteriaceae;g__Methanobacterium;s__Methanobacterium sp020855015	2
GB_GCA_021159465.1	d__Archaea;p__Halobacteriota;c__Syntropharchaeia;o__ANME-1;f__ANME-1;g__G60ANME1;s__G60ANME1 sp021159465	2
GB_GCA_021159475.1	d__Archaea;p__Halobacteriota;c__Syntropharchaeia;o__ANME-1;f__ANME-1;g__G60ANME1;s__G60ANME1 sp021159475	2
GB_GCA_021161765.1	d__Archaea;p__Halobacteriota;c__Syntropharchaeia;o__ANME-1;f__ANME-1;g__QEXZ01;s__QEXZ01 sp021161765	2
GB_GCA_022710665.1	d__Archaea;p__Halobacteriota;c__Methanomicrobia;o__Methanomicrobiales;f__Methanoregulaceae;g__Methanoregula;s__Methanoregula sp022710665	2
GB_GCA_022711635.1	d__Archaea;p__Halobacteriota;c__Methanomicrobia;o__Methanomicrobiales;f__Methanoregulaceae;g__MVRE01;s__MVRE01 sp022711635	2
GB_GCA_023131215.1	d__Archaea;p__Halobacteriota;c__Syntropharchaeia;o__ANME-1;f__ANME-1;g__JAGXOS01;s__JAGXOS01 sp023131215	2
GB_GCA_023227875.1	d__Archaea;p__Halobacteriota;c__Methanomicrobia;o__Methanomicrobiales;f__Methanoregulaceae;g__Methanoregula;s__Methanoregula sp023227875	2
GB_GCA_023228295.1	d__Archaea;p__Halobacteriota;c__Methanomicrobia;o__Methanomicrobiales;f__Methanoregulaceae;g__Methanoregula;s__Methanoregula sp023228295	2
GB_GCA_023249105.1	d__Archaea;p__Halobacteriota;c__Methanosarcinia;o__Methanosarcinales;f__Methanoperedenaceae;g__Methanoperedens;s__Methanoperedens sp023249105	2
GB_GCA_023396065.1	d__Archaea;p__Halobacteriota;c__Methanomicrobia;o__Methanomicrobiales;f__Methanocorpusculaceae;g__Methanocorpusculum;s__Methanocorpusculum sp023396065	2
GB_GCA_023411115.1	d__Archaea;p__Methanobacteriota;c__Methanobacteria;o__Methanobacteriales;f__Methanobacteriaceae;g__Methanobacterium_D;s__Methanobacterium_D sp023411115	2
GB_GCA_023430285.1	d__Archaea;p__Methanobacteriota;c__Methanobacteria;o__Methanobacteriales;f__Methanobacteriaceae;g__Methanobacterium_B;s__Methanobacterium_B sp023430285	2

GB_GCA_023436175.1	d__Archaea;p__Methanobacteriota;c__Methanobacteria;o__Methanobacteriales;f__Methanobacteriaceae;g__Methanobacterium_D;s__Methanobacterium_D sp023436175	2
GB_GCA_023659775.1	d__Archaea;p__Halobacteriota;c__Syntropharchaeia;o__ANME-1;f__ANME-1;g__JAGXOS01;s__JAGXOS01 sp023659775	2
GB_GCA_023659785.1	d__Archaea;p__Halobacteriota;c__Syntropharchaeia;o__ANME-1;f__ANME-1;g__JAGXOR01;s__JAGXOR01 sp023659785	2
GB_GCA_024518585.1	d__Archaea;p__Halobacteriota;c__Methanomicrobia;o__Methanomicrobiales;f__Methanoregulaceae;g__Methanolinea_A;s__Methanolinea_A sp024518585	2
GB_GCA_902384525.1	d__Archaea;p__Halobacteriota;c__Methanosarcinia;o__Methanosarcinales;f__Methanoperedenaceae;g__Methanoperedens;s__Methanoperedens sp902384525	2
GB_GCA_902386115.1	d__Archaea;p__Halobacteriota;c__Methanosarcinia;o__Methanosarcinales;f__Methanoperedenaceae;g__Methanoperedens;s__Methanoperedens sp902386115	2
GB_GCA_903819595.1	d__Archaea;p__Halobacteriota;c__Methanomicrobia;o__Methanomicrobiales;f__Methanoregulaceae;g__CAIKOD01;s__CAIKOD01 sp903819595	2
GB_GCA_903828975.1	d__Archaea;p__Halobacteriota;c__Methanomicrobia;o__Methanomicrobiales;f__Methanoregulaceae;g__CAIKOD01;s__CAIKOD01 sp903828975	2
GB_GCA_903900025.1	d__Archaea;p__Halobacteriota;c__Methanomicrobia;o__Methanomicrobiales;f__Methanoregulaceae;g__MVRE01;s__MVRE01 sp903900025	2
GB_GCA_903926075.1	d__Archaea;p__Halobacteriota;c__Methanomicrobia;o__Methanomicrobiales;f__Methanospirillaceae;g__CAIYHQ01;s__CAIYHQ01 sp903926075	2
RS_GCF_000011005.1	d__Archaea;p__Halobacteriota;c__Methanocellia;o__Methanocellales;f__Methanocellaceae;g__Methanocella;s__Methanocella paludicola	2
RS_GCF_000015765.1	d__Archaea;p__Halobacteriota;c__Methanomicrobia;o__Methanomicrobiales;f__Methanocorpusculaceae;g__Methanocorpusculum;s__Methanocorpusculum labreanum	2
RS_GCF_000021965.1	d__Archaea;p__Halobacteriota;c__Methanomicrobia;o__Methanomicrobiales;f__Methanosphaerulaceae;g__Methanosphaerula;s__Methanosphaerula palustris	2
RS_GCF_000063445.1	d__Archaea;p__Halobacteriota;c__Methanocellia;o__Methanocellales;f__Methanocellaceae;g__Methanocella_A;s__Methanocella_A arvoryzae	2
RS_GCF_000191585.1	d__Archaea;p__Methanobacteriota;c__Methanobacteria;o__Methanobacteriales;f__Methanobacteriaceae;g__Methanobacterium_B;s__Methanobacterium_B lacus	2
RS_GCF_000214725.1	d__Archaea;p__Methanobacteriota;c__Methanobacteria;o__Methanobacteriales;f__Methanobacteriaceae;g__Methanobacterium_C;s__Methanobacterium_C paludis	2
RS_GCF_000251105.1	d__Archaea;p__Halobacteriota;c__Methanocellia;o__Methanocellales;f__Methanocellaceae;g__Methanocella;s__Methanocella conradii	2
RS_GCF_000302455.1	d__Archaea;p__Methanobacteriota;c__Methanobacteria;o__Methanobacteriales;f__Methanobacteriaceae;g__Methanobacterium;s__Methanobacterium formicicum_A	2
RS_GCF_000327485.1	d__Archaea;p__Halobacteriota;c__Methanomicrobia;o__Methanomicrobiales;f__Methanoregulaceae;g__Methanoregula;s__Methanoregula formicica	2
RS_GCF_000685155.1	d__Archaea;p__Halobacteriota;c__Methanosarcinia;o__Methanosarcinales;f__Methanoperedenaceae;g__Methanoperedens;s__Methanoperedens nitroreducens	2
RS_GCF_000745485.1	d__Archaea;p__Methanobacteriota;c__Methanobacteria;o__Methanobacteriales;f__Methanobacteriaceae;g__Methanobacterium_D;s__Methanobacterium_D veterum	2
RS_GCF_002287175.1	d__Archaea;p__Methanobacteriota;c__Methanobacteria;o__Methanobacteriales;f__Methanobacteriaceae;g__Methanobacterium_D;s__Methanobacterium_D bryantii	2
RS_GCF_002813695.1	d__Archaea;p__Methanobacteriota;c__Methanobacteria;o__Methanobacteriales;f__Methanobacteriaceae;g__Methanobacterium;s__Methanobacterium subterraneum	2
RS_GCF_003173355.1	d__Archaea;p__Halobacteriota;c__Methanomicrobia;o__Methanomicrobiales;f__Methanospirillaceae;g__Methanospirillum;s__Methanospirillum lacunae	2
RS_GCF_017873625.1	d__Archaea;p__Methanobacteriota;c__Methanobacteria;o__Methanobacteriales;f__Methanobacteriaceae;g__Methanobacterium;s__Methanobacterium petrolearium	2
RS_GCF_017873855.1	d__Archaea;p__Halobacteriota;c__Methanomicrobia;o__Methanomicrobiales;f__Methanoregulaceae;g__Methanolinea_B;s__Methanolinea_B mesophila	2
RS_GCF_018141185.1	d__Archaea;p__Methanobacteriota;c__Methanobacteria;o__Methanobacteriales;f__Methanobacteriaceae;g__UBA588;s__UBA588 sp002509085	2
RS_GCF_021023085.1	d__Archaea;p__Halobacteriota;c__Methanocellia;o__Methanocellales;f__Methanocellaceae;g__PGCK01;s__PGCK01 sp021023085	2
RS_GCF_023227715.1	d__Archaea;p__Methanobacteriota;c__Methanobacteria;o__Methanobacteriales;f__Methanobacteriaceae;g__Methanobacterium_E;s__Methanobacterium_E alcaliphilum	2
RS_GCF_900196725.1	d__Archaea;p__Halobacteriota;c__Methanosarcinia;o__Methanosarcinales;f__Methanoperedenaceae;g__Methanoperedens;s__Methanoperedens nitroreducens_A	2

GB_GCA_000306725.1	d__Archaea;p__Halobacteriota;c__Methanosarcinia;o__Methanosarcinales;f__Methanosarcinaceae;g__Methanolobus;s__Methanolobus psychrophilus	1
GB_GCA_000350305.1	d__Archaea;p__Thermoplasmatota;c__Thermoplasmata;o__Methanomassiliicoccales;f__Methanomethylophilaceae;g__Methanomethylophilus;s__Methanomethylophilus sp000350305	1
GB_GCA_001399795.1	d__Archaea;p__Thermoproteota;c__Bathyarchaeia;o__B26-1;f__BA1;g__BA2;s__BA2 sp001399795	1
GB_GCA_001412355.1	d__Archaea;p__Halobacteriota;c__Methanomicrobia;o__Methanomicrobiales;f__Methanomicrobiaceae;g__LKUD01;s__LKUD01 sp001412355	1
GB_GCA_001421175.1	d__Archaea;p__Thermoplasmatota;c__Thermoplasmata;o__Methanomassiliicoccales;f__Methanomethylophilaceae;g__RumEn-M2;s__RumEn-M2 sp001421175	1
GB_GCA_001421185.1	d__Archaea;p__Thermoplasmatota;c__Thermoplasmata;o__Methanomassiliicoccales;f__Methanomassiliicoccaceae;g__DTU008;s__DTU008 sp001421185	1
GB_GCA_001507955.1	d__Archaea;p__Methanobacteriota;c__Methanobacteria;o__Methanobacteriales;f__Methanothermobacteraceae_A;g__Methanothermobacter_A;s__Methanothermobacter_A sp001507955	1
GB_GCA_001509375.1	d__Archaea;p__Halobacteriota;c__Methanosarcinia;o__Methanotrichales;f__Methanotrichaceae;g__Methanothrix_A;s__Methanothrix_A harundinacea_D	1
GB_GCA_001512965.1	d__Archaea;p__Thermoplasmatota;c__Thermoplasmata;o__Methanomassiliicoccales;f__Methanomassiliicoccaceae;g__DTU008;s__DTU008 sp001512965	1
GB_GCA_001560915.1	d__Archaea;p__Thermoplasmatota;c__Thermoplasmata;o__Methanomassiliicoccales;f__Methanomethylophilaceae;g__Methanomethylophilus;s__Methanomethylophilus sp001560915	1
GB_GCA_001563305.1	d__Archaea;p__Thermoplasmatota;c__Thermoplasmata;o__Methanomassiliicoccales;f__Methanomethylophilaceae;g__UBA71;s__UBA71 sp001563305	1
GB_GCA_001602645.1	d__Archaea;p__Halobacteriota;c__Methanosarcinia;o__Methanotrichales;f__Methanotrichaceae;g__Methanothrix_A;s__Methanothrix_A sp001602645	1
GB_GCA_001714685.2	d__Archaea;p__Halobacteriota;c__Methanosarcinia;o__Methanosarcinales;f__Methanosarcinaceae;g__Methanosarcina;s__Methanosarcina sp001714685	1
GB_GCA_001717005.1	d__Archaea;p__Thermoproteota;c__Methanomethylicia;o__Methanomethylicales;f__Methanomethylicaceae;g__Methanomethylicus;s__Methanomethylicus mesodigestus	1
GB_GCA_001717015.1	d__Archaea;p__Thermoproteota;c__Methanomethylicia;o__Methanomethylicales;f__Methanomethylicaceae;g__Methanosuratincola;s__Methanosuratincola petrocarbonis	1
GB_GCA_001717025.1	d__Archaea;p__Thermoproteota;c__Methanomethylicia;o__Methanomethylicales;f__Methanomethylicaceae;g__Methanomethylicus;s__Methanomethylicus oleisabuli	1
GB_GCA_001896715.1	d__Archaea;p__Halobacteriota;c__Methanomicrobia;o__Methanomicrobiales;f__Methanoculleaceae;g__Methanoculleus;s__Methanoculleus sp001896715	1
GB_GCA_001896725.1	d__Archaea;p__Halobacteriota;c__Methanosarcinia;o__Methanosarcinales;f__Methanosarcinaceae;g__Methanomethylovorans;s__Methanomethylovorans sp001896725	1
GB_GCA_001914405.1	d__Archaea;p__Halobacteriota;c__Methanonatronarchaeia;o__Methanonatronarchaeales;f__Methanonatronarchaeaceae;g__Methanohalarchaeum;s__Methanohalarchaeum thermophilum	1
GB_GCA_002067275.1	d__Archaea;p__Halobacteriota;c__Methanosarcinia;o__Methanosarcinales;f__Methanosarcinaceae;g__Methanomethylovorans;s__Methanomethylovorans sp002067275	1
GB_GCA_002067365.1	d__Archaea;p__Halobacteriota;c__Methanosarcinia;o__Methanotrichales;f__Methanotrichaceae;g__Methanothrix;s__Methanothrix sp002067365	1
GB_GCA_002067705.1	d__Archaea;p__Halobacteriota;c__Methanosarcinia;o__Methanotrichales;f__Methanotrichaceae;g__Methanothrix;s__Methanothrix sp002067705	1
GB_GCA_002067755.1	d__Archaea;p__Halobacteriota;c__Methanosarcinia;o__Methanotrichales;f__Methanotrichaceae;g__Methanothrix;s__Methanothrix sp002067755	1
GB_GCA_002067795.1	d__Archaea;p__Halobacteriota;c__Methanosarcinia;o__Methanotrichales;f__Methanotrichaceae;g__MVQI01;s__MVQI01 sp002067795	1
GB_GCA_002067865.1	d__Archaea;p__Thermoplasmatota;c__Thermoplasmata;o__Methanomassiliicoccales;f__UBA472;g__MVRC01;s__MVRC01 sp002067865	1
GB_GCA_002254825.2	d__Archaea;p__Halobacteriota;c__Methanosarcinia;o__Methanosarcinales;f__EX4572-44;g__EX4572-44;s__EX4572-44 sp002254825	1
GB_GCA_002256595.1	d__Archaea;p__Halobacteriota;c__Methanosarcinia;o__Methanotrichales;f__Methanotrichaceae;g__Methanothrix;s__Methanothrix sp002256595	1
GB_GCA_002495225.1	d__Archaea;p__Halobacteriota;c__Methanomicrobia;o__Methanomicrobiales;f__Methanosphaerulaceae;g__UBA288;s__UBA288 sp002495225	1

GB_GCA_002495325.1	d__Archaea;p__Thermoplasmatota;c__Thermoplasmata;o__Methanomassiliicoccales;f__Methanomethylophilaceae;g__Methanomethylophilus;s__Methanomethylophilus sp002495325	1
GB_GCA_002495685.1	d__Archaea;p__Methanobacteriota;c__Methanobacteria;o__Methanobacteriales;f__Methanobacteriaceae;g__UBA412;s__UBA412 sp002495685	1
GB_GCA_002496395.1	d__Archaea;p__Halobacteriota;c__Methanomicrobia;o__Methanomicrobiales;f__Methanocorpusculaceae;g__Methanocalculus;s__Methanocalculus sp002496395	1
GB_GCA_002496565.1	d__Archaea;p__Halobacteriota;c__Methanosarcinia;o__Methanosarcinales;f__Methanosarcinaceae;g__Methanosarcina;s__Methanosarcina sp002496565	1
GB_GCA_002497075.1	d__Archaea;p__Thermoplasmatota;c__Thermoplasmata;o__Methanomassiliicoccales;f__UBA472;g__UBA472;s__UBA472 sp002497075	1
GB_GCA_002497965.1	d__Archaea;p__Halobacteriota;c__Methanomicrobia;o__Methanomicrobiales;f__Methanoculleaceae;g__Methanoculleus;s__Methanoculleus sp002497965	1
GB_GCA_002498065.1	d__Archaea;p__Halobacteriota;c__Methanomicrobia;o__Methanomicrobiales;f__Methanoculleaceae;g__Methanoculleus;s__Methanoculleus sp002498065	1
GB_GCA_002498315.1	d__Archaea;p__Halobacteriota;c__Methanomicrobia;o__Methanomicrobiales;f__Methanofollaceae;g__Methanofollis;s__Methanofollis sp002498315	1
GB_GCA_002498365.1	d__Archaea;p__Thermoplasmatota;c__Thermoplasmata;o__Methanomassiliicoccales;f__Methanomethylophilaceae;g__VadinCA11;s__VadinCA11 sp002498365	1
GB_GCA_002498385.1	d__Archaea;p__Methanobacteriota;c__Methanobacteria;o__Methanobacteriales;f__Methanobacteriaceae;g__Methanobacterium_C;s__Methanobacterium_C sp002498385	1
GB_GCA_002499445.1	d__Archaea;p__Halobacteriota;c__Methanosarcinia;o__Methanosarcinales;f__Methanosarcinaceae;g__Methanosarcina;s__Methanosarcina sp002499445	1
GB_GCA_002499455.1	d__Archaea;p__Halobacteriota;c__Methanomicrobia;o__Methanomicrobiales;f__Methanoculleaceae;g__Methanoculleus;s__Methanoculleus sp002499455	1
GB_GCA_002501655.1	d__Archaea;p__Halobacteriota;c__Methanomicrobia;o__Methanomicrobiales;f__Methanoculleaceae;g__Methanoculleus;s__Methanoculleus sp002501655	1
GB_GCA_002501695.1	d__Archaea;p__Halobacteriota;c__Methanosarcinia;o__Methanosarcinales;f__Methanosarcinaceae;g__Methanolobus;s__Methanolobus sp002501695	1
GB_GCA_002501765.1	d__Archaea;p__Halobacteriota;c__Methanosarcinia;o__Methanotrichales;f__Methanotrichaceae;g__UBA204;s__UBA204 sp002501765	1
GB_GCA_002502785.1	d__Archaea;p__Halobacteriota;c__Methanosarcinia;o__Methanotrichales;f__Methanotrichaceae;g__Methanothrix_A;s__Methanothrix_A harundinacea_A	1
GB_GCA_002502965.1	d__Archaea;p__Thermoplasmatota;c__Thermoplasmata;o__Methanomassiliicoccales;f__Methanomethylophilaceae;g__RumEn-M2;s__RumEn-M2 sp002502965	1
GB_GCA_002503105.1	d__Archaea;p__Halobacteriota;c__Methanomicrobia;o__Methanomicrobiales;f__Methanoculleaceae;g__UBA206;s__UBA206 sp002503105	1
GB_GCA_002503135.1	d__Archaea;p__Halobacteriota;c__Methanomicrobia;o__Methanomicrobiales;f__Methanoculleaceae;g__UBA207;s__UBA207 sp002503135	1
GB_GCA_002503545.1	d__Archaea;p__Thermoplasmatota;c__Thermoplasmata;o__Methanomassiliicoccales;f__Methanomethylophilaceae;g__Methanomethylophilus;s__Methanomethylophilus sp002503545	1
GB_GCA_002503595.1	d__Archaea;p__Halobacteriota;c__Methanosarcinia;o__Methanosarcinales;f__Methanogasteraceae;g__Methanogaster;s__Methanogaster sp002503595	1
GB_GCA_002503885.1	d__Archaea;p__Halobacteriota;c__Methanomicrobia;o__Methanomicrobiales;f__Methanoculleaceae;g__Methanoculleus;s__Methanoculleus marisnigri_B	1
GB_GCA_002504405.1	d__Archaea;p__Thermoplasmatota;c__Thermoplasmata;o__Methanomassiliicoccales;f__Methanomethylophilaceae;g__UBA71;s__UBA71 sp002504405	1
GB_GCA_002504525.1	d__Archaea;p__Thermoplasmatota;c__Thermoplasmata;o__Methanomassiliicoccales;f__Methanomassiliicoccaceae;g__DTU008;s__DTU008 sp002504525	1
GB_GCA_002505345.1	d__Archaea;p__Thermoplasmatota;c__Thermoplasmata;o__Methanomassiliicoccales;f__Methanomethylophilaceae;g__VadinCA11;s__VadinCA11 sp002505345	1
GB_GCA_002505485.1	d__Archaea;p__Halobacteriota;c__Methanosarcinia;o__Methanosarcinales;f__Methanosarcinaceae;g__Methanosarcina;s__Methanosarcina sp002505485	1
GB_GCA_002506015.1	d__Archaea;p__Halobacteriota;c__Methanosarcinia;o__Methanosarcinales;f__Methanogasteraceae;g__Methanogaster;s__Methanogaster sp002506015	1
GB_GCA_002506255.1	d__Archaea;p__Thermoplasmatota;c__Thermoplasmata;o__Methanomassiliicoccales;f__Methanomethylophilaceae;g__RumEn-M2;s__RumEn-M2 sp002506255	1
GB_GCA_002506425.1	d__Archaea;p__Thermoplasmatota;c__Thermoplasmata;o__Methanomassiliicoccales;f__Methanomethylophilaceae;g__UBA71;s__UBA71 sp002506425	1

GB_GCA_002506535.1	d__Archaea;p__Halobacteriota;c__Methanosarcinia;o__Methanotrichales;f__Methanotrichaceae;g__Methanothrix_A;s__Methanothrix_A harundinacea_B	1
GB_GCA_002506585.1	d__Archaea;p__Halobacteriota;c__Methanomicrobia;o__Methanomicrobiales;f__Methanoculleaceae;g__Methanoculleus;s__Methanoculleus sp002506585	1
GB_GCA_002506905.1	d__Archaea;p__Thermoplasmatota;c__Thermoplasmata;o__Methanomassiliicoccales;f__Methanomethylophilaceae;g__Methanogranum;s__Methanogranum sp002506905	1
GB_GCA_002507205.1	d__Archaea;p__Halobacteriota;c__Methanosarcinia;o__Methanosarcinales;f__Methanosarcinaceae;g__Methanolobus;s__Methanolobus sp002507205	1
GB_GCA_002508425.1	d__Archaea;p__Halobacteriota;c__Methanosarcinia;o__Methanosarcinales;f__Methanosarcinaceae;g__Methanomethylovorans;s__Methanomethylovorans sp002508425	1
GB_GCA_002508545.1	d__Archaea;p__Thermoplasmatota;c__Thermoplasmata;o__Methanomassiliicoccales;f__Methanomassiliicoccaceae;g__UBA6;s__UBA6 sp002508545	1
GB_GCA_002508705.1	d__Archaea;p__Halobacteriota;c__Methanomicrobia;o__Methanomicrobiales;f__Methanoculleaceae;g__Methanoculleus;s__Methanoculleus sp002508705	1
GB_GCA_002509325.1	d__Archaea;p__Halobacteriota;c__Methanosarcinia;o__Methanosarcinales;f__Methanosarcinaceae;g__Methanosarcina;s__Methanosarcina sp002509325	1
GB_GCA_002509405.1	d__Archaea;p__Thermoplasmatota;c__Thermoplasmata;o__Methanomassiliicoccales;f__Methanomethylophilaceae;g__VadinCA11;s__VadinCA11 sp002509405	1
GB_GCA_002509745.1	d__Archaea;p__Methanobacteriota;c__Methanobacteria;o__Methanobacteriales;f__Methanobacteriaceae;g__UBA349;s__UBA349 sp002509745	1
GB_GCA_002839545.1	d__Archaea;p__Halobacteriota;c__Methanosarcinia;o__Methanosarcinales;f__Methanoperedenaceae;g__Methanoperedens_A;s__Methanoperedens_A sp002839545	1
GB_GCA_002839575.1	d__Archaea;p__Halobacteriota;c__Methanomicrobia;o__Methanomicrobiales;f__Methanoculleaceae;g__Methanoculleus;s__Methanoculleus sp002839575	1
GB_GCA_002839645.1	d__Archaea;p__Halobacteriota;c__Methanomicrobia;o__Methanomicrobiales;f__Methanoculleaceae;g__Methanoculleus;s__Methanoculleus sp002839645	1
GB_GCA_002926195.1	d__Archaea;p__Halobacteriota;c__Methanosarcinia;o__Methanosarcinales;f__Methanocomedenaceae;g__Methanomarinus;s__Methanomarinus sp002926195	1
GB_GCA_003104905.1	d__Archaea;p__Halobacteriota;c__Methanosarcinia;o__Methanosarcinales;f__Methanoperedenaceae;g__Methanoperedens;s__Methanoperedens sp003104905	1
GB_GCA_003139855.1	d__Archaea;p__Halobacteriota;c__Bog-38;o__Bog-38;f__Bog-38;g__Bog-38;s__Bog-38 sp003139855	1
GB_GCA_003154335.1	d__Archaea;p__Halobacteriota;c__Methanomicrobia;o__Methanomicrobiales;f__Methanoregulaceae;g__Methanoregula;s__Methanoregula sp003154335	1
GB_GCA_003157895.1	d__Archaea;p__Halobacteriota;c__Methanomicrobia;o__Methanomicrobiales;f__Methanoregulaceae;g__Methanoregula;s__Methanoregula sp003157895	1
GB_GCA_003158275.1	d__Archaea;p__Halobacteriota;c__Bog-38;o__Bog-38;f__Bog-38;g__Bog-38;s__Bog-38 sp003158275	1
GB_GCA_003161815.1	d__Archaea;p__Methanobacteriota;c__Methanobacteria;o__Methanobacteriales;f__Methanobacteriaceae;g__Methanobacterium_A;s__Methanobacterium_A sp003161815	1
GB_GCA_003162175.1	d__Archaea;p__Halobacteriota;c__Bog-38;o__Bog-38;f__Bog-38;g__Bog-38;s__Bog-38 sp003162175	1
GB_GCA_003162615.1	d__Archaea;p__Halobacteriota;c__Methanosarcinia;o__Methanotrichales;f__Methanotrichaceae;g__Fen-7;s__Fen-7 sp003162615	1
GB_GCA_003170935.1	d__Archaea;p__Halobacteriota;c__Bog-38;o__Bog-38;f__Bog-38;g__Bog-38;s__Bog-38 sp003170935	1
GB_GCA_003194445.1	d__Archaea;p__Halobacteriota;c__Methanosarcinia;o__Methanosarcinales;f__Methanogasteraceae;g__Methanogaster;s__Methanogaster sp003194445	1
GB_GCA_003251955.1	d__Archaea;p__Halobacteriota;c__Methanomicrobia;o__Methanomicrobiales;f__Methanospirillaceae;g__Methanospirillum;s__Methanospirillum hungatei_A	1
GB_GCA_003266075.1	d__Archaea;p__Methanobacteriota;c__Methanobacteria;o__Methanobacteriales;f__Methanobacteriaceae;g__Methanosphaera;s__Methanosphaera sp003266075	1
GB_GCA_003266105.1	d__Archaea;p__Methanobacteriota;c__Methanobacteria;o__Methanobacteriales;f__Methanobacteriaceae;g__Methanosphaera;s__Methanosphaera sp003266105	1
GB_GCA_003266145.1	d__Archaea;p__Methanobacteriota;c__Methanobacteria;o__Methanobacteriales;f__Methanobacteriaceae;g__Methanosphaera;s__Methanosphaera sp003266145	1
GB_GCA_003315655.1	d__Archaea;p__Methanobacteriota;c__Methanobacteria;o__Methanobacteriales;f__Methanobacteriaceae;g__Methanobrevibacter_C;s__Methanobrevibacter_C sp003315655	1
GB_GCA_003491285.1	d__Archaea;p__Methanobacteriota;c__Methanobacteria;o__Methanobacteriales;f__Methanobacteriaceae;g__UBA117;s__UBA117 sp002494785	1

GB_GCA_003550345.1	d__Archaea;p__Thermoplasmatota;c__Thermoplasmata;o__Methanomassiliicoccales;f__Methanomethylophilaceae;g__PWHV01;s__PWHV01 sp003550345	1
GB_GCA_003555025.1	d__Archaea;p__Thermoplasmatota;c__Thermoplasmata;o__Methanomassiliicoccales;f__Methanomethylophilaceae;g__PWHV01;s__PWHV01 sp003555025	1
GB_GCA_003558085.1	d__Archaea;p__Methanobacteriota;c__Methanobacteria;o__Methanobacteriales;f__Methanobacteriaceae;g__UBA588;s__UBA588 sp003558085	1
GB_GCA_003560875.1	d__Archaea;p__Thermoplasmatota;c__Thermoplasmata;o__Methanomassiliicoccales;f__Methanomethylophilaceae;g__PWHV01;s__PWHV01 sp003560875	1
GB_GCA_003565715.1	d__Archaea;p__Halobacteriota;c__Methanosarcinia;o__Methanosarcinales;f__Methanosarcinaceae;g__Methanolobus;s__Methanolobus sp003565715	1
GB_GCA_003584625.1	d__Archaea;p__Methanobacteriota;c__Methanobacteria;o__Methanobacteriales;f__Methanothermobacteraceae_A;g__Methanothermobacter_A;s__Methanothermobacter_A sp003584625	1
GB_GCA_003601535.1	d__Archaea;p__Halobacteriota;c__Methanosarcinia;o__Methanosarcinales;f__Methanogasteraceae;g__Methanogaster;s__Methanogaster sp003601535	1
GB_GCA_003649565.1	d__Archaea;p__Thermoproteota;c__Methanomethylicia;o__Nezhaarchaeales;f__WYZ-LMO8;g__WYZ-LMO8;s__WYZ-LMO8 sp003649565	1
GB_GCA_003650865.1	d__Archaea;p__Thermoproteota;c__Methanomethylicia;o__Nezhaarchaeales;f__WYZ-LMO8;g__WYZ-LMO8;s__WYZ-LMO8 sp003650865	1
GB_GCA_003661105.1	d__Archaea;p__Halobacteriota;c__Methanosarcinia;o__Methanosarcinales;f__Methanogasteraceae;g__Methanogaster;s__Methanogaster sp003661105	1
GB_GCA_003838065.1	d__Archaea;p__Halobacteriota;c__Methanomicrobia;o__Methanomicrobiales;f__Methanocorpusculaceae;g__Methanocalculus;s__Methanocalculus sp003838065	1
GB_GCA_003857025.1	d__Archaea;p__Halobacteriota;c__Methanosarcinia;o__Methanotrichales;f__Methanotrichaceae;g__Methanothrix;s__Methanothrix sp003857025	1
GB_GCA_004028775.1	d__Archaea;p__Thermoproteota;c__Methanomethylicia;o__Methanomethylicales;f__Methanomethylicaceae;g__Methanosuratincola;s__Methanosuratincola subterraneus	1
GB_GCA_004193545.1	d__Archaea;p__Halobacteriota;c__Methanosarcinia;o__Methanosarcinales;f__EX4572-44;g__Ethanoperedens;s__Ethanoperedens ethanivorans	1
GB_GCA_004211975.1	d__Archaea;p__Halobacteriota;c__Methanosarcinia;o__Methanosarcinales;f__Methanogasteraceae;g__Methanogaster;s__Methanogaster sp004211975	1
GB_GCA_004212135.1	d__Archaea;p__Halobacteriota;c__Syntropharchaeia;o__ANME-1;f__ANME-1;g__ANME-1-THS;s__ANME-1-THS sp004212135	1
GB_GCA_004332335.1	d__Archaea;p__Halobacteriota;c__Methanomicrobia;o__Methanomicrobiales;f__Methanosphaerulaceae;g__UBA288;s__UBA288 sp004332335	1
GB_GCA_004347865.1	d__Archaea;p__Halobacteriota;c__Archaeoglobi;o__Archaeoglobales;f__Archaeoglobaceae;g__WYZ-LMO2;s__WYZ-LMO2 sp004347865	1
GB_GCA_004347955.1	d__Archaea;p__Thermoproteota;c__Methanomethylicia;o__Methanomethylicales;f__Methanomethylicaceae;g__WYZ-LMO10;s__WYZ-LMO10 sp004347955	1
GB_GCA_004347965.1.2	d__Archaea;p__Thermoproteota;c__Methanomethylicia;o__Nezhaarchaeales;f__WYZ-LMO8;g__WYZ-LMO8;s__WYZ-LMO8 sp004347965	1
GB_GCA_004348015.1	d__Archaea;p__Thermoproteota;c__Methanomethylicia;o__Methanomethylicales;f__Methanomethylicaceae;g__WYZ-LMO11;s__WYZ-LMO11 sp004348015	1
GB_GCA_004525545.1	d__Archaea;p__Thermoplasmatota;c__Thermoplasmata;o__Methanomassiliicoccales;f__UBA472;g__UBA472;s__UBA472 sp004525545	1
GB_GCA_004553595.1	d__Archaea;p__Methanobacteriota;c__Methanobacteria;o__Methanobacteriales;f__Methanobacteriaceae;g__Methanobrevibacter;s__Methanobrevibacter ruminantium_A	1
GB_GCA_005191425.1	d__Archaea;p__Asgardarchaeota;c__Lokiarchaeia;o__Helarchaeales;f__HEL-GB-B;g__HEL-GB-B;s__HEL-GB-B sp005191425	1
GB_GCA_006954405.1	d__Archaea;p__Thermoplasmatota;c__Thermoplasmata;o__Methanomassiliicoccales;f__Methanomethylophilaceae;g__Methanarcanum;s__Methanarcanum hacksteinii	1
GB_GCA_006954465.1	d__Archaea;p__Thermoplasmatota;c__Thermoplasmata;o__Methanomassiliicoccales;f__Methanomethylophilaceae;g__UBA71;s__UBA71 sp006954465	1
GB_GCA_007116915.1	d__Archaea;p__Thermoplasmatota;c__Thermoplasmata;o__Methanomassiliicoccales;f__Methanomethylophilaceae;g__PWHV01;s__PWHV01 sp007116915	1
GB_GCA_007127385.1	d__Archaea;p__Halobacteriota;c__Methanosarcinia;o__Methanosarcinales;f__Methanosarcinaceae;g__Methanosalsum;s__Methanosalsum sp007127385	1
GB_GCA_009618475.1	d__Archaea;p__Halobacteriota;c__Syntropharchaeia;o__ANME-1;f__ANME-1;g__WJOV01;s__WJOV01 sp009618475	1

GB_GCA_009649835.1	d__Archaea;p__Halobacteriota;c__Methanosarcinia;o__Methanosarcinales;f__Methanocomedenaceae;g__Methanocomedens;s__Methanocomedens sp009649835	1
GB_GCA_009776495.1	d__Archaea;p__Methanobacteriota;c__Methanobacteria;o__Methanobacteriales;f__Methanobacteriaceae;g__Methanobrevibacter_C;s__Methanobrevibacter_C sp009776495	1
GB_GCA_009776625.1	d__Archaea;p__Thermoplasmatota;c__Thermoplasmata;o__Methanomassiliicoccales;f__Methanomethylophilaceae;g__Methanoplasma;s__Methanoplasma sp009776625	1
GB_GCA_009776675.1	d__Archaea;p__Halobacteriota;c__Methanosarcinia;o__Methanosarcinales;f__Methanosarcinaceae;g__Methanimicrococcus;s__Methanimicrococcus sp009776675	1
GB_GCA_009776695.1	d__Archaea;p__Thermoplasmatota;c__Thermoplasmata;o__Methanomassiliicoccales;f__Methanomethylophilaceae;g__WRKA01;s__WRKA01 sp009776695	1
GB_GCA_009777005.1	d__Archaea;p__Methanobacteriota;c__Methanobacteria;o__Methanobacteriales;f__Methanobacteriaceae;g__Methanobrevibacter_C;s__Methanobrevibacter_C sp009777005	1
GB_GCA_009777615.1	d__Archaea;p__Thermoplasmatota;c__Thermoplasmata;o__Methanomassiliicoccales;f__Methanomethylophilaceae;g__Methanoplasma;s__Methanoplasma sp009777615	1
GB_GCA_009778575.1	d__Archaea;p__Thermoplasmatota;c__Thermoplasmata;o__Methanomassiliicoccales;f__Methanomethylophilaceae;g__Methanoplasma;s__Methanoplasma sp009778575	1
GB_GCA_009779205.1	d__Archaea;p__Halobacteriota;c__Methanomicrobia;o__Methanomicrobiales;f__Methanospirillaceae;g__WRER01;s__WRER01 sp009779205	1
GB_GCA_009780575.1	d__Archaea;p__Thermoplasmatota;c__Thermoplasmata;o__Methanomassiliicoccales;f__Methanomethylophilaceae;g__WRKA01;s__WRKA01 sp009780575	1
GB_GCA_009780795.1	d__Archaea;p__Thermoplasmatota;c__Thermoplasmata;o__Methanomassiliicoccales;f__Methanomethylophilaceae;g__WRKA01;s__WRKA01 sp009780795	1
GB_GCA_009783635.1	d__Archaea;p__Halobacteriota;c__Methanosarcinia;o__Methanosarcinales;f__Methanosarcinaceae;g__Methanimicrococcus;s__Methanimicrococcus sp009783635	1
GB_GCA_009784005.1	d__Archaea;p__Halobacteriota;c__Methanosarcinia;o__Methanosarcinales;f__Methanosarcinaceae;g__Methanimicrococcus;s__Methanimicrococcus sp009784005	1
GB_GCA_009784145.1	d__Archaea;p__Methanobacteriota;c__Methanobacteria;o__Methanobacteriales;f__Methanobacteriaceae;g__Methanobrevibacter_C;s__Methanobrevibacter_C sp009784145	1
GB_GCA_009784745.1	d__Archaea;p__Thermoplasmatota;c__Thermoplasmata;o__Methanomassiliicoccales;f__Methanomethylophilaceae;g__WRKA01;s__WRKA01 sp009784745	1
GB_GCA_009786295.1	d__Archaea;p__Thermoplasmatota;c__Thermoplasmata;o__Methanomassiliicoccales;f__Methanomethylophilaceae;g__Methanoplasma;s__Methanoplasma sp009786295	1
GB_GCA_009911715.1	d__Archaea;p__Thermoplasmatota;c__Thermoplasmata;o__Methanomassiliicoccales;f__Methanomethylophilaceae;g__UBA71;s__UBA71 sp006954425	1
GB_GCA_011045995.1	d__Archaea;p__Halobacteriota;c__Methanomicrobia;o__Methanomicrobiales;f__Methanomicrobiaceae;g__Methanogenium;s__Methanogenium sp011045995	1
GB_GCA_011048835.1	d__Archaea;p__Halobacteriota;c__Methanomicrobia;o__Methanomicrobiales;f__Methanomicrobiaceae;g__DSDF01;s__DSDF01 sp011048835	1
GB_GCA_011365055.1	d__Archaea;p__Asgardarchaeota;c__Lokiarchaeia;o__Helarchaeales;f__RDOG01;g__RDOG01;s__RDOG01 sp011365055	1
GB_GCA_011620785.1	d__Archaea;p__Halobacteriota;c__Methanosarcinia;o__Methanotrichales;f__Methanotrichaceae;g__Methanothrix;s__Methanothrix sp011620785	1
GB_GCA_011620825.1	d__Archaea;p__Thermoplasmatota;c__Thermoplasmata;o__Methanomassiliicoccales;f__Methanomethylophilaceae;g__VadinCA11;s__VadinCA11 sp011620825	1
GB_GCA_011620845.1	d__Archaea;p__Methanobacteriota;c__Methanobacteria;o__Methanobacteriales;f__Methanobacteriaceae;g__Methanobacterium_A;s__Methanobacterium_A sp011620845	1
GB_GCA_012026795.1	d__Archaea;p__Halobacteriota;c__Methanosarcinia;o__Methanosarcinales;f__Methanoperedenaceae;g__Methanoperedens;s__Methanoperedens sp012026795	1
GB_GCA_012329085.1	d__Archaea;p__Halobacteriota;c__Methanosarcinia;o__Methanosarcinales;f__Methanosarcinaceae;g__JAAXQB01;s__JAAXQB01 sp012329085	1
GB_GCA_012510295.1	d__Archaea;p__Halobacteriota;c__Methanomicrobia;o__Methanomicrobiales;f__Methanoculleaceae;g__Methanoculleus;s__Methanoculleus sp012510295	1
GB_GCA_012510335.1	d__Archaea;p__Halobacteriota;c__Methanomicrobia;o__Methanomicrobiales;f__Methanoculleaceae;g__Methanoculleus;s__Methanoculleus sp012510335	1
GB_GCA_012511245.1	d__Archaea;p__Halobacteriota;c__Methanomicrobia;o__Methanomicrobiales;f__Methanoculleaceae;g__Methanoculleus;s__Methanoculleus sp012511245	1
GB_GCA_012515075.1	d__Archaea;p__Thermoplasmatota;c__Thermoplasmata;o__Methanomassiliicoccales;f__Methanomethylophilaceae;g__JAAYZC01;s__JAAYZC01 sp012515075	1
GB_GCA_012518185.1	d__Archaea;p__Thermoplasmatota;c__Thermoplasmata;o__Methanomassiliicoccales;f__Methanomassiliicoccaceae;g__DTU008;s__DTU008 sp012518185	1

GB_GCA_012518265.1	d__Archaea;p__Halobacteriota;c__Methanosarcinia;o__Methanosarcinales;f__Methanosarcinaceae;g__Methanimicrococcus;s__Methanimicrococcus sp012518265	1
GB_GCA_012519255.1	d__Archaea;p__Thermoplasmatota;c__Thermoplasmata;o__Methanomassiliicoccales;f__Methanomassiliicoccaceae;g__DTU008;s__DTU008 sp012519255	1
GB_GCA_012520015.1	d__Archaea;p__Halobacteriota;c__Methanomicrobia;o__Methanomicrobiales;f__Methanospirillaceae;g__Methanospirillum;s__Methanospirillum sp012520015	1
GB_GCA_012520845.1	d__Archaea;p__Thermoplasmatota;c__Thermoplasmata;o__Methanomassiliicoccales;f__Methanomethylophilaceae;g__JAAYNL01;s__JAAYNL01 sp012520845	1
GB_GCA_012521035.1	d__Archaea;p__Halobacteriota;c__Methanomicrobia;o__Methanomicrobiales;f__Methanoculleaceae;g__Methanoculleus;s__Methanoculleus sp012521035	1
GB_GCA_012522645.1	d__Archaea;p__Thermoplasmatota;c__Thermoplasmata;o__Methanomassiliicoccales;f__Methanomethylophilaceae;g__RumEn-M2;s__RumEn-M2 sp012522645	1
GB_GCA_012523385.1	d__Archaea;p__Halobacteriota;c__Methanomicrobia;o__Methanomicrobiales;f__Methanomicrobiaceae;g__Methanogenium;s__Methanogenium sp012523385	1
GB_GCA_012719175.1	d__Archaea;p__Thermoplasmatota;c__Thermoplasmata;o__Methanomassiliicoccales;f__Methanomassiliicoccaceae;g__UBA6;s__UBA6 sp012719175	1
GB_GCA_012719315.1	d__Archaea;p__Thermoplasmatota;c__Thermoplasmata;o__Methanomassiliicoccales;f__Methanomethylophilaceae;g__Methanogranum;s__Methanogranum sp012719315	1
GB_GCA_012729095.1	d__Archaea;p__Thermoplasmatota;c__Thermoplasmata;o__Methanomassiliicoccales;f__UBA472;g__UBA472;s__UBA472 sp012729095	1
GB_GCA_012729535.1	d__Archaea;p__Halobacteriota;c__Methanomicrobia;o__Methanomicrobiales;f__Methanospirillaceae;g__Methanospirillum;s__Methanospirillum sp012729535	1
GB_GCA_012797575.1	d__Archaea;p__Halobacteriota;c__Methanomicrobia;o__Methanomicrobiales;f__Methanoculleaceae;g__Methanoculleus;s__Methanoculleus sp012797575	1
GB_GCA_012798025.1	d__Archaea;p__Halobacteriota;c__Methanosarcinia;o__Methanotrichales;f__Methanotrichaceae;g__Methanothrix;s__Methanothrix sp012798025	1
GB_GCA_012798365.1	d__Archaea;p__Halobacteriota;c__Methanomicrobia;o__Methanomicrobiales;f__Methanoregulaceae;g__Methanoregula;s__Methanoregula sp012798365	1
GB_GCA_012910725.1	d__Archaea;p__Halobacteriota;c__Methanosarcinia;o__Methanosarcinales;f__EX4572-44;g__Ethanoperedens;s__Ethanoperedens thermophilum	1
GB_GCA_012961645.1	d__Archaea;p__Halobacteriota;c__Methanosarcinia;o__Methanosarcinales;f__Methanogasteraceae;g__Methanogaster;s__Methanogaster sp012961645	1
GB_GCA_013153845.1	d__Archaea;p__Methanobacteriota;c__Methanococci;o__Methanococcales;f__Methanocaldococcaceae;g__Methanocaldococcus;s__Methanocaldococcus sp013153845	1
GB_GCA_013154335.1	d__Archaea;p__Methanobacteriota;c__Methanopyri;o__Methanopyrales;f__Methanopyraceae;g__Methanopyrus;s__Methanopyrus sp013154335	1
GB_GCA_013178225.1	d__Archaea;p__Halobacteriota;c__Methanosarcinia;o__Methanotrichales;f__Methanotrichaceae;g__JABLXE01;s__JABLXE01 sp013178225	1
GB_GCA_013329105.1	d__Archaea;p__Thermoplasmatota;c__Thermoplasmata;o__Methanomassiliicoccales;f__Methanomethylophilaceae;g__UBA9915;s__UBA9915 sp9915u	1
GB_GCA_013329165.1	d__Archaea;p__Halobacteriota;c__Methanomicrobia;o__Methanomicrobiales;f__Methanocorpusculaceae;g__Methanocalculus;s__Methanocalculus sp9912u	1
GB_GCA_013329415.1	d__Archaea;p__Halobacteriota;c__Methanosarcinia;o__Methanosarcinales;f__Methanosarcinaceae;g__MTP4;s__MTP4 sp9310u	1
GB_GCA_013329455.1	d__Archaea;p__Halobacteriota;c__Methanosarcinia;o__Methanotrichales;f__Methanotrichaceae;g__Methanothrix_A;s__Methanothrix_A sp9297u	1
GB_GCA_013329495.1	d__Archaea;p__Thermoplasmatota;c__E2;o__UBA9212;f__UBA9212;g__UBA9212;s__UBA9212 sp9212u	1
GB_GCA_013329565.1	d__Archaea;p__Thermoplasmatota;c__Thermoplasmata;o__Methanomassiliicoccales;f__UBA472;g__UBA472;s__UBA472 sp8940u	1
GB_GCA_013329575.1	d__Archaea;p__Halobacteriota;c__Methanoliparia;o__Methanoliparales;f__Methanoliparaceae;g__Methanoliparum;s__Methanoliparum sp8915u	1
GB_GCA_013330315.1	d__Archaea;p__Halobacteriota;c__Methanosarcinia;o__Methanosarcinales;f__Methanosarcinaceae;g__Methanosarcina;s__Methanosarcina sp8098u	1
GB_GCA_013330915.1	d__Archaea;p__Methanobacteriota;c__Methanobacteria;o__Methanobacteriales;f__Methanobacteriaceae;g__Methanosphaera;s__Methanosphaera sp11921u	1
GB_GCA_013331225.1	d__Archaea;p__Halobacteriota;c__Methanomicrobia;o__Methanomicrobiales;f__Methanoregulaceae;g__Methanolinea_A;s__Methanolinea_A sp11423u	1
GB_GCA_013331265.1	d__Archaea;p__Halobacteriota;c__Methanosarcinia;o__Methanosarcinales;f__Methanosarcinaceae;g__Methanosarcina;s__Methanosarcina sp10923u	1

GB_GCA_013331275.1	d__Archaea;p__Halobacteriota;c__Methanosarcinia;o__Methanosarcinales;f__Methanosarcinaceae;g__Methanosarcina;s__Methanosarcina sp11020u	1
GB_GCA_013331375.1	d__Archaea;p__Halobacteriota;c__Methanosarcinia;o__Methanosarcinales;f__Methanoperedenaceae;g__UBA10536;s__UBA10536 sp10536u	1
GB_GCA_013331415.1	d__Archaea;p__Halobacteriota;c__Methanomicrobia;o__Methanomicrobiales;f__Methanoregulaceae;g__UBA9949;s__UBA9949 sp10516u	1
GB_GCA_013374385.1	d__Archaea;p__Halobacteriota;c__Methanosarcinia;o__Methanosarcinales;f__Methanocomedenaceae;g__QBUR01;s__QBUR01 sp013374385	1
GB_GCA_013415575.1	d__Archaea;p__Halobacteriota;c__Methanomicrobia;o__Methanomicrobiales;f__Methanoregulaceae;g__UBA9949;s__UBA9949 sp013415575	1
GB_GCA_013415595.1	d__Archaea;p__Halobacteriota;c__Methanosarcinia;o__Methanotrichales;f__Methanotrichaceae;g__JAAEEW01;s__JAAEEW01 sp013415595	1
GB_GCA_013415665.1	d__Archaea;p__Halobacteriota;c__Methanomicrobia;o__Methanomicrobiales;f__Methanomicrobiaceae;g__LKUD01;s__LKUD01 sp013415665	1
GB_GCA_013415865.1	d__Archaea;p__Thermoplasmatota;c__Thermoplasmata;o__Methanomassiliicoccales;f__UBA472;g__MVRC01;s__MVRC01 sp013415865	1
GB_GCA_013572355.1	d__Archaea;p__Halobacteriota;c__Methanosarcinia;o__Methanosarcinales;f__Methanogasteraceae;g__Methanogaster;s__Methanogaster sp013572355	1
GB_GCA_014061035.1	d__Archaea;p__Halobacteriota;c__Syntropharchaeia;o__ANME-1;f__ANME-1;g__JACGMN01;s__JACGMN01 sp014061035	1
GB_GCA_014237145.1	d__Archaea;p__Halobacteriota;c__Methanosarcinia;o__Methanosarcinales;f__Methanocomedenaceae;g__Methanocomedens;s__Methanocomedens sp014237145	1
GB_GCA_014361205.1	d__Archaea;p__Halobacteriota;c__Methanosarcinia;o__Methanosarcinales;f__Methanosarcinaceae;g__Methanomethylovorans;s__Methanomethylovorans sp014361205	1
GB_GCA_014361295.1	d__Archaea;p__Thermoplasmatota;c__Thermoplasmata;o__Methanomassiliicoccales;f__JACIVX01;g__JACIVX01;s__JACIVX01 sp014361295	1
GB_GCA_014361445.1	d__Archaea;p__Thermoproteota;c__Methanomethylicia;o__Methanomethylicales;f__Methanomethylicaceae;g__WYZ-LMO10;s__WYZ-LMO10 sp014361445	1
GB_GCA_014361455.1	d__Archaea;p__Thermoproteota;c__Methanomethylicia;o__Methanomethylicales;f__Methanomethylicaceae;g__Methanosuratincola;s__Methanosuratincola sp014361455	1
GB_GCA_014859725.1	d__Archaea;p__Halobacteriota;c__Methanosarcinia;o__Methanosarcinales;f__Methanocomedenaceae;g__Kmv04;s__Kmv04 sp014859725	1
GB_GCA_014859735.1	d__Archaea;p__Halobacteriota;c__Syntropharchaeia;o__ANME-1;f__ANME-1;g__ANME-1-THS;s__ANME-1-THS sp014859735	1
GB_GCA_014859785.1	d__Archaea;p__Halobacteriota;c__Methanosarcinia;o__Methanosarcinales;f__Methanoperedenaceae;g__Methanoperedens_A;s__Methanoperedens_A sp014859785	1
GB_GCA_015062805.1	d__Archaea;p__Methanobacteriota;c__Methanobacteria;o__Methanobacteriales;f__Methanobacteriaceae;g__Methanosphaera;s__Methanosphaera stadtmanae_C	1
GB_GCA_015062815.1	d__Archaea;p__Methanobacteriota;c__Methanobacteria;o__Methanobacteriales;f__Methanobacteriaceae;g__Methanosphaera;s__Methanosphaera stadtmanae_B	1
GB_GCA_015062825.1	d__Archaea;p__Methanobacteriota;c__Methanobacteria;o__Methanobacteriales;f__Methanobacteriaceae;g__Methanosphaera;s__Methanosphaera stadtmanae_A	1
GB_GCA_015062905.1	d__Archaea;p__Methanobacteriota;c__Methanobacteria;o__Methanobacteriales;f__Methanobacteriaceae;g__Methanobrevibacter_A;s__Methanobrevibacter_A thaueri_A	1
GB_GCA_015062915.1	d__Archaea;p__Methanobacteriota;c__Methanobacteria;o__Methanobacteriales;f__Methanobacteriaceae;g__Methanobrevibacter_A;s__Methanobrevibacter_A thaueri_B	1
GB_GCA_015062925.1	d__Archaea;p__Methanobacteriota;c__Methanobacteria;o__Methanobacteriales;f__Methanobacteriaceae;g__Methanobrevibacter_A;s__Methanobrevibacter_A thaueri_C	1
GB_GCA_015062935.1	d__Archaea;p__Methanobacteriota;c__Methanobacteria;o__Methanobacteriales;f__Methanobacteriaceae;g__Methanobrevibacter_A;s__Methanobrevibacter_A sp015062935	1
GB_GCA_015062985.1	d__Archaea;p__Methanobacteriota;c__Methanobacteria;o__Methanobacteriales;f__Methanobacteriaceae;g__Methanobrevibacter_A;s__Methanobrevibacter_A sp015062985	1
GB_GCA_015063035.1	d__Archaea;p__Methanobacteriota;c__Methanobacteria;o__Methanobacteriales;f__Methanobacteriaceae;g__Methanobrevibacter;s__Methanobrevibacter olleyae_A	1
GB_GCA_015063085.1	d__Archaea;p__Halobacteriota;c__Methanomicrobia;o__Methanomicrobiales;f__Methanocorpusculaceae;g__Methanocorpusculum;s__Methanocorpusculum parvum_A	1
GB_GCA_015063125.1	d__Archaea;p__Thermoplasmatota;c__Thermoplasmata;o__Methanomassiliicoccales;f__Methanomethylophilaceae;g__UBA71;s__UBA71 sp015063125	1
GB_GCA_015063135.1	d__Archaea;p__Thermoplasmatota;c__Thermoplasmata;o__Methanomassiliicoccales;f__Methanomethylophilaceae;g__UBA71;s__UBA71 sp015063135	1

GB_GCA_015063165.1	d__Archaea;p__Thermoplasmatota;c__Thermoplasmata;o__Methanomassiliicoccales;f__Methanomethylophilaceae;g__UBA71;s__UBA71 sp015063165	1
GB_GCA_015063185.1	d__Archaea;p__Thermoplasmatota;c__Thermoplasmata;o__Methanomassiliicoccales;f__Methanomethylophilaceae;g__SIG5;s__SIG5 sp015063185	1
GB_GCA_015063195.1	d__Archaea;p__Thermoplasmatota;c__Thermoplasmata;o__Methanomassiliicoccales;f__Methanomethylophilaceae;g__SIG5;s__SIG5 sp015063195	1
GB_GCA_015063225.1	d__Archaea;p__Thermoplasmatota;c__Thermoplasmata;o__Methanomassiliicoccales;f__Methanomethylophilaceae;g__Methanomethylophilus;s__Methanomethylophilus sp015063225	1
GB_GCA_015063235.1	d__Archaea;p__Thermoplasmatota;c__Thermoplasmata;o__Methanomassiliicoccales;f__Methanomethylophilaceae;g__UBA71;s__UBA71 sp015063235	1
GB_GCA_015063245.1	d__Archaea;p__Thermoplasmatota;c__Thermoplasmata;o__Methanomassiliicoccales;f__Methanomethylophilaceae;g__UBA71;s__UBA71 sp015063245	1
GB_GCA_015063285.1	d__Archaea;p__Thermoplasmatota;c__Thermoplasmata;o__Methanomassiliicoccales;f__Methanomethylophilaceae;g__UBA71;s__UBA71 sp015063285	1
GB_GCA_015523155.1	d__Archaea;p__Methanobacteriota;c__Methanococci;o__Methanococcales;f__Methanococcaceae;g__Methanothermococcus_A;s__Methanothermococcus_A sp015523155	1
GB_GCA_015523685.1	d__Archaea;p__Halobacteriota;c__Archaeoglobi;o__Archaeoglobales;f__JdFR-42;g__WAJW01;s__WAJW01 sp015523685	1
GB_GCA_015660865.1	d__Archaea;p__Halobacteriota;c__Methanomicrobia;o__Methanomicrobiales;f__JACTUA01;g__JACTUA01;s__JACTUA01 sp015660865	1
GB_GCA_015660885.1	d__Archaea;p__Halobacteriota;c__Methanomicrobia;o__Methanomicrobiales;f__Methanoregulaceae;g__Methanoregula;s__Methanoregula sp015660885	1
GB_GCA_015660915.1	d__Archaea;p__Halobacteriota;c__Bog-38;o__Bog-38;f__Bog-38;g__Bog-38;s__Bog-38 sp015660915	1
GB_GCA_015660995.1	d__Archaea;p__Thermoproteota;c__Methanomethylicia;o__Methanomethylicales;f__Methanomethylicaceae;g__JACTUC01;s__JACTUC01 sp015660995	1
GB_GCA_015661395.1	d__Archaea;p__Halobacteriota;c__Bog-38;o__Bog-38;f__Bog-38;g__Bog-38;s__Bog-38 sp015661395	1
GB_GCA_015661405.1	d__Archaea;p__Methanobacteriota;c__Methanobacteria;o__Methanobacteriales;f__Methanobacteriaceae;g__Methanobacterium_A;s__Methanobacterium_A sp015661405	1
GB_GCA_015661555.1	d__Archaea;p__Methanobacteriota;c__Methanococci;o__Methanococcales;f__Methanococcaceae;g__Methanofervidicoccus;s__Methanofervidicoccus okinawensis_B	1
GB_GCA_015661585.1	d__Archaea;p__Methanobacteriota;c__Methanococci;o__Methanococcales;f__Methanococcaceae;g__Methanofervidicoccus;s__Methanofervidicoccus okinawensis_D	1
GB_GCA_015662355.1	d__Archaea;p__Methanobacteriota;c__Methanococci;o__Methanococcales;f__Methanococcaceae;g__Methanofervidicoccus;s__Methanofervidicoccus okinawensis_A	1
GB_GCA_015663075.1	d__Archaea;p__Methanobacteriota;c__Methanococci;o__Methanococcales;f__Methanococcaceae;g__Methanofervidicoccus;s__Methanofervidicoccus okinawensis_C	1
GB_GCA_016109435.1	d__Archaea;p__Thermoplasmatota;c__Thermoplasmata;o__Methanomassiliicoccales;f__Methanomassiliicoccaceae;g__UBA6;s__UBA6 sp016109435	1
GB_GCA_016222945.1	d__Archaea;p__Methanobacteriota;c__Methanobacteria;o__Methanobacteriales;f__Methanobacteriaceae;g__Methanobacterium_D;s__Methanobacterium_D sp016222945	1
GB_GCA_016278365.1	d__Archaea;p__Halobacteriota;c__Methanosarcinia;o__Methanosarcinales;f__Methanosarcinaceae;g__Methanolobus;s__Methanolobus sp016278365	1
GB_GCA_016278385.1	d__Archaea;p__Halobacteriota;c__Methanosarcinia;o__Methanosarcinales;f__Methanosarcinaceae;g__Methanolobus;s__Methanolobus sp016278385	1
GB_GCA_016281925.1	d__Archaea;p__Thermoplasmatota;c__Thermoplasmata;o__Methanomassiliicoccales;f__Methanomethylophilaceae;g__UBA71;s__UBA71 sp016281925	1
GB_GCA_016282555.1	d__Archaea;p__Thermoplasmatota;c__Thermoplasmata;o__Methanomassiliicoccales;f__Methanomethylophilaceae;g__UBA71;s__UBA71 sp016282555	1
GB_GCA_016282985.1	d__Archaea;p__Methanobacteriota;c__Methanobacteria;o__Methanobacteriales;f__Methanobacteriaceae;g__Methanosphaera;s__Methanosphaera sp016282985	1
GB_GCA_016284295.1	d__Archaea;p__Thermoplasmatota;c__Thermoplasmata;o__Methanomassiliicoccales;f__Methanomethylophilaceae;g__UBA71;s__UBA71 sp016284295	1
GB_GCA_016291275.1	d__Archaea;p__Methanobacteriota;c__Methanobacteria;o__Methanobacteriales;f__Methanobacteriaceae;g__Methanobrevibacter;s__Methanobrevibacter sp016291275	1
GB_GCA_016297775.1	d__Archaea;p__Thermoplasmatota;c__Thermoplasmata;o__Methanomassiliicoccales;f__Methanomethylophilaceae;g__SIG5;s__SIG5 sp016297775	1

GB_GCA_016699325.1	d__Archaea;p__Halobacteriota;c__Methanomicrobia;o__Methanomicrobiales;f__Methanoregulaceae;g__UBA9949;s__UBA9949 sp016699325	1
GB_GCA_016706325.1	d__Archaea;p__Halobacteriota;c__Methanosarcinia;o__Methanotrichales;f__Methanotrichaceae;g__Methanothrix;s__Methanothrix sp016706325	1
GB_GCA_016782355.1	d__Archaea;p__Halobacteriota;c__Syntropharchaeia;o__ANME-1;f__ANME-1;g__WJOV01;s__WJOV01 sp016782355	1
GB_GCA_016838945.1	d__Archaea;p__Methanobacteriota;c__Methanobacteria;o__Methanobacteriales;f__Methanobacteriaceae;g__Methanobrevibacter;s__Methanobrevibacter sp016838945	1
GB_GCA_016841265.1	d__Archaea;p__Halobacteriota;c__Methanosarcinia;o__Methanosarcinales;f__Methanosarcinaceae;g__MTP4;s__MTP4 sp016841265	1
GB_GCA_016841385.1	d__Archaea;p__Halobacteriota;c__Methanomicrobia;o__Methanomicrobiales;f__Methanoculleaceae;g__Methanoculleus;s__Methanoculleus sp016841385	1
GB_GCA_016841485.1	d__Archaea;p__Halobacteriota;c__Methanomicrobia;o__Methanomicrobiales;f__Methanomicrobiaceae;g__Methanogenium;s__Methanogenium sp016841485	1
GB_GCA_016841625.1	d__Archaea;p__Halobacteriota;c__Methanosarcinia;o__Methanosarcinales;f__Methanosarcinaceae;g__MTP4;s__MTP4 sp016841625	1
GB_GCA_016841665.1	d__Archaea;p__Halobacteriota;c__Methanomicrobia;o__Methanomicrobiales;f__Methanomicrobiaceae;g__DSDF01;s__DSDF01 sp016841665	1
GB_GCA_016841955.1	d__Archaea;p__Halobacteriota;c__Methanomicrobia;o__Methanomicrobiales;f__Methanoculleaceae;g__Methanoculleus;s__Methanoculleus sp016841955	1
GB_GCA_016882195.1	d__Archaea;p__Thermoproteota;c__Methanomethylicia;o__Methanomethylicales;f__Methanomethylicaceae;g__VGLU01;s__VGLU01 sp016882195	1
GB_GCA_016919565.1	d__Archaea;p__Thermoplasmatota;c__Thermoplasmata;o__Methanomassiliicoccales;f__UBA472;g__FEN-33;s__FEN-33 sp016919565	1
GB_GCA_016919625.1	d__Archaea;p__Thermoplasmatota;c__Thermoplasmata;o__Methanomassiliicoccales;f__UBA472;g__JACXTP01;s__JACXTP01 sp016919625	1
GB_GCA_016926075.1	d__Archaea;p__Thermoplasmatota;c__Thermoplasmata;o__Methanomassiliicoccales;f__UBA472;g__UBA472;s__UBA472 sp016926075	1
GB_GCA_016926505.1	d__Archaea;p__Halobacteriota;c__Methanomicrobia;o__Methanomicrobiales;f__Methanospirillaceae;g__JAFGOM01;s__JAFGOM01 sp016926505	1
GB_GCA_016926855.1	d__Archaea;p__Halobacteriota;c__Methanomicrobia;o__Methanomicrobiales;f__Methanomicrobiaceae;g__LKUD01;s__LKUD01 sp016926855	1
GB_GCA_016927055.1	d__Archaea;p__Halobacteriota;c__Methanosarcinia;o__Methanotrichales;f__Methanotrichaceae;g__Methanothrix;s__Methanothrix sp016927055	1
GB_GCA_016927425.1	d__Archaea;p__Halobacteriota;c__Methanosarcinia;o__Methanotrichales;f__Methanotrichaceae;g__JAFGMR01;s__JAFGMR01 sp016927425	1
GB_GCA_016932675.1	d__Archaea;p__Halobacteriota;c__Methanosarcinia;o__Methanosarcinales;f__Methanosarcinaceae;g__Methanolobus;s__Methanolobus sp016932675	1
GB_GCA_016935475.1	d__Archaea;p__Halobacteriota;c__Methanosarcinia;o__Methanosarcinales;f__Methanosarcinaceae;g__JAFGQV01;s__JAFGQV01 sp016935475	1
GB_GCA_016937345.1	d__Archaea;p__Halobacteriota;c__Methanomicrobia;o__Methanomicrobiales;f__Methanomicrobiaceae;g__Methanomicrobium;s__Methanomicrobium sp016937345	1
GB_GCA_017387505.1	d__Archaea;p__Halobacteriota;c__Methanomicrobia;o__Methanomicrobiales;f__Methanocorpusculaceae;g__Methanocorpusculum;s__Methanocorpusculum sp017387505	1
GB_GCA_017395275.1	d__Archaea;p__Thermoplasmatota;c__Thermoplasmata;o__Methanomassiliicoccales;f__Methanomethylophilaceae;g__SIG5;s__SIG5 sp017395275	1
GB_GCA_017404125.1	d__Archaea;p__Methanobacteriota;c__Methanobacteria;o__Methanobacteriales;f__Methanobacteriaceae;g__Methanobrevibacter;s__Methanobrevibacter sp017404125	1
GB_GCA_017406825.1	d__Archaea;p__Methanobacteriota;c__Methanobacteria;o__Methanobacteriales;f__Methanobacteriaceae;g__Methanobrevibacter_A;s__Methanobrevibacter_A sp017406825	1
GB_GCA_017407115.1	d__Archaea;p__Methanobacteriota;c__Methanobacteria;o__Methanobacteriales;f__Methanobacteriaceae;g__Methanobrevibacter_A;s__Methanobrevibacter_A sp017407115	1
GB_GCA_017408885.1	d__Archaea;p__Halobacteriota;c__Methanomicrobia;o__Methanomicrobiales;f__Methanocorpusculaceae;g__Methanocorpusculum;s__Methanocorpusculum sp017408885	1
GB_GCA_017409525.1	d__Archaea;p__Methanobacteriota;c__Methanobacteria;o__Methanobacteriales;f__Methanobacteriaceae;g__Methanobrevibacter_A;s__Methanobrevibacter_A sp017409525	1
GB_GCA_017410345.1	d__Archaea;p__Methanobacteriota;c__Methanobacteria;o__Methanobacteriales;f__Methanobacteriaceae;g__Methanobrevibacter;s__Methanobrevibacter sp017410345	1
GB_GCA_017412625.1	d__Archaea;p__Halobacteriota;c__Methanomicrobia;o__Methanomicrobiales;f__Methanomicrobiaceae;g__Methanomicrobium;s__Methanomicrobium sp017412625	1

GB_GCA_017427765.1	d__Archaea;p__Methanobacteriota;c__Methanobacteria;o__Methanobacteriales;f__Methanobacteriaceae;g__Methanobrevibacter_A;s__Methanobrevibacter_A sp017427765	1
GB_GCA_017430835.1	d__Archaea;p__Methanobacteriota;c__Methanobacteria;o__Methanobacteriales;f__Methanobacteriaceae;g__Methanosphaera;s__Methanosphaera sp017430835	1
GB_GCA_017431845.1	d__Archaea;p__Methanobacteriota;c__Methanobacteria;o__Methanobacteriales;f__Methanobacteriaceae;g__Methanosphaera;s__Methanosphaera sp017431845	1
GB_GCA_017431965.1	d__Archaea;p__Methanobacteriota;c__Methanobacteria;o__Methanobacteriales;f__Methanobacteriaceae;g__Methanobrevibacter_A;s__Methanobrevibacter_A sp017431965	1
GB_GCA_017432245.1	d__Archaea;p__Methanobacteriota;c__Methanobacteria;o__Methanobacteriales;f__Methanobacteriaceae;g__Methanobrevibacter;s__Methanobrevibacter sp017432245	1
GB_GCA_017434525.1	d__Archaea;p__Methanobacteriota;c__Methanobacteria;o__Methanobacteriales;f__Methanobacteriaceae;g__Methanobrevibacter_A;s__Methanobrevibacter_A sp017434525	1
GB_GCA_017434555.1	d__Archaea;p__Methanobacteriota;c__Methanobacteria;o__Methanobacteriales;f__Methanobacteriaceae;g__Methanobrevibacter_A;s__Methanobrevibacter_A sp017434555	1
GB_GCA_017447225.1	d__Archaea;p__Methanobacteriota;c__Methanobacteria;o__Methanobacteriales;f__Methanobacteriaceae;g__Methanobrevibacter_A;s__Methanobrevibacter_A sp017447225	1
GB_GCA_017455785.1	d__Archaea;p__Thermoplasmatota;c__Thermoplasmata;o__Methanomassiliicoccales;f__Methanomethylophilaceae;g__Methanarcanum;s__Methanarcanum sp017455785	1
GB_GCA_017460025.1	d__Archaea;p__Methanobacteriota;c__Methanobacteria;o__Methanobacteriales;f__Methanobacteriaceae;g__Methanobrevibacter_A;s__Methanobrevibacter_A sp017460025	1
GB_GCA_017461225.1	d__Archaea;p__Thermoplasmatota;c__Thermoplasmata;o__Methanomassiliicoccales;f__Methanomethylophilaceae;g__UBA71;s__UBA71 sp017461225	1
GB_GCA_017468685.1	d__Archaea;p__Methanobacteriota;c__Methanobacteria;o__Methanobacteriales;f__Methanobacteriaceae;g__Methanobrevibacter_A;s__Methanobrevibacter_A sp017468685	1
GB_GCA_017468935.1	d__Archaea;p__Thermoplasmatota;c__Thermoplasmata;o__Methanomassiliicoccales;f__Methanomethylophilaceae;g__UBA71;s__UBA71 sp017468935	1
GB_GCA_017473945.1	d__Archaea;p__Methanobacteriota;c__Methanobacteria;o__Methanobacteriales;f__Methanobacteriaceae;g__Methanobrevibacter_A;s__Methanobrevibacter_A sp017473945	1
GB_GCA_017475875.1	d__Archaea;p__Thermoplasmatota;c__Thermoplasmata;o__Methanomassiliicoccales;f__Methanomethylophilaceae;g__UBA71;s__UBA71 sp017475875	1
GB_GCA_017507885.1	d__Archaea;p__Thermoplasmatota;c__Thermoplasmata;o__Methanomassiliicoccales;f__Methanomethylophilaceae;g__UBA71;s__UBA71 sp017507885	1
GB_GCA_017508065.1	d__Archaea;p__Thermoplasmatota;c__Thermoplasmata;o__Methanomassiliicoccales;f__Methanomethylophilaceae;g__SIG5;s__SIG5 sp017508065	1
GB_GCA_017519045.1	d__Archaea;p__Thermoplasmatota;c__Thermoplasmata;o__Methanomassiliicoccales;f__Methanomethylophilaceae;g__UBA71;s__UBA71 sp017519045	1
GB_GCA_017524805.1	d__Archaea;p__Thermoplasmatota;c__Thermoplasmata;o__Methanomassiliicoccales;f__Methanomethylophilaceae;g__UBA71;s__UBA71 sp017524805	1
GB_GCA_017539065.1	d__Archaea;p__Methanobacteriota;c__Methanobacteria;o__Methanobacteriales;f__Methanobacteriaceae;g__Methanobrevibacter_A;s__Methanobrevibacter_A sp017539065	1
GB_GCA_017540825.1	d__Archaea;p__Thermoplasmatota;c__Thermoplasmata;o__Methanomassiliicoccales;f__Methanomethylophilaceae;g__UBA71;s__UBA71 sp017540825	1
GB_GCA_017553245.1	d__Archaea;p__Halobacteriota;c__Methanomicrobia;o__Methanomicrobiales;f__Methanomicrobiaceae;g__Methanomicrobium;s__Methanomicrobium sp017553245	1
GB_GCA_017553445.1	d__Archaea;p__Methanobacteriota;c__Methanobacteria;o__Methanobacteriales;f__Methanobacteriaceae;g__Methanobrevibacter_A;s__Methanobrevibacter_A sp017553445	1
GB_GCA_017555685.1	d__Archaea;p__Halobacteriota;c__Methanomicrobia;o__Methanomicrobiales;f__Methanocorpusculaceae;g__Methanocorpusculum;s__Methanocorpusculum sp017555685	1
GB_GCA_017613335.1	d__Archaea;p__Halobacteriota;c__Methanosarcinia;o__Methanosarcinales;f__Methanosarcinaceae;g__Methanimicrococcus;s__Methanimicrococcus sp017613335	1
GB_GCA_017616575.1	d__Archaea;p__Thermoplasmatota;c__Thermoplasmata;o__Methanomassiliicoccales;f__Methanomethylophilaceae;g__UBA71;s__UBA71 sp017616575	1
GB_GCA_017622255.1	d__Archaea;p__Halobacteriota;c__Methanomicrobia;o__Methanomicrobiales;f__Methanocorpusculaceae;g__Methanocorpusculum;s__Methanocorpusculum sp017622255	1
GB_GCA_017646885.1	d__Archaea;p__Methanobacteriota;c__Methanobacteria;o__Methanobacteriales;f__Methanobacteriaceae;g__Methanobrevibacter;s__Methanobrevibacter sp017646885	1
GB_GCA_017883605.1	d__Archaea;p__Methanobacteriota;c__Methanobacteria;o__Methanobacteriales;f__Methanobacteriaceae;g__Methanobacterium_A;s__Methanobacterium_A sp017883605	1
GB_GCA_017935945.1	d__Archaea;p__Thermoplasmatota;c__Thermoplasmata;o__Methanomassiliicoccales;f__Methanomethylophilaceae;g__UBA71;s__UBA71 sp017935945	1

GB_GCA_017940815.1	d__Archaea;p__Methanobacteriota;c__Methanobacteria;o__Methanobacteriales;f__Methanobacteriaceae;g__Methanobrevibacter_A;s__Methanobrevibacter_A sp017940815	1
GB_GCA_017994055.1	d__Archaea;p__Halobacteriota;c__Methanosarcinia;o__Methanotrichales;f__Methanotrichaceae;g__Methanothrix;s__Methanothrix sp017994055	1
GB_GCA_018052825.1	d__Archaea;p__Halobacteriota;c__Methanosarcinia;o__Methanotrichales;f__Methanotrichaceae;g__Methanothrix;s__Methanothrix sp018052825	1
GB_GCA_018065685.1	d__Archaea;p__Halobacteriota;c__Methanomicrobia;o__Methanomicrobiales;f__Methanocorpusculaceae;g__Methanocorpusculum;s__Methanocorpusculum sp018065685	1
GB_GCA_018262895.1	d__Archaea;p__Thermoplasmatota;c__Thermoplasmata;o__Methanomassiliicoccales;f__Methanomassiliicoccaceae;g__UBA6;s__UBA6 sp018262895	1
GB_GCA_018433835.1	d__Archaea;p__Halobacteriota;c__Methanomicrobia;o__Methanomicrobiales;f__Methanoculleaceae;g__Methanoculleus;s__Methanoculleus sp018433835	1
GB_GCA_018609725.1	d__Archaea;p__Halobacteriota;c__Methanosarcinia;o__Methanosarcinales;f__Methanosarcinaceae;g__Methanohalobium;s__Methanohalobium sp018609725	1
GB_GCA_018687785.1	d__Archaea;p__Halobacteriota;c__Methanomicrobia;o__Methanomicrobiales;f__Methanomicrobiaceae;g__Methanogenium;s__Methanogenium sp018687785	1
GB_GCA_019136335.1	d__Archaea;p__Halobacteriota;c__Methanomicrobia;o__Methanomicrobiales;f__Methanoculleaceae;g__Methanoculleus;s__Methanoculleus sp019136335	1
GB_GCA_019262145.1	d__Archaea;p__Thermoplasmatota;c__Thermoplasmata;o__Methanomassiliicoccales;f__Methanomethylophilaceae;g__Methanogranum;s__Methanogranum sp019262145	1
GB_GCA_019429385.1	d__Archaea;p__Halobacteriota;c__Methanosarcinia;o__Methanosarcinales;f__Methanocomedenaceae;g__QBUR01;s__QBUR01 sp019429385	1
GB_GCA_019561555.1	d__Archaea;p__Methanobacteriota;c__Methanococci;o__Methanococcales;f__Methanococcaceae;g__Methanofervidicoccus;s__Methanofervidicoccus sp019561555	1
GB_GCA_019561565.1	d__Archaea;p__Methanobacteriota;c__Methanococci;o__Methanococcales;f__Methanococcaceae;g__Methanofervidicoccus;s__Methanofervidicoccus sp019561565	1
GB_GCA_019561615.1	d__Archaea;p__Methanobacteriota;c__Methanococci;o__Methanococcales;f__Methanococcaceae;g__Methanofervidicoccus;s__Methanofervidicoccus sp019561615	1
GB_GCA_019695435.1	d__Archaea;p__Halobacteriota;c__Methanomicrobia;o__Methanomicrobiales;f__Methanoregulaceae;g__Methanoregula;s__Methanoregula sp019695435	1
GB_GCA_020055655.1	d__Archaea;p__Halobacteriota;c__Methanosarcinia;o__Methanosarcinales;f__Methanosarcinaceae;g__Methanolobus;s__Methanolobus sp020055655	1
GB_GCA_020216685.1	d__Archaea;p__Halobacteriota;c__Methanomicrobia;o__Methanomicrobiales;f__Methanospirillaceae;g__Methanospirillum;s__Methanospirillum hungatei_B	1
GB_GCA_020696975.1	d__Archaea;p__Halobacteriota;c__Methanomicrobia;o__Methanomicrobiales;f__Methanoculleaceae;g__Methanoculleus;s__Methanoculleus sp020696975	1
GB_GCA_020725315.1	d__Archaea;p__Halobacteriota;c__Syntropharchaeia;o__ANME-1;f__ANME-1;g__ANME-1-THS;s__ANME-1-THS sp020725315	1
GB_GCA_020793555.1	d__Archaea;p__Halobacteriota;c__Methanosarcinia;o__Methanosarcinales;f__Methanosarcinaceae;g__DQIP01;s__DQIP01 sp020793555	1
GB_GCA_020793565.1	d__Archaea;p__Halobacteriota;c__Methanosarcinia;o__Methanosarcinales;f__Methanosarcinaceae;g__DQIP01;s__DQIP01 sp020793565	1
GB_GCA_020832905.1	d__Archaea;p__Thermoproteota;c__Methanomethylicia;o__Methanomethylicales;f__Methanomethylicaceae;g__WYZ-LMO11;s__WYZ-LMO11 sp020832905	1
GB_GCA_020844795.1	d__Archaea;p__Halobacteriota;c__Methanosarcinia;o__Methanotrichales;f__Methanotrichaceae;g__Methanothrix_A;s__Methanothrix_A sp020844795	1
GB_GCA_020854755.1	d__Archaea;p__Halobacteriota;c__Methanomicrobia;o__Methanomicrobiales;f__Methanoculleaceae;g__JAHKLN01;s__JAHKLN01 sp020854755	1
GB_GCA_020854785.1	d__Archaea;p__Halobacteriota;c__Methanosarcinia;o__Methanosarcinales;f__Methanosarcinaceae;g__Methanomethylovorans;s__Methanomethylovorans sp020854785	1
GB_GCA_020854915.1	d__Archaea;p__Methanobacteriota;c__Methanobacteria;o__Methanobacteriales;f__Methanobacteriaceae;g__JAHKLT01;s__JAHKLT01 sp020854915	1
GB_GCA_021106765.1	d__Archaea;p__Halobacteriota;c__Methanosarcinia;o__Methanosarcinales;f__Methanosarcinaceae;g__JAIOTO01;s__JAIOTO01 sp021106765	1
GB_GCA_021108185.1	d__Archaea;p__Halobacteriota;c__Methanosarcinia;o__Methanosarcinales;f__Methanosarcinaceae;g__Methanococcoides;s__Methanococcoides sp021108185	1
GB_GCA_021108275.1	d__Archaea;p__Halobacteriota;c__Methanosarcinia;o__Methanosarcinales;f__Methanosarcinaceae;g__Methanococcoides;s__Methanococcoides sp021108275	1
GB_GCA_021108405.1	d__Archaea;p__Halobacteriota;c__Methanosarcinia;o__Methanosarcinales;f__Methanocomedenaceae;g__Methanomarinus;s__Methanomarinus sp021108405	1

GB_GCA_021159385.1	d__Archaea;p__Halobacteriota;c__Methanosarcinia;o__Methanosarcinales;f__Methanogasteraceae;g__Methanogaster;s__Methanogaster sp021159385	1
GB_GCA_021160575.1	d__Archaea;p__Thermoproteota;c__Methanomethylicia;o__Methanomethylicales;f__JAGHCH01;g__JAGHCH01;s__JAGHCH01 sp021160575	1
GB_GCA_021199865.1	d__Archaea;p__Methanobacteriota;c__Methanobacteria;o__Methanobacteriales;f__Methanobacteriaceae;g__Methanosphaera;s__Methanosphaera sp021199865	1
GB_GCA_021371995.1	d__Archaea;p__Halobacteriota;c__Methanomicrobia;o__Methanomicrobiales;f__Methanoregulaceae;g__UBA9949;s__UBA9949 sp021371995	1
GB_GCA_021372315.1	d__Archaea;p__Thermoplasmatota;c__Thermoplasmata;o__Methanomassiliicoccales;f__UBA472;g__MVRC01;s__MVRC01 sp021372315	1
GB_GCA_021372335.1	d__Archaea;p__Thermoplasmatota;c__Thermoplasmata;o__Methanomassiliicoccales;f__UBA472;g__UBA472;s__UBA472 sp021372335	1
GB_GCA_021767785.1	d__Archaea;p__Halobacteriota;c__Methanosarcinia;o__Methanosarcinales;f__Methanosarcinaceae;g__Methanolobus;s__Methanolobus sp021767785	1
GB_GCA_022353185.1	d__Archaea;p__Halobacteriota;c__Methanosarcinia;o__Methanosarcinales;f__Methanocomedenaceae;g__QBUR01;s__QBUR01 sp022353185	1
GB_GCA_022768985.1	d__Archaea;p__Methanobacteriota;c__Methanobacteria;o__Methanobacteriales;f__Methanobacteriaceae;g__Methanosphaera;s__Methanosphaera sp022768985	1
GB_GCA_022775905.1	d__Archaea;p__Methanobacteriota;c__Methanobacteria;o__Methanobacteriales;f__Methanobacteriaceae;g__Methanobrevibacter_A;s__Methanobrevibacter_A sp022775905	1
GB_GCA_022841205.1	d__Archaea;p__Halobacteriota;c__Methanomicrobia;o__Methanomicrobiales;f__Methanoregulaceae;g__UBA9949;s__UBA9949 sp022841205	1
GB_GCA_022865315.1	d__Archaea;p__Halobacteriota;c__Methanosarcinia;o__Methanotrichales;f__Methanotrichaceae;g__JALHSR01;s__JALHSR01 sp022865315	1
GB_GCA_023136155.1	d__Archaea;p__Halobacteriota;c__Methanosarcinia;o__Methanosarcinales;f__Methanocomedenaceae;g__QBUR01;s__QBUR01 sp023136155	1
GB_GCA_023229165.1	d__Archaea;p__Halobacteriota;c__Methanosarcinia;o__Methanotrichales;f__Methanotrichaceae;g__Methanothrix;s__Methanothrix sp023229165	1
GB_GCA_023230065.1	d__Archaea;p__Thermoplasmatota;c__Thermoplasmata;o__Methanomassiliicoccales;f__Methanomethylophilaceae;g__JALNYB01;s__JALNYB01 sp023230065	1
GB_GCA_023230425.1	d__Archaea;p__Halobacteriota;c__Methanomicrobia;o__Methanomicrobiales;f__Methanoculleaceae;g__Methanoculleus;s__Methanoculleus sp023230425	1
GB_GCA_023249275.1	d__Archaea;p__Halobacteriota;c__Methanosarcinia;o__Methanosarcinales;f__Methanoperedenaceae;g__Methanoperedens;s__Methanoperedens sp023249275	1
GB_GCA_023249725.1	d__Archaea;p__Methanobacteriota;c__Methanobacteria;o__Methanobacteriales;f__Methanobacteriaceae;g__UBA349;s__UBA349 sp023249725	1
GB_GCA_023393455.1	d__Archaea;p__Halobacteriota;c__Methanomicrobia;o__Methanomicrobiales;f__Methanoculleaceae;g__Methanoculleus;s__Methanoculleus sp023393455	1
GB_GCA_023396365.1	d__Archaea;p__Halobacteriota;c__Methanomicrobia;o__Methanomicrobiales;f__Methanomicrobiaceae;g__Methanomicrobium;s__Methanomicrobium sp023396365	1
GB_GCA_023399215.1	d__Archaea;p__Halobacteriota;c__Methanosarcinia;o__Methanosarcinales;f__Methanosarcinaceae;g__Methanosarcina;s__Methanosarcina sp023399215	1
GB_GCA_023402275.1	d__Archaea;p__Thermoplasmatota;c__Thermoplasmata;o__Methanomassiliicoccales;f__Methanomethylophilaceae;g__Methanoplasma;s__Methanoplasma sp023402275	1
GB_GCA_023409695.1	d__Archaea;p__Methanobacteriota;c__Methanobacteria;o__Methanobacteriales;f__Methanobacteriaceae;g__Methanobacterium_D;s__Methanobacterium_D sp023409695	1
GB_GCA_023436075.1	d__Archaea;p__Halobacteriota;c__Methanocellia;o__Methanocellales;f__Methanocellaceae;g__Methanocella_A;s__Methanocella_A sp023436075	1
GB_GCA_023440975.1	d__Archaea;p__Methanobacteriota;c__Methanobacteria;o__Methanobacteriales;f__Methanobacteriaceae;g__UBA412;s__UBA412 sp023440975	1
GB_GCA_023544565.1	d__Archaea;p__Halobacteriota;c__Methanosarcinia;o__Methanosarcinales;f__Methanosarcinaceae;g__DQIP01;s__DQIP01 sp023544565	1
GB_GCA_023544605.1	d__Archaea;p__Halobacteriota;c__Methanosarcinia;o__Methanosarcinales;f__Methanocomedenaceae;g__QBUR01;s__QBUR01 sp023544605	1
GB_GCA_023955635.1	d__Archaea;p__Halobacteriota;c__Methanosarcinia;o__Methanosarcinales;f__Methanosarcinaceae;g__Methanosarcina;s__Methanosarcina barkeri_C	1
GB_GCA_024167805.1	d__Archaea;p__Methanobacteriota;c__Methanobacteria;o__Methanobacteriales;f__Methanobacteriaceae;g__Methanobacterium_B;s__Methanobacterium_B sp024167805	1
GB_GCA_024256265.1	d__Archaea;p__Thermoproteota;c__Nitrososphaeria;o__Nitrososphaerales;f__JACAEJ01;g__JACAEJ01;s__JACAEJ01 sp024256265	1

GB_GCA_024256285.1	d__Archaea;p__Thermoproteota;c__Nitrososphaeria;o__Nitrososphaerales;f__JACAEJ01;g__HK02M2;s__HK02M2 sp024256285	1
GB_GCA_024280975.1	d__Archaea;p__Halobacteriota;c__Methanosarcinia;o__Methanosarcinales;f__Methanosarcinaceae;g__Methanosarcina;s__Methanosarcina sp024280975	1
GB_GCA_024399155.1	d__Archaea;p__Thermoplasmatota;c__Thermoplasmata;o__Methanomassiliicoccales;f__Methanomethylophilaceae;g__JAKSHX01;s__JAKSHX01 sp024399155	1
GB_GCA_024399175.1	d__Archaea;p__Thermoplasmatota;c__Thermoplasmata;o__Methanomassiliicoccales;f__Methanomethylophilaceae;g__Methanomethylophilus;s__Methanomethylophilus sp024399175	1
GB_GCA_024399195.1	d__Archaea;p__Thermoplasmatota;c__Thermoplasmata;o__Methanomassiliicoccales;f__Methanomethylophilaceae;g__Methanomethylophilus;s__Methanomethylophilus sp024399195	1
GB_GCA_024399215.1	d__Archaea;p__Thermoplasmatota;c__Thermoplasmata;o__Methanomassiliicoccales;f__Methanomethylophilaceae;g__JAKSHX01;s__JAKSHX01 sp024399215	1
GB_GCA_024399275.1	d__Archaea;p__Thermoplasmatota;c__Thermoplasmata;o__Methanomassiliicoccales;f__Methanomethylophilaceae;g__JAKSHX01;s__JAKSHX01 sp024399275	1
GB_GCA_024409145.1	d__Archaea;p__Methanobacteriota;c__Methanobacteria;o__Methanobacteriales;f__Methanobacteriaceae;g__Methanobrevibacter;s__Methanobrevibacter sp024409145	1
GB_GCA_024409165.1	d__Archaea;p__Methanobacteriota;c__Methanobacteria;o__Methanobacteriales;f__Methanobacteriaceae;g__Methanobrevibacter;s__Methanobrevibacter sp024409165	1
GB_GCA_024409185.1	d__Archaea;p__Methanobacteriota;c__Methanobacteria;o__Methanobacteriales;f__Methanobacteriaceae;g__Methanobrevibacter;s__Methanobrevibacter sp024409185	1
GB_GCA_024413395.1	d__Archaea;p__Methanobacteriota;c__Methanobacteria;o__Methanobacteriales;f__Methanobacteriaceae;g__Methanobrevibacter_A;s__Methanobrevibacter_A sp024413395	1
GB_GCA_024464195.1	d__Archaea;p__Thermoplasmatota;c__Thermoplasmata;o__Methanomassiliicoccales;f__JACIVX01;g__JACIVX01;s__JACIVX01 sp024464195	1
GB_GCA_024464205.1	d__Archaea;p__Thermoproteota;c__Methanomethylicia;o__Methanomethylicales;f__Methanomethylicaceae;g__Methanomethylicus;s__Methanomethylicus sp024464205	1
GB_GCA_024490875.1	d__Archaea;p__Methanobacteriota;c__Methanococci;o__Methanococcales;f__Methanocaldococcaceae;g__Methanocaldococcus;s__Methanocaldococcus sp024490875	1
GB_GCA_024518575.1	d__Archaea;p__Halobacteriota;c__Methanosarcinia;o__Methanotrichales;f__Methanotrichaceae;g__Methanothrix_B;s__Methanothrix_B sp024518575	1
GB_GCA_024649985.1	d__Archaea;p__Halobacteriota;c__Methanosarcinia;o__Methanotrichales;f__Methanotrichaceae;g__Methanothrix_A;s__Methanothrix_A sp024649985	1
GB_GCA_024689425.1	d__Archaea;p__Methanobacteriota;c__Methanobacteria;o__Methanobacteriales;f__Methanobacteriaceae;g__Methanobrevibacter_A;s__Methanobrevibacter_A sp024689425	1
GB_GCA_024699715.1	d__Archaea;p__Halobacteriota;c__Syntropharchaeia;o__ANME-1;f__ANME-1;g__JANPRD01;s__JANPRD01 sp024699715	1
GB_GCA_025057955.1	d__Archaea;p__Thermoproteota;c__Methanomethylicia;o__Methanomethylicales;f__Methanomethylicaceae;g__JANXER01;s__JANXER01 sp025057955	1
GB_GCA_025058955.1	d__Archaea;p__Halobacteriota;c__Archaeoglobi;o__Archaeoglobales;f__Archaeoglobaceae;g__WYZ-LMO2;s__WYZ-LMO2 sp025058955	1
GB_GCA_025059375.1	d__Archaea;p__Thermoproteota;c__Methanomethylicia;o__Nezhaarchaeales;f__WYZ-LMO8;g__WYZ-LMO8;s__WYZ-LMO8 sp025059375	1
GB_GCA_025059545.1	d__Archaea;p__Halobacteriota;c__Archaeoglobi;o__Archaeoglobales;f__Archaeoglobaceae;g__WYZ-LMO2;s__WYZ-LMO2 sp025059545	1
GB_GCA_900095815.1	d__Archaea;p__Methanobacteriota;c__Methanobacteria;o__Methanobacteriales;f__Methanothermobacteraceae;g__Methanothermobacter;s__Methanothermobacter wolfei	1
GB_GCA_900314605.1	d__Archaea;p__Methanobacteriota;c__Methanobacteria;o__Methanobacteriales;f__Methanobacteriaceae;g__Methanobrevibacter_B;s__Methanobrevibacter_B sp900314605	1
GB_GCA_900314615.1	d__Archaea;p__Methanobacteriota;c__Methanobacteria;o__Methanobacteriales;f__Methanobacteriaceae;g__Methanobrevibacter_A;s__Methanobrevibacter_A sp900314615	1
GB_GCA_900314635.1	d__Archaea;p__Methanobacteriota;c__Methanobacteria;o__Methanobacteriales;f__Methanobacteriaceae;g__Methanobrevibacter;s__Methanobrevibacter sp900314635	1
GB_GCA_900314695.1	d__Archaea;p__Methanobacteriota;c__Methanobacteria;o__Methanobacteriales;f__Methanobacteriaceae;g__Methanobrevibacter_A;s__Methanobrevibacter_A sp900314695	1
GB_GCA_900316895.1	d__Archaea;p__Methanobacteriota;c__Methanobacteria;o__Methanobacteriales;f__Methanobacteriaceae;g__Methanobrevibacter_A;s__Methanobrevibacter_A sp900316895	1
GB_GCA_900317865.1	d__Archaea;p__Methanobacteriota;c__Methanobacteria;o__Methanobacteriales;f__Methanobacteriaceae;g__Methanobrevibacter_A;s__Methanobrevibacter_A sp900317865	1

GB_GCA_900318035.1	d__Archaea;p__Methanobacteriota;c__Methanobacteria;o__Methanobacteriales;f__Methanobacteriaceae;g__Methanobrevibacter_A;s__Methanobrevibacter_A sp900318035	1
GB_GCA_900319985.1	d__Archaea;p__Methanobacteriota;c__Methanobacteria;o__Methanobacteriales;f__Methanobacteriaceae;g__Methanobrevibacter_A;s__Methanobrevibacter_A sp900319985	1
GB_GCA_900320515.1	d__Archaea;p__Methanobacteriota;c__Methanobacteria;o__Methanobacteriales;f__Methanobacteriaceae;g__Methanobrevibacter_A;s__Methanobrevibacter_A sp900320515	1
GB_GCA_900320955.1	d__Archaea;p__Methanobacteriota;c__Methanobacteria;o__Methanobacteriales;f__Methanobacteriaceae;g__Methanobrevibacter_A;s__Methanobrevibacter_A sp900320955	1
GB_GCA_900766745.1	d__Archaea;p__Methanobacteriota;c__Methanobacteria;o__Methanobacteriales;f__Methanobacteriaceae;g__Methanobrevibacter_A;s__Methanobrevibacter_A sp900766745	1
GB_GCA_900767505.1	d__Archaea;p__Thermoplasmatota;c__Thermoplasmata;o__Methanomassiliicoccales;f__Methanomethylophilaceae;g__UBA71;s__UBA71 sp900767505	1
GB_GCA_900769095.1	d__Archaea;p__Methanobacteriota;c__Methanobacteria;o__Methanobacteriales;f__Methanobacteriaceae;g__Methanobrevibacter_A;s__Methanobrevibacter_A sp900769095	1
GB_GCA_902385025.1	d__Archaea;p__Halobacteriota;c__Methanosarcinia;o__Methanotrichales;f__Methanotrichaceae;g__Methanothrix;s__Methanothrix sp902385025	1
GB_GCA_902386085.1	d__Archaea;p__Halobacteriota;c__Methanosarcinia;o__Methanosarcinales;f__Methanoperedenaceae;g__Methanoperedens;s__Methanoperedens sp902386085	1
GB_GCA_902386205.1	d__Archaea;p__Halobacteriota;c__Methanosarcinia;o__Methanosarcinales;f__Methanoperedenaceae;g__Methanoperedens;s__Methanoperedens sp902386205	1
GB_GCA_902386255.1	d__Archaea;p__Halobacteriota;c__Methanosarcinia;o__Methanosarcinales;f__Methanoperedenaceae;g__Methanoperedens;s__Methanoperedens sp902386255	1
GB_GCA_902763685.1	d__Archaea;p__Thermoplasmatota;c__Thermoplasmata;o__Methanomassiliicoccales;f__Methanomethylophilaceae;g__Methanomethylophilus;s__Methanomethylophilus sp902763685	1
GB_GCA_902764015.1	d__Archaea;p__Methanobacteriota;c__Methanobacteria;o__Methanobacteriales;f__Methanobacteriaceae;g__Methanobrevibacter_A;s__Methanobrevibacter_A sp902764015	1
GB_GCA_902764455.1	d__Archaea;p__Methanobacteriota;c__Methanobacteria;o__Methanobacteriales;f__Methanobacteriaceae;g__Methanobrevibacter_A;s__Methanobrevibacter_A sp902764455	1
GB_GCA_902769175.1	d__Archaea;p__Methanobacteriota;c__Methanobacteria;o__Methanobacteriales;f__Methanobacteriaceae;g__Methanobrevibacter;s__Methanobrevibacter sp902769175	1
GB_GCA_902770715.1	d__Archaea;p__Methanobacteriota;c__Methanobacteria;o__Methanobacteriales;f__Methanobacteriaceae;g__Methanobrevibacter_A;s__Methanobrevibacter_A sp902770715	1
GB_GCA_902771225.1	d__Archaea;p__Methanobacteriota;c__Methanobacteria;o__Methanobacteriales;f__Methanobacteriaceae;g__Methanobrevibacter_A;s__Methanobrevibacter_A sp900319535	1
GB_GCA_902771435.1	d__Archaea;p__Methanobacteriota;c__Methanobacteria;o__Methanobacteriales;f__Methanobacteriaceae;g__Methanobrevibacter_A;s__Methanobrevibacter_A sp902771435	1
GB_GCA_902774605.1	d__Archaea;p__Methanobacteriota;c__Methanobacteria;o__Methanobacteriales;f__Methanobacteriaceae;g__Methanobrevibacter_A;s__Methanobrevibacter_A sp902774605	1
GB_GCA_902774685.1	d__Archaea;p__Methanobacteriota;c__Methanobacteria;o__Methanobacteriales;f__Methanobacteriaceae;g__Methanobrevibacter;s__Methanobrevibacter sp902774685	1
GB_GCA_902777885.1	d__Archaea;p__Methanobacteriota;c__Methanobacteria;o__Methanobacteriales;f__Methanobacteriaceae;g__Methanobrevibacter_A;s__Methanobrevibacter_A sp902777885	1
GB_GCA_902782945.1	d__Archaea;p__Methanobacteriota;c__Methanobacteria;o__Methanobacteriales;f__Methanobacteriaceae;g__Methanosphaera;s__Methanosphaera sp900322125	1
GB_GCA_902783085.1	d__Archaea;p__Methanobacteriota;c__Methanobacteria;o__Methanobacteriales;f__Methanobacteriaceae;g__Methanobrevibacter_A;s__Methanobrevibacter_A sp902783085	1
GB_GCA_902784195.1	d__Archaea;p__Methanobacteriota;c__Methanobacteria;o__Methanobacteriales;f__Methanobacteriaceae;g__Methanobrevibacter;s__Methanobrevibacter sp902784195	1
GB_GCA_902785855.1	d__Archaea;p__Methanobacteriota;c__Methanobacteria;o__Methanobacteriales;f__Methanobacteriaceae;g__Methanobrevibacter_A;s__Methanobrevibacter_A sp902785855	1
GB_GCA_902787415.1	d__Archaea;p__Thermoplasmatota;c__Thermoplasmata;o__Methanomassiliicoccales;f__Methanomethylophilaceae;g__Methanomethylophilus;s__Methanomethylophilus sp902787415	1
GB_GCA_902788255.1	d__Archaea;p__Methanobacteriota;c__Methanobacteria;o__Methanobacteriales;f__Methanobacteriaceae;g__Methanobrevibacter_A;s__Methanobrevibacter_A sp902788255	1
GB_GCA_902789505.1	d__Archaea;p__Methanobacteriota;c__Methanobacteria;o__Methanobacteriales;f__Methanobacteriaceae;g__Methanobrevibacter_A;s__Methanobrevibacter_A sp902789505	1
GB_GCA_902794475.1	d__Archaea;p__Methanobacteriota;c__Methanobacteria;o__Methanobacteriales;f__Methanobacteriaceae;g__Methanobrevibacter_A;s__Methanobrevibacter_A sp902794475	1

GB_GCA_902795935.1	d__Archaea;p__Methanobacteriota;c__Methanobacteria;o__Methanobacteriales;f__Methanobacteriaceae;g__CADBMS01;s__CADBMS01 sp902795935	1
GB_GCA_902796575.1	d__Archaea;p__Methanobacteriota;c__Methanobacteria;o__Methanobacteriales;f__Methanobacteriaceae;g__Methanobrevibacter_A;s__Methanobrevibacter_A sp902796575	1
GB_GCA_902797085.1	d__Archaea;p__Methanobacteriota;c__Methanobacteria;o__Methanobacteriales;f__Methanobacteriaceae;g__Methanosphaera;s__Methanosphaera sp902797085	1
GB_GCA_902801725.1	d__Archaea;p__Methanobacteriota;c__Methanobacteria;o__Methanobacteriales;f__Methanobacteriaceae;g__Methanobrevibacter_A;s__Methanobrevibacter_A sp902801725	1
GB_GCA_902827205.1	d__Archaea;p__Methanobacteriota;c__Methanococci;o__Methanococcales;f__Methanocaldococcaceae;g__Methanocaldococcus;s__Methanocaldococcus sp902827205	1
GB_GCA_903871465.1	d__Archaea;p__Halobacteriota;c__Methanosarcinia;o__Methanotrichales;f__Methanotrichaceae;g__Methanothrix;s__Methanothrix sp903871465	1
GB_GCA_904501935.1	d__Archaea;p__Methanobacteriota;c__Methanobacteria;o__Methanobacteriales;f__Methanobacteriaceae;g__Methanobrevibacter_A;s__Methanobrevibacter_A sp904501935	1
GB_GCA_905067555.1	d__Archaea;p__Halobacteriota;c__Methanosarcinia;o__Methanosarcinales;f__EX4572-44;g__Ethanoperedens;s__Ethanoperedens ethanivorans_C	1
GB_GCA_905171695.1	d__Archaea;p__Halobacteriota;c__Methanosarcinia;o__Methanosarcinales;f__EX4572-44;g__EX4572-44;s__EX4572-44 sp905171695	1
GB_GCA_905187815.1	d__Archaea;p__Thermoplasmatota;c__Thermoplasmata;o__Methanomassiliicoccales;f__Methanomethylophilaceae;g__UBA71;s__UBA71 sp905187815	1
GB_GCA_905202485.1	d__Archaea;p__Thermoplasmatota;c__Thermoplasmata;o__Methanomassiliicoccales;f__Methanomassiliicoccaceae;g__Methanomassiliicoccus_A;s__Methanomassiliicoccus_A sp905202485	1
GB_GCA_905203995.1	d__Archaea;p__Thermoplasmatota;c__Thermoplasmata;o__Methanomassiliicoccales;f__Methanomassiliicoccaceae;g__Methanomassiliicoccus_A;s__Methanomassiliicoccus_A sp905203995	1
GB_GCA_905235195.1	d__Archaea;p__Methanobacteriota;c__Methanobacteria;o__Methanobacteriales;f__Methanobacteriaceae;g__Methanobrevibacter_B;s__Methanobrevibacter_B sp905235195	1
GB_GCA_905235495.1	d__Archaea;p__Methanobacteriota;c__Methanobacteria;o__Methanobacteriales;f__Methanobacteriaceae;g__Methanobrevibacter;s__Methanobrevibacter sp905235495	1
GB_GCA_934234005.1	d__Archaea;p__Thermoplasmatota;c__Thermoplasmata;o__Methanomassiliicoccales;f__Methanomethylophilaceae;g__UBA71;s__UBA71 sp934234005	1
GB_GCA_934702355.1	d__Archaea;p__Thermoplasmatota;c__Thermoplasmata;o__Methanomassiliicoccales;f__Methanomethylophilaceae;g__UBA71;s__UBA71 sp934702355	1
GB_GCA_934746965.1	d__Archaea;p__Methanobacteriota;c__Methanobacteria;o__Methanobacteriales;f__Methanobacteriaceae;g__Methanobrevibacter_A;s__Methanobrevibacter_A sp934746965	1
GB_GCA_944319735.1	d__Archaea;p__Thermoplasmatota;c__Thermoplasmata;o__Methanomassiliicoccales;f__Methanomassiliicoccaceae;g__Methanomassiliicoccus_A;s__Methanomassiliicoccus_A sp944319735	1
GB_GCA_944320485.1	d__Archaea;p__Thermoplasmatota;c__Thermoplasmata;o__Methanomassiliicoccales;f__Methanomethylophilaceae;g__UBA71;s__UBA71 sp944320485	1
GB_GCA_944320495.1	d__Archaea;p__Thermoplasmatota;c__Thermoplasmata;o__Methanomassiliicoccales;f__Methanomethylophilaceae;g__UBA71;s__UBA71 sp944320495	1
GB_GCA_944321505.1	d__Archaea;p__Thermoplasmatota;c__Thermoplasmata;o__Methanomassiliicoccales;f__Methanomethylophilaceae;g__SIG5;s__SIG5 sp944321505	1
GB_GCA_944321985.1	d__Archaea;p__Thermoplasmatota;c__Thermoplasmata;o__Methanomassiliicoccales;f__Methanomethylophilaceae;g__UBA71;s__UBA71 sp944321985	1
GB_GCA_944322255.1	d__Archaea;p__Thermoplasmatota;c__Thermoplasmata;o__Methanomassiliicoccales;f__Methanomethylophilaceae;g__UBA71;s__UBA71 sp944322255	1
RS_GCF_000007185.1	d__Archaea;p__Methanobacteriota;c__Methanopyri;o__Methanopyrales;f__Methanopyraceae;g__Methanopyrus;s__Methanopyrus kandleri	1
RS_GCF_000007345.1	d__Archaea;p__Halobacteriota;c__Methanosarcinia;o__Methanosarcinales;f__Methanosarcinaceae;g__Methanosarcina;s__Methanosarcina acetivorans	1
RS_GCF_000008645.1	d__Archaea;p__Methanobacteriota;c__Methanobacteria;o__Methanobacteriales;f__Methanothermobacteraceae;g__Methanothermobacter;s__Methanothermobacter thermautotrophicus	1
RS_GCF_000012545.1	d__Archaea;p__Methanobacteriota;c__Methanobacteria;o__Methanobacteriales;f__Methanobacteriaceae;g__Methanosphaera;s__Methanosphaera stadtmanae	1
RS_GCF_000013445.1	d__Archaea;p__Halobacteriota;c__Methanomicrobia;o__Methanomicrobiales;f__Methanospirillaceae;g__Methanospirillum;s__Methanospirillum hungatei	1

RS_GCF_000013725.1	d__Archaea;p__Halobacteriota;c__Methanosarcinia;o__Methanosarcinales;f__Methanosarcinaceae;g__Methanococcoides;s__Methanococcoides burtonii	1
RS_GCF_000014945.1	d__Archaea;p__Halobacteriota;c__Methanosarcinia;o__Methanotrichales;f__Methanotrichaceae;g__Methanothrix_B;s__Methanothrix_B thermoacetophila	1
RS_GCF_000015825.1	d__Archaea;p__Halobacteriota;c__Methanomicrobia;o__Methanomicrobiales;f__Methanoculleaceae;g__Methanoculleus;s__Methanoculleus marisnigri	1
RS_GCF_000016125.1	d__Archaea;p__Methanobacteriota;c__Methanococci;o__Methanococcales;f__Methanococcaceae;g__Methanococcus;s__Methanococcus maripaludis_D	1
RS_GCF_000016525.1	d__Archaea;p__Methanobacteriota;c__Methanobacteria;o__Methanobacteriales;f__Methanobacteriaceae;g__Methanobrevibacter_A;s__Methanobrevibacter_A smithii	1
RS_GCF_000017165.1	d__Archaea;p__Methanobacteriota;c__Methanococci;o__Methanococcales;f__Methanococcaceae;g__Methanococcus;s__Methanococcus vannielii	1
RS_GCF_000017185.1	d__Archaea;p__Methanobacteriota;c__Methanococci;o__Methanococcales;f__Methanococcaceae;g__Methanothermococcus_A;s__Methanothermococcus_A aeolicus	1
RS_GCF_000017625.1	d__Archaea;p__Halobacteriota;c__Methanomicrobia;o__Methanomicrobiales;f__Methanoregulaceae;g__Methanoregula;s__Methanoregula boonei	1
RS_GCF_000023985.1	d__Archaea;p__Methanobacteriota;c__Methanococci;o__Methanococcales;f__Methanocaldococcaceae;g__Methanocaldococcus;s__Methanocaldococcus fervens	1
RS_GCF_000024185.1	d__Archaea;p__Methanobacteriota;c__Methanobacteria;o__Methanobacteriales;f__Methanobacteriaceae;g__Methanobrevibacter;s__Methanobrevibacter ruminantium	1
RS_GCF_000024625.1	d__Archaea;p__Methanobacteriota;c__Methanococci;o__Methanococcales;f__Methanocaldococcaceae;g__Methanocaldococcus;s__Methanocaldococcus vulcanius	1
RS_GCF_000025525.1	d__Archaea;p__Methanobacteriota;c__Methanococci;o__Methanococcales;f__Methanocaldococcaceae;g__Methanocaldococcus;s__Methanocaldococcus sp000025525	1
RS_GCF_000025865.1	d__Archaea;p__Halobacteriota;c__Methanosarcinia;o__Methanosarcinales;f__Methanosarcinaceae;g__Methanohalophilus;s__Methanohalophilus mahii	1
RS_GCF_000091665.1	d__Archaea;p__Methanobacteriota;c__Methanococci;o__Methanococcales;f__Methanocaldococcaceae;g__Methanocaldococcus;s__Methanocaldococcus jannaschii	1
RS_GCF_000092305.1	d__Archaea;p__Methanobacteriota;c__Methanococci;o__Methanococcales;f__Methanocaldococcaceae;g__Methanocaldococcus_A;s__Methanocaldococcus_A infernus	1
RS_GCF_000145295.1	d__Archaea;p__Methanobacteriota;c__Methanobacteria;o__Methanobacteriales;f__Methanothermobacteraceae;g__Methanothermobacter;s__Methanothermobacter marburgensis	1
RS_GCF_000147875.1	d__Archaea;p__Halobacteriota;c__Methanomicrobia;o__Methanomicrobiales;f__Methanomicrobiaceae;g__Methanolacinia;s__Methanolacinia petrolearia	1
RS_GCF_000166095.1	d__Archaea;p__Methanobacteriota;c__Methanobacteria;o__Methanobacteriales;f__Methanothermaceae;g__Methanothermus;s__Methanothermus fervidus	1
RS_GCF_000179575.2	d__Archaea;p__Methanobacteriota;c__Methanococci;o__Methanococcales;f__Methanococcaceae;g__Methanothermococcus_A;s__Methanothermococcus_A okinawensis	1
RS_GCF_000196655.1	d__Archaea;p__Halobacteriota;c__Methanosarcinia;o__Methanosarcinales;f__Methanosarcinaceae;g__Methanohalobium;s__Methanohalobium evestigatum	1
RS_GCF_000204415.1	d__Archaea;p__Halobacteriota;c__Methanosarcinia;o__Methanotrichales;f__Methanotrichaceae;g__Methanothrix;s__Methanothrix soehngenii	1
RS_GCF_000214415.1	d__Archaea;p__Methanobacteriota;c__Methanococci;o__Methanococcales;f__Methanococcaceae;g__Methanotorris;s__Methanotorris igneus	1
RS_GCF_000217995.1	d__Archaea;p__Halobacteriota;c__Methanosarcinia;o__Methanosarcinales;f__Methanosarcinaceae;g__Methanosalsum;s__Methanosalsum zhilinae	1
RS_GCF_000235565.1	d__Archaea;p__Halobacteriota;c__Methanosarcinia;o__Methanotrichales;f__Methanotrichaceae;g__Methanothrix_A;s__Methanothrix_A harundinacea_E	1
RS_GCF_000243255.1	d__Archaea;p__Halobacteriota;c__Methanomicrobia;o__Methanomicrobiales;f__Methanomicrobiaceae;g__Methanoplanus;s__Methanoplanus limicola	1
RS_GCF_000243455.1	d__Archaea;p__Methanobacteriota;c__Methanococci;o__Methanococcales;f__Methanococcaceae;g__Methanotorris;s__Methanotorris formicicus	1
RS_GCF_000275865.1	d__Archaea;p__Halobacteriota;c__Methanomicrobia;o__Methanomicrobiales;f__Methanofollaceae;g__Methanofollis;s__Methanofollis liminatans	1
RS_GCF_000300255.2	d__Archaea;p__Thermoplasmatota;c__Thermoplasmata;o__Methanomassiliicoccales;f__Methanomethylophilaceae;g__Methanomethylophilus;s__Methanomethylophilus alvus	1
RS_GCF_000304355.2	d__Archaea;p__Halobacteriota;c__Methanomicrobia;o__Methanomicrobiales;f__Methanoculleaceae;g__Methanoculleus;s__Methanoculleus bourgensis	1
RS_GCF_000308215.1	d__Archaea;p__Thermoplasmatota;c__Thermoplasmata;o__Methanomassiliicoccales;f__Methanomassiliicoccaceae;g__Methanomassiliicoccus;s__Methanomassiliicoccus luminyensis	1

RS_GCF_000320505.1	d__Archaea;p__Methanobacteriota;c__Methanobacteria;o__Methanobacteriales;f__Methanobacteriaceae;g__Methanobrevibacter_B;s__Methanobrevibacter_B boviskoreani	1
RS_GCF_000328665.1	d__Archaea;p__Halobacteriota;c__Methanosarcinia;o__Methanosarcinales;f__Methanosarcinaceae;g__Methanomethylovorans;s__Methanomethylovorans hollandica	1
RS_GCF_000371805.1	d__Archaea;p__Methanobacteriota;c__Methanococci;o__Methanococcales;f__Methanocaldococcaceae;g__Methanocaldococcus_A;s__Methanocaldococcus_A villosus	1
RS_GCF_000376965.1	d__Archaea;p__Methanobacteriota;c__Methanococci;o__Methanococcales;f__Methanococcaceae;g__Methanothermococcus;s__Methanothermococcus thermolithotrophicus	1
RS_GCF_000404225.1	d__Archaea;p__Thermoplasmatota;c__Thermoplasmata;o__Methanomassiliicoccales;f__Methanomassiliicoccaceae;g__Methanomassiliicoccus_A;s__Methanomassiliicoccus_A intestinalis	1
RS_GCF_000504205.1	d__Archaea;p__Halobacteriota;c__Methanosarcinia;o__Methanosarcinales;f__Methanosarcinaceae;g__Methanolobus;s__Methanolobus tindarius	1
RS_GCF_000621965.1	d__Archaea;p__Methanobacteriota;c__Methanobacteria;o__Methanobacteriales;f__Methanobacteriaceae;g__Methanobrevibacter_B;s__Methanobrevibacter_B wolinii	1
RS_GCF_000711215.1	d__Archaea;p__Halobacteriota;c__Methanomicrobia;o__Methanomicrobiales;f__Methanomicrobiaceae;g__Methanomicrobium;s__Methanomicrobium mobile	1
RS_GCF_000711905.1	d__Archaea;p__Halobacteriota;c__Methanosarcinia_A;o__Methanosarcinales_A;f__Methermicoccaceae;g__Methermicoccus;s__Methermicoccus shengliensis	1
RS_GCF_000739065.1	d__Archaea;p__Methanobacteriota;c__Methanococci;o__Methanococcales;f__Methanocaldococcaceae;g__Methanocaldococcus;s__Methanocaldococcus bathoardescens	1
RS_GCF_000744455.1	d__Archaea;p__Methanobacteriota;c__Methanobacteria;o__Methanobacteriales;f__Methanobacteriaceae;g__Methanobacterium_B;s__Methanobacterium_B sp000744455	1
RS_GCF_000765475.1	d__Archaea;p__Halobacteriota;c__Methanosarcinia;o__Methanosarcinales;f__Methanosarcinaceae;g__Methanococcoides;s__Methanococcoides methylutens	1
RS_GCF_000784355.1	d__Archaea;p__Halobacteriota;c__Methanomicrobia;o__Methanomicrobiales;f__Methanomicrobiaceae;g__Methanolacinia;s__Methanolacinia paynteri	1
RS_GCF_000800805.1	d__Archaea;p__Thermoplasmatota;c__Thermoplasmata;o__Methanomassiliicoccales;f__Methanomethylophilaceae;g__Methanoplasma;s__Methanoplasma termitum	1
RS_GCF_000828575.1	d__Archaea;p__Methanobacteriota;c__Methanobacteria;o__Methanobacteriales;f__Methanothermobacteraceae;g__Methanothermobacter;s__Methanothermobacter sp000828575	1
RS_GCF_000969885.1	d__Archaea;p__Halobacteriota;c__Methanosarcinia;o__Methanosarcinales;f__Methanosarcinaceae;g__Methanosarcina;s__Methanosarcina thermophila	1
RS_GCF_000969905.1	d__Archaea;p__Halobacteriota;c__Methanosarcinia;o__Methanosarcinales;f__Methanosarcinaceae;g__Methanosarcina;s__Methanosarcina vacuolata	1
RS_GCF_000969965.1	d__Archaea;p__Halobacteriota;c__Methanosarcinia;o__Methanosarcinales;f__Methanosarcinaceae;g__Methanosarcina;s__Methanosarcina sp000969965	1
RS_GCF_000969985.1	d__Archaea;p__Halobacteriota;c__Methanosarcinia;o__Methanosarcinales;f__Methanosarcinaceae;g__Methanosarcina;s__Methanosarcina barkeri_B	1
RS_GCF_000970025.1	d__Archaea;p__Halobacteriota;c__Methanosarcinia;o__Methanosarcinales;f__Methanosarcinaceae;g__Methanosarcina;s__Methanosarcina barkeri	1
RS_GCF_000970045.1	d__Archaea;p__Halobacteriota;c__Methanosarcinia;o__Methanosarcinales;f__Methanosarcinaceae;g__MTP4;s__MTP4 sp000970045	1
RS_GCF_000970085.1	d__Archaea;p__Halobacteriota;c__Methanosarcinia;o__Methanosarcinales;f__Methanosarcinaceae;g__Methanosarcina;s__Methanosarcina siciliae	1
RS_GCF_000970205.1	d__Archaea;p__Halobacteriota;c__Methanosarcinia;o__Methanosarcinales;f__Methanosarcinaceae;g__Methanosarcina;s__Methanosarcina mazei	1
RS_GCF_000970265.1	d__Archaea;p__Halobacteriota;c__Methanosarcinia;o__Methanosarcinales;f__Methanosarcinaceae;g__Methanosarcina;s__Methanosarcina lacustris	1
RS_GCF_000970285.1	d__Archaea;p__Halobacteriota;c__Methanosarcinia;o__Methanosarcinales;f__Methanosarcinaceae;g__Methanosarcina;s__Methanosarcina horonobensis	1
RS_GCF_000970305.1	d__Archaea;p__Halobacteriota;c__Methanosarcinia;o__Methanosarcinales;f__Methanosarcinaceae;g__Methanosarcina;s__Methanosarcina barkeri_A	1
RS_GCF_000970325.1	d__Archaea;p__Halobacteriota;c__Methanosarcinia;o__Methanosarcinales;f__Methanosarcinaceae;g__Methanococcoides;s__Methanococcoides methylutens_A	1
RS_GCF_000979455.1	d__Archaea;p__Halobacteriota;c__Methanosarcinia;o__Methanosarcinales;f__Methanosarcinaceae;g__Methanosarcina;s__Methanosarcina sp000979455	1
RS_GCF_001017125.1	d__Archaea;p__Halobacteriota;c__Methanomicrobia;o__Methanomicrobiales;f__Methanoculleaceae;g__Methanoculleus;s__Methanoculleus sediminis	1

RS_GCF_001304615.2	d__Archaea;p__Halobacteriota;c__Methanosarcinia;o__Methanosarcinales;f__Methanosarcinaceae;g__Methanosarcina;s__Methanosarcina flavescens	1
RS_GCF_001315945.1	d__Archaea;p__Halobacteriota;c__Methanomicrobia;o__Methanomicrobiales;f__Methanomicrobiaceae;g__Methanogenium;s__Methanogenium cariaci	1
RS_GCF_001316325.1	d__Archaea;p__Methanobacteriota;c__Methanobacteria;o__Methanobacteriales;f__Methanobacteriaceae;g__Methanobacterium;s__Methanobacterium formicicum	1
RS_GCF_001477655.1	d__Archaea;p__Methanobacteriota;c__Methanobacteria;o__Methanobacteriales;f__Methanobacteriaceae;g__Methanobrevibacter_A;s__Methanobrevibacter_A millerae_A	1
RS_GCF_001481295.1	d__Archaea;p__Thermoplasmatota;c__Thermoplasmata;o__Methanomassiliicoccales;f__Methanomethylophilaceae;g__Methanomethylophilus;s__Methanomethylophilus sp001481295	1
RS_GCF_001548675.1	d__Archaea;p__Methanobacteriota;c__Methanobacteria;o__Methanobacteriales;f__Methanobacteriaceae;g__Methanobrevibacter_A;s__Methanobrevibacter_A sp001548675	1
RS_GCF_001571385.1	d__Archaea;p__Halobacteriota;c__Methanomicrobia;o__Methanomicrobiales;f__Methanofollaceae;g__Methanofollis;s__Methanofollis ethanolicus	1
RS_GCF_001571405.1	d__Archaea;p__Halobacteriota;c__Methanomicrobia;o__Methanomicrobiales;f__Methanoculleaceae;g__Methanoculleus;s__Methanoculleus thermophilus	1
RS_GCF_001602375.1	d__Archaea;p__Halobacteriota;c__Methanomicrobia;o__Methanomicrobiales;f__Methanoculleaceae;g__Methanoculleus;s__Methanoculleus horonobensis	1
RS_GCF_001639265.1	d__Archaea;p__Methanobacteriota;c__Methanobacteria;o__Methanobacteriales;f__Methanobacteriaceae;g__Methanobrevibacter_D;s__Methanobrevibacter_D filiformis	1
RS_GCF_001639275.1	d__Archaea;p__Methanobacteriota;c__Methanobacteria;o__Methanobacteriales;f__Methanobacteriaceae;g__Methanobrevibacter_A;s__Methanobrevibacter_A oralis	1
RS_GCF_001639285.1	d__Archaea;p__Methanobacteriota;c__Methanobacteria;o__Methanobacteriales;f__Methanobacteriaceae;g__Methanobrevibacter_C;s__Methanobrevibacter_C cuticularis	1
RS_GCF_001639295.1	d__Archaea;p__Methanobacteriota;c__Methanobacteria;o__Methanobacteriales;f__Methanobacteriaceae;g__Methanobrevibacter_D;s__Methanobrevibacter_D curvatus	1
RS_GCF_001729965.1	d__Archaea;p__Methanobacteriota;c__Methanobacteria;o__Methanobacteriales;f__Methanobacteriaceae;g__Methanosphaera;s__Methanosphaera sp001729965	1
RS_GCF_001889405.1	d__Archaea;p__Halobacteriota;c__Methanosarcinia;o__Methanosarcinales;f__Methanosarcinaceae;g__Methanohalophilus;s__Methanohalophilus halophilus	1
RS_GCF_002072215.1	d__Archaea;p__Methanobacteriota;c__Methanobacteria;o__Methanobacteriales;f__Methanobacteriaceae;g__Methanobrevibacter_C;s__Methanobrevibacter_C arboriphilus	1
RS_GCF_002153915.1	d__Archaea;p__Halobacteriota;c__Methanonatronarchaeia;o__Methanonatronarchaeales;f__Methanonatronarchaeaceae;g__Methanonatronarchaeum;s__Methanonatronarchaeum thermophilum	1
RS_GCF_002201895.1	d__Archaea;p__Methanobacteriota;c__Methanopyri;o__Methanopyrales;f__Methanopyraceae;g__Methanopyrus;s__Methanopyrus sp002201895	1
RS_GCF_002208625.1	d__Archaea;p__Methanobacteriota;c__Methanobacteria;o__Methanobacteriales;f__Methanobacteriaceae;g__Methanobrevibacter_B;s__Methanobrevibacter_B sp002208625	1
RS_GCF_002243045.1	d__Archaea;p__Halobacteriota;c__Methanosarcinia;o__Methanosarcinales;f__Methanosarcinaceae;g__Methanolobus;s__Methanolobus psychrotolerans	1
RS_GCF_002287235.1	d__Archaea;p__Halobacteriota;c__Methanosarcinia;o__Methanosarcinales;f__Methanosarcinaceae;g__Methanosarcina;s__Methanosarcina spelaei	1
RS_GCF_002487355.1	d__Archaea;p__Halobacteriota;c__Methanosarcinia;o__Methanosarcinales;f__Methanoperedenaceae;g__Methanoperedens;s__Methanoperedens sp002487355	1
RS_GCF_002761295.1	d__Archaea;p__Halobacteriota;c__Methanosarcinia;o__Methanosarcinales;f__Methanosarcinaceae;g__Methanohalophilus;s__Methanohalophilus portucalensis	1
RS_GCF_002945325.1	d__Archaea;p__Methanobacteriota;c__Methanococci;o__Methanococcales;f__Methanococcaceae;g__Methanococcus;s__Methanococcus maripaludis	1
RS_GCF_003111605.1	d__Archaea;p__Methanobacteriota;c__Methanobacteria;o__Methanobacteriales;f__Methanobacteriaceae;g__Methanobrevibacter_A;s__Methanobrevibacter_A woesei	1
RS_GCF_003111625.1	d__Archaea;p__Methanobacteriota;c__Methanobacteria;o__Methanobacteriales;f__Methanobacteriaceae;g__Methanobrevibacter_A;s__Methanobrevibacter_A thaueri	1
RS_GCF_003149675.1	d__Archaea;p__Methanobacteriota;c__Methanobacteria;o__Methanobacteriales;f__Methanobacteriaceae;g__Methanosphaera;s__Methanosphaera cuniculi	1
RS_GCF_003173335.1	d__Archaea;p__Halobacteriota;c__Methanomicrobia;o__Methanomicrobiales;f__Methanospirillaceae;g__Methanospirillum;s__Methanospirillum stamsii	1

RS_GCF_003264935.1	d__Archaea;p__Methanobacteriota;c__Methanobacteria;o__Methanobacteriales;f__Methanothermobacteraceae_A;g__Methanothermobacter_A;s__Methanothermobacter_A tenebrarum_A	1
RS_GCF_003268005.1	d__Archaea;p__Methanobacteriota;c__Methanobacteria;o__Methanobacteriales;f__Methanobacteriaceae;g__Methanosphaera;s__Methanosphaera sp003268005	1
RS_GCF_003351865.1	d__Archaea;p__Methanobacteriota;c__Methanococci;o__Methanococcales;f__Methanococcaceae;g__Methanofervidicoccus;s__Methanofervidicoccus sp003351865	1
RS_GCF_003722075.1	d__Archaea;p__Halobacteriota;c__Methanosarcinia;o__Methanosarcinales;f__Methanosarcinaceae;g__Methanohalophilus;s__Methanohalophilus sp003722075	1
RS_GCF_003814835.1	d__Archaea;p__Methanobacteriota;c__Methanobacteria;o__Methanobacteriales;f__Methanobacteriaceae;g__Methanobrevibacter_A;s__Methanobrevibacter_A gottschalkii	1
RS_GCF_003947435.1	d__Archaea;p__Thermoproteota;c__Korarchaeia;o__Korarchaeales;f__Korarchaeaceae;g__Methanodesulfokores;s__Methanodesulfokores washburnensis	1
RS_GCF_004099695.1	d__Archaea;p__Halobacteriota;c__Methanosarcinia;o__Methanosarcinales;f__Methanosarcinaceae;g__Methanosarcina;s__Methanosarcina sp004099695	1
RS_GCF_004102725.1	d__Archaea;p__Halobacteriota;c__Methanomicrobia;o__Methanomicrobiales;f__Methanoculleaceae;g__Methanoculleus_A;s__Methanoculleus_A taiwanensis	1
RS_GCF_004137855.1	d__Archaea;p__Halobacteriota;c__Methanosarcinia;o__Methanosarcinales;f__Methanosarcinaceae;g__Methanohalophilus;s__Methanohalophilus profundi	1
RS_GCF_004297185.1	d__Archaea;p__Halobacteriota;c__Methanomicrobia;o__Methanomicrobiales;f__Methanofollaceae;g__Methanofollis;s__Methanofollis fontis	1
RS_GCF_004310395.1	d__Archaea;p__Methanobacteriota;c__Methanococci;o__Methanococcales;f__Methanococcaceae;g__Methanofervidicoccus;s__Methanofervidicoccus abyssi	1
RS_GCF_004363215.1	d__Archaea;p__Halobacteriota;c__Methanosarcinia;o__Methanosarcinales;f__Methanosarcinaceae;g__Methanimicrococcus;s__Methanimicrococcus blatticola	1
RS_GCF_004745425.1	d__Archaea;p__Halobacteriota;c__Methanosarcinia;o__Methanosarcinales;f__Methanosarcinaceae;g__Methanolobus;s__Methanolobus halotolerans	1
RS_GCF_006546655.1	d__Archaea;p__Halobacteriota;c__Methanosarcinia;o__Methanosarcinales;f__Methanosarcinaceae;g__Methanolobus;s__Methanolobus vulcani_A	1
RS_GCF_009914725.1	d__Archaea;p__Halobacteriota;c__Methanomicrobia;o__Methanomicrobiales;f__Methanomicrobiaceae;g__Methanogenium;s__Methanogenium sp009914725	1
RS_GCF_013377755.1	d__Archaea;p__Halobacteriota;c__Methanomicrobia;o__Methanomicrobiales;f__Methanofollaceae;g__Methanofollis;s__Methanofollis tationis	1
RS_GCF_013388255.1	d__Archaea;p__Halobacteriota;c__Methanosarcinia;o__Methanosarcinales;f__Methanosarcinaceae;g__Methanolobus;s__Methanolobus zinderi	1
RS_GCF_013760955.1	d__Archaea;p__Methanobacteriota;c__Methanococci;o__Methanococcales;f__Methanococcaceae;g__Methanococcus;s__Methanococcus maripaludis_A	1
RS_GCF_014889545.1	d__Archaea;p__Methanobacteriota;c__Methanobacteria;o__Methanobacteriales;f__Methanothermobacteraceae;g__Methanothermobacter;s__Methanothermobacter thermautotrophicus_A	1
RS_GCF_017873415.1	d__Archaea;p__Halobacteriota;c__Methanosarcinia;o__Methanosarcinales;f__Methanosarcinaceae;g__Methanolobus;s__Methanolobus bombayensis	1
RS_GCF_017874375.1	d__Archaea;p__Halobacteriota;c__Methanosarcinia;o__Methanosarcinales;f__Methanosarcinaceae;g__Methanohalophilus;s__Methanohalophilus levihalophilus	1
RS_GCF_017874455.1	d__Archaea;p__Methanobacteriota;c__Methanobacteria;o__Methanobacteriales;f__Methanobacteriaceae;g__Methanobacterium_C;s__Methanobacterium_C aggregans	1
RS_GCF_017875315.1	d__Archaea;p__Halobacteriota;c__Methanomicrobia;o__Methanomicrobiales;f__Methanomicrobiaceae;g__Methanomicrobium;s__Methanomicrobium sp017875315	1
RS_GCF_017875325.1	d__Archaea;p__Halobacteriota;c__Methanomicrobia;o__Methanomicrobiales;f__Methanofollaceae;g__Methanofollis;s__Methanofollis sp017875325	1
RS_GCF_017875395.1	d__Archaea;p__Methanobacteriota;c__Methanococci;o__Methanococcales;f__Methanococcaceae;g__Methanococcus;s__Methanococcus voltae_C	1
RS_GCF_018132105.1	d__Archaea;p__Halobacteriota;c__Methanomicrobia;o__Methanomicrobiales;f__Methanocorpusculaceae;g__Methanocalculus;s__Methanocalculus chunghsingensis	1
RS_GCF_019263745.1	d__Archaea;p__Halobacteriota;c__Methanomicrobia;o__Methanomicrobiales;f__Methanospirillaceae;g__Methanospirillum;s__Methanospirillum sp012729995	1
RS_GCF_019633745.1	d__Archaea;p__Halobacteriota;c__Methanomicrobia;o__Methanomicrobiales;f__Methanofollaceae;g__Methanofollis;s__Methanofollis formosanus	1
RS_GCF_019669925.1	d__Archaea;p__Methanobacteriota;c__Methanobacteria;o__Methanobacteriales;f__Methanobacteriaceae;g__Methanobrevibacter_C;s__Methanobrevibacter_C arboriphilus_A	1

RS_GCF_019669965.1	d__Archaea;p__Halobacteriota;c__Methanomicrobia;o__Methanomicrobiales;f__Methanoculleaceae;g__Methanoculleus;s__Methanoculleus chikugoensis	1
RS_GCF_020148105.1	d__Archaea;p__Methanobacteriota;c__Methanobacteria;o__Methanobacteriales;f__Methanobacteriaceae;g__Methanobrevibacter_C;s__Methanobrevibacter_C sp020148105	1
RS_GCF_020804225.1	d__Archaea;p__Halobacteriota;c__Methanosarcinia;o__Methanosarcinales;f__Methanosarcinaceae;g__Methanosarcina;s__Methanosarcina sp020804225	1
RS_GCF_021184045.1	d__Archaea;p__Halobacteriota;c__Methanosarcinia;o__Methanosarcinales;f__Methanosarcinaceae;g__Methanococcoides;s__Methanococcoides orientis	1
RS_GCF_022014235.1	d__Archaea;p__Methanobacteriota;c__Methanobacteria;o__Methanobacteriales;f__Methanothermobacteraceae;g__Methanothermobacter;s__Methanothermobacter sp022014235	1
RS_GCF_023016325.1	d__Archaea;p__Halobacteriota;c__Methanonatronarchaeia;o__Methanonatronarchaeales;f__Methanonatronarchaeaceae;g__Methanonatronarchaeum;s__Methanonatronarchaeum sp004212035	1
RS_GCF_023167465.1	d__Archaea;p__Methanobacteriota;c__Methanobacteria;o__Methanobacteriales;f__Methanothermobacteraceae_A;g__Methanothermobacter_A;s__Methanothermobacter_A tenebrarum	1
RS_GCF_023195915.1	d__Archaea;p__Halobacteriota;c__Methanomicrobia;o__Methanomicrobiales;f__Methanoculleaceae;g__Methanoculleus;s__Methanoculleus sp023195915	1
RS_GCF_023617305.1	d__Archaea;p__Methanobacteriota;c__Methanobacteria;o__Methanobacteriales;f__Methanobacteriaceae;g__Methanobrevibacter_A;s__Methanobrevibacter_A smithii_A	1
RS_GCF_023684405.1	d__Archaea;p__Halobacteriota;c__Methanosarcinia;o__Methanosarcinales;f__Methanosarcinaceae;g__Methanococcoides;s__Methanococcoides seepicolus	1
RS_GCF_023702065.1	d__Archaea;p__Halobacteriota;c__Methanomicrobia;o__Methanomicrobiales;f__Methanoculleaceae;g__Methanoculleus;s__Methanoculleus sp023702065	1
RS_GCF_024170265.1	d__Archaea;p__Halobacteriota;c__Methanomicrobia;o__Methanomicrobiales;f__Methanocorpusculaceae;g__Methanocalculus;s__Methanocalculus sp003838185	1
RS_GCF_024170505.1	d__Archaea;p__Halobacteriota;c__Methanomicrobia;o__Methanomicrobiales;f__Methanocorpusculaceae;g__Methanocalculus;s__Methanocalculus alkaliphilus	1
RS_GCF_024372725.1	d__Archaea;p__Halobacteriota;c__Methanosarcinia;o__Methanosarcinales;f__Methanosarcinaceae;g__Methanosarcina;s__Methanosarcina sp024372725	1
RS_GCF_024372745.1	d__Archaea;p__Halobacteriota;c__Methanomicrobia;o__Methanomicrobiales;f__Methanocorpusculaceae;g__Methanocalculus;s__Methanocalculus taiwanensis	1
RS_GCF_024500045.1	d__Archaea;p__Halobacteriota;c__Methanosarcinia;o__Methanosarcinales;f__Methanosarcinaceae;g__Methanolobus;s__Methanolobus chelungpuianus	1
RS_GCF_024662215.1	d__Archaea;p__Halobacteriota;c__Methanomicrobia;o__Methanomicrobiales;f__Methanomicrobiaceae;g__Methanoplanus;s__Methanoplanus endosymbiosus	1
RS_GCF_024807035.1	d__Archaea;p__Methanobacteriota;c__Methanococci;o__Methanococcales;f__Methanococcaceae;g__Methanococcus;s__Methanococcus voltae	1
RS_GCF_024807655.1	d__Archaea;p__Methanobacteriota;c__Methanococci;o__Methanococcales;f__Methanococcaceae;g__Methanococcus;s__Methanococcus voltae_D	1
RS_GCF_024808815.1	d__Archaea;p__Halobacteriota;c__Methanosarcinia;o__Methanosarcinales;f__Methanosarcinaceae;g__Methanosalsum;s__Methanosalsum natronophilum	1
RS_GCF_900095295.1	d__Archaea;p__Methanobacteriota;c__Methanobacteria;o__Methanobacteriales;f__Methanobacteriaceae;g__Methanobacterium_C;s__Methanobacterium_C congolense	1
RS_GCF_900095385.1	d__Archaea;p__Halobacteriota;c__Methanomicrobia;o__Methanomicrobiales;f__Methanoculleaceae;g__Methanoculleus;s__Methanoculleus chikugoensis_A	1
RS_GCF_900100715.1	d__Archaea;p__Halobacteriota;c__Methanosarcinia;o__Methanosarcinales;f__Methanosarcinaceae;g__Methanolobus;s__Methanolobus vulcani	1
RS_GCF_900103415.1	d__Archaea;p__Methanobacteriota;c__Methanobacteria;o__Methanobacteriales;f__Methanobacteriaceae;g__Methanobrevibacter_A;s__Methanobrevibacter_A millerae	1
RS_GCF_900111645.1	d__Archaea;p__Halobacteriota;c__Methanosarcinia;o__Methanosarcinales;f__Methanosarcinaceae;g__Methanococcoides;s__Methanococcoides vulcani	1
RS_GCF_900114585.1	d__Archaea;p__Methanobacteriota;c__Methanobacteria;o__Methanobacteriales;f__Methanobacteriaceae;g__Methanobrevibacter;s__Methanobrevibacter olleyae	1
RS_GCF_900114835.1	d__Archaea;p__Halobacteriota;c__Methanosarcinia;o__Methanosarcinales;f__Methanosarcinaceae;g__Methanolobus;s__Methanolobus profundi	1
RS_GCF_900215215.1	d__Archaea;p__Halobacteriota;c__Methanosarcinia;o__Methanosarcinales;f__Methanosarcinaceae;g__Methanohalophilus;s__Methanohalophilus euhalobius	1
RS_GCF_900774055.1	d__Archaea;p__Halobacteriota;c__Methanosarcinia;o__Methanosarcinales;f__Methanosarcinaceae;g__Methanococcoides;s__Methanococcoides sp900774055	1

Table S2.8 Sequence and genome identifiers used to build phylogenetic tree in Figure 2.2.6.1. Sequences from Table S2.7 were clustered based on 70% sequence similarity using Cluster Database at High Identity with Tolerance (CD-HIT)[119]. See section *2.4.14* for further detail.

Genome reference for component A2 sequences	
GB_GCA_000350305.1	GB_GCA_016926505.1
GB_GCA_001399795.1	GB_GCA_016927055.1
GB_GCA_001766815.1	GB_GCA_017613335.1
GB_GCA_001766825.1	GB_GCA_019058315.1
GB_GCA_001766825.1 2	GB_GCA_020832905.1
GB_GCA_001766825.1 3	GB_GCA_021159385.1
GB_GCA_001914405.1	GB_GCA_021160575.1
GB_GCA_002067315.1	GB_GCA_022710385.1
GB_GCA_002503825.1	GB_GCA_022768985.1
GB_GCA_002506105.1	GB_GCA_023396365.1
GB_GCA_003336485.1	GB_GCA_023436175.1
GB_GCA_003661185.1	GB_GCA_024256265.1
GB_GCA_004193545.1	GB_GCA_024464205.1
GB_GCA_004212075.1	GB_GCA_025057955.1
GB_GCA_004212075.1 2	GB_GCA_025059545.1
GB_GCA_004332335.1	GB_GCA_902158735.1
GB_GCA_004347955.1	GB_GCA_902158745.1
GB_GCA_004347965.1.2	GB_GCA_902158745.1 2
GB_GCA_009618475.1	GB_GCA_902386255.1
GB_GCA_009777615.1	GB_GCA_902783085.1
GB_GCA_009780575.1	GB_GCA_903832665.1
GB_GCA_011620825.1	GB_GCA_905171695.1
GB_GCA_012329085.1	GB_GCA_934702355.1
GB_GCA_012518265.1	GB_GCA_944321505.1
GB_GCA_012520845.1	RS_GCF_000007345.1
GB_GCA_013154335.1	RS_GCF_000063445.1
GB_GCA_013329105.1	RS_GCF_000166095.1
GB_GCA_013329495.1	RS_GCF_000196655.1
GB_GCA_013375455.1	RS_GCF_000308215.1
GB_GCA_013375455.1 2	RS_GCF_000320505.1
GB_GCA_013415565.1	RS_GCF_000711905.1
GB_GCA_013415865.1	RS_GCF_001639265.1
GB_GCA_014361455.1	RS_GCF_003947435.1
GB_GCA_015523685.1	RS_GCF_017873855.1
GB_GCA_015660995.1	RS_GCF_021023085.1
GB_GCA_015661395.1	RS_GCF_023016325.1
GB_GCA_015661555.1	RS_GCF_024372745.1
GB_GCA_016840125.1	RS_GCF_024807655.1
GB_GCA_016919565.1	RS_GCF_024808815.1
GB_GCA_016926075.1	RS_GCF_900774055.1

Accession of outgroup sequences
WP_048038079.1
WP_048142278.1
WP_048177517.1
WP_128507879.1
WP_255333748.1
WP_292389363.1
WP_310574945.1
WP_324445388.1
WP_422543076.1
WP_424716364.1
HET8688081.1
HJH32081.1
MBN2488851.1
MDD3043193.1
MDD4750015.1
MDM7919529.1
MDQ1251115.1
MGB9930053.1
MHB8102642.1
NLO31043.1

Appendix B. Supplementary information to Chapter 3

Table S3.1 Table of all primers and gblocks used in this study

Name	Sequence	Description
DN1005	TGATTTTAATAAATTAAGGAGGAAATTCATATGGAT AAGAAATACTCAATAG	Forward primer to amplify dCas9 from pBHC0103. 30 bp Gibson overhang at 5'end upstream of NdeI cut site in pJK027A
DN1006	GCATACATTATACGAAGTTATCAAGAAGCTTTTAGT CACCTCCTAGCTGAC	Reverse primer to amplify dCas9 from pBHC0103. 30 bp Gibson overhang at 5'end downstream of HindIII cut site in pJK027A
SA067	ATTGCAGATAGCCACATGGGAC	forward primer for rpo1 qPCR with 68 (product is 91 bp)
SA068	CCATCTGGGTAAGGTTCAGGAT	reverse primer for rpo1 qPCR with 67(product is 91 bp)
SA100	CGCAGACAATGGACCTCATG	reverse primer for McrB qPCR with 101 (product is 82 bp)
SA101	AGGGAGAAGCCAAGACCTTC	forward primer for McrB qPCR with 100 (product is 82 bp)
SA104	CGGCCGTCAGATTGTTGAAG	reverse primer for McrG qPCR with 105 (product is 125 bp)
SA105	CAGAGTGACCGTGGACTGTT	forward primer for McrG qPCR with 104 (product is 125 bp)
SA112	TGGTGCCACAAACGTTCTG	reverse primer for McrA qPCR with 113 (product is 125 bp)
SA113	CCTGAGCGATACCTGCGTAT	forward primer for McrA qPCR with 112 (product is 125 bp)
SA116	TCCCTACAAGCCCGAAAATCT	forward primer MMP A2 w/ 117 (product is 125 bp)
SA117	AGAGCCCATTATCCGCGTAA	reverse primer MMP A2 w/ 116 (product is 125 bp)
SA121	ACTTTAAGCCTGCGTTTCTC	forward primer MMP 6 w/ 124 (product is 125 bp)
SA124	AGACCGGGATTCCATTTCCT	reverse primer MMP 6 w/ 121 (product is 125 bp)
SA127	ACGACTCCTTCATCAAACT	forward primer MMP 7 w/ 129 (product is 125 bp)
SA129	CGGAAATCCAAAGAGTCCTCTCT	reverse primer MMP 7 w/ 127 (product is 124 bp)
SA132	ATTGCCTTGTTGTCCATACCT	forward primer MMP 15 w/ 133 (product is 124 bp)
SA133	ATTTCAACGCCCAGCTTGTT	reverse primer MMP 15 w/ 132 (product is 124 bp)
SA138	CAGGACTTGCCCAGTGGATA	forward primer MMP 3 w/ 139 (product is 125 bp)
SA139	CGCTATCAAGACGCCCAGA	reverse primer MMP 3 w/ 138 (product is 125 bp)
gSAA001B	GCCTTTTTTTTTTCGAAGTTTCTGGTTGGTTTTCTA AATCAATGTGTTCTTAGTTCCTATCCGAAAAGCGG TACTGTTAAGTCTTAGGGGGATGGTTATAATTGCAT GTTCACCTATAACTGGAAAATTTCTTATCCCCCTA AGTCTTAACAGTACCAAAAAAGGAAAAGATTGCGC CCTGAATACCTGCGAGTTTTAGAGCTAGAAATAGC AAGTTAAAATAAGGCTAGTCCGTTATCAACTTGAA AAAGTGGCACCGAGTCGGTGCTTTTACTCAATAAA TCAAACACTTTAAAACAGAGTAGGCCTTCGGGCCT GCTTTTTTCCCTCTTTTTTCCATACTGGCTTTTCT TTACTGTTTTTCCGGAAATCAAACCTGCAGGCGCG CCG	gblock for cloning mcrB guide into dCas9 plasmid
gSAA002	GCCTTTTTTTTTTCGAAGTTTCTGGTTGGTTTTCTA AATCAATGTGTTCTTAGTTCCTATCCGAAAAGCGG TACTGTTAAGTCTTAGGGGGATGGTTATAATTGCAT GTTCACCTATAACTGGAAAATTTCTTATCCCCCTA AGTCTTAACAGTACCAAAAAAGGAAAAGATGGTCT CGATACCGTAGAGTGGTTTTAGAGCTAGAAATAGC AAGTTAAAATAAGGCTAGTCCGTTATCAACTTGAA AAAGTGGCACCGAGTCGGTGCTTTTACTCAATAAA TCAAACACTTTAAAACAGAGTAGGCCTTCGGGCCT GCTTTTTTCCCTCTTTTTTCCATACTGGCTTTTCT	gblock for cloning mcrA guide into dCas9 plasmid

	TTACTGTTTTTCCGGAAATCAAACCTGCAGGCGCG CCG	
gSAA003	GCCTTTTTTTTTTCGAAGTTTCTGGTTGGTTTTCTA AATCAATGTGTTCTTAGTTCCTATCCGAAAAGCGG TACTGTTAAGTCTTAGGGGGATGGTTATAATTGCAT GTTCACCTATAACTGGAAAATTTCTTATCCCCCTA AGTCTTAACAGTACCAAAAAAGGAAAAGATCATAA AGGGCAAAGGTCCTCGTTTTAGAGCTAGAAATAGC AAGTTAAAATAAGGCTAGTCCGTTATCAACTTGAA AAAGTGGCACCGAGTCGGTGCTTTTACTCAATAAA TCAAACACTTTAAAACAGAGTAGGCCTTCGGGCCT GCTTTTTTCCCTCTTTTTTCCATACTGGCTTTTCT TTACTGTTTTTCCGGAAATCAAACCTGCAGGCGCG CCG	gblock for cloning component A2 guide into dCas9 plasmid

Table S3.2 Table of all plasmids used in this study.

Plasmid	Description	Reference
pJK027A	Vector with PmcrB(tetO1) promoter fusion to uidA that contains φC31-attB and λattP	17
pAMG40	Vector for fosmid retrofitting containing pC2A and λattB	17
pBFC0103	Vector containing dSpyCas9 sequence for cloning into pGLC014	150
pGLC014	Backbone: pJK027A digested by NdeI, HindIII; Insert: dSpyCas9 from pBFC0103	This study
pSAA017	Backbone: pGLC014 digested by PmeI; Insert: mcrB_sgRNA_expression_construct	This study
pSAA018	Backbone: pGLC014 digested by PmeI; Insert: mcrA_sgRNA_expression_construct	This study
pSAA021	cointegrate of pAMG40 with pSAA017 using BP clonase II master mix	This study
pSAA022	cointegrate of pAMG40 with pSAA018 using BP clonase II master mix	This study
pSAA031	Backbone: pGLC014 digested by PmeI; insert: gSAA003 (gblock to insert A2 sgRNA expression construct)	This study
pSAA039	cointegrate of pAMG40 and pSAA031 using BP clonase II master mix	This study

Table S3.3 Table of all strains used in this study.

Strain	Description	Reference
WWM60	M. acetivorans delta hpt:: PmcrB-tetR	17
DDN223	M. acetivorans delta hpt:: PmcrB-tetR / pSAA021 [mcrB KD construct]	This study
DDN224	M. acetivorans delta hpt:: PmcrB-tetR / pSAA022 [mcrA KD construct]	This study
DDN249	M. acetivorans delta hpt:: PmcrB-tetR / pSAA039 [component A2 KD construct]	This study